

TECHNISCHE UNIVERSITÄT MÜNCHEN

Wissenschaftszentrum Weihenstephan
für Ernährung, Landnutzung und Umwelt

Lehrstuhl für Experimentelle Genetik

Developmental gene *Pax6* in adult pancreas homeostasis and energy metabolism

Nirav Florian Chhabra

Vollständiger Abdruck der von der Fakultät Wissenschaftszentrum Weihenstephan für Ernährung, Landnutzung und Umwelt der Technischen Universität München zur Erlangung des akademischen Grades eines

Doktors der Naturwissenschaften

genehmigten Dissertation.

Vorsitzender: Prof. Dr. Wolfgang Wurst

Prüfer der Dissertation: 1. Prof. Dr. Martin Hrabě de Angelis
2. Prof. Dr. Matrin Klingenspor

Die Dissertation wurde am 14.06.2017 bei der Technischen Universität München eingereicht und durch die Fakultät Wissenschaftszentrum Weihenstephan für Ernährung, Landnutzung und Umwelt am 18.10.2017 angenommen.

I. TABLE OF CONTENTS

| | |
|--|------------|
| I. TABLE OF CONTENTS ----- | I |
| II. TABLES AND FIGURES ----- | IV |
| III. ABBREVIATIONS ----- | VII |
| IV. SUMMARY/ZUSAMMENFASSUNG ----- | X |
| 1. INTRODUCTION ----- | 1 |
| 1.1 β-cell identity and function ----- | 1 |
| 1.1.1 Islets of Langerhans----- | 1 |
| 1.1.2 Pancreatic development and the endocrine lineage----- | 1 |
| 1.1.3 Insulin secretory mechanism----- | 3 |
| 1.1.3.1 Glucose stimulated insulin secretion----- | 3 |
| 1.1.3.2 Incretin effects on insulin secretion----- | 4 |
| 1.1.4 Postnatal β -cell identity and regulation----- | 6 |
| 1.1.5 Type 2 Diabetes Mellitus----- | 7 |
| 1.1.5.1 Overview----- | 7 |
| 1.1.5.2 β -cell dysfunction in T2DM----- | 8 |
| 1.2 Central and peripheral metabolic pathways ----- | 9 |
| 1.2.1 Islet-liver axis----- | 9 |
| 1.2.2 Hypothalamic control of metabolism----- | 13 |
| 1.3 PAX family of transcription factors ----- | 14 |
| 1.3.1 PAX family----- | 14 |
| 1.3.2 Paired box protein 6----- | 16 |
| 1.3.2.1 PAX6: Master regulator----- | 16 |
| 1.3.2.2 PAX6 and metabolism----- | 16 |
| 1.4 Aims and hypothesis ----- | 21 |
| 2. MATERIALS AND METHODS ----- | 22 |
| 2.1 Materials ----- | 22 |
| 2.1.1 Buffers and solutions----- | 22 |
| 2.1.2 <i>In vitro</i> insulin secretion assay materials----- | 24 |
| 2.1.3 PCR Primers----- | 24 |
| 2.1.3.1 Housekeeping genes----- | 24 |
| 2.1.3.2 Target genes----- | 25 |
| 2.1.4 Primary Antibodies----- | 26 |
| 2.1.4.1 Western blot and chromatin immunoprecipitation----- | 26 |
| 2.1.4.2 Immunohistochemistry----- | 26 |

| | |
|--|-----------|
| 2.1.5 Secondary Antibodies ----- | 27 |
| 2.1.5.1 Western blot ----- | 27 |
| 2.1.5.2 Immunohistochemistry ----- | 27 |
| 2.1.6 Chemicals and kits ----- | 27 |
| 2.1.6.1 Consumables ----- | 27 |
| 2.1.6.2 Chemicals ----- | 28 |
| 2.1.6.3 Reagents ----- | 28 |
| 2.1.6.4 Kits ----- | 29 |
| 2.1.6.5 Laboratory devices and equipment ----- | 29 |
| 2.2 Methods----- | 30 |
| 2.2.1 Mouse line maintenance ----- | 30 |
| 2.2.2 Metabolic and physiological methods ----- | 30 |
| 2.2.2.1 Body composition and metabolic studies ----- | 30 |
| 2.2.2.2 Dietary challenge test ----- | 30 |
| 2.2.2.3 Leptin sensitivity assay ----- | 30 |
| 2.2.2.4 Euglycemic-hyperinsulinemic clamps ----- | 31 |
| 2.2.2.5 Plasma collection and Clinical chemistry ----- | 31 |
| 2.2.3 <i>In vitro</i> methods ----- | 31 |
| 2.2.3.1 Islet isolation ----- | 31 |
| 2.2.3.2 Insulin stimulatory studies ----- | 32 |
| 2.2.3.3 Hepatocyte isolation ----- | 33 |
| 2.2.3.4 Primary hepatocyte sandwich culture ----- | 34 |
| 2.2.3.5 Glucose secretion assay ----- | 35 |
| 2.2.3.6 Hepatocyte mitochondrial respiration ----- | 35 |
| 2.2.3.7 Maintenance of β TC-3 cell line ----- | 35 |
| 2.2.4 Molecular methods ----- | 36 |
| 2.2.4.1 RNA isolation ----- | 36 |
| 2.2.4.2 Microarray ----- | 37 |
| 2.2.4.3 cDNA synthesis ----- | 38 |
| 2.2.4.4 Quantitative real-time Polymerase Chain Reaction (qRT-PCR) ----- | 38 |
| 2.2.4.5 Protein isolation ----- | 39 |
| 2.2.4.6 Western blot ----- | 40 |
| 2.2.4.7 Measurement of insulin and glucagon ----- | 40 |
| 2.2.4.8 FGF21 and Leptin ELISA ----- | 41 |
| 2.2.5 Histology ----- | 41 |
| 2.2.5.1 Pancreatic tissue preparation for frozen sections ----- | 41 |
| 2.2.5.2 Hypothalamic tissue preparation for frozen sections ----- | 41 |
| 2.2.5.3 Immunohistochemistry for frozen pancreatic sections ----- | 42 |
| 2.2.5.4 Immunohistochemistry for frozen hypothalamic sections ----- | 42 |
| 2.2.5.5 Acquisition and quantification of insulin and glucagon expression ----- | 42 |
| 2.2.6 Tissue preparation for chromatin immunoprecipitation and next generation sequencing (ChIP-seq) ----- | 43 |
| 3. RESULTS ----- | 44 |
| 3.1 Characterization of islets of homozygous <i>Pax6^{Leca2}</i> mice----- | 44 |
| 3.1.1 Reduction in the number of beta cells and centralization of alpha cells in mutant islets ----- | 44 |
| 3.1.2 Differential expression of transcriptome of <i>Pax6^{Leca2}</i> isolated islets ----- | 49 |
| 3.1.3 Loss of insulin secretory mechanism in <i>Pax6^{Leca2}</i> mice ----- | 53 |
| 3.2 Metabolic features of homozygous <i>Pax6^{Leca2}</i> mice----- | 56 |
| 3.2.1 Lower body weight and blood glucose levels ----- | 56 |

| | |
|--|--------------|
| 3.2.2 Differences in energy expenditure, food intake and locomotor activity ----- | 58 |
| 3.2.3 Increased insulin sensitivity and reduced hepatic glucose output ----- | 60 |
| 3.2.4 Molecular signatures for insulin signaling and compensatory liver function ----- | 63 |
| 3.2.5 Resistance to diet induced obesity but not a hyperglycemic state ----- | 72 |
| 3.3 Possible contribution of hypothalamus to changes in the metabolic phenotype of <i>Pax6^{Leca2}</i> mice ----- | 79 |
| 3.3.1 Expression of <i>Pax6</i> in adult murine hypothalamus ----- | 79 |
| 3.3.2 ChIP-sequencing reveals differentially bound targets of PAX6 in <i>Pax6^{Leca2}</i> mutants ----- | 84 |
| 4. DISCUSSION ----- | 88 |
| 4.1 The islet story ----- | 88 |
| 4.1.1 Structural changes in the islets of homozygous <i>Pax6^{Leca2}</i> mice ----- | 88 |
| 4.1.2 R128C contributes to changes in gene expression pattern in isolated islets ----- | 89 |
| 4.1.2.1 Partial loss of β -cell identity ----- | 89 |
| 4.1.2.2 Loss of insulin secretory mechanism ----- | 91 |
| 4.1.2.3 Changes in RED subdomain DNA binding: A speculation ----- | 93 |
| 4.2 The metabolic story ----- | 94 |
| 4.2.1 <i>Pax6^{Leca2}</i> mice maintain normoglycemia with low insulin levels ----- | 94 |
| 4.2.2 Changes in the metabolic state of <i>Pax6^{Leca2}</i> mice ----- | 95 |
| 4.2.2.1 Increased energy expenditure and food intake ----- | 95 |
| 4.2.2.2 Increased insulin sensitivity and reduced hepatic glucose production ----- | 96 |
| 4.2.2.3 HFD fed <i>Pax6^{Leca2}</i> mice are resistant to DIO but not to hyperglycemia ----- | 100 |
| 4.2.2.4 Contribution of the hypothalamus to the metabolic phenotype of <i>Pax6^{Leca2}</i> mice ----- | 103 |
| 4.3 General remarks and future perspectives ----- | 109 |
| 4.4 Closing remarks ----- | 111 |
| 5. APPENDIX ----- | 112 |
| 5.1 Supplementary methods ----- | 112 |
| 5.2 Supplementary figures ----- | 114 |
| 5.3 Supplementary tables ----- | 118 |
| 6. REFERENCES ----- | 205 |
| V. ACKNOWLEDGEMENT ----- | XIII |
| VI. AFFIRMATION ----- | XV |
| VII. PUBLICATIONS, TALKS AND POSTERS ----- | XVI |
| VIII. CURRICULUM VITAE ----- | XVIII |

II. TABLES AND FIGURES

| | |
|---|-----|
| Figure 1.1: Transcription factors involved in islet cell development and maturation..... | 3 |
| Figure 1.2: Insulin secretion from the pancreatic β -cell..... | 6 |
| Figure 1.3: Fasting liver metabolism..... | 10 |
| Figure 1.4: Regulation of POMC and AGRP neurons..... | 14 |
| Figure 1.5: PAX DNA binding domains..... | 15 |
| Figure 3.1: Effects of <i>Leca2</i> mutation on islet morphology..... | 45 |
| Figure 3.2: Quantification of hormone positive endocrine cells..... | 46 |
| Figure 3.3: Histological expression and localization of islet hormones..... | 47 |
| Figure 3.4: Histological expression of β -cell markers..... | 48 |
| Figure 3.5: Transcriptome changes contributed by the <i>Leca2</i> mutation..... | 49 |
| Figure 3.6: Dysregulated genes conferring identity to β -cells..... | 51 |
| Figure 3.7: Dysregulated genes conferring functional attributes to β -cells..... | 53 |
| Figure 3.8: In vitro analysis of hormonal content and secretory capacity in 10 weeks old mice..... | 55 |
| Figure 3.9: Insulin secretion upon forskolin stimulation..... | 56 |
| Figure 3.10: Glucose homeostasis..... | 57 |
| Figure 3.11: Energy expenditure and body composition..... | 59 |
| Figure 3.12: Glucose lowering efficiency in response to exogenous insulin..... | 61 |
| Figure 3.13: Hepatic glucose production and glucose uptake..... | 62 |
| Figure 3.14: mRNA expressions of gluconeogenic enzymes..... | 64 |
| Figure 3.15: Protein expressions of gluconeogenic enzymes and insulin signaling intermediates..... | 65 |
| Figure 3.16: Glycogenolytic and gluconeogenic capacity..... | 66 |
| Figure 3.17: Evident change in fasting glycogen but normal glucagon levels in <i>Pax6^{Leca2}</i> mice..... | 68 |
| Figure 3.18: Glucose secretory capacity of primary hepatocytes..... | 70 |
| Figure 3.19: Increased FGF21 in <i>Pax6^{Leca2}</i> mice..... | 71 |
| Figure 3.20: mRNA expression of liver genes involved in fat metabolism..... | 72 |
| Figure 3.21: Weekly body weight and blood glucose of HFD fed mice..... | 73 |
| Figure 3.22: Resistance to DIO in HFD fed <i>Pax6^{Leca2}</i> mice..... | 74 |
| Figure 3.23: Glucose homeostasis of HFD fed mice..... | 75 |
| Figure 3.24: Absence of compensatory increase in insulin in HFD fed <i>Pax6^{Leca2}</i> mice..... | 76 |
| Figure 3.25: Loss of insulin sensitivity in <i>Pax6^{Leca2}</i> mice fed with HFD..... | 77 |
| Figure 3.26: mRNA expression of <i>Pax6</i> in various tissues..... | 79 |
| Figure 3.27: Expression and localization of PAX6 in hypothalamus..... | 80 |
| Figure 3.28: mRNA expressions of genes involved in feeding and leptin signaling in hypothalamus..... | 82 |
| Figure 3.29: Leptin assay reveals a non-significant trend towards increased leptin sensitivity..... | 83 |
| Figure 3.30: Peak locations in hypothalamus of PAX6 bound sites..... | 84 |
| Figure 3.31: Motif enrichment in PAX6 bound regions..... | 86 |
| Figure 3.32: Comparison of bound and regulated gene targets..... | 87 |
| Figure 4.1: Graphical summary of <i>Pax6^{Leca2}</i> mouse model..... | 109 |
| | |
| Table 3.1: GO term analysis of dysregulated gene set in <i>Pax6^{Leca2}</i> mice..... | 50 |
| Table 3.2: Biochemical parameters in chow fed mice..... | 69 |
| Table 3.3: Biochemical parameters in HFD fed mice..... | 78 |
| | |
| Supplementary method 1: Chromatin Immunoprecipitation..... | 112 |
| Supplementary method 2: ChIP Sequencing (Illumina)..... | 112 |

| | |
|--|-----|
| <i>Supplementary figure 1: In vitro analysis of hormonal content and secretory capacity in 4 weeks old mice</i> | 114 |
| <i>Supplementary figure 2: In vitro analysis of hormonal content and secretory capacity in 6 weeks old mice</i> | 115 |
| <i>Supplementary figure 3: Linear regression model for analysis of body composition.....</i> | 116 |
| <i>Supplementary figure 4: RER of mice fed with HFD and LFCD.....</i> | 116 |
| <i>Supplementary figure 5: Plasma glucagon levels in mice fed with HFD</i> | 117 |

| | |
|---|-----|
| <i>Supplementary table 1: Differential expression of genes in isolated islets of 4 weeks old male Pax6^{Leca2} (Leca2) and wildtype (WT) mice filtered for a minimum FC 1.5 and <10% FDR.....</i> | 118 |
| <i>Supplementary table 2: Differential expression of genes in isolated islets of 6 weeks old male Pax6^{Leca2} (Leca2) and wildtype (WT) mice filtered for a minimum FC 1.5 and <10% FDR.....</i> | 130 |
| <i>Supplementary table 3: Differential expression of genes in isolated islets of 10 weeks old male Pax6^{Leca2} (Leca2) and wildtype (WT) mice filtered for a minimum FC 1.5 and <10% FDR.....</i> | 165 |
| <i>Supplementary table 4: ChIP-sequencing for PAX6 in hypothalamic tissue.....</i> | 198 |

III. ABBREVIATIONS

| ABBREVIATION | FULL NAME |
|---------------------|---|
| °C | Degree Celsius |
| μL | Microliter |
| μM | Micromolar |
| AC | Adenylyl cyclase |
| Acetyl CoA | Acetyl coenzyme A |
| AgRP/AGRP | Agouti-related peptide |
| AKT | Protein kinase B (PKB) |
| ANOVA | Analysis of variance |
| ARH | Arcuate hypothalamic nucleus |
| Arx | Aristaless Related Homeobox |
| ATP | Adenosine triphosphate |
| bHLH | Basic-helix-loop-helix |
| bp | Basepair |
| BSA | Bovine albumin serum |
| Ca ²⁺ | Calcium |
| cAMP | Cyclic adenosine monophosphate |
| CART/ <i>Cartpt</i> | Cocaine- and amphetamine-regulated transcript |
| CCK | Cholecystokinin |
| cDNA | Complementary DNA |
| CO ₂ | Carbon dioxide |
| Cp | Crossing point |
| DIO | Diet induced obesity |
| DNA | Desoxyribonuclein acid |
| dNTPs | Desoxynucleotides |
| E | Embryonic day |
| EDTA | Ethylenediaminetetraacetic acid |
| EGF | Epidermal growth factor |
| ELISA | Enzyme-linked immunosorbent assay |
| EPAC2 | Exchange protein activated by cAMP 2 |
| ER | Endoplasmatic reticulum |
| FBP1 | Fructose-1,6-bisphosphatase |
| FC | Fold change |
| FDR | False discovery rate |
| FFAR1 | Free fatty acid receptor 1 |
| FGF21 | Fibroblast growth factor 21 |
| FOXO1 | Forkhead box O1 |
| G6PC | Glucose-6-phosphatase |
| GCGR | Glucagon receptor |
| GCK | Glucokinase |
| GIP | Glucose-dependent insulintropic peptide |

| | |
|------------------|---|
| GIPR | Glucose-dependent insulinotropic peptide receptor |
| GIR | Glucose infusion rate |
| GLP1 | Glucagon-like protein1 |
| GIP1R | Glucagon-like protein1 receptor |
| GLUT2 | Glucose transporter 2 |
| GPCR | G-protein coupled receptor |
| GSIS | Glucose-stimulated insulin secretion |
| GTT | Glucose tolerance test |
| H ₂ O | Water |
| HGP | Hepatic glucose production |
| HNF4A | Hepatocyte nuclear factor-4A |
| IA1 | Insulinoma associated 1 |
| ip | Intraperitoneal |
| IP3 | Inositol 1,4,5-trisphosphate |
| ipGTT | Intraperitoneal glucose tolerance test |
| IRS1 | Insulin receptor substrate 1 |
| IRS2 | Insulin receptor substrate 2 |
| K _{ATP} | ATP sensitive potassium channels |
| Kir6.2 | Inward-rectifier potassium ion channel |
| LDHA | Lactate dehydrogenase A |
| LHA | Lateral hypothalamic area |
| MAFA | v-maf musculoaponeurotic fibrosarcoma oncogene family A |
| MAFB | v-maf musculoaponeurotic fibrosarcoma oncogene family B |
| mL | Milliliter |
| mM | Millimolar |
| MODY | Maturity onset diabetes of the young. |
| MSLN | Mesothelin |
| NAADP | Nicotinic acid-adenine dinucleotide phosphate |
| NAD | Nicotinamide adenine dinucleotide |
| NEUROD1 | Neurogenic differentiation 1 |
| NEUROG3 | Neurogenin 3 |
| NKX2-2 | NK type homeodomain 2.2 |
| NKX6-1 | NK type homeodomain 6.1 |
| nM | Nanomolar |
| NMR | Nuclear magnetic resonance |
| NPY | Neuropeptide Y |
| OAA | Oxaloacetate |
| oGTT | Oral glucose tolerance test |
| PAS | Periodic acid-Schiff |
| PAX6 | Paired box protein 6 |
| PC1/3 | Prohormone convertase 1/3 |
| PC2 | Prohormone convertase 2 |
| PCX | Pyruvate carboxylase |
| PDH | Pyruvate dehydrogenase |
| PDK1 | Phosphoinositide-dependent protein kinase 1 |
| PDK2 | Pyruvate Dehydrogenase Kinase 2 |

| | |
|---------------|--|
| PDX1 | Pancreatic duodenal homeobox 1 |
| PEP | Phosphoenolpyruvate |
| PEPCK | Phosphoenolpyruvate carboxykinase |
| PFA | Paraformaldehyde |
| PGC-1A | Coactivator peroxisome proliferator-activated receptor γ coactivator-1 α |
| PI3K | Phosphatidylinositol 3-kinase |
| PKA | Activating protein kinase A |
| PKA | Protein kinase A |
| POMC | Pro-opiomelanocortin |
| PP | Pancreatic polypeptide |
| PPAR α | Peroxisome proliferator-activated receptor α |
| PTF1A | Pancreas-specific transcription factor 1a |
| PVH | Paraventricular hypothalamus |
| qRT-PCR | Quantitative real-time polymerase chain reaction |
| RFX | Regulatory factor X |
| RIN | RNA integrity number |
| RNA | Ribonucleic acid |
| rpm | Rounds per minute |
| RRP | Readily releasable pool |
| RT | Room temperature |
| SDS | Sodium dodecyl Sulfate |
| SEM | Standard error of the mean |
| SLC2A2 | Solute Carrier Family 2 Member 2 |
| SOX9 | Sry-related HMG box transcription factor 9 |
| SPF | Specific-pathogen-free |
| T1DM | Type 1 diabetes mellitus |
| T2DM | Type 2 diabetes mellitus |
| TCA | Tricarboxylic acid cycle |
| TF | Transcription factor |
| UCN3 | Urocortin 3 |
| WAT | White adipose tissue |
| ZI | Zona incerta |
| α | Alpha |
| β | Beta |
| δ | Delta |
| ϵ | Epsilon |

IV. SUMMARY/ZUSAMMENFASSUNG

The paired box protein 6 (PAX6) is a major transcription factor involved in eye development, and the olfactory lobe. Additionally, its role in the development of the pancreas has previously been well established and seems to also play an important role in the homeostasis of the adult islet. Furthermore, studies have indicated that PAX6 is involved in extra-islet tissues and the overall metabolism although the underlying mechanisms remain largely unknown. The present study attempted to shed light on this by making use of an *ENU*-generated *Pax6*^{Leca2} mouse line with a point mutation (R128C) in the RED subdomain of the PAX6 protein that recapitulates a previously documented human mutation causing foveal hypoplasia.

In addition to the retinal defects, the mutation translates into numerous observable abnormalities in the pancreas. Using *in vitro* assays and molecular tools, the mouse model was analyzed for effects of the mutation on pancreatic β -cell identity and function. Islet distortion was discernible from the age of 4 weeks including various dysregulated genes. More specifically, partial loss of identity pertaining to reduction in *Ucn3* and increase in *Neurog3* expression in the islets and reduction of insulin content seems to be the most profound effects. Moreover, failure of the insulin secretory mechanism, possibly due to dysfunction of mitochondrial machinery and downregulation of incretin-associated receptors exacerbated the β -cell failure. Surprisingly, no change in circulating or islet glucagon content and secretion was found in the *Pax6*^{Leca2} mice.

Furthermore, *in vivo* investigations on contributions of the mutation on the peripheral metabolism revealed similar results as demonstrated by *in vitro* assays, indicating reduced insulin content and secretion. However, this reduction was surprisingly accompanied with a decreased fasting and *ad libitum* fed blood glucose level as well as a normal glucose clearance. This was in accordance to an enhanced liver insulin sensitivity and decreased hepatic glucose production, specifically due to the loss of gluconeogenic output. Additionally, increase in locomotor activity and energy expenditure indicated an effect mediated via the hypothalamus. Presence of PAX6 was found in various parts of the hypothalamus and ChIP-sequencing exposed several targets differentially bound by the mutated TF including *Foxo1*, which is an integral part of the insulin signaling mechanism. This shows that alterations in DNA binding properties of the RED subdomain of PAX6 are capable of inducing changes in the islets and in

the hypothalamus affecting the overall metabolism. Taken together, the data suggests, as yet, an unknown systemic function of PAX6 that affect metabolic pathways and consequently protect the organism from hyperglycemia in absence of insulin increment.

Das Paired-Box-Protein 6 (PAX6) ist ein wichtiger Transkriptionsfaktor, der an der Augenentwicklung sowie am olfaktorischen Lappen beteiligt ist. Seine Rolle bei der Entwicklung der Bauchspeicheldrüse ist schon früher nachgewiesen worden und scheint auch eine wichtige Rolle bei der Homöostase der erwachsenen Inselzellen zu spielen. Ferner haben Untersuchungen auf eine Beteiligung von PAX6 an Geweben außerhalb der Inseln und dem Gesamtmetabolismus hingewiesen, obwohl die zugrundeliegenden Mechanismen weitgehend unbekannt sind. In der vorliegenden Studie wurde der Versuch unternommen, dies zu beleuchten, und zwar unter Verwendung der ENU-generierten *Pax6^{Leca2}* Mauslinie, die eine Punktmutation (R128C) in der RED Subdomäne des PAX6 Proteins aufweist und einer bereits dokumentierten, foveale Hypoplasie verursachenden Mutation des Menschen entspricht.

Zusätzlich zu den Schädigungen der Netzhaut führt die Mutation zu zahlreichen beobachtbaren Anomalien in der Bauchspeicheldrüse. Unter Verwendung von *in vitro* Versuchen und molekularbiologischer Methoden wurde das Mausmodell im Hinblick auf die Auswirkungen der Mutation auf die pankreatische β -Zellenidentität und -funktion analysiert. Veränderungen in den Inselzellen waren ab einem Alter von 4 Wochen erkennbar, einschließlich einer Deregulation verschiedener Gene. Genauer gesagt scheinen ein partieller Identitätsverlust, der auf eine Verringerung der *Ucn3*- und Zunahme der *Neurog3*-Expression in den Inselzellen zurückzuführen ist, sowie eine Reduzierung des Insulingehaltes die tiefgreifenden Auswirkungen zu sein. Darüber hinaus verschärfte ein Ausfall des insulin-sekretorischen Mechanismus, möglicherweise aufgrund einer Fehlfunktion von Mitochondrien und inkretin-assoziierten Rezeptoren, das Versagen der Beta-Zellen. Überraschenderweise wurden bei *Pax6^{Leca2}* Mäusen keine Änderungen beim Gehalt, der Sekretion oder der Zirkulation von Glukagon festgestellt.

Darüber hinaus zeigten *in vivo* Untersuchungen über die Auswirkungen der Mutation auf den Stoffwechsel ähnliche Ergebnisse wie *in vitro* Versuche, die einen verminderten Gehalt und Sekretion von Insulin offenlegten. Allerdings war diese Verminderung überraschenderweise begleitet von einem verminderten Blutglukosespiegel sowohl nach Fasten als auch bei *ad libitum* Fütterung sowie einer normalen Glukosetoleranz. Dies war in Übereinstimmung mit

einer erhöhten Zunahme der Insulinsensibilität der Leber und einer verminderten hepatischen Glukoseproduktion, insbesondere aufgrund des Verlustes der glukoneogenen Produktion. Darüber hinaus deutete die Erhöhung der Bewegungsaktivität und des Energieverbrauchs eine Wirkung an, die über den Hypothalamus vermittelt wird. Die Expression von PAX6 wurde in verschiedenen Teilen des Hypothalamus gefunden, und eine ChIP-Sequenzierung lieferte mehrere Targets, die durch den mutierten Transkriptionsfaktor unterschiedlich gebunden sind, darunter *Foxo1*, das einen integralen Bestandteil des Insulin-Signalmechanismus darstellt. Dies zeigt, dass Veränderungen der DNA-Bindungseigenschaften der RED Subdomäne von PAX6 in der Lage sind, Veränderungen in den Inselzellen und im Hypothalamus zu induzieren, die Auswirkungen auf den Gesamtmetabolismus haben können.

Zusammengenommen deuten die Daten auf eine bislang unbekannte systemische Funktion von PAX6 hin, die Stoffwechselwege beeinflusst und damit den Organismus vor Hyperglykämie bei Abwesenheit eines Insulinanstiegs schützt.

1. INTRODUCTION

1.1 β -cell identity and function

1.1.1 Islets of Langerhans

Pancreatic insulin secretion is central to postprandial mammalian metabolism. Although the pivotal discovery of islets in the pancreas was made by Paul Langerhans in 1869^[1], it wasn't until von Mering and Minkowski's famous experiment with pancreatic excision that suggested a "secreted hormone" from the gland that caused diabetes in dogs^[2]. Finally, in 1922, works of Banting and Best elucidated that the hormone is in fact secreted from the pancreas and termed it insulin^[3,4], paving the way for its production and helping diabetics all over the world.

The islet of Langerhans typically consists of 5 different cell types, namely; glucagon secreting α -cell, insulin secreting β -cell, somatostatin secreting δ -cell, pancreatic polypeptide secreting PP cell and ghrelin secreting ϵ -cell. In rodents, β -cells occupy about 1% of pancreas, making ~60% of islet population^[5]. Interestingly, islet composition is subject to change within the same species depending on the part of the pancreas^[6]. Nevertheless, β -cells are centrally arranged while the other cell types take a peripheral position in rodents^[7,8], unlike in human islets, wherein, a definitive arrangement although evident, the pattern is highly variable^[9].

1.1.2 Pancreatic development and the endocrine lineage

The development of different islet cell types including β -cells has been widely studied which was made possible by crucial advancement in molecular tools such as gene knockin and knockout models and lineage tracing. With the help of these techniques, developmental steps of β -cells during embryogenesis have been elucidated in great detail. During the early stages of development, the homeodomain transcription factor (TF) PDX1, the trimeric pancreas transcription factor 1 (PTF1) and Sry-related HMG box transcription factor 9 (SOX9) appear in the initial progenitor pool and are expressed in the ventral and dorsal pancreatic buds around embryonic day (E) 9.0^[10-13], thereby committing to a pancreatic fate as endocrine granules become visible^[14]. At this stage around E9.5, called the primary transition^[15], a conglomerate of TFs such as hepatocyte nuclear factor 1b, HNF1B, FOXA2 and HES1 via the Notch pathway activate *Neurog3* (Neurogenin 3) in cells as they emerge from the gut endoderm which sets the endocrinal lineage in motion^[16-19]. Indeed, *Neurog3*-null mice completely lack islet cells and are devoid of early and late endocrinal progenitors expressing *Isl1* (Islet 1), *Pax4* (Paired box

protein 4), *Pax6* (Paired box protein 6) and *Neurod1* (neural differentiation 1) ^[20], making it indispensable for endocrine development. By E12.5, two primordial pancreatic organs (exocrine and endocrine) are formed ^[21] where multipotent pancreatic progenitor cells are present in discrete domains in the epithelial branches ^[22]. Around E14.5, the second transition ushers in, the expression of *Neurog3* peaks and glucagon and insulin positive cells of the endocrinal descent become detectable, albeit at low expression levels ^[16, 20, 23]. Finally, the pancreas continues to expansively branch out until birth.

During the early and late phases of pancreatic development, the aforementioned transcription factors keep a tight control over each developmental step and differentiation into separate cell types. *Neurog3*⁺ endocrine progenitor cells differentiate into different islet cell types as the expressions of islet progenitor genes and its direct targets such as *Neurod1*, *Insm1* (insulinoma associated 1), *Arx* (Aristaless Related Homeobox), *Pax4* and *Pax6* become more apparent ^[23]. Loss of *Neurod1* and *Insm1* in rodents reduces the number of hormone positive cells and negatively affects endocrinal differentiation, thereby accumulating islet progenitors ^[24-26]. Paired box DNA binding domain containing TF PAX6 is another important endocrine marker, loss of which results in prenatal death of pups with massive reduction in β - and δ -cells but a particular effect on α -cells as they are found undetectable ^[27, 28]. Furthermore, studies have shown that mice lacking *Pax4*, which is first noticeable at E9.5, have an increased number of α -cells while a reciprocal effect on β - and δ - cells ^[29]. Interestingly, homozygous knockout of the homeobox TF gene *Arx* has the opposite effect to *Pax4*-null mice wherein, α -cells are dramatically reduced and pups die shortly after birth due to hypoglycemia, suggesting opposing actions in endocrinal specificity ^[30]. Of note, PAX4 seems to interact with NKX2-2, another target of NEUROG3, to exert its functional aspects ^[31]. Hence, these TFs are considered to be key elements in the precise differentiation of precursor cells into hormone expressing islet cells.

By 15.5, expression of somatostatin in δ -cells is evident and expression of *Nkx2-2* becomes restricted to α -, β - and δ -islet cells ^[32]. Downstream of NKX2-2 lies another NK type homeodomain TF NKX6-1 which first appears around E10.5 in NEUROG3⁺ cells and plays a role in providing identity to islet cells, particularly to β -cells ^[23, 33, 34]. The basic leucine zipper TF V-Maf Avian Musculoaponeurotic Fibrosarcoma Oncogene Homolog A and B, MAF A and MAF B are placed downstream of *Nkx6-1* and appear at E13.5 and E12.5, respectively ^[23, 35, 36]. *Mafa* exclusively marks insulin positive cells and is expressed in prenatal as well as mature β -cells in adult islets, maintaining identity and secretory function ^[35, 37, 38]. *Mafb* on the other hand is transiently present in both α - and β -cells at embryonic stages but becomes restricted to

α -cells in the adult [36, 39]. Interestingly, although the mRNA of all islet hormones are expressed early on during embryonic development [40], however, protein expressions are detected much later, especially ghrelin and pancreatic polypeptide (PP) that appear only at E15.5 and at birth [41, 42], respectively. The Figure 1.1 displays a schematic diagram of TFs involved in pancreatic development.

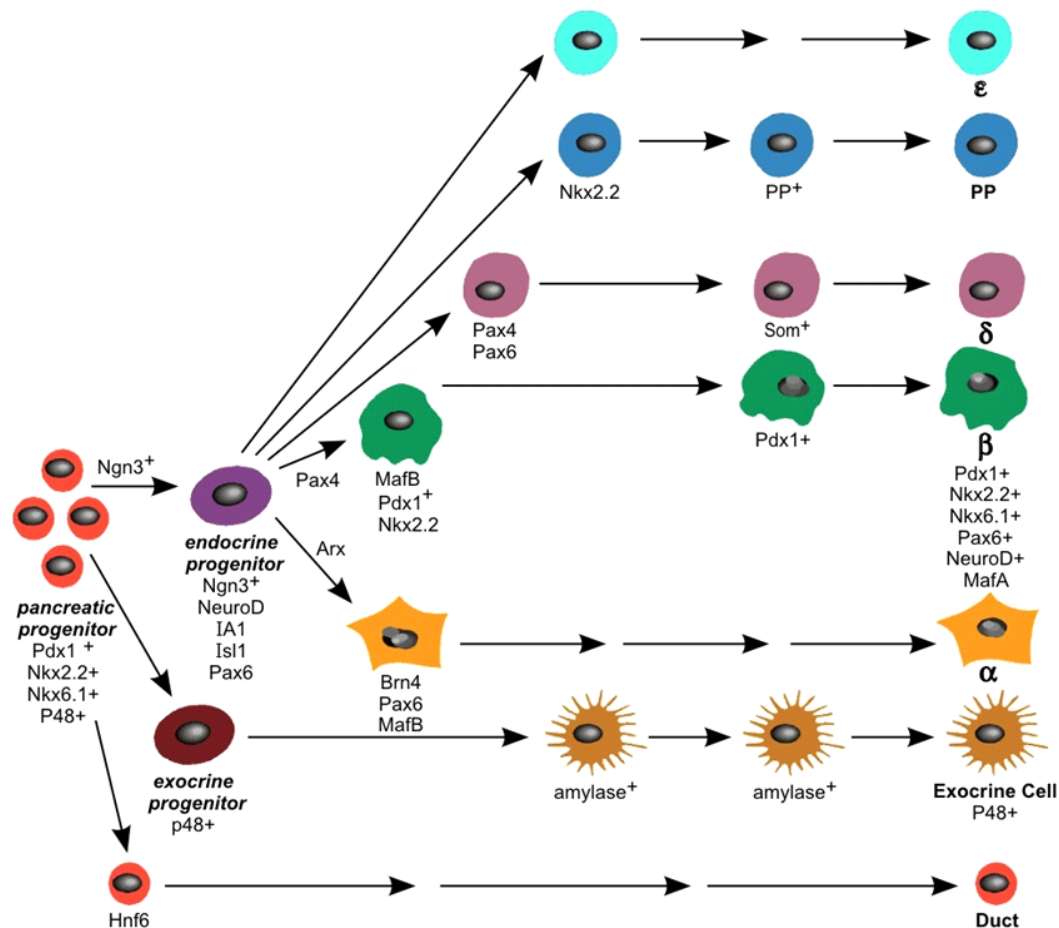


Figure 1.1: Transcription factors involved in islet cell development and maturation

Development of endocrinal lineage and the transcription factors involved at every step. Pancreatic progenitors expressing *Neurog3* (*Ngn3*) demarcate the difference in endocrine and exocrine lineages. Arrows depict the direction of differentiation. Details are provided in the text. Adapted and edited from [43].

1.1.3 Insulin secretory mechanism

1.1.3.1 Glucose stimulated insulin secretion

Insulin positive cells can be first detected at E9.5, simultaneously when glucagon is over 1000 fold higher [15]. This status quickly changes as glucagon positive cells become less apparent, possibly due to competitive inhibition of PAX6 binding to the glucagon promoter by NKX6-1 which selectively promotes transcription of the insulin gene [44, 45]. The increase in amounts of detectable insulin itself is much higher than the increase in the number of insulin positive cells

between E12-20 in rodents ^[14, 46]. As the islet matures, the number of β -cells increases drastically and in the adult they mount up to 55% of the islet cells in humans and 70-80% in rodents, while α -cells take up to 35% and δ -cells 11% of a total human islet as compared to 19% and 6%, respectively in rodents ^[47]. Interestingly, the number of islets varies across species but the typical size of islets remain confined within the range of 100-200 μm ^[48] suggesting a functional optimization. Insulin is the principle hormone and marker for a fully functional and mature β -cell and in turn its release by the cell in response to glucose, otherwise termed as glucose stimulated insulin secretion (GSIS), the most basic of functions. Prenatal, *Neurog3* expressing β -cells have poor response to glucose in rodents ^[49] and lack second phase insulin secretion during gestation in humans ^[50]. However, this process substantially improves postnatal as the β -cells acquire functional maturity ^[50] and continue to do so over months after birth ^[51]. Moreover, as the islets begin to assemble in definitive structures, the β -cells become more functionally competent ^[52]. Importantly, weaning itself acts as a strong trigger for β -cell maturation as several key cell-cycle genes take into effect and induce proliferation ^[53].

Glucose transporter (GLUT1, encoded by *Slc2a1* in humans and GLUT2, encoded by *Slc2a2* in rodents) ^[54] in adult β -cells allows the entry of glucose into the cell. Glucokinase (GCK), the first enzyme in the glycolytic pathway, but not GLUT2, is termed as the “glucose sensor” as it initiates glucose metabolism ^[54, 55]. The end product of glycolysis is pyruvate (pyruvic acid) that enters the mitochondria from the cytosol via pyruvate transporters, two of which were recently characterized in humans and other species ^[56, 57]. Pyruvate then enters the tricarboxylic acid (TCA) cycle in turn switching on the oxidative phosphorylation within the lumen of the mitochondria which ultimately results in the generation of ATP ^[58]. As the ATP/ADP ratio increases in the cytosol, ATP sensitive potassium channels (K_{ATP}) close ^[59, 60], leading to depolarization of cell membrane ^[61]. Upon firing of action potential, voltage-gated calcium (Ca^{2+}) channels open. Additionally, Ca^{2+} is secreted by intracellular organelles like golgi via inositol 1,4,5-trisphosphate (IP3) ^[62], endoplasmic reticulum (ER) ^[63] and others ^[64], which together increase Ca^{2+} concentrations. At this juncture, insulin vesicles from the readily releasable pool (RRP) ^[65] adhere to the cell membrane and secrete insulin. These steps constitute what is considered as the canonical pathway of insulin secretion.

1.1.3.2 Incretin effects on insulin secretion

In addition to the insulin stimulation by glucose, various other insulin secretagogues exist in parallel. Of these, hormones such as glucagon like peptide-1 (GLP-1) and glucose-dependent insulinotropic peptide (GIP) are of particular relevance. As the food is ingested and leads its

way into the gut, GLP-1 and GIP are secreted from the L and K intestinal cells, respectively. These incretins act via their G-coupled receptors (GPCRs) GLP-1R and GIPR, placed on the cellular membrane of β -cells [66-68]. Furthermore, these receptors in turn stimulate adenylyl cyclase [69] which increases the concentrations of the secondary messenger cyclic adenosine monophosphate (cAMP) and in turn activate protein kinase A (PKA) [70] and exchange protein activated by cAMP2 (EPAC2) [71]. Ultimately, this increases cellular Ca^{2+} and intensifies the release of insulin exocytosis [66]. In the context of β -cell insulin secretion, GLP-1 and GIP produce very similar physiological effects via similar downstream effectors [72]. Importantly, glucose not only stimulates the release of incretins from the gut but the effects exerted by incretins on β -cells essentially require glucose in humans and rodents, *in vivo* and *in vitro* [72-75]. Hence, the influence of incretin action is to merely potentiate the release of insulin and not to initiate it. Interestingly, loss of the Kir6.2 subunit (encoded by *Kcnj11*) of the K_{ATP} channel in β -cells still allows for an effect mediated by GLP-1 but not GIP, suggesting possible differences in downstream targets [76]. Of note, the canonical incretin pathway via intestinal GLP-1 was recently reconsidered and islet derived GLP-1 was shown to have higher importance in glucose metabolism [77]. Additionally, several other sources of insulin secretagogues are present such as free fatty acids which act via the free fatty acid receptor 1 (GPR40/FFAR1) [78] including acetylcholine via muscarinic M3 receptors and cholecystokinin (CCK) via CCK1R to increase intracellular Ca^{2+} [79].

The intra-islet hormone glucagon also stimulates insulin secretion from the β -cells via glucagon receptor (GCGR) by activating the cAMP pathway [80, 81]. On the other hand, somatostatin secreted by the δ -cells acts via GPCR to inhibit both insulin and glucagon secretion [82, 83]. Furthermore, epinephrine and norepinephrine recognize adrenergic receptors coupled to G_{ia} (G protein subunit) which decrease cAMP levels by inhibiting adenylyl cyclase [84, 85]. Hence, K_{ATP} channels are opened and in turn hyperpolarize the cell membrane of β -cells and inhibit insulin secretion, while in the postprandial state, norepinephrine stimulates glucagon and somatostatin [86-88]. These together contribute to a response in the β -cells, covering pre- and postprandial states and display physiological relevance as compared to a response produced through glucose administration via intravenous (iv) or intraperitoneal (ip) injections. Figure 1.2 depicts insulin secretion from β -cells.

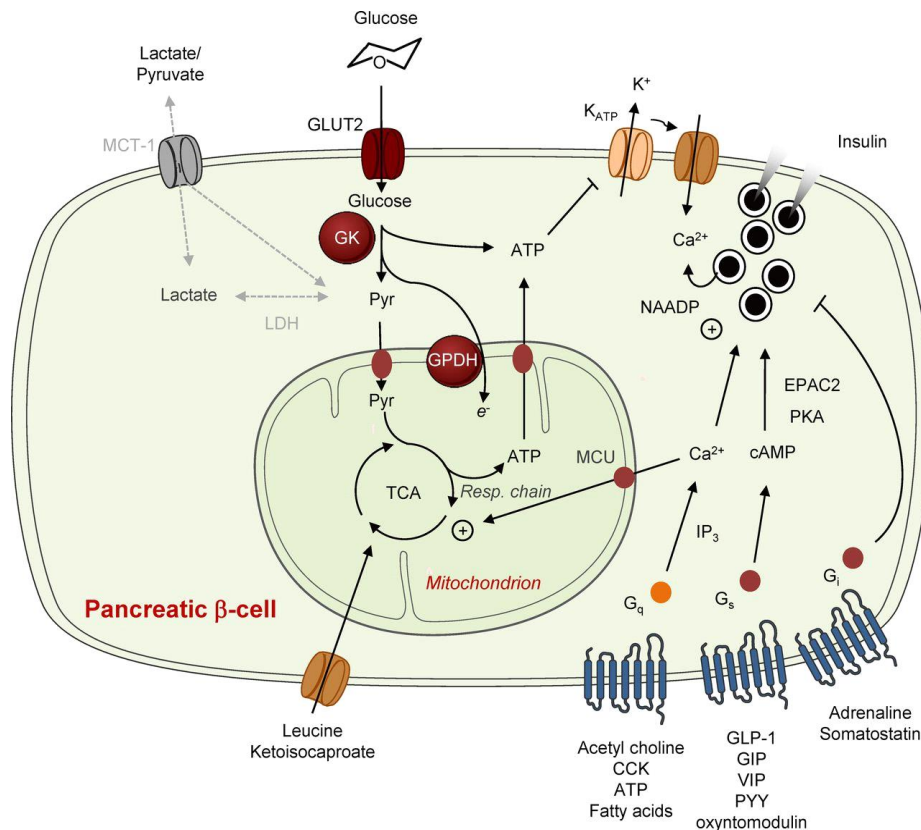


Figure 1.2: Insulin secretion from the pancreatic β -cell

The figure depicts effect of glucose, incretin and other stimulants leading to changes in membrane polarization and subsequently opening or closure of K_{ATP} channels, which affects intracellular Ca^{2+} concentrations and determines commencement or halt of β -cell insulin secretion. Details are provided in the text. GK, Glucokinase (GCK); Pyr, Pyruvate; NAADP, LDH, lactate dehydrogenase; Nicotinic acid adenine dinucleotide phosphate; MCT-1, Monocarboxylate transporter 1; MCU, Mitochondrial calcium uniporter. Adapted from [64].

Another important aspect of insulin secretion is that its occurrence follows a biphasic fashion with a short and marked first and a low sustained second phase *in vivo* and *in vitro* [89, 90]. In addition to the biphasic nature, β -cell insulin secretion also possess a pulsatile feature, occurring at distinct time periods in rodents, monkeys, dogs and humans although the time periods themselves differ among the species [89, 91]. Fascinatingly, glucagon, insulin and even somatostatin follow a periodic pulsatile nature of secretion [91-93]. These characteristics, together, contribute to the complex secretory mechanism of islet cells.

1.1.4 Postnatal β -cell identity and regulation

A number of TFs that are discussed in section 1.1.2 although first appear during development, a number of them are also involved in providing β -cells functional and morphological identity postnatally and are responsible for transcriptional regulation of the insulin gene of which two isoforms *Ins1* and *Ins2*, exist in rodents and a single *INS* gene in human [94, 95]. In this regard, endocrinal markers PAX6 and NEUROD1 and mature β -cell markers MAFA, NKX6-1, RFX3,

RFX6 and PDX1 among others have all been reported to regulate insulin gene expression [94, 95] and play an important role either as functional regulators or maintaining maturity. Indeed, *Neurod1*-null mice die shortly after birth with poorly differentiated islet cells and dramatic loss of β -cells [24]. In adult β -cell specific knockouts of *Neurod1*, islets display blunted GSIS and increased expressions of disallowed genes [96] such as lactate dehydrogenase A (*Ldha*) as well as that of genes conferring glycolytic properties, all of which point at reversion to an immature state [97]. Likewise, PAX6 is a marker for all endocrine cells and therefore *Pax6*-null mice have dramatically reduced α -, β - as well as δ -cells and new born homozygous mice die within minutes after birth [27]. Adult whole body [98] and β -cell specific [99, 100] conditional knockouts of *Pax6* rendered the mice expectedly hyperglycemic with dramatic loss of all β -cells along with a trans-differentiation of β -cells to ghrelin positive ϵ -cells [101]. The early pancreatic progenitor PDX1 is confined specifically to β -cells postnatally [102] and although it is not required for their postnatal formation, PDX1 is essential for maturation of functional β -cell [10, 103]. Interestingly, PDX1 has also been found to repress α -cell identity in order to preferentially maintain the mature characteristics and function of β -cells [104]. Similarly, it was reported that over expression of NKX6-1 caused suppression of glucagon mRNA expression [44] although no difference in the same was reported for the *Nkx6-1* adult β -cell knockout mouse model [105]. Nevertheless, NKX6-1 has been shown to promote postnatal β -cell proliferation [106] and control insulin secretion by regulating glucose import into the cell [105]. Another important TF for postnatal β -cell proliferation is MAFA [107]. It is indeed further required for maintenance of β -cells and *Mafa* knockout mice show a diabetic phenotype and the downregulation of β -cell markers [38]. In addition, a small population of cells seems to transdifferentiate into α -cells with a higher expression of *Mafb* [38], which itself is required for β -cell maturation [36]. Recently, the TFs regulatory factor X (RFX) -3 and -6 have been further characterized for their role in early endocrinal development, downstream of *Neurog3* [108, 109]. Additionally, RFX3 directly controls *Gck* expression by promoter binding [110] while *Rfx6*-null mice fail to produce any islet cells except for PP secreting cells [111]. Thus, careful regulation of TFs ensure the maintenance of β -cell identity and functional maturity while simultaneously inhibiting differentiation or neonatal markers, the so called “disallowed” genes and markers for α -, δ - and ϵ -cells [97, 101, 104, 112].

1.1.5 Type 2 Diabetes Mellitus

1.1.5.1 Overview

Diabetes Mellitus (DM) is the most prevalent metabolic disease to date afflicting over 380 million people worldwide, 45% of whom remain undiagnosed as of 2014 [113]. This is further

expected to increase up to 600 million, especially in the developing countries ^[113]. Broadly, two forms of diabetes mellitus have been well characterized depending on the source of chronic hyperglycemia, which is the hallmark of the disease. Type 1 diabetes mellitus (T1DM) is primarily an autoimmune disease wherein T-cell mediated immune response kills β -cells which is finally responsible for a lifelong dependency on exogenous insulin. This form of diabetes has been attributed to viruses but has largely unknown causes and accounts for about 10% ^[114] of the diabetic population. Type 2 diabetes mellitus (T2DM) on the other hand, is essentially characterized by hyperglycemia due to either dysfunctional β -cells, peripheral insulin resistance or both, accounting for the majority of diabetics worldwide. Risk factors include a range of known genetic predispositions including lifestyle, family history, age and even ethnicity ^[115]. Furthermore, DM also comprises of monogenic forms such as neonatal diabetes and maturity onset diabetes of the young (MODY), prevalence of which is rather low, between 1-4% ^[116]. Some of the aforementioned TFs conferring β -cell functional identity such as PDX1, RFX6 and NEUROD1 among others have been reported as causes of monogenic diabetes ^[114].

1.1.5.2 β -cell dysfunction in T2DM

Although defective insulin secretion in T2DM was already reported decades earlier, the β -cell as such came into focus only in the late 1980s ^[117]. The biphasic insulin secretion has been previously shown to be perturbed in T2DM patients, with a marked reduction in first phase and low second phase insulin secretion ^[118]. Additionally, pulsatile nature of insulin secretion, which incidentally has a higher glucose clearance potential than continuous secretion ^[119] was found to be abnormal in T2DM ^[120]. Moreover, changes in oscillatory insulin secretion ^[121] have been implicated in the pathogenesis of T2DM. This implies that the insulin secretory capacity of β -cells seems to play an important role in the manifestation of T2DM.

Several studies have shown the impact of changing transcriptional regulations within the β -cell that initiate a reversion to a dedifferentiated state and/or drive trans-differentiation into other cell types as elegantly exemplified in β -cell specific *Foxo1* knockout study ^[122]. Even though similar findings in human islets have been published ^[123, 124], results on the contrary exist ^[125-127] and therefore considering such a mechanism as a potential consequence in T2DM patients, remains to be a matter of much debate ^[128]. Moreover, hyperglycemia itself seems to be a trigger that can elicit changes in β -cell identity and function ^[129, 130], which may even include trans-differentiation from β - to α -cell ^[130]. Although, genetic ablation and mutations regarding TFs such as NKX6-1 ^[105], NEUROD1 ^[97] and PAX6 ^[131, 132] might display reduced β -cell markers and a decrease in regulation of insulin gene expression, the phenotypes are always

accompanied by a distorted insulin secretion. Incidentally, evidence collected over decades suggests that lower insulin content in the β -cell can be, to some extent, compensated for and therefore it is conceivable that reduced amount of insulin in the β -cell is secondary to a secretory failure, at least in the initial phases of T2DM [114]. However, mice displaying reduced efficiency to convert proinsulin into insulin by prohormone convertase 1/3 and 2 (PCSK1 and PCSK2) [133, 134] are still likely to show a diabetic phenotype due to loss of mature insulin rather than a defective insulin secretion. Nonetheless, by the time fasting hyperglycemia is detected, about 50% of β -cell function is reduced thereby suggesting that smaller differences in insulin secretion may contribute at the onset of glucose intolerance [135].

1.2 Central and peripheral metabolic pathways

β -cell function underlines an important aspect in the initiation and progression of T2DM. Peripheral insulin sensitivity is another measure to accurately follow the development of a diabetic phenotype. Initially, it is rather common to find hyperinsulinemia accompanied with hyperglycemia, as β -cells cope with the increased demands due insulin resistance. Finally, as the β -cells exhaust themselves and sustained hyperglycemia affects their survival, full scale diabetes comes into effect. Therefore, it is highly pertinent to understand the efficacy with which peripheral organs respond to insulin and the defects associated with it.

1.2.1 Islet-liver axis

The human brain has immense energy demands and requires up to 5.6 g of glucose per 100 g tissue per minute [136]. Therefore, it is imperative for the body to maintain a constant flow of glucose in the blood within a narrow physiological range. Although other sources of endogenous glucose production are present, the liver remains to be the organ contributing the most [137] and it does so via two distinct mechanisms, glycogenolysis and gluconeogenesis which ultimately result in increased glucose output. A graphical overview is displayed in Figure 1.3. As discussed earlier, the β -cell secretes insulin in response to glucose, thereafter other incretins and nutrients during the digestive process. Insulin stimulates peripheral organs such as fat and muscle which contain GLUT4 to take up glucose [138]. In the liver, glucose is either stored away as glycogen or enters the glycolytic pathway and is eventually converted into pyruvate. Upon entering the mitochondria, pyruvate drives the TCA cycle, intermediates of which either produce ATP via oxidative phosphorylation or are subsequently stored away as fats. In humans, up to one third of ingested glucose from a mixed meal is taken up by the liver and stored as glycogen and this exact mechanism has been widely reported to be distorted in T2DM [139]. As the glucose levels fall after postprandial period, insulin levels drop in the

absence of external stimuli. Concomitantly, glucagon levels slowly rise with the decrease of the inhibitory effects of insulin on α -cells^[140]. Glucagon released into the blood stream reaches the liver where it binds to the glucagon receptor (GCGR) which is coupled with G protein $G_{\alpha s}$ ^[141] and consequently activates adenylate cyclase, increasing cAMP levels and the subsequent activation of PKA^[142]. Activated PKA then phosphorylates glycogen phosphorylase that in turn phosphorylates and cleaves glycogen into glucose-1-phosphate which is first converted to glucose-6-phosphate by phosphoglucomutase and finally to glucose by the enzyme glucose-6-phosphatase (G6PC). Simultaneously, glucagon inhibits the action of glycogen synthase by the means of phosphorylation of the enzyme and halts the storage of glucose as glycogen^[143].

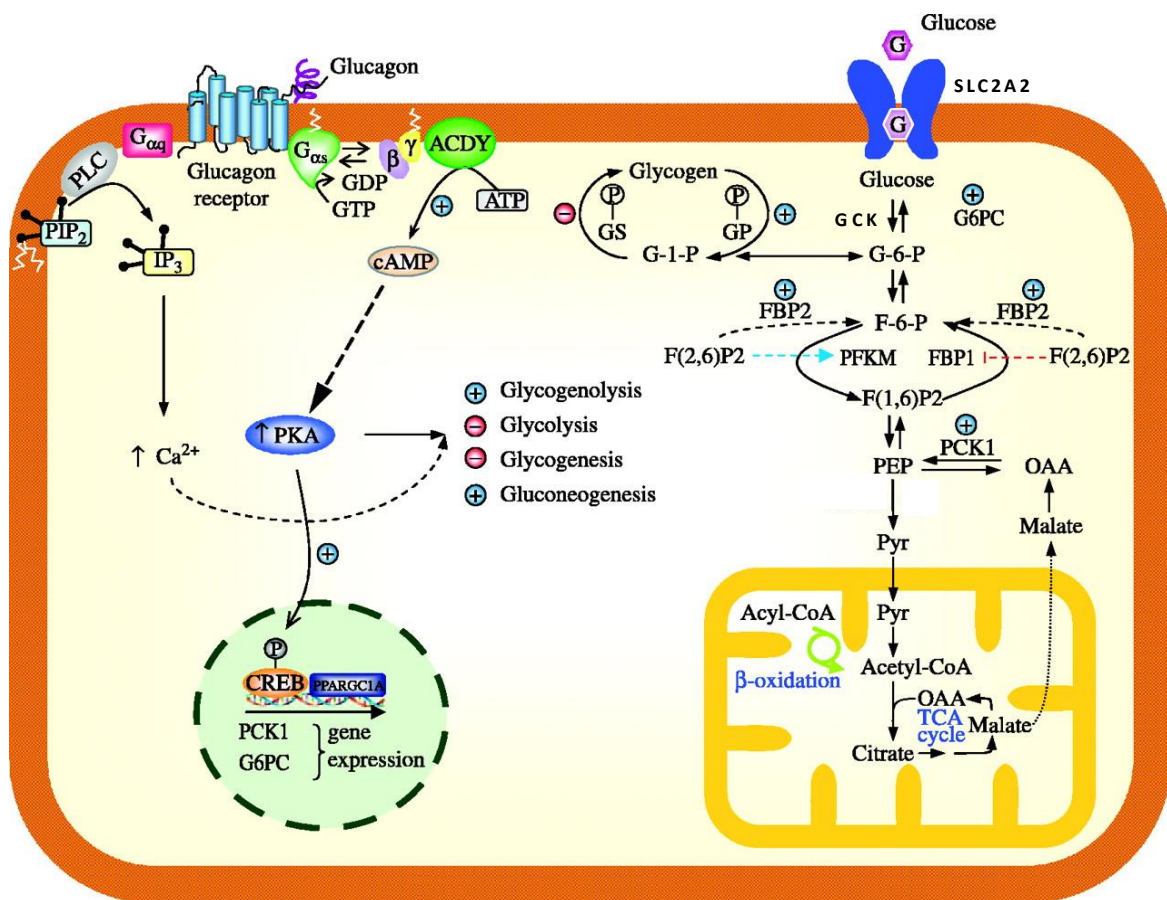


Figure 1.3: Fasting liver metabolism

Glucagon binds to the glucagon receptor and fires the signaling cascade shown here in positively (+) or negatively (–) regulations in the multiple steps of the hepatic glucose production. Details are provided in the text. ADCY, Adenylate cyclase; CREB, cAMP response element binding; F(1,6)P2, fructose-1,6-bisphosphate; F(2,6)P2, fructose-2,6-bisphosphate; F-6-P, fructose 6-phosphate; FBP1, fructose-1,6-bisphosphatase; FBP2, fructose-2,6-bisphosphatase; G-1-P; GP, glycogen phosphorylase; GS, glycogen synthase; PFKM, phosphofruktokinase-1; PPARGC1A, peroxisome proliferators-activated receptor- γ coactivator-1; PLC, phospholipase C; Pyr, pyruvate. Dashed lines: red, inhibition; blue, stimulation. Adapted and edited from^[142].

The other wing of hepatic glucose production (HGP) is gluconeogenesis, which utilizes non-carbohydrate substrates such as free fatty acids, glycerol and amino acids to produce glucose. Whereas fatty acids are essentially oxidized into acetyl CoA only to provide two carbon atoms to the TCA cycle, glycerol and certain amino acids can be directly used for glucose synthesis. This pathway becomes predominant in prolonged fasting and poorly controlled diabetes wherein sustained hyperglycemia and lipolysis overloads the liver with gluconeogenic substrates further perpetuating hyperglycemia ^[144]. Under normal fasting conditions, oxaloacetate (OAA) is formed from pyruvate by the enzyme pyruvate carboxylase (PCX) which then gets reduced to malate to enter the cytosol. Malate is re-oxidized to OAA and converted into phosphoenolpyruvate (PEP) by phosphoenolpyruvate carboxykinase (PEPCK). The next steps involve reactions of reverse glycolysis although including two other enzymes, fructose-1,6-bisphosphatase (FBP1) and G6PC, which is the rate limiting step in the process. Indeed, *G6pc* knockout mice display significantly reduced blood glucose levels and an accumulation of glycogen in the liver ^[145, 146]. Interestingly, knockdown of PEPCK (*Pck1*) in the liver also results in lower blood glucose levels as well as improved glucose clearance without any increase in glycogen storage but rather a decrease, possibly due to a compensatory increase in glycogenolysis ^[147].

The molecular signals following fed and fasted state require maintenance of a balance. Typically, insulin secretion directly inhibits glucagon secretion ^[140], while simultaneously stimulating peripheral organs to take up glucose. Likewise, glucose acts on the α -cell to inhibit glucagon secretion ^[148] and in poorly controlled diabetics, this inhibitory effect is lost causing hyperglucagonemia ^[149] which extenuates the extent of hyperglycemia. Paradoxically, higher glucose levels itself can even stimulate glucagon secretion ^[150]. On the other hand, loss of counter-regulatory mechanism to increase glucose during hypoglycemia seems to be a major concern for insulin treated patients ^[151]. Nevertheless, development of insulin resistance remains to be one of the major reasons for the incidence of T2DM. Therefore, it is essential to understand the signaling pathways of this hormone, especially in relation to HGP.

Insulin secreted by the β -cells binds to insulin receptors on hepatocytes which initiates signaling cascade that results in phosphorylation of insulin receptor substrates (IRS) and switching on of the phosphatidylinositol 3-kinase (PI3K)–AKT pathway ^[152]. Phosphorylated AKT in turn phosphorylates forkhead box O1 (FOXO1), allowing its nuclear exclusion ^[153, 154]. FOXO1 and hepatocyte nuclear factor-4 α (HNF4A) along with transcriptional coactivator peroxisome proliferator-activated receptor γ coactivator-1 α (PGC-1A, encoded by *Pparg1a*),

bind to promoters of *G6pc* and *Pck1* to stimulate gluconeogenesis [155-157]. This interaction under the influence of insulin, in a direct or indirect manner, is abolished and therefore gluconeogenesis is arrested [155]. Consequently, researchers have manipulated critical factors in this pathway to address the possibility of enhancing insulin action. In this regard, liver specific knockout of *Foxo1* in mice shows reduction in blood glucose levels and HGP via blockage of PGC-1A mediated increases in *G6pc* and *Pck1* [158]. Likewise, *Foxo1* deletion in *Akt1* and *Akt2* knockout mice rescues hyperglycemia, demonstrating that the role of AKT in this pathway is to restrict FOXO1 mediated transcriptional activity [159].

During fasting periods, gluconeogenic substrates can arise from within the liver via mitochondrial β -oxidation that breaks down fatty acids to produce acetyl CoA. In presence of low insulin or low carbohydrate diet, sufficient energy production takes place via gluconeogenesis and hence acetyl CoA is diverted towards formation of ketone bodies such as acetoacetate and β -hydroxybutyrate. These ketone bodies are then released into the blood stream to be taken up by several tissues. This is of particular importance because ketone bodies can cross the blood brain barrier and hence present as an alternative energy source for the brain during prolonged starvation periods when glycogen storages have been depleted. Central to this pathway are the peroxisome proliferator-activated receptors (PPARs) which regulate fatty acid metabolism. PPARA is the most abundant of PPARs in the liver and is therefore of particular relevance to HGP [160]. PPARA, in combination with PGC-1A in the liver, promotes insulin resistance by increasing gluconeogenic output and inducing high fat diet induced obesity [161, 162]. Importantly, fibroblast growth factor 21 (FGF21), a liver derived hormone, is regulated by PPARA [163-166]. FGF21 is induced during prolonged fasting periods and it regulates carbohydrate and lipid metabolism by activating PGC-1A [167]. In addition, circulating FGF21 in humans increases after 7 days of fasting and glucagon secretion reduces in parallel, possibly due to inhibition by FGF21 exemplifying a balancing feature in liver where further induction of gluconeogenesis is required because HGP via glycogenolysis diminishes [164, 166, 167]. On the other hand, subcutaneous administration of FGF21 reduced circulating triglycerides and plasma glucose levels in *db/db* and *ob/ob* mice that lack leptin signaling, thereby suggesting increased insulin sensitivity and glucose uptake [166, 168]. Therefore, the data collectively points to an important role of PPARA and FGF21 is maintenance of adaptive fasting-response [169].

1.2.2 Hypothalamic control of metabolism

Although involvement of brain in metabolic control and energy homeostasis was established, much has been learnt about molecular pathways in the hypothalamus regulating satiety, food intake and glycemia in the last couple of decades. Many nutrients, hormones and other biochemical signals are involved in the cross talk between hypothalamus and the peripheral organs. In particular, leptin and insulin have emerged as important hormones in mediating this communication. In 1979, a study showed that intracerebroventricular infusion of insulin reduced food intake and body weight in primates ^[170]. Similarly, intrahypothalamic infusion of insulin in rats resulted in decreased body weight and increased activity suggesting alterations in energy expenditure ^[171]. Moreover, infusion of insulin in third cerebral ventricle reduced HGP, possibly via the K_{ATP} channels ^[172] and antagonism of the same pathway blocked this effect resulting in hepatic insulin resistance ^[173, 174]. Conversely, attenuating insulin signaling in the brain caused increase in body weight ^[175] and damping it in the whole body including brain caused severe hyperglycemia, lipomatrophy and hypoleptinemia ^[176]. In the same study, leptin therapy restored normoglycemia suggesting that central control of insulin signaling modulates glucose and lipid metabolism ^[176]. Leptin is a white adipose tissue (WAT) derived hormone, which is released in proportion to the amount of fat mass ^[177, 178]. Leptin binding to its receptors in the hypothalamus not only activates the JAK/STAT pathway but also the PI3K-AKT pathway, which eventually regulates FOXO1 and its downstream effects ^[179, 180]. Hence, this node in the pathway presents itself as a synergistic point of action for leptin and insulin ^[181].

These pathways are particularly relevant in pro-opiomelanocortin (POMC) and agouti-related peptide (AGRP) expressing neurons in the arcuate nucleus region of the hypothalamus. Orexigenic (appetite stimulating) AGRP neurons and anorexigenic (appetite suppressing) POMC neurons are involved in food intake. Whereas AGRP neurons are directly involved in the feeding circuitry, POMC neurons require the melanocortin pathway to exert its effects ^[182]. Leptin and insulin induce effects on POMC that is opposite to those in AGRP neurons. Both hormones regulate FOXO1 expression which in turn regulates transcriptional activation of *Agrp* while repression of *Pomc* for which it competes with STAT3 that produces opposite effects to FOXO1 ^[183, 184]. Furthermore, increased *Foxo1* activity in the hypothalamus increased food intake and body weight while attenuation of the same produced opposite effects ^[183, 185]. Moreover, insulin receptor knockout in either of the two neuronal subtypes did not produce an overt glycemic effect but increased HGP in mice with decreased insulin signaling

in AGRP neurons ^[186]. Therefore, these data suggest that insulin acting via the AKT pathway and leptin via the JAK/STAT pathway reduces expression of FOXO1 to inhibit *Agrp* expression and promote that of *Pomc* ^[183, 184, 187]. Thus, central control of hormone regulation ultimately affects energy expenditure and peripheral glycemia. These pathways are summarized in figure 1.4.

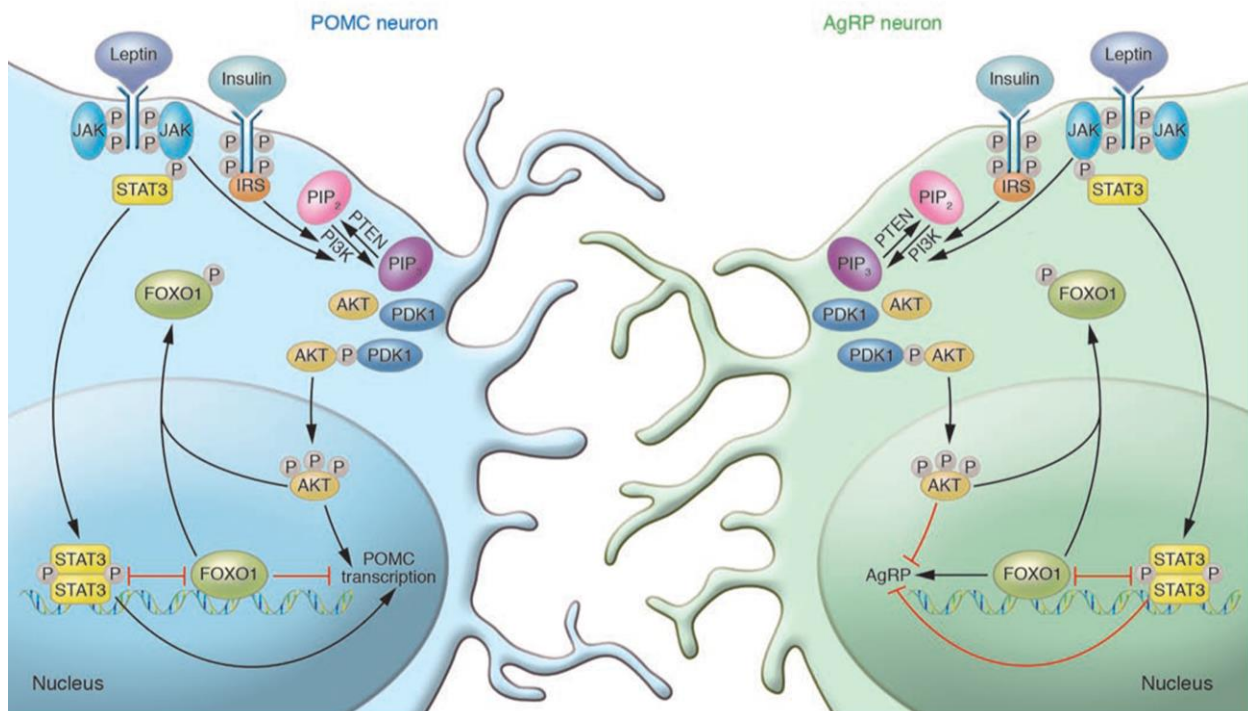


Figure 1.4: Regulation of POMC and AGRP neurons

Image depicts different pathways activated by insulin and leptin in POMC and AGRP neurons. Insulin binds to its receptor and initiates its signaling cascade wherein PI3K phosphorylates phosphatidylinositol-4,5-bisphosphate (PIP₂) to generate PIP₃, which can be antagonized by phosphatase and tensin homolog (PTEN). Phosphoinositide-dependent protein kinase 1 (PDK1, PDPK1) phosphorylates AKT that upon entering the nucleus, phosphorylates FOXO1, causing its nuclear exclusion and thereby inhibiting the transcription of AGRP on one hand and revealing its inhibition of POMC transcription on the other. Similarly, Leptin activates POMC transcription by recruiting STAT3 while inhibiting that of AGRP. Further details are provided in the text. Adapted from ^[179].

1.3 PAX family of transcription factors

1.3.1 PAX family

Paired box (PAX) family of TFs contains with the so-called paired domain (PD), a highly conserved DNA-binding domain, which consists of two helix-turn-helix (HTH) resembling subdomains, PAI and RED. In addition, PAX proteins contain a Proline-Serine-Threonine (PST) rich transactivation domain at the C-terminal end. There are a total of 9 TFs in this family that have been identified in the mammals PAX1-PAX9 ^[188]. They are divided into four groups

according to the presence or absence of both or either of an additional DNA-binding domain; homeodomain (HD) and an octapeptide region ^[189] (Figure 1.5).

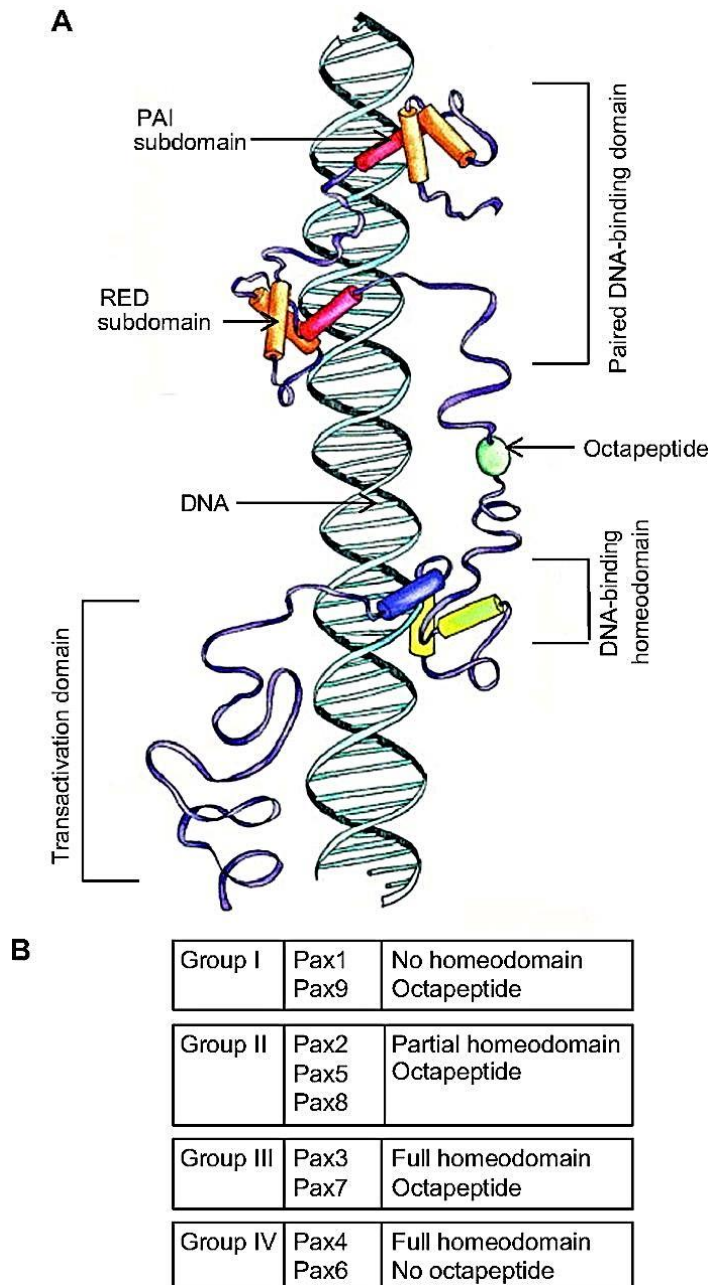


Figure 1.5: PAX DNA binding domains.

PAX proteins are divided into groups according to the presence or absence of DNA binding domains. Details are provided in the text. Adapted from ^[189].

PAX TFs cover a whole spectrum of functions, including developmental of several parts of the central nervous system (CNS) and endocrinal organs such as the thyroid and pancreatic islets

among others ^[188]. Moreover, PAX proteins are also found to be involved in maintenance of differentiated or progenitor cell pools in the adult and some may even play a role in tissue regeneration ^[190]. In support of the particular importance of the PAX family of TFs, studies have demonstrated that most homozygous *Pax(1-9)*-null models either display prenatal or neonatal death ^[191]. Furthermore, some members of the PAX family are also used as markers for tumor growth, illustrating the potential of these TFs in proliferation ^[192].

Although PAX2 and PAX8 have been identified in either developing or adult pancreas ^[191], PAX4 and PAX6 are of particular importance as discussed in section 1.1. PAX4 is required for cells involved in the endocrinal lineage as well as subsequent differentiation into β - and δ -cells ^[29]. Its expression is thereafter restricted to β -cells and decreases with age ^[193]. PAX6 on the other hand is important for the late endocrine lineage and is further required for maintenance of all islet cells in the adult ^[28, 98], although decrease in PAX6 expression favors trans-differentiation of α - and β -cells to ghrelin positive ϵ -cells ^[101]. Therefore, PAX6 emerges as the key PAX TF in function and regulation of the adult islet cell population.

1.3.2 Paired box protein 6

1.3.2.1 PAX6: Master regulator

Paired box protein 6 (PAX6) is a 422 amino acid long TF with pleiotropic functions contributing to and directing development in CNS, eye, olfactory lobes, and endocrine pancreas ^[188, 194]. In fact, PAX6 alone can drive the formation of a whole organ in *Drosophila*, thereby earning its title of ‘master regulator’ ^[188]. PAX6 consists of PAI and RED DNA binding subdomains ^[195] on the N-terminal followed by a linker region and DNA binding HD ^[196], thereby belonging to group IV of the PAX family of TFs and a transactivation PST domain towards the C-terminal end ^[197] as shown in figure 1.5 above. Importantly, an alternative splice variant exists which causes a 14 bp insertion at the N-terminus producing a PAX6 (5a) and binds to a site different from that of the canonical PAX6 ^[198, 199]. The nucleotide sequence of murine *Pax6* shares over 92% homology with the human ortholog *PAX6* and an identical amino acid sequence within the PD and HD ^[200].

1.3.2.2 PAX6 and metabolism

PAX6 expression in murine embryos first appears as early as E9.0 during pancreatic development in discrete cells and later becomes restricted to hormone positive cells, thus PAX6 is a late endocrinal marker ^[27, 28]. Over the past two decades several mouse models and human patients have been studied to elucidate functional aspects of PAX6 driven through separate

DNA binding domains. In this regard, first reports were that of the naturally occurring *Pax6*^{Sey} (*small eye*)^[201] and the ethylnitrosourea (ENU)-generated *Pax6*^{Sey-Neu}^[28] mouse model which lacks both HD and PST or only the PST, respectively. As the name suggests, the mutation is characterized by small eyes and iris hypoplasia^[201-203] with craniofacial abnormalities in rodents, aniridia and Peter's anomaly in humans^[204] and the failure to develop eye in *Drosophila* (*eyeless*)^[205]. Due to the homology between the human and rodent *Pax6* gene, the data collectively points at an evolutionary conserved TF that possess one of most fundamental functionalities present across species^[205, 206].

Homozygous *small eye* mutant mice die at birth and can be noticeably distinguished from heterozygous and wildtype littermates due to the lack of eyes and a shortened snout^[201]. Moreover, these mice display a decrease in all islet cell types^[28] thereby suggesting abnormality in development of the pancreas. Lineage tracing experiments in mice have revealed that in the adult mice, *Pax6* is important for maintenance of α - and β - but not that of δ - and PP cells in the adult^[98, 101]. Inactivating *Pax6* during development only in the endocrine cells resulted in successful birth of pups, which died within a few days due to overt diabetes^[207]. Similarly, conditional knockout of *Pax6* in islets or specifically in β -cells produced a diabetic phenotype with profound changes in islet content^[98-100]. Similar phenotypes were observed with *Pax6*^{Aey18}, a mouse model harboring a point mutation in the exon 6 encoding for the paired domain that results in greatly reduced islet cell number although the authors also demonstrated a retention of PAX6 in the cytoplasm thereby suggesting nuclear localization may be driven via exon 6^[208]. Interestingly, *Pax6*^{14Neu} and *Pax6*^{4Neu} mutants display completely different phenotypes although they have adjacent point mutations, F272I and S273P respectively, in the HD^[208]. Whereas the homozygous *Pax6*^{4Neu} mutants with S273P are embryonic lethal, homozygous *Pax6*^{14Neu} mutants with F272I mutation are viable without any overt pancreatic phenotype^[208]. Figure 1.6 summarizes the PAX6 mutants discussed above.

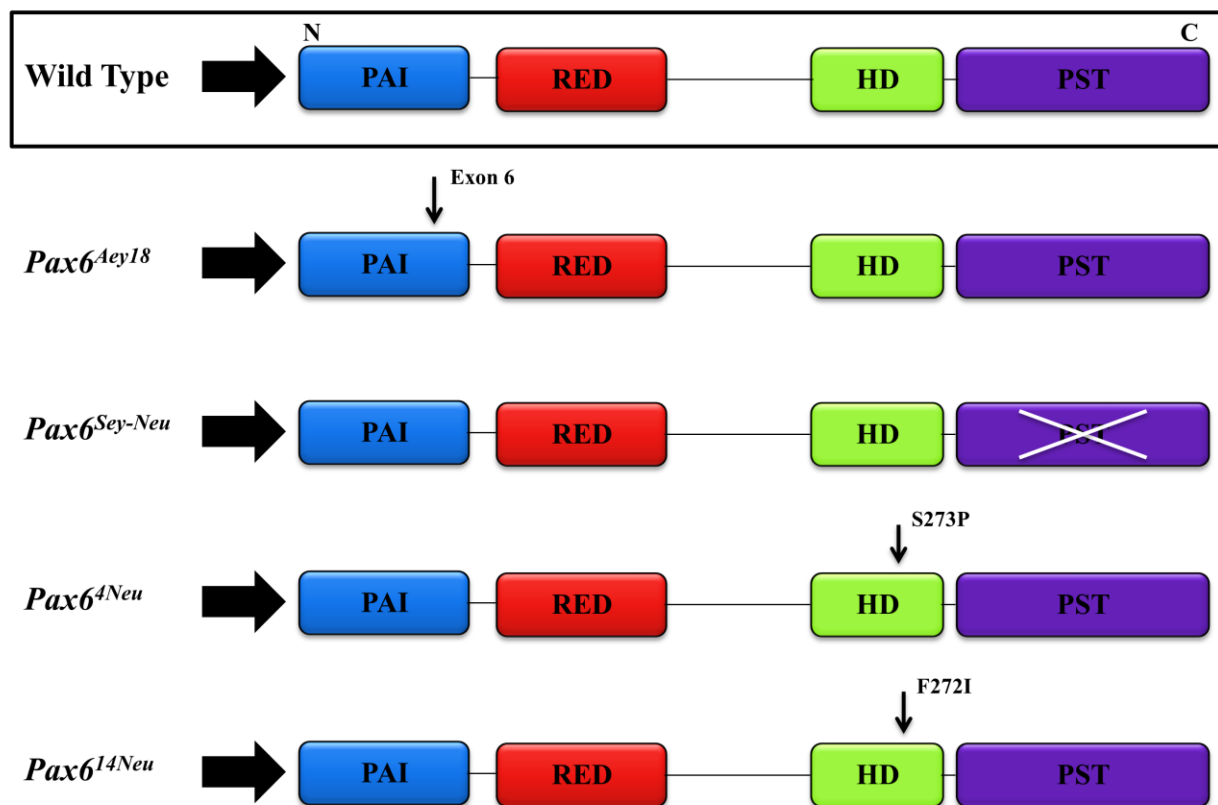


Figure 1.6: Summary of published *Pax6* mutations. Arrows depict presence of mutations. Details are provided in the text. PAI and RED, PAIRED subdomains; HD, Homeodomain; PST, Proline-Serine-Threonine transactivation domain; C, carboxy terminal; N, amino terminal.

Unsurprisingly, some patients afflicted with aniridia due to mutations in *PAX6*, also showed signs of glucose intolerance ^[209] and the absence or hypoplasia of the pineal gland ^[210]. Moreover, some MODY and MODY-like cases have also previously reported *PAX6* mutations as the causal element resulting in aniridia and diabetes in young adults ^[209, 211]. Thus, to further study effects of *Pax6* mutation on overall metabolism and draw parallels with human studies, heterozygous mouse models were taken up for investigation. A direct comparison was made in one study where a mouse model heterozygous for a R266Stop mutation showed similar phenotypes to that in humans with a heterozygous R240Stop mutation ^[212], both displaying glucose intolerance. In the same study, a direct target of *PAX6*, prohormone convertase PC1/3 (*Psc1*), was blunted ^[213, 214], resulting in increased proinsulin to insulin ratio and consequently glucose intolerance without any compensatory change in insulin sensitivity ^[212]. Interestingly, an *in vitro* investigation reported presence of a single nucleotide polymorphism (SNP) associated with reduced *PAX6* and *PSCK1* in human islets ^[215].

Another important characteristic of TF is that in the adult, PAX6 is also required for conferring functionality to the endocrine cells. Indeed, PAX6 not only binds to the promoter regions of glucagon, insulin and somatostatin ^[28] but also controls processing of prohormone convertases PC1/3 ^[212, 214] and PC2 ^[216, 217] and hence formation of mature insulin. Moreover, *in vitro* knockdown studies in primary mouse α - and β -cells has demonstrated direct regulation of insulin and glucagon secretion ^[213, 217] which is in line with previously shown attenuation of insulin secretion in primary islets from rats carrying heterozygous *small eye* mutation ^[132]. In addition, it was recently shown that glucose sensing in the adult β -cell specific *Pax6* knockout mice is distorted and may represent one mechanism contributing to faulty insulin secretion ^[100]. Therefore, these studies have brought aspects of PAX6 into focus that in addition to identity provide functional attributes to islet cells.

Furthermore, genes for receptors on the β -cells responsible for contributing to the incretin effect such as *Glp1r* and *Gipr* are directly regulated by PAX6 ^[213]. Previously, it was shown that PAX6 binds to the G1 and G3 elements of the preproglucagon gene in α -cells ^[28]. Similarly, the other spliced products of the gene GLP-1, GLP-2 as well as GIP, all of which were found to be reduced in the mouse intestine of *small eye* mutants ^[218] were later found to be directly regulated by PAX6 *in vivo* ^[219]. Therefore, PAX6 not only regulates incretin expression and thereby its effects on pancreatic β -cells but also peripheral effects of GLP-1 as shown in mice heterozygous for a PAX6 mutation in the HD ^[131]. Here, the authors observed that circulating GLP-1 levels as well as intestinal transcripts were reduced, leading to increase in blood glucose levels due to reduced β -cell function and increased food intake, which was corrected via Exendin-4 (GLP-1 analog) therapy ^[131]. Moreover, dual studies investigating *Pax6* mutations in mice and humans found decreased levels of α -MSH and POMC in human blood plasma and mouse hypothalamus suggesting effects might be driven via the hypothalamus ^[212]. Indeed, scattered *Pax6* positive cells were found in the hypothalamus during development of the mouse brain ^[220]. More recently, clusters with *Pax6* positive cells in adult mice were recently found in the zona incerta region, an area of the hypothalamic tissue which is functionally rather poorly understood ^[221]. Taken together, these data strongly points at the role of PAX6 in providing functional identity which is certainly not limited to islet cells. Considering the scale at which PAX6 might function in different tissues, it warrants further investigations taking other peripheral tissues as well as the hypothalamus under study.

1.3.3 *Pax6*^{Leca2} model

In 1996, Azuma et al, reported a novel PAX6 mutation R128C (R125C was originally published, which was subject to change in nomenclature of the gene) was identified in a human patient [222]. The mutation lies within the RED subdomain, substituting arginine for cysteine as a consequence of which *Pax6* displays differential transactivation properties [223]. An ENU-mutant carrying this particular mutation was screened [224] and then later studied in the embryonic homozygous condition, for understanding functional differences between PAI and RED subdomains during brain development [225]. Interestingly, the authors also reported homozygous viability of this mouse model with a mildly reduced Mendelian ratio and that these mice live a normal span of life [225].

Previously, this mouse model was taken into study in our group for histological examination of pancreatic islets and transcriptome analysis of the same. Preliminary data indicated normal embryonic development based on similar number of insulin and glucagon positive cells compared to wildtype littermates. However, reduced insulin positive cells in the islets were observed in adult mice from ages 6 weeks and above. Moreover, mircoarray analysis of isolated islets at ages 4 and 20 weeks showed dramatic changes in the transcriptome which taken together with immunohistochemistry (IHC) results demonstrated a progressive loss of β -cell function [226]. Furthermore, no hyperglycemia or an overt diabetic phenotype was observed although significantly reduced insulin levels in plasma were reported (Daniel Gradinger, unpublished results). Therefore, this being the only *Pax6* mouse model with a mutation in the RED subdomain and homozygous viable with a pancreatic phenotype [208], it deserves further investigation as a major discrepancy exists between reduced plasma insulin and absence of hyperglycemia.

1.4 Aims and hypothesis

The TF PAX6, as mentioned above in great detail, is a pleiotropic player not only during developmental stages but also in the adulthood. It indeed has various roles to play in the islets and gut affecting overall metabolism. Moreover, *PAX6* in human patients of diabetes have also been studied including the identification of an SNP [211]. Several mutations have thus been studied that specifically target the PAI subdomain, HD and/or the PST domain. In addition, the phenotypic similarities reported for mutations between the rodent and human studies support a translational component to these investigations. Unfortunately, none of the rodent models can be studied in a homozygous condition in the adult due to prenatal death [225]. Considering this and the preliminary data obtained for homozygous *Pax6^{Leca2}* mutant, the following research questions were attempted;

- a. How does the *Leca2* mutation in PAX6 affect islet functionality?
- b. Why do the homozygous *Pax6^{Leca2}* mice not show signs of hyperglycemia or a metabolic syndrome?
- c. Do functional differences in peripheral tissues contribute to this apparent absence of hyperglycemia?

Isolated islets from mice homozygous for the *Leca2* mutation were subjected to transcriptome analysis as well as histological examinations and *in vitro* functional studies determining the capacity of β -cells to secrete insulin. Moreover, *in vivo* physiological tests were performed to test the capability of the mice to metabolize glucose and generate glucose in addition to hyperinsulinemic-euglycemic clamp studies to test response of peripheral tissues to glucose. Furthermore, diet challenge tests and indirect calorimetry was performed to investigate energy expenditure. Finally, an attempt was made to dissect the role of liver and hypothalamus in contribution to the prevailing phenotype by utilizing various molecular methods and physiological studies.

2. MATERIALS AND METHODS

2.1 Materials

2.1.1 Buffers and solutions

| Buffers and solutions | Recipes |
|---|--|
| G-solution for islet isolation | 500 mL Hanks' Balanced Salt Solution (Lonza Verviers) 5 mL antibiotic antimycotic solution (Sigma-Aldrich) 5 g BSA (Sigma-Aldrich) Dissolved and sterile filtered, stored at 4 °C for up to a month |
| 40% Optiprep | 20 mL 60% Optiprep® (Sigma-Aldrich) 9.7 mL DBPS (Lonza Verviers) 300 µl 1M HEPES (Lonza Verviers) Stored at 4 °C for up to a week |
| 15% Optiprep | 5 mL 40% Optiprep® (Sigma-Aldrich) 3 mL 10% RPMI1640 (Lonza Verviers) in HBSS (Lonza Verviers) Freshly prepared on the day of use |
| Modified Krebs Ringer Bicarbonate Buffer (mKRBH) (10x) | 14 g NaCl 0.7 g KCl 0.7 g CaCl ₂ ·2H ₂ O 0.23 g MgCl ₂ ddH ₂ O added to a final volume of 200 mL Stored sterile filtered at 4°C for up to two months or freeze aliquots at -20°C up to several months |
| Acid ethanol (0.18M HCl in 71% ethanol) | 375 mL absolute ethanol 117.5 mL ddH ₂ O 7.5 mL concentrated (37%) HCl Stored at -20°C |
| mKRB (1x) | To approx. 75 mL of ddH ₂ O, add 20 mL 10x mKRB 2 mL 1M HEPES 9.6 mL 0.5M NaHCO ₃ (freshly prepared) Components added in the exact order detailed above and adjusted to pH 7.4 ddH ₂ O added to a final volume of 200 mL Add 0.1% BSA before use and check pH again |
| RPMI medium | 440 mL RPMI medium (Lonza Verviers) 50 mL Fetal calf serum (Life technologies) 5 mL antibiotic antimycotic solution (Sigma) 5 mL 5.5 mM glucose solution (Sigma) |

| | |
|--|--|
| PBS (10x) | 80 g NaCl 2 g KCl 17.8 g Na ₂ HPO ₄ ·2H ₂ O 2.72 g KH ₂ PO ₄ Dissolved in ddH ₂ O and adjusted to pH 7.3 ddH ₂ O added to a final volume of 1 L |
| PBST | 100 mL 10x PBS 500 µL Tween20 900 mL ddH ₂ O |
| TNT Buffer | 10 ml of 1M Tris HCl, pH 8.0 17.53 g NaCl 0.1% Tween20 Dissolved in ddH ₂ O to a final volume of 1 L |
| SDS lysis Buffer | 10 mL of 1M Tris pH 7.5 75 mL of 1M NaCl 1 mL of 0.5M EDTA 1 mL of 0.5M EGTA 50 mL of 10% SDS 5 mL of 100% NP40 Dissolved in ddH ₂ O to a final volume of 500 mL |
| 6x SDS loading buffer | 3 mL Glycerol 7 mL 4×Tris·Cl/SDS pH 6.8 3 mg Bromphenol blue 375 µL β-mercaptoethanol 1 g SDS Stored at 4°C |
| 5x SDS electrophoresis running buffer | 15.1 g Trizma base 72.0 g Glycine 5.0 g SDS ddH ₂ O added to a final volume of 1L Stored at RT for up to one month |
| 10x western blotting transfer buffer | 30.03 g Trizma base 144.1 g Glycine ddH ₂ O added to a final volume of 1 L Stored at RT for up to one month |
| 1x western blotting transfer buffer | 100 mL 10x Transfer buffer 200 mL Methanol 700 mL ddH ₂ O |
| Paraformaldehyde fixative (20%) | Stock prepared under a fume hood 70 mL PBS 8 g PFA Heat to 70°C Add 1 drop of concentrated NaOH until the solution is clear, remove from the heat Add 30 mL PBS, cool to room temperature Adjust pH to 7.2 with HCl Store at -20°C, dilute to 4% before use |

| | |
|---|--|
| 11% Formaldehyde solution | Prepared fresh before use 6 mL of 37% Formaldehyde 0.4 mL of 5 M NaCl 40 µL of 0.5 M EDTA, pH 8.0 1 mL of 1 M HEPES, pH 7.9 Dissolved in 20 mL ddH ₂ O |
| 2.5 M Glycine solution | 3.75 g Glycine Dissolved in 20 mL ddH ₂ O |
| PBS-Igepal | 100 mL PBS pH 7.5 0.5 mL Igepal |
| Cryoprotectant (500 mL) (30 µm brain sections) | 150 mL Glycerol 150 mL Ethylene glycol 200 mL Sucrose-TBS (150 g sucrose in 200 mL TBS) |
| SUMI (250 mL) (Prepared fresh) | 0.625g gelatin 1.25ml TritonX-100 Heated at 60°C to dissolve 250ml TBS (6°C) |

2.1.2 *In vitro* insulin secretion assay materials

| Diluent solution | Insulin secretagogues (stock solutions) | Volume added to mKRB (1x) (freshly prepared) |
|------------------|--|--|
| 1x PBS | Glucose (2M) (Sigma-Aldrich) | for 1.5 mM glucose, add 0.75 µL/mL, for 2.8 mM glucose, add 1.4 µL/mL, for 6 mM glucose, add 3 µL/mL, for 12 mM glucose, add 6 µL/mL, for 16.7 mM glucose, add 8.35µL/mL |
| 1x PBS | KCl (3M) | for 30 mM, add 10 µL/mL |
| 1x PBS | Exendin-4 (100 µM) (Sigma-Aldrich) | for 100 nM, add 1 µL/mL |
| DMSO | Forskolin (2,5 mM) (Sigma-Aldrich) | for 2,5 µM, add 1 µL/mL |

2.1.3 PCR Primers

2.1.3.1 Housekeeping genes

| Gene | Forward sequence | Reverse sequence |
|------------------|-----------------------|-------------------------|
| <i>Atp5b</i> | GGTTTGACCGTTGCTGAATAC | TAAGGCAGACACCTCTGAGC |
| <i>Atp5b</i> (2) | CCTCGGTGCAGGCTATCTATG | GTAGCATCCAAATGGGCAAAG |
| <i>B2m</i> | GCTATCCAGAAAACCCCTCA | GGGGTGAATTTCAGTGTGAGC |
| <i>Cyc1</i> | GTTTCGAGCTAGGCATGGTG | CGGGAAAGTAAGGGTTGAAATAG |

| | | |
|---------------------------------|--------------------------|--------------------------|
| <i>Cyc1</i> | ATGGGTCTCAAGATGTTGTTG | GGCAAGATGACAAGCAGATAC |
| <i>Fbxw2</i> | ATGGGTACCAAGGTGGT | TCCCAATTGGCCAAATCTT |
| <i>Hmbs</i> | GCTGAAAGGGCTTTTCTGAG | TGCCATCTTTCATCACTGT |
| <i>Hprt1</i> (<i>Hprt</i>) | CCTAAGATGAGCGCAAGTTGAA | CCACAGGACTAGAACACCTGCTAA |
| <i>Rpl13a</i> | TGAAGCCTACCAGAAAGTTTGC | GCCTGTTTCCGTAACCTCAA |
| <i>Sdha</i> | GCAATTTCTACTCAATACCCAGTG | CTCCCTGTGCTGCAACAGTA |
| <i>Tbp</i> | CCCCACAACCTTTCCATTCT | GCAGGAGTGATAGGGGTCAT |
| <i>Tuba1a</i> | AAGGAGGATGCTGCCAATAA | GCTGTGGAAAACCAAGAAGC |
| <i>Ubc</i> | AGCCCAGTGTTACCACCAAG | ACCCAAGAACAAGCACAAGG |
| <i>Ywhaz</i> | TGCAGCCAGAAGAATATCCA | AAGAGACAGTACATCGTTGCAGA |
| <i>Ywhaz</i> (2) | TGCAAAAACAGCTTTCGATG | TCCGATGTCCACAATGTTAAGT |
| <i>Zfp91</i> | TTGCAGCACCATTAATAAC | ATCCCTCTGGTCTGTATGATG |
| <i>Zfp91</i> (2) | CCAGGAAGAGAGGGAGAAG | CACATCCTTCCATCTCACAAC |

2.1.3.2 Target genes

| Gene | Forward sequence | Reverse sequence |
|----------------|-----------------------------|----------------------------|
| <i>Abcc8</i> | TCAACTTGTCTGGTGGTCAGC | GAGCTGAGAAAGGGTCATCCA |
| <i>Acaca</i> | TTTCCCAGCCAGCAGAT | TCGGTACCTCTGCACCA |
| <i>Acly</i> | CCCGAGGAAGCCTACATT | AGATGGTGTCACTGTACACGA |
| <i>Agrp</i> | GGCCTCAAGAAGACAACCTGC | GCAAAAGGCATTGAAGAAGC |
| <i>Cartpt</i> | CGAGAAGAAGTACGGCCAAG | GGAATATGGGAACCGAAGGT |
| <i>Fasn</i> | ACTGTTGCAGGCTGTCCT | TGACATTGATGCCTGTGAG |
| <i>Fbp1</i> | CCTGAGAAGAGGGGCAAATA | GCTCATCAGTACTTTTCTTTCTGTAA |
| <i>Ffar1</i> | TTCCTAGCTGCTCTCAGCG | TCGGGATCCCAGGCTTC |
| <i>Fgf21</i> | CCGCAGTCCAGAAAGTCT | AGTGAGGCGATCCATAGAG |
| <i>G6pc</i> | TCGGAGACTGGTTCAACCTC | AGGTGACAGGGAAGTCTTTAT |
| <i>G6pc2</i> | CCTACTACGTGTGAAACAGGC | CAGAAAGGACCAGGTCAGTCT |
| <i>Gcgr</i> | TCTGTTTGAGAATGTTCAAGTCT | GGCCAGCCGGAAGTATAG |
| <i>Gck</i> | CTGTTAGCAGGATGGCAGCTT | TTTCTGGAGAGATGCTGTGG |
| <i>Glp1r</i> | ACGGTGTCCCTCTCAGAGAC | ATCAAAGGTCCGGTTGCAGAA |
| <i>Igf1r</i> | GTG GGG GCT CGT GTT TCT C | GAT CAC CGT GCA GTT TTC CA |
| <i>Ins1</i> | GCAAGCAGGTCATTGTTTCA | CACTTGTGGGTCTCCTCACTT |
| <i>Ins2</i> | CAGCAAGCAGGAAGCCTATC | GCTCCAGTTGTGCCACTTGT |
| <i>Jak2</i> | ATACTCTACAGGATAAGGTTCTACTTC | CCGCCACTGAGCAAAAAG |
| <i>Kcnj11</i> | AAGGGCATTATCCCTGAGGAA | TTGCCTTTCTTGGACACGAAG |
| <i>Lepr</i> | CGTGGTGAAGCATCGTACTG | GGGCCATGAGAAGGTAAGGT |
| <i>Mafa</i> | CAGCAGCGGCACATTCTG | GCCCGCCAAGTCTCGTAT |
| <i>Mc3r</i> | TCAAACGCGAAGAAAGTGCA | AGACAACGCACTTACCAGGA |
| <i>Mc4r</i> | GGACTCTGAAAAGACCCCGA | TGCCTGTAGAAGTTGGGAGG |
| <i>Msln</i> | CATCCCCAAGGATGTCAAAG | GCAGGCTTTCTGTTCTGCAT |
| <i>Neurog3</i> | GTCGGGAGAACTAGGATGGC | GGAGCAGTCCCTAGGTATG |
| <i>Npy</i> | TCGCTCTATCTCTGCTCGTG | AATCAGTGTCTCAGGGCTGG |

| | | |
|-----------------|-------------------------|-----------------------|
| <i>Pax6</i> | CAGAGAAGACAGGCCAGCAA | AAGGAGGAGACAGGTGTGGT |
| <i>Pck1</i> | CTTCTCTGCCAAGGTCATCC | TTTTGGGGATGGGCAC |
| <i>Pcx</i> | CTGAAGTTCCAAACAGTTCGAGG | CGCACGAAACACTCGGATG |
| <i>Pcx (2)</i> | ACATTACCTCGGACATGTCA | CTGGAGGTGGGCCTATG |
| <i>Pdx1</i> | CAGTGGGCAGGAGGTGCTTA | GCCCCGGTGTAGGCAGTAC |
| <i>Pfkfb2</i> | AAGGCGCAGATGAGTTACCA | TGGGGAAGTTGTGAGTTGGC |
| <i>Pi3k</i> | CACCCAAGCCCCTACTGTA | GAGTGTAATCGCCGTGCATT |
| <i>Pomc</i> | CATTAGGCTTGGAGCAGGTC | TCTTGATGATGGCGTTCTTG |
| <i>Pp2a</i> | GATGGGCAGATCTTCTGTCTAC | CCTCATGAGGAACCTCCTGT |
| <i>Ppara</i> | VMPS-4940 (Biomol) | VMPS-4940 (Biomol) |
| <i>Ptp1b</i> | CTCGTTAAAATGTGCCCAGTAT | TCCTTGGTAGTCAGGTTTTCC |
| <i>Slc2a2</i> | GGGGACAAACTTGGAAAGGAT | TGAGGCCAGCAATCTGACTA |
| <i>Srebp1c</i> | GGAGCCATGGATTGCACATT | GGCCCCGGGAAGTCACTGT |
| <i>Stat3</i> | CAAGAGCCAAGGAGACAT | CTCACAATGCTTCTCCGC |
| <i>Syt14</i> | ATCATTTAGTGTGCCGAGAATGC | CCTGTTCGGTAATCAAAGCGA |
| <i>Ucn3</i> | AAGCTGCAACCCTGAACAGT | AGCATCGCTCCCTGTAAGTG |
| <i>Ucn3 (2)</i> | GGGAAGCTGTACCCAGACAA | AATTCTTGGCCTTGTCGATG |

2.1.4 Primary Antibodies

2.1.4.1 Western blot and chromatin immunoprecipitation

| Antibody | MW (kDa) | Host | Clonality | Catalogue number | Company | Working dilution |
|------------------------|----------|--------|------------|------------------|----------------|------------------|
| AKT | 60 | Rabbit | Polyclonal | 9272 S | Cell Signaling | 1:1000 |
| G6PC | 40 | Rabbit | Polyclonal | 70R-8595 | Fitzgerald | 1:1000 |
| GAPDH | 37 | Rabbit | Polyclonal | 2118 | Cell Signaling | 1:10000 |
| P-AKT (Ser 473) | 62 | Rabbit | Polyclonal | 9271 S | Cell Signaling | 1:1000 |
| P-AKT (Thr 308) | 62 | Rabbit | Polyclonal | 4056 S | Cell Signaling | 1:1000 |
| PAX6 | 52 | Rabbit | Polyclonal | 61611 | Active Motif | 1:1000 |
| PCX | 137 | Rabbit | Polyclonal | 70R-50176 | Fitzgerald | 1:1000 |
| PEPCK | 63 | Rabbit | Monoclonal | D12F5 (12940S) | NEB | 1:1000 |

2.1.4.2 Immunohistochemistry

| Antibody | Host | Clonality | Catalogue number | Company | Working dilution |
|---------------------|------------|------------|------------------|---------------|------------------|
| Ghrelin | Goat | Polyclonal | sc-10368 | Santa-cruz | 1:200 |
| Glucagon | Mouse | Monoclonal | G2654 | Sigma-Aldrich | 1:1000 |
| Insulin | Guinea pig | Polyclonal | A0564 | Dako | 1:200 |
| Pax6 | Rabbit | Polyclonal | AB2237 | Millipore | 1:200 |
| Pdx1 | Mouse | Monoclonal | F6A11-c | DSHB | 1:500 |
| Somatostatin | Rabbit | Polyclonal | A0566 | Dako | 1:200 |

2.1.5 Secondary Antibodies

2.1.5.1 Western blot

| Antibody | Host | Catalogue number | Company | Working dilution |
|-----------------------|------------------|------------------|---------------|------------------|
| HRP-conjugated | Goat-anti-rabbit | A6154-1ML | Sigma-Aldrich | 1:20000 |

2.1.5.2 Immunohistochemistry

| Antibody | Host | Catalogue number | Company | Working dilution |
|-------------------------|----------------------|------------------|------------|------------------|
| Alexa Flour® 488 | Goat-anti-guinea pig | A11073 | Invitrogen | 1:500 |
| Alexa Flour® 488 | Donkey-anti-rabbit | A21206 | Invitrogen | 1:500 |
| Alexa Flour® 488 | Donkey-anti-goat | A11055 | Invitrogen | 1:500 |
| Alexa Flour® 594 | Donkey-anti-mouse | A21203 | Invitrogen | 1:500 |
| Alexa Flour® 594 | Donkey-anti-rabbit | A21207 | Invitrogen | 1:500 |
| Alexa Flour® 594 | Donkey-anti-goat | A11058 | Invitrogen | 1:500 |

2.1.6 Chemicals and kits

2.1.6.1 Consumables

| Consumable | Company |
|--|-------------------|
| 384 well plates (LC480 Lightcycler) | Roche |
| 6-well tissue culture plate | Falcon |
| Accu-check Aviva (blood glucose meter) | Roche |
| Cell strainer 70 µm nylon mesh, sterile | BD Bioscience |
| Corning 100mmx20mm style dishes | Corning |
| Corning filter system 0.22 µm | Corning |
| Disposable centrifuge tubes, sterile, polypropylene, 15 mL/50 mL | Sarstedt |
| Eppendorf reaction tube | Sarstedt |
| Gloves | Meditrade |
| Matrix Liquid Handling Tips 30 µL, 125 µL | Thermo Fischer |
| Microvette® CB 300 LH | Sarstedt |
| O.C.T. compound | Thermo Fischer |
| Omnican F 1.0 mL | B Braun |
| Omnifix 1 mL, 5mL, 50 mL | B Braun |
| Pap Pen | Enzo Life Science |
| Serological pipets 5, 10, 25 and 50 mL | Greiner Bio One |
| S-Monovette® 1,2 ml, K3 EDTA | Sarstedt |
| S-Monovette®-Needle 21Gx1½ | Sarstedt |
| Sterican® Insulin Einmalkanüle für spezielle Indikationen "- G 30 x 1/2" / Ø 0,30 x 12 mm" | Neolab |
| Sterile Syringe Filter 0.20 µm | Corning |
| SuperFrost® Plus slides | VWR |
| Tips | Sarstedt |

2.1.6.2 Chemicals

| Chemical | Company | Catalogue number |
|--|-------------------|------------------|
| 1M HEPES | Lonza Verviers | 882120 |
| 60% Optiprep® | Sigma-Aldrich | D1556-250ML |
| Antibiotic Antimycotic Solution | Sigma-Aldrich | A5955-100ML |
| Bovine Serum Albumin | Sigma-Aldrich | A3311-100G |
| Dexamethasone | Sigma-Aldrich | D4902-500MG |
| DMEM | Biozol | 1-25K34-I |
| Dulbecco's Phosphate-buffered Saline | Lonza Verviers | 882110 |
| Exendin-4 | Sigma-Aldrich | E7144 |
| Fetal Calf serum | Life technologies | 10500064 |
| Formaldehyde solution | Sigma-Aldrich | F-8775 |
| Forskolin | Sigma-Aldrich | F3917-10MG |
| Glucagon | Sigma-Aldrich | G2044-5MG |
| Glucose solution | Sigma-Aldrich | G8644-100ML |
| Hanks' Balanced Salt Solution | Lonza Verviers | 882005 |
| Human insulin | Lilly | HI0219 |
| Igepal® | Sigma-Aldrich | I8896-50ML |
| KCl | Sigma-Aldrich | P5405-250G |
| Ketamine | Heinrich Fromme | |
| Rompun | Ble-Pharm | |
| Phenylmethanesulfonyl fluoride | Sigma-Aldrich | P7626-1G |
| Phosphate-buffered Saline | Lonza Verviers | BE17-516F |
| Rat tail collagen | Roche | 11179179001 |
| RPMI 1640 | Lonza Verviers | 880181 |
| Sera Plus (Special processed FBS) | Pan Biotech | P30-3702 |
| Sodium pyruvate | Sigma-Aldrich | P5280-25G |
| Tween20 | Biotium | 22002 |
| William's Medium E with L-Glutamine with 2.24 g/L NaHCO ₃ | Pan Biotech | P04-29500 |

2.1.6.3 Reagents

| Molecular Biology Reagents | Company | Catalogue number |
|---|----------------|------------------|
| Antipain dihydrochloride | Sigma-Aldrich | A6191-25MG |
| APMSF | Sigma-Aldrich | A6664-50MG |
| Aprotinin | Sigma-Aldrich | A1153-10MG |
| Chymostatin | Sigma-Aldrich | C7268-25MG |
| cOmplete™, Mini Protease Inhibitor Cocktail | Roche | 11836153001 |
| Leupeptin | Sigma-Aldrich | L2884-5MG |
| Pepstatin A | Sigma-Aldrich | P4265-5MG |
| Phosphatase Inhibitor Cocktail 2 & 3 | Sigma-Aldrich | P5726 & P0044 |
| QuantiFast SYBR Green PCR Kit (4000) | Qiagen | 204057 |
| Random Primer Mix | NEB | S1330S |
| RIPA Lysis and Extraction Buffer | Roche | 89900 |
| RNaseOUT® | Invitrogen | 10777-019 |
| Spectra Multicolor Broad Range Protein Ladder | Thermo Fischer | 26624 |
| SuperScript® II Reverse Transcriptase | Invitrogen | 18064-014 |
| Taq DNA Polymerase | Qiagen | 201205 |

2.1.6.4 Kits

| Kit | Company | Catalogue number |
|---------------------------------------|----------------------|-------------------------|
| Agilent RNA 6000 Pico Kit | Agilent Technologies | 5067-1513 |
| Mouse/Rat Leptin Quantikine ELISA Kit | R&D Systems | MOB00 |
| FGF-21 Quantikine ELISA | R&D Systems | MF2100 |
| Mouse Glucagon ELISA | Mercodia | 10-1281-01 |
| Mouse Insulin ELISA | Mercodia | 10-1247-10 |
| PicoProbe Acetyl CoA Assay Kit | Abcam | ab87546 |
| Pierce BCA Protein Assay Kit | Thermo Scientific | 23227 |
| Pierce ECL Western Blotting Substrate | Thermo Scientific | 32109 |
| RNeasy® Mini Kit | Qiagen | 74104 |
| RNeasy® Plus Micro Kit | Qiagen | 74004 |

2.1.6.5 Laboratory devices and equipment

| Laboratory equipment | Company |
|---|-------------------------|
| Bio safety cabinet | Schulz Lufttechnik GmbH |
| Centrifuge Biofuge pico | Heraeus |
| Freezer -20°C | Liebherr |
| Fridge +4°C | Liebherr |
| Glassware | Schott |
| Incubator | Heraeus |
| Leica CM1850 Cryostat | Leica Microsystems |
| Leica SP5 Confocal Microscope | Leica |
| Lightscanner | Idaho Technology |
| Magnetic Mixer | IKA Labortechnik |
| Matrixpipette 30 µL, 125 µL | Thermo Fischer |
| Micro bulldog clamp | Roboz |
| Multichannel pipette 300 µL | Gilson |
| Nanodrop ND-1000 | NanoDrop Technologies |
| NanoZoomer 2.0HT | Hamamatsu |
| NanoZoomer –XR Digital slide scanner | Hamamatsu Photonics |
| Pipetman P10, P20, P200, P1000 | Gilson |
| Rocking Platform | VWR |
| Seahorse XFe24 Analyzer | Agilent Technologies |
| SpectraMax190 Plate reader | Molecular Devices |
| Stereo Microscope Stemi SV6 | Zeiss |
| Thermomixer 1.5 mL | Eppendorf |
| Timer | Roth |
| TissueLyser | Qiagen |
| Universal 32R centrifuge | Hettich Zentrifugen |
| Vacuum pump Reglo-Digital (MS-4/12-100) | Techlab |
| Varioskan Plate reader | Thermo Fischer |
| Vortexer | Neolab |
| Water bath | Julabo |

2.2 Methods

2.2.1 Mouse line maintenance

All mice were kept in a specific-pathogen-free environment in compliance with the Federation of European Laboratory Animal Science Associations Protocols (FELASA) and all experimental procedures were performed in accordance with German and European Union guidelines. The *Pax6^{Leca2}* animals [224] were provided by Prof. Dr. Magdalena Götz as part of a scientific collaboration and maintained on a C3HeB/FeJ background. Unless otherwise stated, these mice freely received standard chow diet (Ssniff) and water. All experiments were performed with homozygous *Pax6* mutant mice denoted as *Pax6^{Leca2}* and wildtype littermates as *Pax6^{WT}*, aged 10-12 weeks, unless otherwise specified.

2.2.2 Metabolic and physiological methods

2.2.2.1 **Body composition and metabolic studies**

Food was removed at 8 am, 6 hours [227] prior to an intraperitoneal injection of 2 g/kg of glucose (20% solution, Braun), 0.75 U/kg of human insulin (Lilly), 2 g/kg of sodium pyruvate (Sigma-Aldrich) or 0.5 mg/kg of glucagon (Sigma-Aldrich) depending on the experimental purpose. Blood glucose was measured using Accu-Check (Roche) from tail blood at time periods 0, 15, 30, 60, 90 and/or 120 minutes. Blood plasma was collected at several time points in heparinized-tubes (Sarstedt), snap-frozen in liquid nitrogen and subsequently stored at -80°C until further use.

Body composition was carried out using noninvasive nuclear magnetic resonance (NMR) to measure fat and lean mass. Indirect calorimetry including food intake was measured by keeping mice using the PhenoMaster homecage system (TSE system) in collaboration with Dr. Jan Rozman.

2.2.2.2 **Dietary challenge test**

Mice were put on either low fat control diet (LFCD) or fat high fat diet (HFD). HFD and LFCD (Ssniff) consisted of 60 kJ% and 9 kJ% fat, respectively. Starting at week 4 of age, mice were allowed to eat the given diet freely for a period of 10 weeks. Weekly measurements of body weight and blood glucose were carried out in *ad libitum* state.

2.2.2.3 **Leptin sensitivity assay**

Under sterile conditions, recombinant leptin (R&D systems) was dissolved in 20 mM Tris (pH 8.0) to attain the concentration of 1 mg/mL. Mice were fasted 3 hours before the dark phase which started at 6:00 pm and lasted for 12 hours. 30 minutes before the commencement of the

dark phase, mice were injected intraperitoneal with 5 mg/kg of leptin or PBS vehicle (20 mM Tris-PBS) and were allowed to eat freely in metabolic cages (TSE systems). Food intake and other metabolic parameters were monitored for 24 hours.

2.2.2.4 Euglycemic-hyperinsulinemic clamps

Euglycemic-hyperinsulinemic clamp studies were performed with 9-10 weeks old mice as previously published [228]. To initiate the euglycemic-hyperinsulinemic clamp, a continuous insulin infusion (1.25 mU/kg/min; Humulin R, Lilly) was started and continued for 120 min. Between 90 and 120 min, four blood samples were collected for calculation of insulin-mediated suppression of endogenous glucose appearance rates (EndoRa), a marker of hepatic glucose production. At 120 min, 2-deoxy-D-(1-14C) glucose was injected intravenously (370 kBq), and additional blood samples were collected. Basal EndoRa was calculated as the ratio of (3-3 H) glucose infusion rate and plasma (3-3 H) glucose specific activity. The EndoRa during insulin-stimulated conditions was determined by subtracting the Glucose Infusion Rate (GINF) from rate of disappearance (Rd). Tissue 2-(14C) deoxyglucose-6-phosphate was extracted, and glucose uptake rates (Rg) were calculated as previously described [228].

2.2.2.5 Plasma collection and Clinical chemistry

Mice were sacrificed at *ad libitum* state or after 6 hours of fasting. Whole blood from mice was collected from *vena cava* using Lithium Heparin-containing S-Monovette® (Sarstedt), and centrifuged in a 1.5 mL tube (Eppendorf) for 2 minutes at 10°C and 9000 rpm to obtain plasma which was snap frozen in liquid nitrogen. The following molecules were analyzed through the Clinical Chemistry screen under the supervision of Dr. Birgit Rathkolb in the GMC; non-esterified free fatty acids (NEFA), glycerol, triglycerides (TG), cholesterol, high density lipoproteins (HDL), low density lipoproteins (LDL), lipase and lactate.

2.2.3 In vitro methods

2.2.3.1 Islet isolation

Mice were euthanized by CO₂ and the peritoneum was cut open. The dissected mice were then kept under a microscope with its anterior side towards the experimenter. The gut and the liver were carefully placed aside to expose the common bile duct entering the duodenum at a site called the Ampulla of Vater. This site was then clamped with a micro bulldog clamp (Roboz). The common bile duct was pierced with a 30 G1/2-G needle (Braun), attached to a syringe containing 4 mL of collagenase solution (Roche). The pancreas was then slowly perfused with the solution, subsequently excised and immediately transferred to a 15 mL tube containing 4 mL of collagenase solution kept on ice. Long incubations in the collagenase solution must be

avoided. Once all the samples were collected, the falcon tubes were transferred to a water bath and incubated at 37°C for 15 minutes. Additionally, the tubes were temporarily removed from the water bath after 7.5 minutes and gently shaken to dismember the pancreatic tissue and then transferred back to the water bath. The digested pancreatic tissue was then immediately transferred to an ice box. The following steps were carried out inside a sterile hood. 8 mL ice cold G-solution was added to all the tubes and centrifuged at 290g for 2 minutes at RT. The supernatant, containing mostly fat and exocrine material, was carefully decanted and 10 mL G-solution was added to it and vigorously mixed with reverse pipetting. The solution, now mixed with the pancreatic digest, was then transferred to a 50 mL tube through a metal mesh to remove any undigested piece of tissue. Another 10 mL G-solution was added to the 15 mL tube and then transferred to the 50 mL tube with the residual to avoid islet loss. The metal mesh was then rinsed with 20 mL G-solution for the same purpose. The samples were then centrifuged at 290g for 2 minutes at RT. The supernatant was then decanted and 5.5 mL 15% Optiprep solution (Sigma-Aldrich) was added to the 50 mL tube. After thorough mixing, the resuspension was carefully pipetted along the wall of the 15 mL tube containing 2.5 mL 15% Optiprep solution to obtain a gradient. This gradient was then overlaid with 6 mL G-solution to obtain a third layer of gradient and incubated for 10 minutes at RT. Next, the samples were centrifuged at 290g for 15 minutes, with slow acceleration and without brakes to avoid mixture of gradient layers. The islets were found floating over the second and below the third gradient layer. The islets were carefully collected using a 5 mL serological pipette and filtered through a 70 µm nylon cell strainer to avoid any acinar tissue. The islets were then maintained in RPMI medium (Lonza) overnight in a humidified incubator at 37°C and 5% CO₂.

2.2.3.2 Insulin stimulatory studies

For the purpose of *in vitro* stimulatory experiments, isolated islets were incubated first handpicked using a 20 µL pipette and transferred to a 1.5 mL tube containing 1.5 mM glucose in 1x Krebs-Ringer Buffer (KRB). After several washes, the islets were then transferred to a 6-well plate containing 1.5 mM glucose in 1x KRB for an hour to facilitate equilibration, inside a 37°C and 5% CO₂ incubator. Meanwhile, another 6 well plate containing the same solution was also kept in the incubator, wherein the islets were transferred for an hour after the first incubation. During the second incubation, 1.5 mL tubes containing 500 µL of several concentrations of glucose and other insulin secretagogues (Section 2.1.2) were kept in the incubator with open lids. Next, 5-10 islets per experiment and mouse were transferred to the stimulants for 2 hours. At the end of the incubation period, the solution containing the islets

were gently mixed via reverse pipetting and incubated for further 5 minutes to allow the islets to settle down. Using a 200 μL pipette, 400 μL of the supernatant was transferred to a fresh 1.5 mL tube and the remaining 100 μL of solution was added with 500 μL of acid-ethanol solution to break open the islets and release the islet's insulin content. The supernatant and the lysate were stored at -20°C until use.

2.2.3.3 Hepatocyte isolation

All buffers required were brought to 37°C by placing them in a water bath. Next, EGTA buffer was pumped through the tubing system to rid the tube of any air bubbles. The mouse was then anaesthetized by an intraperitoneal injection with Ketamin:Rompun (1.6:1) and fixed after falling asleep onto an ethanol-sterilized surface. Before cutting into the peritoneum, an alcohol soaked tissue was kept on the side of the mouse where the intestines can be placed. Using a small surgical scissor, the skin was removed from the height of the bladder up to the diaphragm. A small incision at the lower left end of the skin was made so as to allow steady drainage of the perfusion fluids. After removing any hair or dirt with PBS solution, the inner peritoneal wall was incised. The intestine and fat tissue was carefully moved to clearly reveal the *vena cava* and the hepatic portal vein underneath. A small string, attached to a needle, was wrapped around the *vena cava* and a knot was prepared to fix the cannula in the direction of the *vena cava*. Next, a small slit was made into the *vena cava* and the cannula was carefully inserted. Once the knot was closed and the cannula fixed inside the *vena cava*, an incision was made to open the hepatic portal vein to allow the perfusion solutions to exit the system. The liver was then perfused with EGTA buffer for 15 minutes. Simultaneously, the collagenase buffer was prepared by adding 90 mg of collagenase (Roche) and 400 mg of BSA to the suspension buffer. The solutions were then kept in 37°C water bath. The perfusion was now carried out with the collagenase solution at a steady flow rate of 10 mL/minute and a pressure below 20 cm water column. After the perfusion, the liver was carefully excised, still attached to a small part of the diaphragm and placed into a petri dish with 15 mL of suspension buffer inside a sterile hood. To extract hepatocytes, the liver was grabbed with the attached piece of diaphragm and carefully ripped without applying much force. The resulting hepatocyte suspension was filtered through a wire net (pore size 100 μm) followed by a centrifugation for 5 minutes at 50x g and 4°C . The obtained cell pellet was washed with suspension buffer and centrifuged again. By gentle inversion, the resulting pellet was re-suspended in 10 mL suspension buffer. In order to determine the viability of the hepatocytes, the cells were diluted (1:2) in trypan blue solution

(4 g/L Trypan Blue). Using a Neubauer counting chamber, the number of viable cells was calculated (average cell number*dilution factor*volume factor).

2.2.3.4 Primary hepatocyte sandwich culture

Rat tail collagen (Roche) was reconstituted in 0.2% acetic acid to acquire a final concentration of 1 mg/mL and incubated overnight at 4°C without shaking. Then, 10 mL working solution was prepared adding 1 mL of 10x DMEM (Biozol) to 9 mL of reconstituted collagen. Next, 30 µL of 1N NaOH per mL of working solution was added dropwise (a total of 240 µL was added in two additions, each 120 µL) while swirling the tube containing the working solution. Now, 0.1 N NaOH and 0.2% acetic acid was used to adjust to pH 7.4. Next, 100 µL of collagen solution thus obtained was added to each well of a 24-well plate. Pipette tip was used to spread the collagen around the well while tilting the plate and then finally allowed to spread by laying it flat. Of note, collagen solution is viscous and hence the pipette tip end was slightly cut. The collagen was then allowed to condense at 37°C in an incubator for 45 minutes with the lid open. 500 µL of Williams Media E (Pan Biotech) was added and incubated overnight at 37°C.

Hepatocytes were re-suspended gently by dropwise addition of wash buffer to the cell pellet (approximately 10 mL per mouse). A final concentration of 200,000 cells/mL was obtained by carefully adding the cells to a 15 mL tube containing Williams Media E. After removing the media from the collagen-coated 24-well plates, 1 mL/well of hepatocytes were added in a dropwise fashion. Of note, hepatocytes are big in size and quickly settle down at the bottom of a tube. Hence, the solution containing them required resuspension after every 4 wells. The cells were allowed to attach for 2-3 hours.

10 mL working solution was again prepared adding 1 mL of 10x DMEM to 6 mL of reconstituted collagen and 3 mL of 0.2% acetic acid. Next, 30 µL of 1N NaOH per mL of working solution was added (a total of 300 µL was added in two additions, each 150 µL) dropwise while swirling the tube containing the working solution. 0.1 N NaOH and 0.2% acetic acid was used to adjust to pH 7.4. Next, the hepatocytes were washed 2 times by dropping 1 mL of PBS, at RT, directly in the middle of the well. 160 µL of the collagen solution was added to the cells in a dropwise manner and place the remaining solution in a water bath at 37°C to monitor solidification process. Once the collagen was hardened, 500 µL of Williams Media E was added directly to the center of the well. The hepatocytes were maintained in culture for 3-6 days before pursuing further experiments.

2.2.3.5 Glucose secretion assay

The hepatocytes were placed in 24-well plates with starvation medium containing phenol-free DMEM, 0.5% FBS, 5 mM glucose and 4 mM glutamine. After an incubation period of 10 hours, the cells were washed twice with PBS at RT and 200 μ L of DMEM medium containing basal stimulants; 4 mM glutamine, 2 mM pyruvate, 20 mM lactate was added. Next, wells were added with different stimulants; 100 nM glucagon (Sigma-Aldrich), insulin 100 nM (Lilly) and combined stimulant cocktail (1 μ M/100 nM Dexamethasone (Sigma-Aldrich) and 100 μ M Forskolin (Sigma-Aldrich)). Separate batch of wells were kept containing only basal medium and basal stimulants. After an overnight incubation, medium from 3 wells per sample per condition were pooled and centrifuged at RT at 6000 RPM. The supernatant was transferred into a fresh 1.5 mL tube and stored away at -20°C . The remaining cells, attached at the bottom of the well were lysed using 100 μ L of SDS lysis buffer containing Phosphatase inhibitor cocktail 2 and 3 (Sigma-Aldrich) and CLAAP (Chymostatin, Leupeptin, Antipain, Aprotinin, APMSF, Pepstatin) (Sigma-Aldrich) and further taken for protein analysis.

2.2.3.6 Hepatocyte mitochondrial respiration

As described in 2.2.3.4, 24-well Seahorse XFe24 (Seahorse Bioscience) plates were coated with collagen. 30000 cells per well were plated in a volume of 50 μ L of Williams E medium. After three days of primary hepatocyte culture, 1 mL of calibration solution was added to the calibration plate and placed inside a 37°C , non- CO_2 incubator for 20 minutes. Next, 400 μ L of seahorse assay medium (40 mL of Seahorse XF medium + 10 μ L 1M NaOH + 178 μ L 45% Glucose) was added to cells before placing the plate in Seahorse Xfe24 Analyzer (Seahorse Bioscience). The following substrate/inhibitors were applied: Port A – Oligomycin (2 μ M) 56 μ L/well, Port B – FCCP (Carbonyl cyanide-p-trifluoromethoxyphenylhydrazone) (1 μ M) 62 μ L/well, Port C - 2 DG (2-Deoxy-D-glucose) (25 mM) 69 μ L/well and Port D – Rotenone & Antimycin A (1 μ M each) 77 μ L/well. All given numbers represent final concentrations in the assay buffer.

2.2.3.7 Maintenance of β TC-3 cell line

Mouse pancreatic beta cell line β TC-3 (ATCC) was maintained in T-75 cm^2 cell culture flasks containing 13 – 15 mL of cell culture medium with 81.5% 4.5 g/L glucose Dulbecco's MEM (Biozym), 15% heat inactivated horse serum (Life technologies), 2.5% Fetal Bovine Serum (Life technologies) and 5 mL Penicillin-Streptomycin solution (Sigma-Aldrich). Cells were incubated in a humidified incubator at 37°C and 5% CO_2 . These cells have a doubling time of about 34 hours. Cells were sub-cultured upon reaching 80% confluency. All medium from

primary culture was removed with a sterile Pasteur pipette and the adhering cell monolayer was washed once with a small volume of 37°C PBS without Ca^{2+} and Mg^{2+} to remove any residual FBS that may inhibit the action of trypsin. Next, using mechanical disruption by adding 3 mL of 0.25% Trypsin/EDTA (Sigma-Aldrich) and incubation at 37°C for 5 minutes, the cells were dissociated to acquire a single cell suspension. 7 mL of the cell culture medium was added immediately to inactive trypsin. The entire content was transferred to a 15 mL tube and centrifuged at 290g for 5 minutes. The supernatant was discarded and the pellet was re-suspended in a suitable amount of cell culture medium and split accordingly. Alternatively, the cells were frozen down in a solution containing 70% medium, 20% FBS and 10% DMSO with about 2.5×10^6 cells per ampoule.

2.2.4 Molecular methods

2.2.4.1 RNA isolation

For total RNA extraction, tissues such as liver and hypothalamus were homogenized in 4 mL Qiazol (Qiagen) using a Heidolph DIAX 900 (Sigma-Aldrich). 1 mL of the tissue homogenate was added to a 1.5 mL tube containing 200 μL Chloroform, while the rest of the homogenate was stored at -80°C until further use. After vigorous shaking, the samples were allowed to incubate for 2-3 minutes and centrifuged for 15 min at 13000 rpm at 4°C. The colorless aqueous supernatant was transferred to a 1.5 mL and washed with an equal volume of 100% ethanol. The subsequent steps were performed using Rneasy Mini kit (Qiagen), according to the manufacturer's instructions. Briefly, the sample mixed with 100% ethanol was transferred to an Rneasy mini column and centrifuged for 1 minute at 13000 rpm, at RT. The flow through was discarded and the column was washed once with 700 μL RW1 buffer and twice with 400 μL RPE buffer. At each step the samples were centrifuged for 1 minute at 13000 rpm, at RT and decanted flow through. Finally, appropriate amount of RNase-free water was used to elute the RNA in a fresh 1.5 mL tube. RNA concentration was obtained using Nano Drop (Thermo Scientific) and stored at -80°C.

Total RNA from isolated islets was isolated by employing the Rneasy Plus Micro (Qiagen). Briefly, islets were hand-picked under a microscope with a 200 μL pipette and collected in a 1.5 mL tube, stored them on ice until all samples were ready. For a successful RNA isolation, it is advisable never to pick less than 50 islets for any one sample. The islets were collected in a pellet by centrifuging at 12000 rpm for 1 minute at RT. After carefully removing the medium, islets were lysed immediately by adding 350 μL RLT buffer plus β -mercaptoethanol (10

$\mu\text{L}/\text{mL}$) and vortexed for 30 seconds. Next, the complete sample was transferred to a gDNA eliminator spin column and centrifuged at 8000g for 30 seconds. After discarding the column, 350 μL 70% ethanol was added to the flow-through (lysate). The lysate was then transferred to an Rneasy MinElute spin column placed in a 2 mL collection tube and centrifuged at 8000g for 15 seconds. The flow-through was discarded and the bound RNA was washed once with 700 μL RW1 buffer and once with 500 μL RPE buffer and centrifuged at 8000g for 15 seconds after each buffer addition. Next, 500 μL 80% ethanol was added to the spin column and centrifuged at 8000g for 2 minutes. The pellet was dried by centrifugation at full speed for 5 minutes with the lid open. Total RNA was eluted by adding 14 μL Rnase-free water and centrifuged at full speed for 1 minute. The samples were thereafter stored at -80°C until further use.

2.2.4.2 Microarray

The Agilent 2100 Bioanalyzer in combination with the Agilent RNA 6000 Pico Kit was used to assess RNA quality, according to manufacturer's instructions. Briefly, the chip priming station was set up by adjusting the syringe and the Bioanalyzer was washed with Rnase-free water. Next, all reagents were allowed to come to RT. Gel was prepared by placing 550 μL of RNA 6000 Pico gel matrix into a spin filter and centrifuged at 1500g for 10 minutes. RNA 6000 Pico dye was centrifuged and 1 μL was added to 65 μL aliquot of filtered gel and centrifuged at 13000g for 10 minutes. 9 μL of gel-dye mix was then added to a RNA Pico chip. The plunger of the syringe at the priming station was pushed and released after 30 seconds. Next, 9 μL of RNA 6000 Pico conditioning solution, 5 μL of Pico marker and 1 μL of denatured RNA 6000 ladder was added according to marking on the chip. 1 μL of samples were then added to sample wells. The chip was vortexed for 1 minute at 2400 rpm (IKA vortex mixer) and inserted in the receptacle of the Bioanalyzer to start chip run.

Only high quality RNA ($\text{RIN}>7$) was used for further analyses which were performed by Dr. Martin Irmeler. Briefly, Total RNA (15 ng) was amplified using the Ovation PicoSL WTA System V2 in combination with the Encore Biotin Module (Nugen). Amplified cDNA was hybridized on Affymetrix Mouse Gene ST 2.0 arrays containing about 35,000 probe sets. Staining and scanning (GeneChip Scanner 3000 7G) was done according to the Affymetrix expression protocol including minor modifications as suggested in the Encore Biotin protocol. Expression console (v.1.4.1.46, Affymetrix) was used for quality control and to obtain annotated normalized RMA gene-level data (standard settings including median polish and sketch-quantile normalization). Statistical analyses were performed by utilizing the statistical

programming environment R ^[229] implemented in CARMAweb ^[230]. Gene-wise testing for differential expression was done employing the limma t-test and Benjamini-Hochberg multiple testing correction (FDR <10%). Inconsistently expressed genes in Leca2 mutants were removed by applying the following filter: ratio>20 (maximal value of a time point vs minimal value of time point). Also, known acinar-enriched genes were removed ^[231]. Heatmaps were generated with CARMAweb, cluster dendrograms and PCA were done in R (hclust).

2.2.4.3 cDNA synthesis

Synthesis of cDNA from isolated RNA from various tissues was carried out by using Superscript II enzyme, random primer mix and dNTPs. The following pre-annealing step was carried out:

| Component | Amount |
|--------------------------|---|
| RNA | Variable (20-500 ng) |
| Random primer mix (60µM) | 2 µL |
| dNTPs (10 mM) | 1 µL |
| Nuclease-free water | Variable (according to RNA concentration) |
| Final Volume | 12 µL |

The step was carried out at 65°C for 5 minutes, after which the samples were chilled on ice for at least 5 minutes and the following components were added to the test tubes:

| Component | Amount |
|------------------------|---|
| Pre annealing mix | 12 µL |
| 5x First-Strand Buffer | 4 µL |
| 0.1 M DTT | 2 µL |
| kRNaseOUT® | 1 µL (mix gently, incubate for 2 minutes) |
| SuperScript® II | 1 µL |
| Final volume | 20 µL |

After gentle mixing, the samples were first incubated for 10 minutes at 25°C and then at 42°C for 60 minutes to allow reverse transcription to take place. Enzyme activation was achieved by incubating the samples at 70°C for 15 minutes. If the samples required further dilution, nuclease free water was added to achieve a final concentration of 2.5 ng/µL. Samples were then stored –at 20°C, except a small aliquot of cDNA sample was stored at +4°C to avoid numerous freeze/thaw cycles.

2.2.4.4 Quantitative real-time Polymerase Chain Reaction (qRT-PCR)

qRT-PCR was used for the relative quantification of genes in cDNA samples, using the fluorescent cyanine dye SYBR Green I included in the LightCycler® 480 DNA SYBR Green

I Master (Roche) according to the manufacturer's instruction. The results were determined as described elsewhere [232]. cDNA from several tissues was used for relative quantifications of several genes by carrying out qRT-PCR. Primers were either taken from publications or were self-designed specifically to attain products between 100-300 bp and cross exon/exon boundaries so as to prevent the co-amplification of genomic DNA. Every set of samples from each tissue was initially checked for the most appropriate housekeeping genes (Section 2.1.3.1) with the least amount of standard deviation among all samples for normalization of relative quantities of a given target gene (Section 2.1.3.2). Two of the chosen candidate genes were then used as references for normalization, assuming the ratio between them to be identical among all samples, at all times. The following components were added to a 384 well plate in the order given below:

| Component | Amount |
|---|-----------------------------|
| Gene-specific primers (Fw+Rv) (3 μ M) | 2 μ L (0.3 μ M) |
| Nuclease-free water | Variable |
| LightCycler® 480 DNA SYBR Green I Master (2x) | 10 μ L |
| cDNA (2.5 ng/ μ L) | Variable (0.5 ng/well) |
| Final volume | 20 μL |

2.2.4.5 Protein isolation

Isolated islets collected from mice were hand-picked under a microscope with a P200 micropipette and collected in a 1.5 mL tube and stored on ice until all samples were ready. Of note, for western blots, it is advisable not to pick less than 100 islets per sample. After a brief centrifugation at 12,000 rpm for 1 minute at RT, the culture medium was removed carefully with a micropipette. The pellet was washed once with PBS without Ca²⁺ and Mg²⁺ (Lonza Verviers) and then centrifuged again at 12,000 rpm for 1 minute. The supernatant was discarded and the islets were re-suspended in 100 μ L ice-cold RIPA Lysis and Extraction Buffer (Thermo Scientific) supplemented with 1x cOmplete® Mini Protease Inhibitor Cocktail (Roche) and shaken for 30 minutes at 1,400 rpm and 4°C. Next, the samples were centrifuged at 13,000 rpm and 4°C for 10 minutes in order to dispose of any insoluble material. The supernatant was transferred to a new 1.5 mL reaction tube and stored at -80°C until use.

Liver tissue excised from mice was snap frozen in liquid nitrogen. The tissue was then homogenized at -80°C using TissueLyser (Qiagen), and lysed in 500 μ L SDS lysis Buffer containing freshly prepared CLAAAP (1:1000) (Chymostatin, Leupeptin, Antipain, Aprotinin, APMSF, Pepstatin), Phosphatase Inhibitor Cocktail 2 and 3 (1:100). Protein concentrations were obtained using Pierce BCA Protein Assay Kit (Thermo Scientific) according to

manufacturer's instructions. Briefly, 25 μL of the protein samples and albumin standards were placed in to a 96-well plate. 200 μL of the working reagent was added and incubated for 30 minutes on a plate shaker at 37°C. After allowing the plate to cool, the absorbance was measured at 562 nm using Spectramax plate reader (Molecular Devices) and corresponding protein concentrations were derived from the standard curve.

2.2.4.6 Western blot

20-40 μg of protein sample was added with 6% SDS loading buffer and heated for 5 min at 95°C. The samples and the protein ladder (Thermo Scientific) were loaded onto a 10% SDS-polyacrylamide gel (Bio-Rad). Samples were run on through the gel at 60 V for 45 minutes and then at 80-100 V for 45 minutes. PVDF membrane was activated for 10 seconds in 100% methanol, washed in Milli-Q for 5 minutes and equilibrated together with Whatman paper (GE Healthcare) and the sponges in 1x transfer buffer until use. Protein was then transferred to a PVDF membrane (GE healthcare) while running the blot at 200 mA for 90 minutes at 4°C. The membrane was blocked with 5% BSA in 1x TBST for 3 hours at RT. The blots were incubated overnight in primary antibody (Section 2.1.4.1) and washed thrice with 1x TBST before being incubated in secondary antibody (Section 2.1.5.1) for 2 hours. The membrane was washed again thrice with 1x TBST. For the detection of phosphorylated proteins, 1x TNT buffer was used instead of 1x TBST. ECL detection kit (Thermo Scientific) was used to visualize bands on a chemiluminescence film (GE Healthcare) or using ChemiDoc (Bio-Rad). Quantification of western blot images was performed using Image Studio Lite version 5.2 (LI-COR) and ImageLab® software (Bio-Rad) and expressed in arbitrary units (AU).

2.2.4.7 Measurement of insulin and glucagon

Insulin and glucagon obtained from *in vitro* stimulatory studies were analyzed using mouse insulin and glucagon ELISA kits (Mercodia) according to the manufacturer's instructions. Briefly, the supernatant and lysate samples were appropriately diluted with the calibrator 0. 10 μL of the 6 calibrators were added to the enzyme pre-coated 96 well plate. 10 μL of the samples were then added to the wells. Both samples and calibrators were added in duplicates. 100 μL of the enzyme conjugate was added and the plate was incubated at RT for 2 hours on a shaker at 800 rpm. Next, after several washing steps, 200 μL of TMB substrate was added and incubated for 15 minutes at RT. To end the reaction, 50 μL of Stop solution was added to acquire a faint yellow coloration. After briefly shaking the plate, the optical density (OD) was read at 450 nm using Spectramax 190 plate reader (Molecular Devices). Using pre-designed

Excel sheet layouts by Mercodia, OD values were calculated and insulin and glucagon concentrations were obtained.

2.2.4.8 FGF21 and Leptin ELISA

Plasma samples from fed and 6 hours fasted mice were collected as described in section 2.2.2.5. These samples were used for measuring the amount of circulating FGF21 or Leptin levels using Mouse/Rat FGF-21 or leptin Quantikine ELISA Kit (R&D Systems) according to the manufacturer's instructions. Briefly, standards were prepared by serial dilution to attain a range of 31.3-2000 pg/mL for FGF21 and 62.5-4000 pg/mL for leptin ELISA. Next, 50 μ L of Assay diluent was added to each well of a 96 well plate and 50 μ L of standards and samples (1:2 and 1:10 dilution for FGF21 and leptin ELISA, respectively) were added to the wells. After incubating for 2 hours at RT, the plate was washed using wash buffer 5 times and then 100 μ L conjugate was added and incubated for another 2 hours. After washing 5 times, 100 μ L substrate solution was added to the wells and incubated for 30 minutes in the dark. Thereafter, 100 μ L Stop Solution was added and absorbance was measured at 450 nm using a plate reader (Molecular Devices). FGF21 or leptin values were calculated by generating a log-log best fit standard curve.

2.2.5 Histology

2.2.5.1 Pancreatic tissue preparation for frozen sections

Mice were sacrificed and the excised pancreatic tissue along with the spleen was dipped into 1xPBS solution to remove any blood carryover and transferred to a 15 mL containing 1xPBS kept on ice. After all samples were collected, the pancreases were fixed in 4% PFA/PBS solution for 20 minutes on ice. The tissues were then serially incubated for one hour at each step in 9%, 15% and 30% sucrose/PBS solutions. After this, any other tissue such as fat and blood vessels attached to the pancreatic tissue was excised and the tissue was cut in the middle to obtain the head and tail part of the pancreas. The two pancreatic tissues were then embedded in optimum cutting temperature (OCT) solution (Thermo Scientific). 9-10 μ m thick sections were obtained with Leica CM1850 Cryostat (Leica Microsystems) and 3-4 sections, >300 μ m apart, were placed on a single SuperFrost® Plus slide (Menzel-Gläser). Slides were stored at -20°C.

2.2.5.2 Hypothalamic tissue preparation for frozen sections

The mice were sacrificed with CO₂ and the chest cavity was immediately opened. The heart was exposed and a needle, attached to the perfusion pump (Techlab) was inserted into the

protrusion of the left ventricle and extended straight up to 5 mm and the needle was clamped to maintain position. The pump was turned on and a slow, steady flow of 0.9% saline solution was applied to drain out the blood through a small cut made into the atrium. After clearing out the blood from the organism, the saline solution was exchanged with 4% PFA/PBS to perfuse the whole body. Next, whole the brains was excised and placed in a 50 mL tube, containing 4% PFA/TBS and stored at 4°C for 24 hours. The brains were then transferred to 30% sucrose/TBS solution for 2 days. The posterior part in the middle of the spinal cord was abscised and the brains were then embedded in OCT, with their anterior part facing out. Cross-sectional cuts, with thickness of 30 µm, were achieved from anterior to posterior. The hypothalamic slices were collected and stored at -20°C.

2.2.5.3 Immunohistochemistry for frozen pancreatic sections

The slides with pancreatic sections were washed twice with 1x PBS for 10 minutes and once with ddH₂O. The sections were then permeabilized twice with 0.1% Tween20/PBS for 10 minutes each. After two further washes with 1x PBS for 10 minutes each, the sections were marked with PAP-Pen (Enzo) so as to contain the solutions over the sections and avoid slippage. The sections were then blocked with 5% BSA for 3 hours at RT. and subsequently incubated with appropriate primary antibodies (Section 2.1.4.2) overnight at 4°C. The sections were then incubated with the appropriate secondary antibodies (Section 2.1.5.2), at RT for 90 minutes and mounted with Vectashield® Mounting Medium (Vector Laboratories, USA). Slides were examined and analyzed using Nanozoomer (Hammamatsu) and images were acquired using confocal Leica TCS SP5 microscope (Leica).

2.2.5.4 Immunohistochemistry for frozen hypothalamic sections

Free floating hypothalamic slices were blocked with SUMI for 2 hours at RT, following which the sections are incubated with primary antibodies (Section 2.1.4.2) overnight at 4°C. The sections were then washed thrice with 1x TBS and then further incubated with secondary antibodies (Section 2.1.5.2) for 1 hour at RT. The slices were then carefully placed over a slide and dried at RT. DAPI was further added and the slide was finally covered with a cover slide and stored away at 4°C.

2.2.5.5 Acquisition and quantification of insulin and glucagon expression

Whole section images of islets, liver and hypothalamus were acquired from Nanozoomer (Hammamatsu) while separate islet and liver images were obtained using NDP.view 2 (Hammamatsu). Using ImageJ, hormone positive islet cells or hormone positive cell area was measured in the islet images and percent threshold for glycogen storage was measured in

images of liver sections. Final confocal images of islets as well as hypothalamic regions were obtained using Leica TCS SP5 microscope.

2.2.6 Tissue preparation for chromatin immunoprecipitation and next generation sequencing (ChIP-seq)

Mice aged 10-12 weeks were euthanized by the means of cervical dislocation and hypothalami were excised and snap frozen in liquid nitrogen. 6 samples per genotyped were pooled and the company Active Motif performed the next steps of ChIP-seq. Additionally, two ampoules of β -TC3 (section 2.2.3.8) cells were collected and frozen (1×10^6 cells/ampoule) according to Active Motif's instructions for antibody validation. Briefly, 1/10 volume of freshly prepared formaldehyde solution was added to the media in each culture flask (Corning) and agitated for exactly 15 minutes RT to fix the cells. To stop the fixation, 1/20 volume glycine solution was added to the existing media and allowed to incubate for 5 minutes. After the glycine incubation, cells were washed by transferring contents of each container to a 15 mL falcon tube and centrifuged at $800 \times g$ in a refrigerated centrifuge for 10 minutes to pellet the cells. The supernatant was discarded and cells were re-suspended in 10 mL chilled PBS-Igepal and centrifuged again to pellet the cells. The supernatant was discarded and 10 mL chilled PBS-Igepal and 100 μ L PMSF (100 mM prepared in ethanol; Sigma-Aldrich) was added to each tube and the cells re-suspended. After another centrifugation, the cells were pelleted and snap frozen on dry ice and stored away at -80°C .

3. RESULTS

3.1 Characterization of islets of homozygous *Pax6*^{Leca2} mice

3.1.1 Reduction in the number of beta cells and centralization of alpha cells in mutant islets

As discussed earlier, PAX6 plays a role in the development of the endocrine lineage and certain mutations have shown a delay in the eventual consequence of losing functional PAX6 [131]. Therefore, we used immunohistochemistry to delineate whether the mutation affects the islet morphology at prenatal stage or after birth. Previously in our group, no difference was found in the percentage of glucagon and insulin positive cells at the embryonic stage E18.5 between the homozygous mutants and wildtype littermates [226]. Therefore, investigation was taken up to determine the effects of the homozygous Leca2 mutation on hormone positive cells within the islet, shortly after weaning up to adulthood. Thus, pancreata were excised from mutant as well as wildtype mice and processed for immunohistological investigations. We observed normal islet images in the wildtype, displaying glucagon positive α -cells on the periphery and centralized insulin positive β -cells (Figure 3.1). On the other hand, α -cells tended to localize towards the center rather than the periphery of the islet in the *Pax6*^{Leca2} mutants with noticeably reduced insulin positive staining (Figure 3.1). Furthermore, upon quantifying hormone positive cells, a clear decrease in insulin positive beta cells was observed in the islets of *Pax6*^{Leca2} mice wherein >30% less insulin positive cells were found, a pattern seen in all ages that were analyzed (Figure 3.2A-C). Previous studies have shown that *Pax6*-null mice display lower number of β -cells and a virtual lack of α -cells making it indispensable for the development of mature α -cells [27, 28]. Although glucagon positive cells showed a trend towards a modest decrease in their number, surprisingly however, no significant differences were found between the groups (Figure 3.2D-F). In addition, the islet size was found to be similar between the groups (Figure 3.1G-I), suggesting the overall islet architecture to be intact.

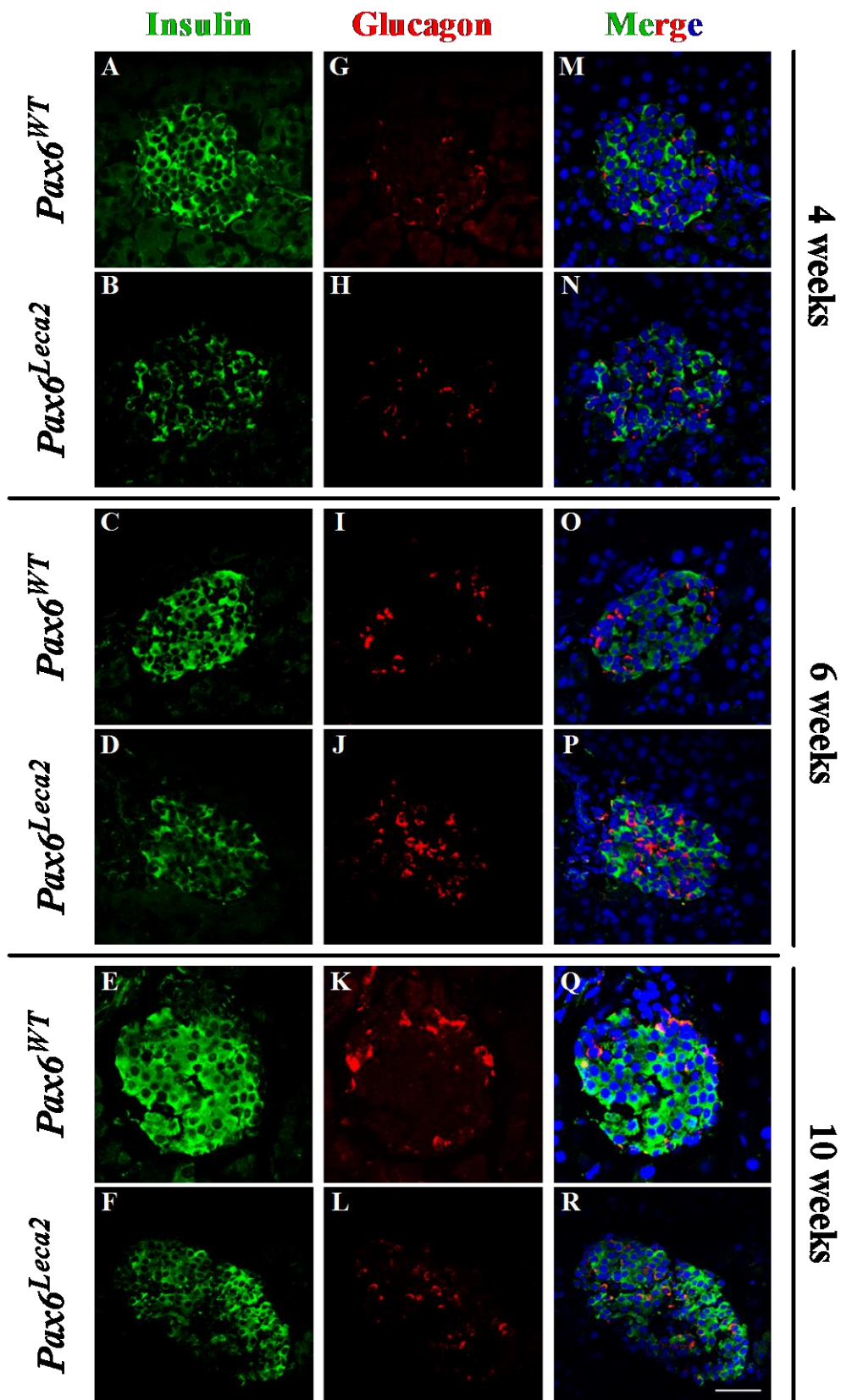


Figure 3.1: Effects of *Leca2* mutation on islet morphology

The left panel (A-F) shows distribution of insulin positive β -cells and the center panel (G-L) glucagon positive α -cells. The right panel (M-R), displays merged images of insulin (green), glucagon (red) and DAPI (blue) stainings; $n=3$. Scale bar (white) represents 50 μm . Images were acquired using Leica TCS SP5 microscope.

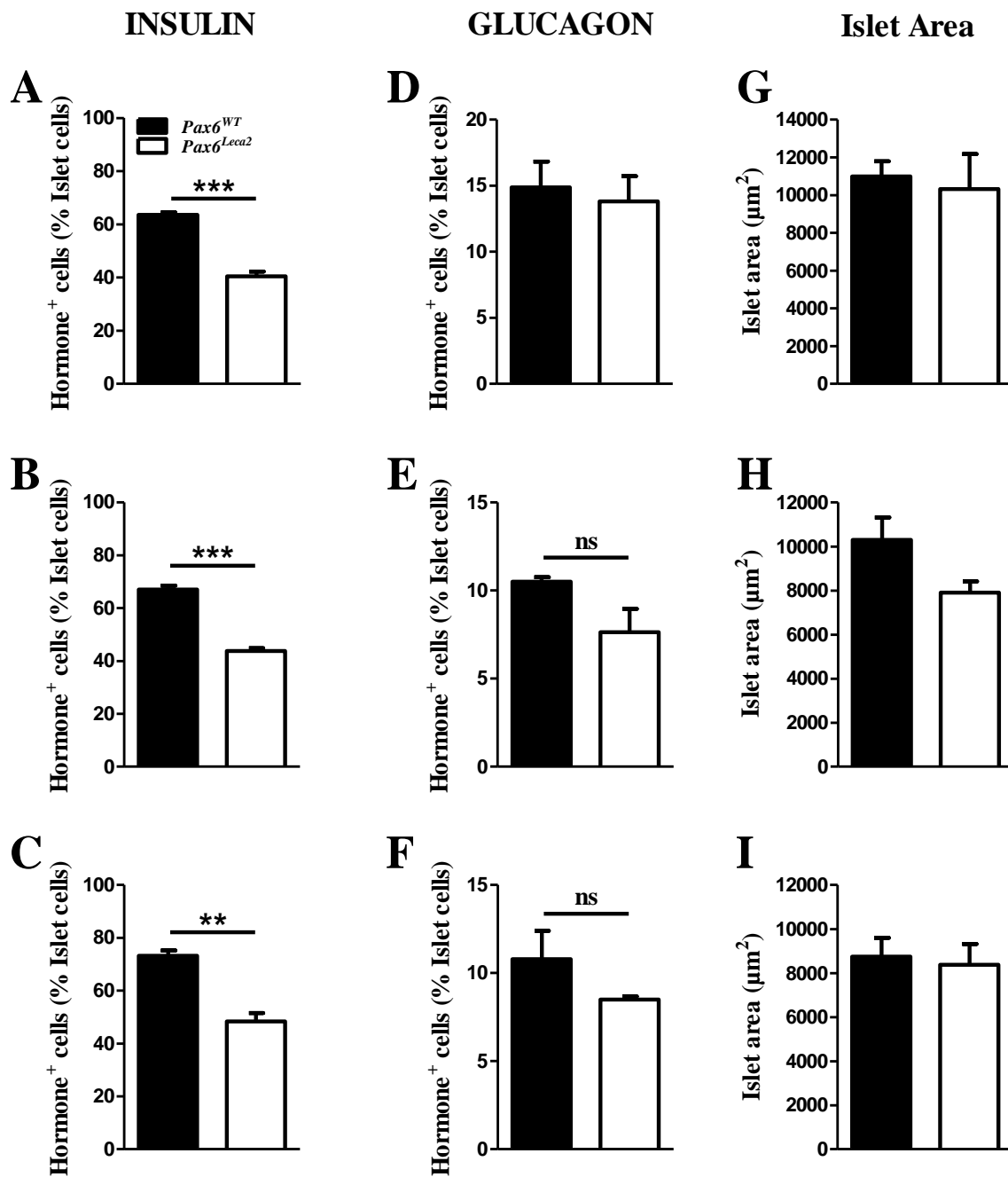


Figure 3.2: Quantification of hormone positive endocrine cells

(A-C) Show quantified insulin positive cells of 4, 6 & 10 week old mice respectively. (D-F) show quantified glucagon positive cells of 4, 6 & 10 week old mice. (G-I) show quantified islet area of 4, 6 & 10 week old mice; $n=3$; 32.1 ± 7.1 $Pax6^{Leca2}$ islets and 44.1 ± 9.0 $Pax6^{WT}$ islets per mouse & age. Error bars display standard error of mean (SEM) values. Differences were considered statistically significant at $p < 0.05$ using a two tailed Student's t test (** < 0.01, *** < 0.001, ns = non-significant).

Since the overall islet size was similar between the groups and the islet structure intact, we wondered whether other hormone positive cells were affected in islets. PAX6 has been shown to bind to promoter regions of somatostatin [28] and loss of $Pax6$ transdifferentiates the β -cells into ghrelin positive ϵ -cells [98-101]. Therefore, we investigated hormone expression in δ - and ϵ -

cells in the islets. As shown in figure 3.3 (A-C), we observed a near-2 fold increase in ghrelin positive cells in islets of *Pax6^{Leca2}* mice was observed without any obvious change the number of somatostatin positive cells (Figure 3.3 D-E), although quantification for it was not carried out.

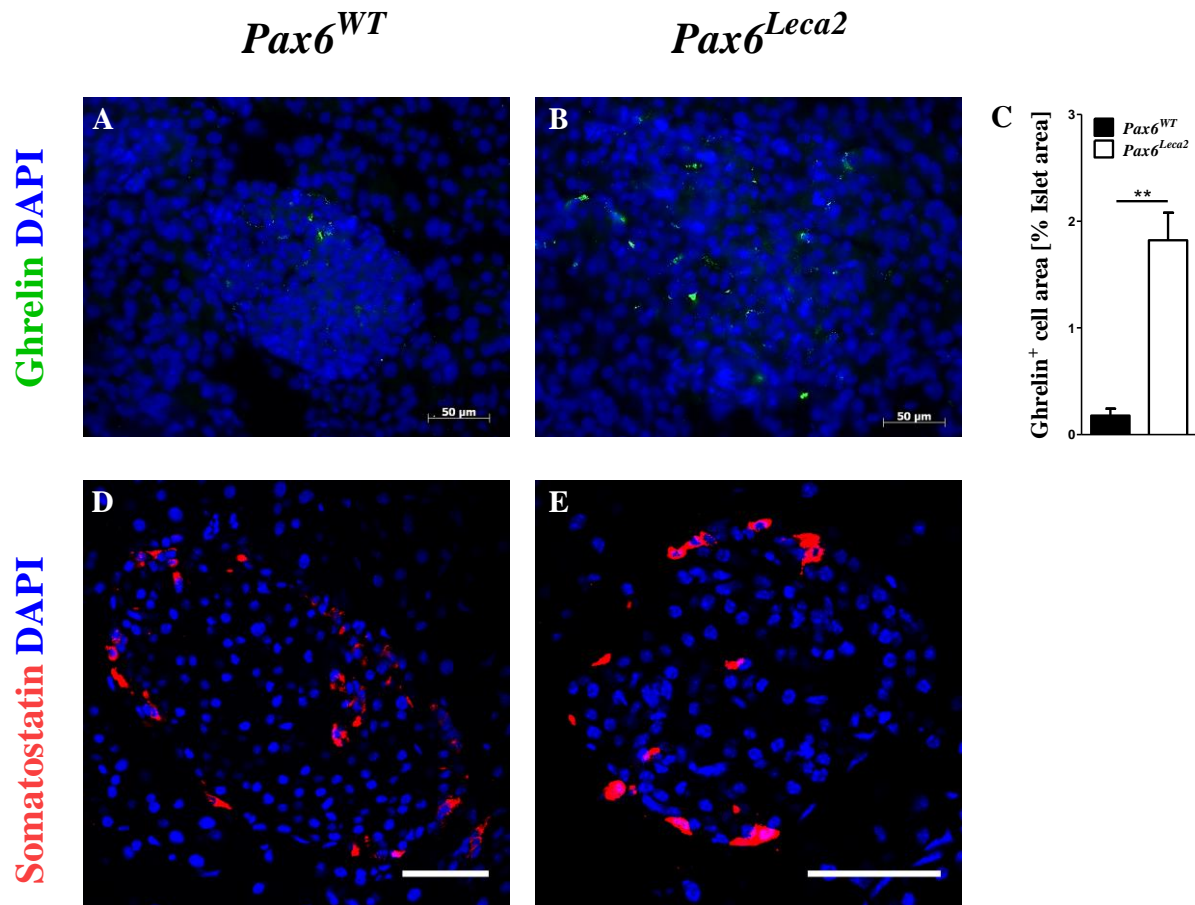


Figure 3.3: Histological expression and localization of islet hormones

(A-B) Expression and localization of ghrelin and (C) quantification of hormone positive cells in the islets; n=3, 14.3±6.3 islets per mouse. (D-E) Expression and localization of somatostatin expression in the islets of 10 week old male mice; n=3. Scale bar (white) represents 50 μm. Error bars display standard error of mean (SEM) values. Differences were considered statistically significant at p < 0.05 using a two tailed Student's t test (** < 0.01). Images were acquired using Axioplan II (Zeiss) and Leica TCS SP5 microscope.

Furthermore, expression of the β-cell marker PDX1 and the endocrine marker PAX6 in islets was investigated. As shown in figure 3.4, the expression of PDX1 and PAX6 positive cells look largely similar between the groups. In summary, the *Leca2* mutation produces major changes in insulin expressing β-cells and shows an inherent increase in ghrelin positive cells as seen in other *Pax6* mutants. This hints at alterations in the transcriptome and possible functional changes in β-cells of the *Pax6^{Leca2}* mice.

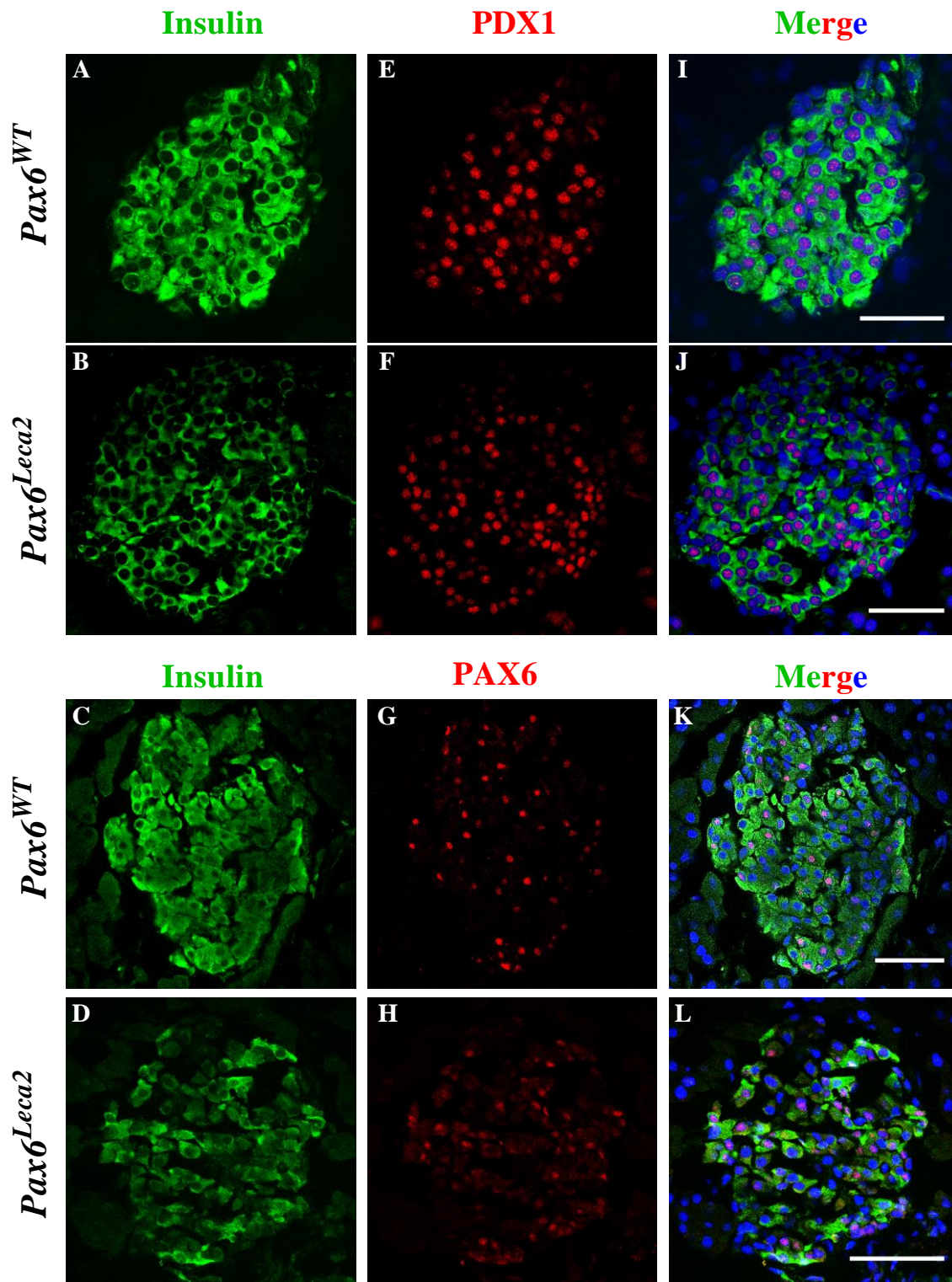


Figure 3.4: Histological expression of β -cell markers

The left panel (A-D) shows distribution of insulin positive β -cells and the center panel (E-H) PDX1 or PAX6 positive endocrine cells. The right panel (I-L), displays merged images of insulin (green), PDX/PAX6 (red) and DAPI (blue) stainings; n=3. Scale bar (white) represents 50 μ m. Images were acquired using Leica TCS SP5 microscope.

3.1.2 Differential expression of transcriptome of *Pax6^{Leca2}* isolated islets

Having observed differences in hormonal expression in the mutant islets, we investigated whether markers for mature and functional β -cells were affected. Using similar strategy as that for histology, RNA from isolated islets of mice from several ages was acquired. Microarray RNA expression analysis was then carried out which revealed numerous genes regulated in the islets of *Pax6^{Leca2}* mice, as depicted in (Figure 3.5A), where a fold change (FC) of 1.5 and FDR <10% was considered statistically significant. As expected, important changes in β -cell markers and genes conferring identity and functional attributes affected in the *Pax6^{Leca2}* mice seem to occur as early as 4 weeks with over 500 genes dysregulated (Supplementary table 1).

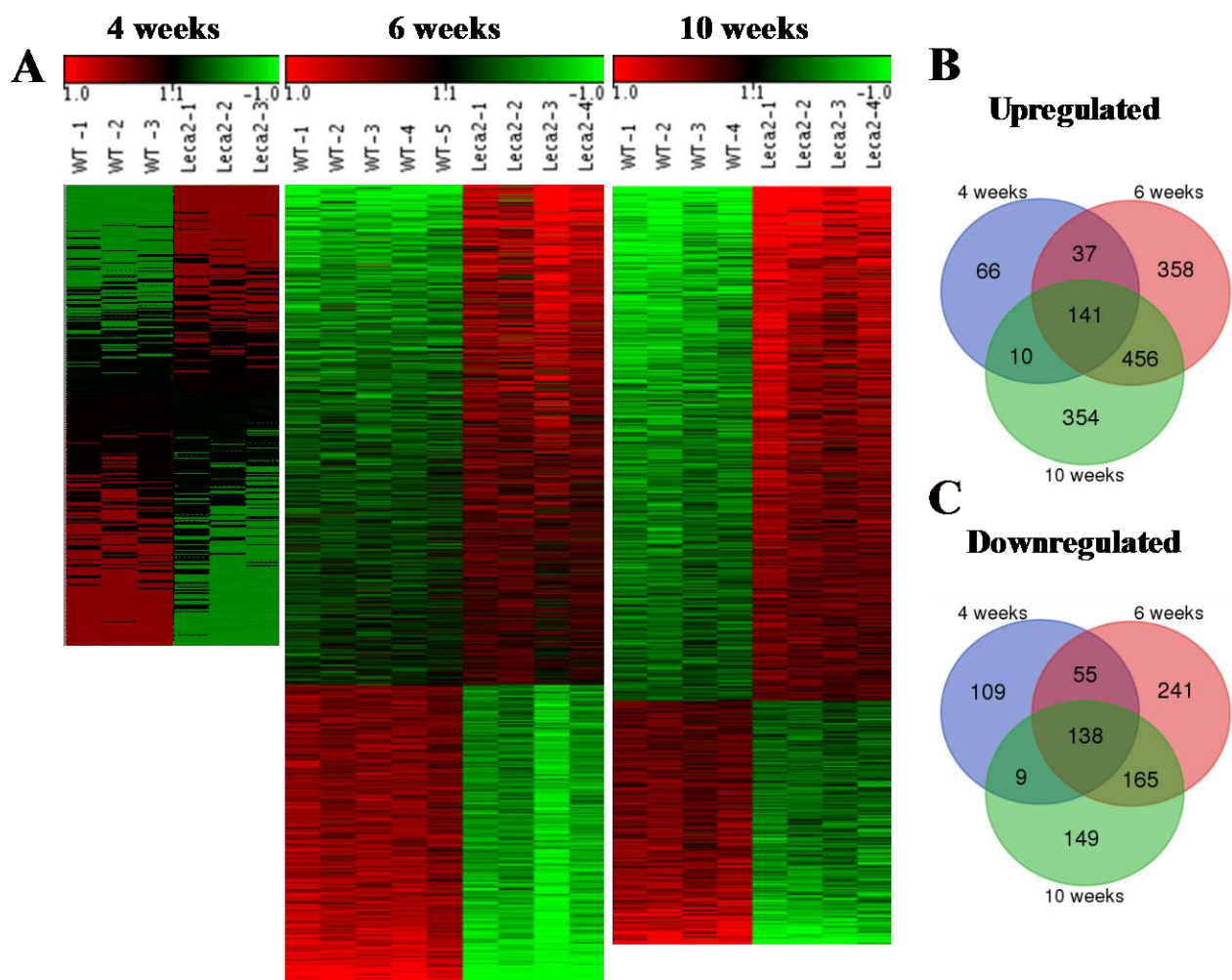


Figure 3.5: Transcriptome changes contributed by the *Leca2* mutation

(A) Microarray heat maps display regulation of various genes using RNA from isolated islets from mice aged 4, 6 & 10 weeks. (B-C) A comparative diagram showing number of genes similarly regulated between the different age groups in the mutant. Genes were filtered for a fold change of at least 1.5 (FDR <10%).

Interestingly, a progressive change in the transcriptome was observed between the ages 4 and 6 weeks with over 1600 genes dysregulated at 6 weeks of age in the *Pax6^{Leca2}* mice (Figure

3.5B-C, Supplementary table 2). A similar result was obtained previously by our lab [226], although the differences were observed between 4 and 20 week old mice. Here, by this new approach, an evident change in the transcriptome is already set in motion in the islets of 6 week old homozygous mutant mice. Moreover, similar changes were found between ages 6 and 10 weeks, suggesting that major changes in the transcriptome already take place by week 6 (Figure 3.5B-C, Supplementary table 3). Recently, a role for PAX6 as TF conferring both repressive and stimulating activity on genes was suggested [99]. Interestingly, a higher number of genes were upregulated in all data sets suggesting that the RED subdomain may confer a repressive role for the TF. Next, using Genomatix GeneRanker® tool, gene ontology (GO) of dysregulated genes in 10 weeks old mice revealed a plethora of significantly affected metabolic pathways, most notable of which were insulin secretion and neurogenesis.

| GO term | P-value | List of observed genes | ID |
|--|----------|---|------------|
| Regulation of neurogenesis | 5,36E-11 | <i>Skil, Itm2c, Nrep, Sgk1, Pax6, Plxna1, Syne1, Cdh2, Adcyap1, Ptprg, Dab2, Gli3, Brinp1, Zswim6, Ptprz1, Tnr, Tgfb1, Serpine2, Ngf, Cxcl12, Cpeb1, Vim, Unc13a, Mef2c, Prrx1, Dusp10, Vldlr, Syt17, Thy1, Magi2, Timp2, Ntrk2, Ptprd, Negr1, Kalrn, Flna, Nap112, Eya1, Ephb2, Etv5, Lyn, Il6st, Kdr, Jag1, Nrcam, Ccl5, Sez6, Lrp1, Cnr1, Robo1, Csf1, Tspo, Tenm4, Ascl1, Rapgef4, Robo2, Prkch, Arhgef2, Star, Nrp1, Tlr2, Sdc2, Neurog3, H2-K1, Sema3e, Igf1r, Ulk1, Ednrb, Map4k4, Heyl, Scn1b, Dbn1, Cdh4, Dnm3, Cit, F2, P2ry12, Spock1, Grin1, Sema4a, Plxnb1, EphA7, Il6</i> | GO:0050767 |
| Insulin secretion | 2,30E-07 | <i>Nnat, Sox4, Nr1d1, Cd38, Gpr119, Nr1h4, Oxct1, Cartpt, Pfkfb2, G6pc2, Vgf, Ucn3, Syt9, Sytl4, Ccl5, Cnr1, Rfx6, Rapgef4, Lrp5, Ffar1, Aacs, Map4k4, Ano1, Cpt1a, Pck2, Rbp4, Abat, Ucp2, Glp1r</i> | GO:0030073 |
| Glucose homeostasis | 5,02E-07 | <i>Ero11b, Pax6, Sox4, Nr1d1, Nr1h4, Oxct1, Cartpt, Icam1, G6pc2, Vgf, Ffar3, Prcp, Rph3al, Aqp4, Cnr1, Rfx6, Ern1, Lrp5, Igf1r, Ffar1, Aacs, Adgrf5, Map4k4, Pdk2, Ano1, Gcgr, Rbp4, Vcam1, Ucp2, Il6</i> | GO:0042593 |
| Carboxylic acid metabolic process | 1,27E-06 | <i>Yars, Sars, Cyp4v3, Iars, Slco1a5, Mars, Nr1d1, Pycr1, Tars, Psph, Cygb, Pdpn, Hdac4, Cbs, Gpt2, Nr1h4, Pfkfb2, Cd74, Adh1, Gnpda1, Aldh5a1, Cryl1, Aldh1a2, Slco1a6, Eprs, Got1, Asns, Psat1, Nmnat2, Idh1, Fa2h, Dhdkd1, Cars, Atp2b4, Galk1, Ggh, Cnr1, Gne, Pcx, Fh1, Aldh1a3, Ddah2, Cad, Gfpt2, Rbp1, Mpc1, C3, Star, Tat, Cyp39a1, Scd2, Tlr2, Gars, Aacs, Slc27a4, Pdk2, Cpt1a, Me2, Eci2, Pck2, Trib3, Btd, Erlin1, Ddc, Lars, Ivd, Abat, Aldh18a1</i> | GO:0019752 |

Table 3.1: GO term analysis of dysregulated gene set in Pax6^{Leca2} mice

GeneRanker® tool was used to reveal GO terms of regulated genes in islets obtained from microarray analysis of 10 week old male mice.

The most relevant and highly enriched GO terms are summarized in (Table 3.1). To get a closer look into possibly affected mechanisms, RT-qPCR was performed to check for individual gene

expressions of genes related to β -cell markers, insulin secretion and several enzymes as well as receptors, and in turn to validate the results acquired from the microarray analysis.

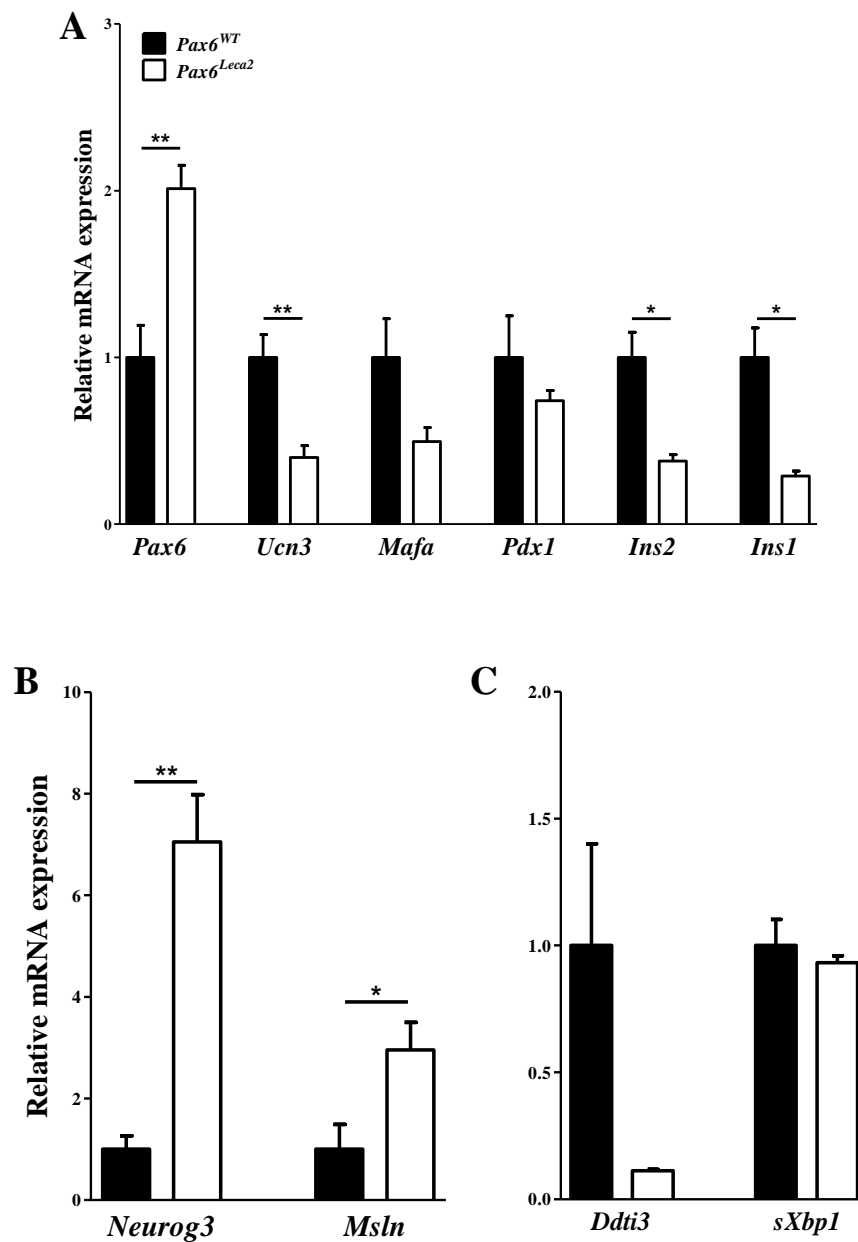


Figure 3.6: Dysregulated genes conferring identity to β -cells

qPCR validation of microarray in RNA isolated from islets of 10 week old male mice display dysregulation of several important (A) β -cell mature (B) dedifferentiation and (C) apoptotic markers; $n=3-4$. Error bars display SEM values. Differences were considered statistically significant at $p < 0.05$ using a two tailed Student's t test (* < 0.05 , ** < 0.01 , *** < 0.001).

Both of the insulin gene isoforms, *Ins1* and *Ins2* were found to be significantly downregulated (Figure 3.6A) and several β -cells markers such as *Mafa* and *Pdx1* showed a non-significant trend towards reduced expression (Figure 6A). *Pax6* itself was not found to be downregulated

(Figure 3.6A). Instead, an increase in its expression was detected at 10 weeks of age in the islets of *Pax6^{Leca2}* mice, a feature observed elsewhere in cortices of the same mutant model [225].

Interestingly, maturity marker urocortin3, *Ucn3* [233] was downregulated and proliferation and dedifferentiation markers mesothelin, *Msln* [234] and *Neurog3* [20, 235] were upregulated in isolated islets of *Pax6^{Leca2}* mice (Figure 3.6A-B). Considering that proliferation was increased in the islets of *Pax6^{Leca2}* mice as previously stated, we hypothesized that β -cell death may not be the reason behind lack of insulin positive cells. Indeed, the endoplasmic reticulum stress markers *Ddit3* and spliced X-box binding protein 1 (*sXbp1*) did not show any significant increase (Figure 3.6C); instead *Ddit3* (encoding CHOP) was downregulated in the microarray dataset (FC -4.64, Supplementary table 3). Additionally, several genes involved in neurogenesis were also seen to be particularly upregulated in the mutant islets, most notably of which was the cannabinoid receptor 1 (*Cnr1*), with an upregulation of 7.21 fold (Supplementary table 3).

Various enzymes such as *Pcx* (pyruvate carboxylase), *G6pc2* (glucose-6-phosphatase catalytic subunit 2) and *Pfkfb2* (6-phosphofructo-2-kinase/fructose-2,6-biphosphatase 2), were among the dysregulated gene set suggesting changes in the glycolytic pathway and TCA cycle (Figure 3.7A). No change in K_{ATP} channel subunits sulfonylurea receptor 1 SUR1, (encoded by *Abcc8*) and inward-rectifier potassium ion channel Kir6.2, (encoded by *Kcnj11*) was observed confirming their absence in the dysregulated gene set in microarray analysis (Figure 3.7A). Recently, a study in rodents lacking the *Pax6* gene specifically in the β -cells showed increase in glucokinase activity accompanied with a reduction in the main glucose transporter GLUT2 (encoded by *Slc2a2*) [100]. Interestingly, expression of *Gck* as well as *Slc2a2* was unchanged (Figure 3.7A) suggesting β -cell glucose sensing and uptake, unlike in the β -cell specific *Pax6* knockout, might be unaffected in *Pax6^{Leca2}* islets. Hence, the data not only suggests partial loss of β -cell identity but also hints at disturbances in pathways contributing to insulin secretion. In support of this conjecture, receptors conferring incretin stimulatory effects such as *Glp1r* (glucagon-like peptide 1 receptor), as well as *Gcgr* (glucagon receptor), *Igf1r* (insulin-like growth factor 1 receptor), and *Syt4* (synaptotagmin-like 4) among others were downregulated (Figure 3.7B). *Ffar1*, (free fatty acid receptor 1), also known as *Gpr40* and a direct target of PAX6 [213], was virtually undetectable in the RNA extracted from islets of *Pax6^{Leca2}* mice (Figure 3.7B). Taken together, the microarray analysis strongly suggests partial loss of β -cell identity and disturbances in insulin secretion in the islets of *Pax6^{Leca2}* mice.

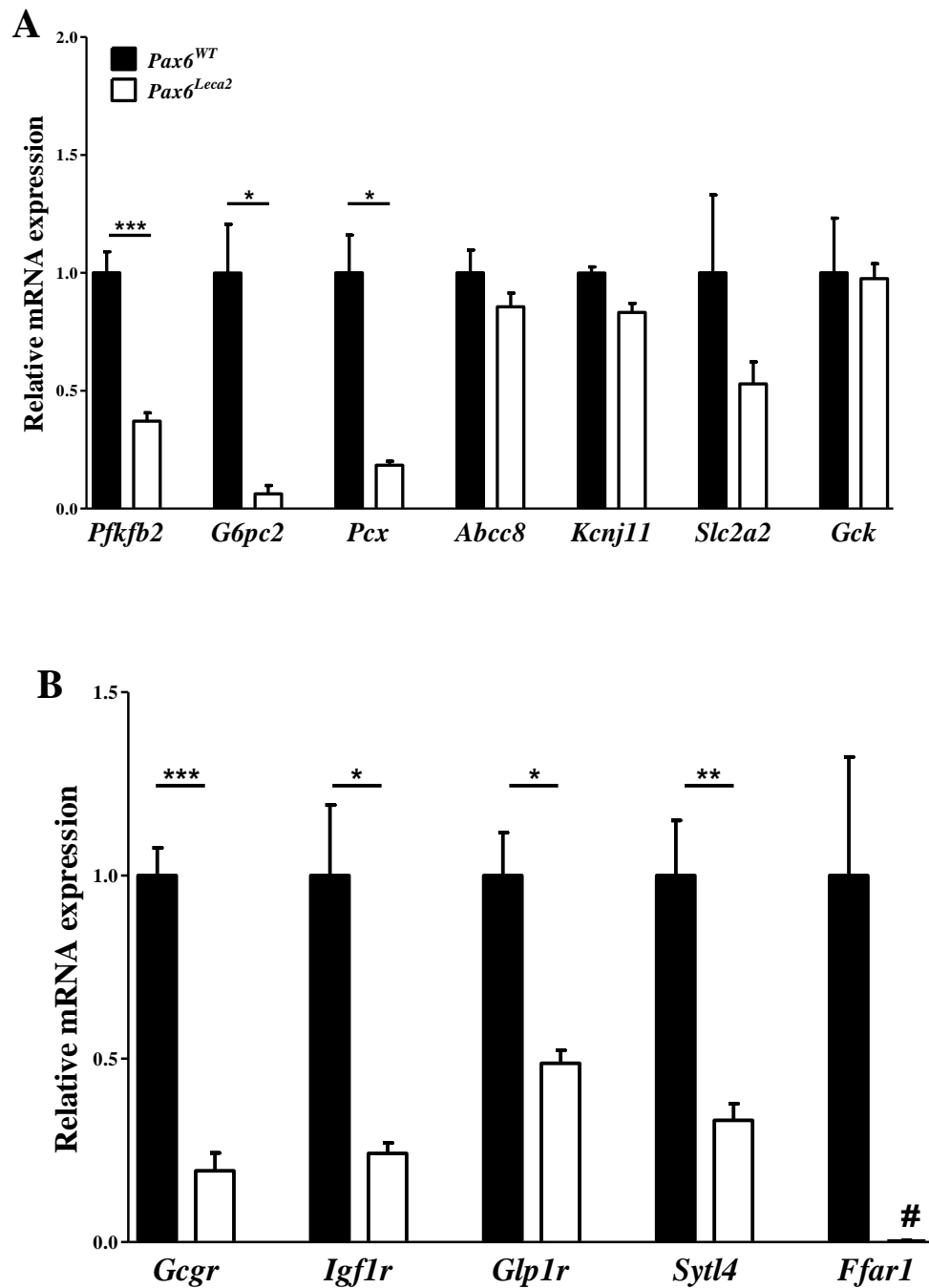


Figure 3.7: Dysregulated genes conferring functional attributes to β -cells

qPCR validation of microarray in RNA isolated from islets of 10 week old male mice display dysregulation of several important (A) enzymes and (B) receptors and genes related to secretion of insulin; n=3-4. Error bars display SEM values. Differences were considered statistically significant at $p < 0.05$ using a two tailed Student's t test (* < 0.05 , ** < 0.01 , *** < 0.001 , # = undetectable, qPCR cycles > 30).

3.1.3 Loss of insulin secretory mechanism in *Pax6*^{Leca2} mice

To further confirm whether the R128C mutation of PAX6 contributes to a faulty insulin secretory mechanism as indicated by dysregulation of genes conferring this particular attribute to the β -cells, islets were isolated from mice and *in vitro* investigations were undertaken at 4,

6 and 10 weeks of age. As observed earlier, the insulin content of islets from *Pax6^{Leca2}* mutants was reduced about 40-50% at all ages analyzed (Figure 3.8A, Supplementary figure 1A & 2A). No significant changes were observed, in the content as well as in the secretion of glucagon at low glucose concentration (2.8 mM), which is in accordance to the histological results where similar number of glucagon positive cells were observed (Figure 3.8B-C, Supplementary figure 1B-C & 2B-C). To test the secretory capacity of the β -cells upon stimulation with glucose, a glucose stimulated insulin secretion (GSIS) assay was carried out. As expected, the results revealed a lack of sufficient increase in insulin secretion between basal (2.8 mM) to high (12 mM) glucose concentrations in the islets of *Pax6^{Leca2}* mutants as compared to the wildtype mice (Figure 3.7D, Supplementary figure 1D & 2D).

Furthermore, stimulation with KCl, which depolarizes the cell membrane and closes the K_{ATP} channels, only slightly, albeit non-significantly increased insulin secretion above the basal level (Figure 3.8D, Supplementary figure 1D & 2D). Moreover, only a modest increase in insulin secretion was observed when *Pax6^{Leca2}* islets were stimulated with the GLP-1 analog exendin-4, in 10 week old mice (Figure 3.8D). However, when stimulated with forskolin, *Pax6^{Leca2}* islets showed a substantial increase in insulin secretion at all ages (Figure 3.8D, Supplementary figure 1D & 2D), suggesting that the reduced capacity to secrete insulin in response to incretins lies at the receptor level as evident by their dysregulation which is bypassed by the cAMP enhancer, forskolin. Indeed, when insulin secretion was calculated as per total insulin content of the islet, no significant difference was found between the 4 and 6 weeks old groups (Figure 3.9A-B). Thus, these data again hints at a progressive nature of the mutation and its effects so that the insulin secretory capacity *per se* is only lost at the age of 10 weeks (Figure 3.9C). Therefore physiologically, incretins cannot act as the stimulus for insulin secretion due to downregulation of GPCRs. Taken together, the gene expression analysis and the *in vitro* assays paint a picture wherein not only the loss of insulin content but also the loss of its subsequent secretion, contribute to the phenotype of *Pax6^{Leca2}* mice.

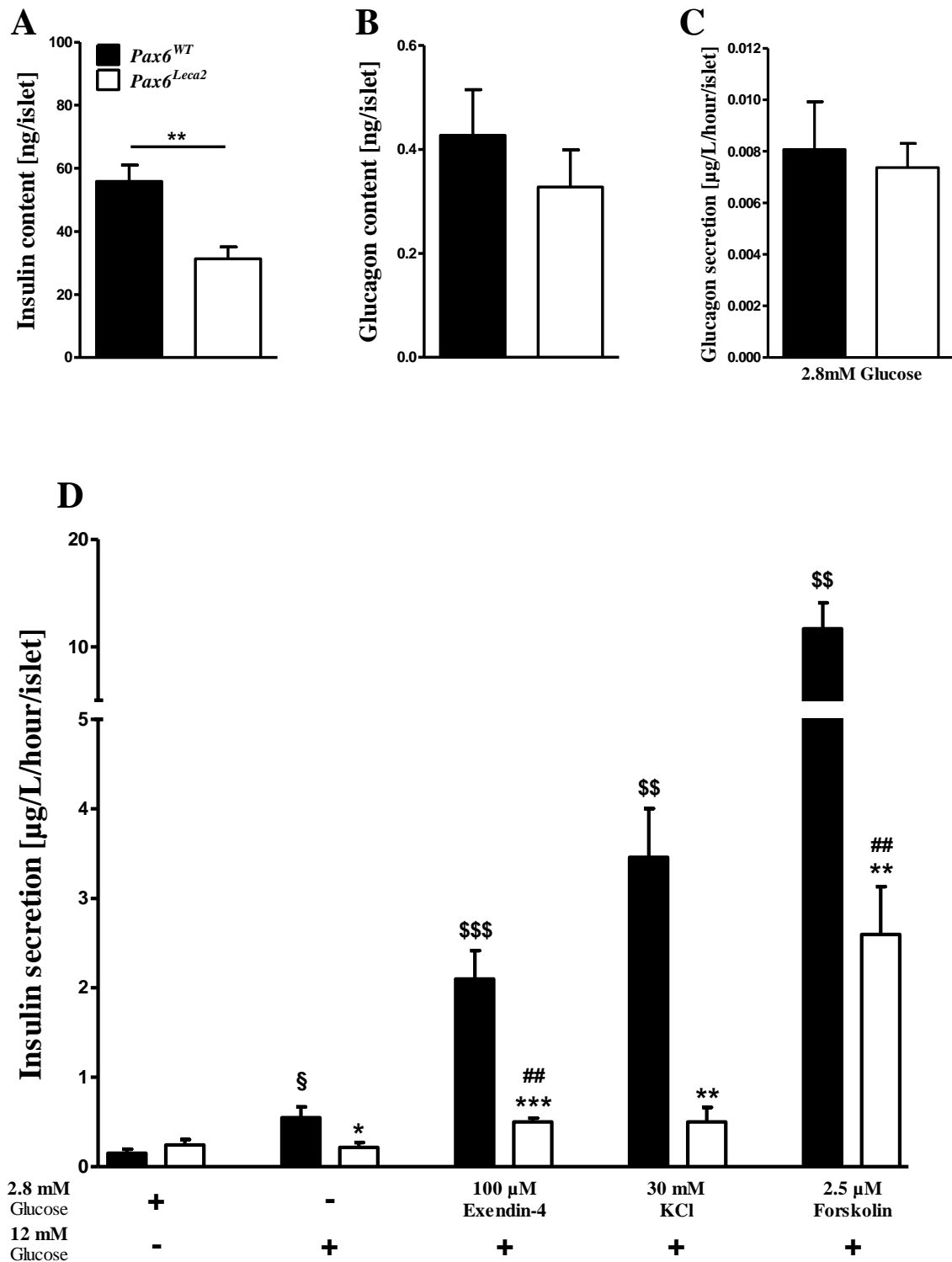


Figure 3.8: In vitro analysis of hormonal content and secretory capacity in 10 weeks old mice

(A) Reduced amount of insulin in isolated islets of 10 weeks old male mice as identified by insulin ELISA. (B) Glucagon content and (C) glucagon secretion seem to be normal in mutants. (D) β -cells in the mutant islets have dramatically reduced capacity to secrete insulin following stimulation with several secretagogues, n=5-10. Error bars display SEM values. Differences were considered statistically significant at $p < 0.05$ using a two tailed Student's *t* test. * = *Pax6*^{Leca2} vs *Pax6*^{WT}, § = vs 2.8mM *Pax6*^{WT}, § = vs 12mM *Pax6*^{WT}, # = vs 12mM *Pax6*^{Leca2}, §, * < 0.05, \$\$, ##, ** < 0.01, \$\$\$, *** < 0.001).

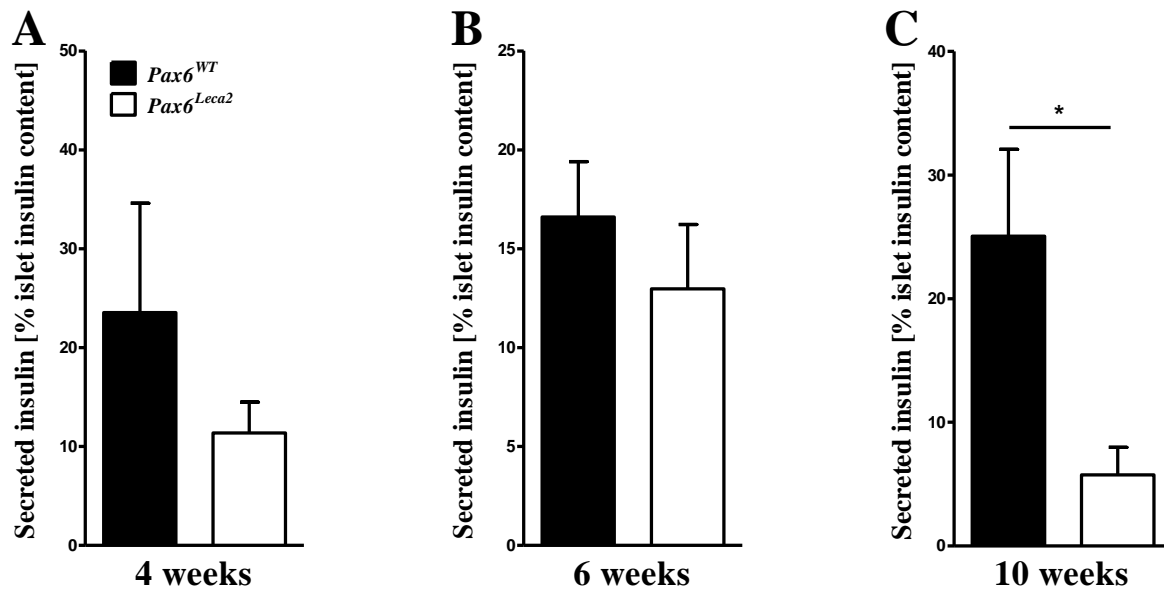


Figure 3.9: Insulin secretion upon forskolin stimulation

(A-C) Insulin secreted by β -cells of mice at different ages. The amount of secreted insulin is normalized to the amount of insulin present in the β -cells; n=5-10 Error bars display SEM values. Differences were considered statistically significant at $p < 0.05$ using a two tailed Student's t test (* < 0.05).

3.2 Metabolic features of homozygous $Pax6^{Leca2}$ mice

3.2.1 Lower body weight and blood glucose levels

Unlike other homozygous $Pax6$ mutants that are either embryonic lethal or die shortly after birth [27, 208, 225], homozygous $Pax6^{Leca2}$ mice grow to adulthood, are fertile and are born with an almost Mendelian ratio [225]. Weekly measurements of *ad libitum* fed body weight and tail blood glucose levels from the stage of weaning until 10 weeks of age revealed significant reduction in body mass (Figure 3.10A), and astonishingly, significantly lower blood glucose levels (Figure 3.10B). This was highly surprising considering the islets display no change in insulin increment upon stimulation with glucose *in vitro* (Figure 3.8D). Moreover, these changes in body weight and blood glucose occur from as early as 3 weeks of age and are maintained throughout lifetime. This unexpected result required further validation, for which *in vivo* glucose challenge tests were performed.

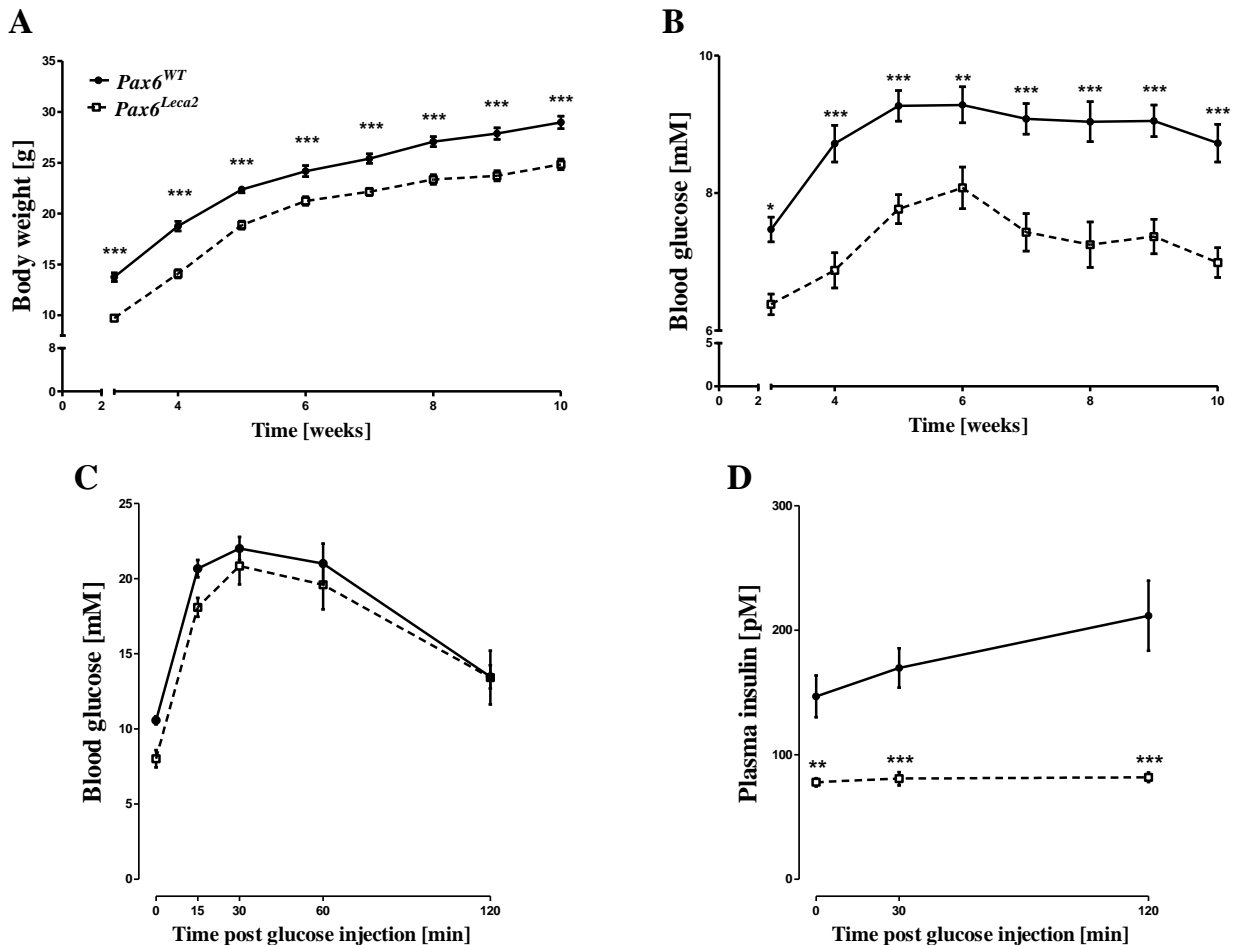


Figure 3.10: Glucose homeostasis

Weekly measurements of (A) body weight and (B) blood glucose demonstrated reduction in both parameters at weaning and beyond; $n=14-19$. A glucose challenge test showed normal tolerance (C) in the absence of insulin increment in 10-12 week old male mutant mice (D); $n=12-13$. Error bars display SEM values. Differences were considered statistically significant at $p < 0.05$ using two-way ANOVA (Bonferroni) (* < 0.05 , ** < 0.01 , *** < 0.001).

An intraperitoneal (ip) administration of glucose to 6 hours fasted mice showed normal disposal of glucose in the $Pax6^{Leca2}$ mice and no significant differences were found between the groups (Figure 3.10C). Moreover, 6 hour fasting plasma insulin levels were reduced in agreement with *in vitro* results. However, insulin increment during a glucose challenge, unlike that observed in the wildtype mice, was completely lost in the mutants and these mice produced only low basal levels of insulin (Figure 3.10D). Although this was expected, it is rather puzzling as to how $Pax6^{Leca2}$ mice are able to metabolize glucose without any inherent increase in insulin levels. The findings essentially show that $Pax6^{Leca2}$ mice maintain below normal blood glucose levels at *ad libitum* fed and 6 hours fasted state while metabolizing glucose at a rate similar to their wildtype counterparts.

3.2.2 Differences in energy expenditure, food intake and locomotor activity

To determine whether physiological traits of the *Pax6^{Leca2}* mice were changed, several parameters were measured using indirect calorimetry. Using this method, conclusions regarding the metabolic state can be made by precisely measuring energy expenditure, food intake as well as physical activity which in turn gives a global view on the metabolic state of an organism, while maintaining certain biochemical assumptions [236]. Therefore, 10-12 week old mice were kept in metabolic cages (TSE Systems) over a period of 6 days. The mice were allowed to acclimate to the cage environment for 24 hours and several parameters were measured thereafter for a period of 5 days. Several genotype-related changes were observed during the active (between 18:00 and 6:00) and inactive phase (between 6:00 and 18:00). Active phase is a reflection of a predominantly fed state while inactive phase mirrors a predominantly fasting state. Mice from both groups showed similar oxygen consumption rate during the active and inactive phase (Figure 3.11A) but *Pax6^{Leca2}* mice showed increased RER (Figure 3.11B), specifically during the inactive phase. Moreover, locomotor activity as well as food intake was significantly and concurrently increased during the inactive phase (Figure 3.11C-D) in the *Pax6^{Leca2}* mice as compared to the wildtype mice. During feeding under normal conditions, carbohydrates take precedence as the primary source of metabolic fuel and therefore an increase in carbohydrate oxidation is observed during feeding, i.e. the active phase and a simultaneous decrease in lipid oxidation. The opposite trend is observed during fasting and this feature is termed 'metabolic flexibility' [237]. Indeed, this was observed in wildtype mice in the present study (Figure 3.11E-F). Conversely, *Pax6^{Leca2}* mice displayed altered substrate utilization and seemed to be inclined towards a higher oxidation of carbohydrates during the inactive phase which is concomitant with overall increased food intake, and consequently resulted in a decrease in lipid oxidation (Figure 3.11E-F). To investigate the possibility of loss of lipids and its derivatives through defecation, a FT/IR was performed (see [238] for method description). This, however, did not indicate any differences in lipid content of the fecal matter (data not shown). Moreover, *Pax6^{Leca2}* mice did not display an increase in absolute fat mass; instead NMR demonstrated decreased fat and lean mass and hence overall body weight in *Pax6^{Leca2}* mice (Figure 3.11G-I).

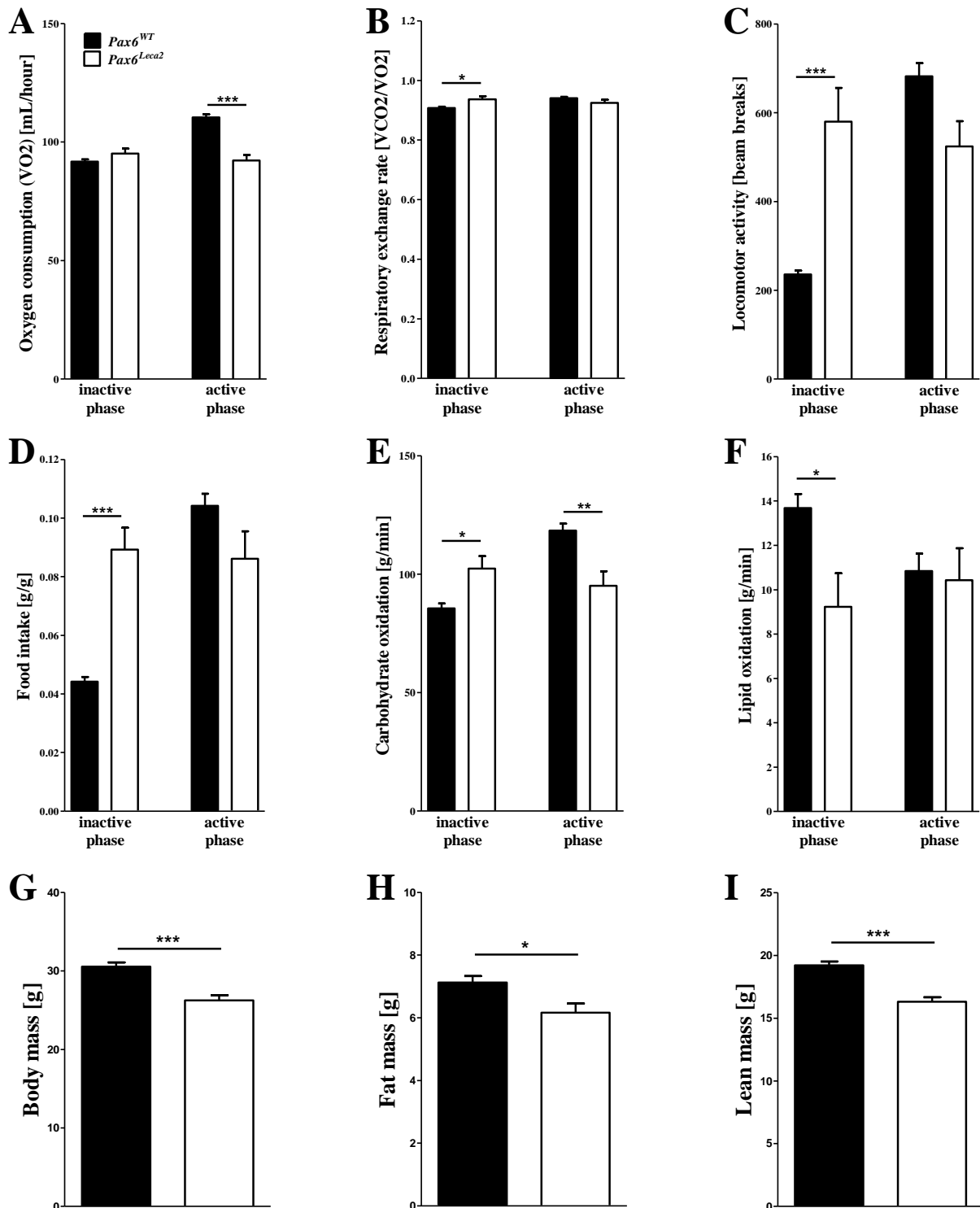


Figure 3.11: Energy expenditure and body composition

Indirect calorimetry, averaged over 5 days in metabolic cages, demonstrated an increase in (F-H) RER, locomotor activity and food intake along with increased carbohydrate oxidation paralleled with decreased lipid oxidation during the inactive phase; n=13-19; 10-12 week old male mice. (G) NMR spectroscopy revealed differences in body mass composition between the groups. (H-I) Reduced lean mass and fat mass was observed in the mutant mice; n=23-25. Error bars display SEM values. Differences were considered statistically significant at $p < 0.05$ using a two tailed Student's t test or one-way ANOVA (Bonferroni) (* < 0.05 , ** < 0.01 , *** < 0.001).

However, linear regression analysis by taking the body mass as a covariate showed an increase in fat mass ($p < 0.0001$) and a decrease in lean mass ($p < 0.0001$) (Supplementary figure 3). Taken together, *Pax6^{Leca2}* mice showed an increase in food intake while at the same time a reduced body weight which leads to strongly suggest an increase in energy expenditure reflected in increased locomotion and RER.

3.2.3 Increased insulin sensitivity and reduced hepatic glucose output

Although increase in energy expenditure positively increases glucose disposal and might to some extent support lower glucose levels at fasting and fed states, it may not completely explain the normal glucose turnover without insulin increment during the glucose tolerance test. This led to the obvious question of how the *Pax6^{Leca2}* mice compensate for the lack of insulin. To this end, we carried out an insulin tolerance test after a 6 hour fasting period. As shown in Figure 3.12A-B, a modest exogenous insulin dose of 0.5 U/kg lowered the blood glucose levels in *Pax6^{Leca2}* mice to a higher degree than in wildtype mice, indicating increased sensitivity to insulin.

To further affirm the acquired enhanced ability to lower glucose in response to insulin, we utilized the gold standard method to evaluate whole body insulin sensitivity, a hyperinsulinemic-euglycaemic clamp. The blood glucose levels were brought to comparable values for the entire length of the experiment (Figure 3.12C). As expected, the amount of glucose required to be infused in the mice to maintain similar levels, termed glucose infusion rate (GIR) was highly increased in *Pax6^{Leca2}* mice indicating increased peripheral insulin sensitivity (Fig 3.12D).

Furthermore, this increased response to insulin could be derived from either increased uptake of glucose by peripheral tissues or by reduced hepatic output. Indeed, *Pax6^{Leca2}* mice showed a dramatic reduction in hepatic glucose production and an increased suppression of glucose secretion from the liver in presence of insulin (Figure 3.13A-B). Surprisingly, no significant alterations were observed in total glucose turnover or glucose uptake by peripheral tissues, although a small trend towards increased glucose uptake by epididymal white adipose tissue (WAT) and liver was observed, albeit non-significantly (Figure 3.13C-D).

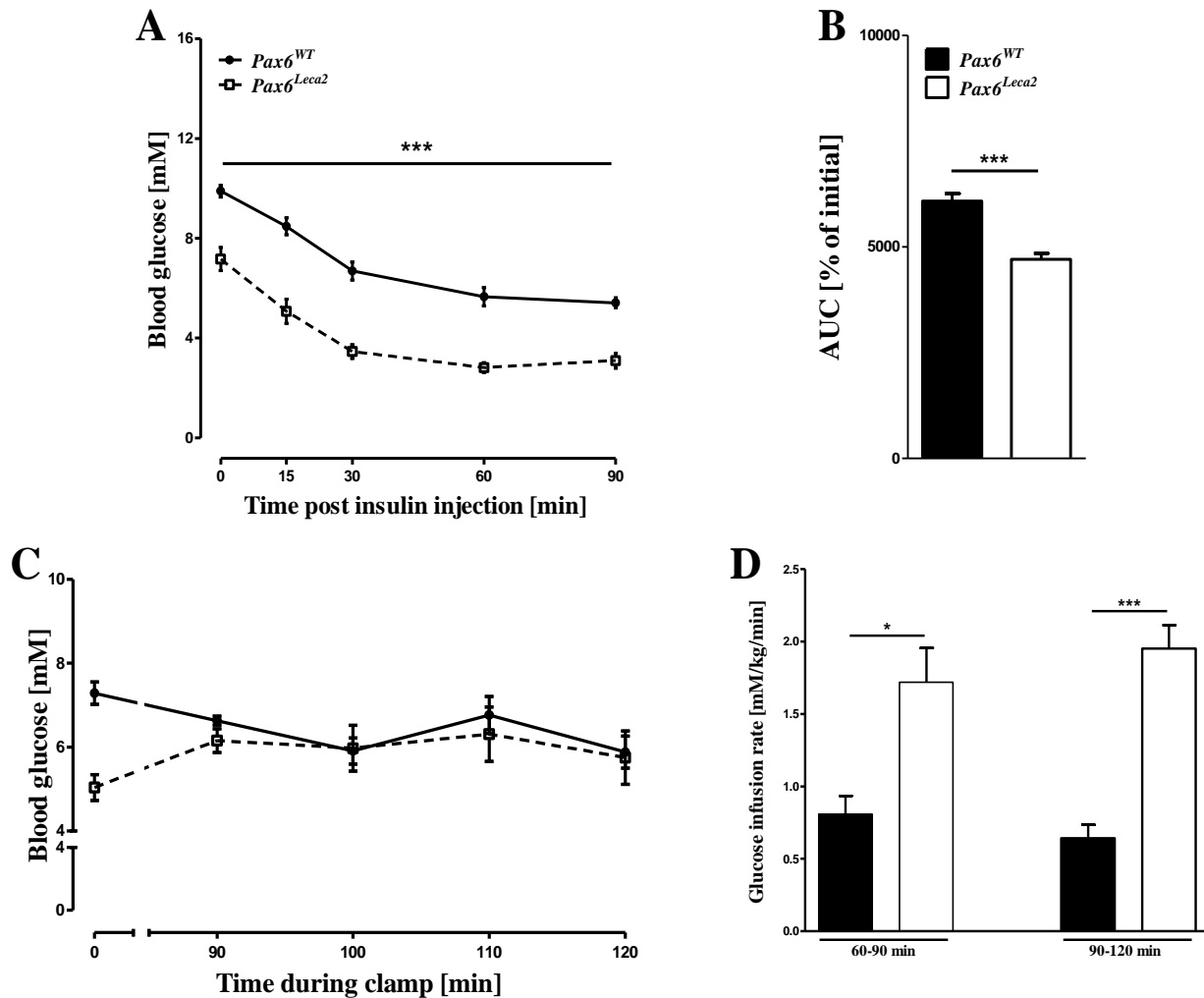


Figure 3.12: Glucose lowering efficiency in response to exogenous insulin

(A) An intraperitoneal insulin tolerance test (0.5 U/Kg of insulin) revealed higher response to the glucose lowering effect of insulin in mutant mice, further exemplified by (B) decrease in blood glucose values against basal values. (C) With the help of hyperinsulinemic-euglycaemic clamp, an increase in the (D) glucose infusion rate was clearly demonstrated in 10-12 week old male mice; n=6-8. Error bars display SEM values. Differences were considered statistically significant at $p < 0.05$ using a two tailed Student's t test, two or one-way ANOVA (Bonferroni) (* < 0.05 , ** < 0.01 , *** < 0.001).

To exclude loss of glucose through micturition, urine was collected at the end of the clamp experiment and glucose values were checked. No significant differences were found in excretion of glucose via the urinary tract suggesting normal absorbance of glucose in the kidneys (Figure 3.13E). Taken together, absence of a hyperglycemic state in *Pax6*^{Leca2} mice, which lack the ability to increase insulin secretion upon glucose stimulation, is at least in part, driven by an increased response of the liver to insulin that ultimately leads to a reduction in glucose output.

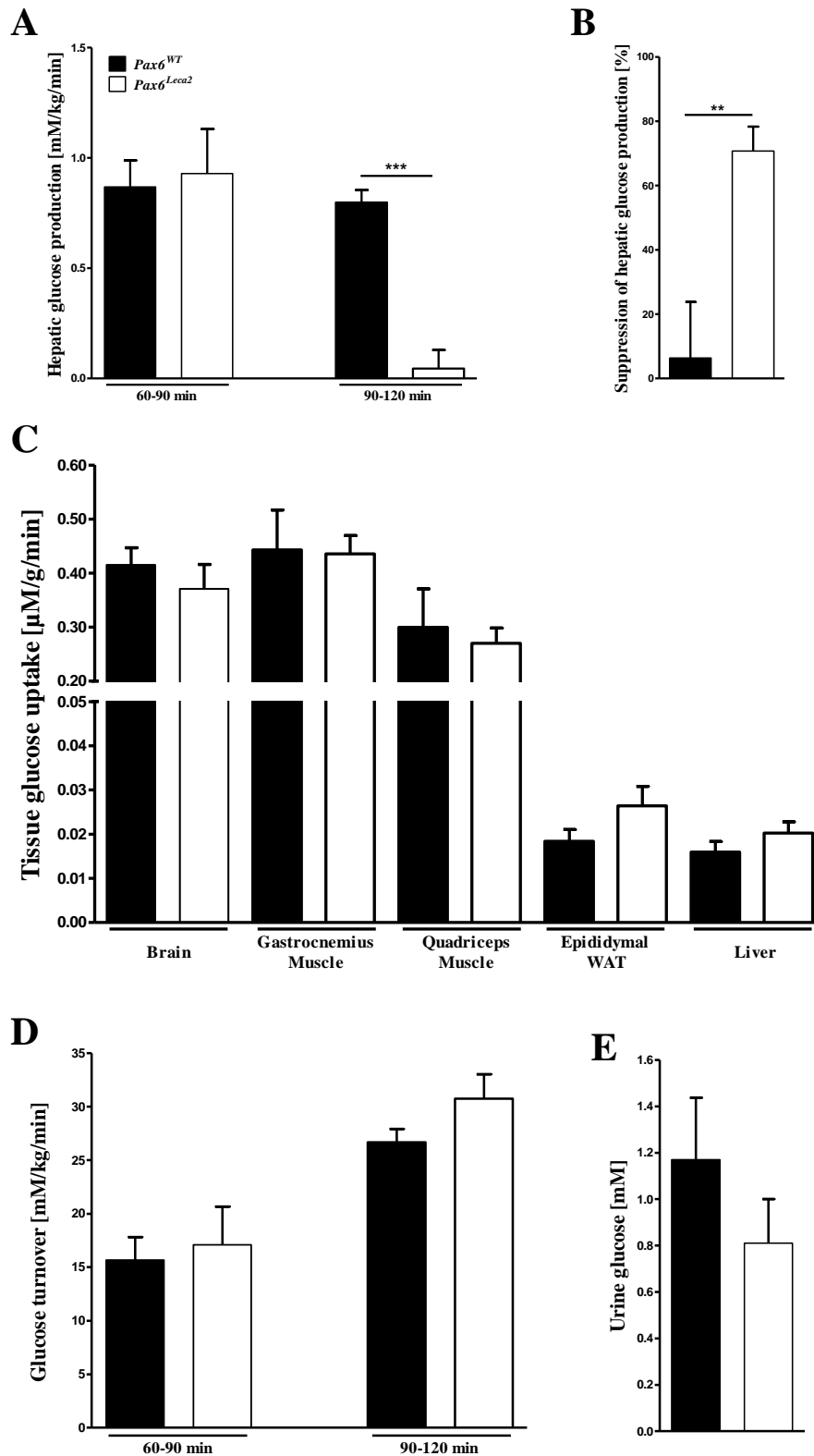


Figure 3.13: Hepatic glucose production and glucose uptake

(A) Hepatic glucose production during hyperinsulinemic-euglycaemic clamp displayed reduced HGP and increased (B) suppression of HGP. (C) Total glucose uptake in peripheral tissues and (D) total glucose turnover were found to be similar between the groups as was the (E) loss of glucose via micturition in 10-12 week old male mice; n=6. Error bars display SEM values. Differences were considered statistically significant at $p < 0.05$ using a two tailed Student's t test or one-way ANOVA (Bonferroni) (** < 0.01 , *** < 0.001).

3.2.4 Molecular signatures for insulin signaling and compensatory liver function

The data collected thus far strongly pointed at liver having acquired increased sensitivity to insulin whereby glucose secretion from the organ was dramatically reduced in the *Pax6^{Leca2}* mice (Figure 3.12 & 3.13). Indirect calorimetry data clearly showed that changes between the inactive phase and active phase were rather small for *Pax6^{Leca2}* mutants as opposed to changes for the wildtype. This prompted an investigation into the function of liver during fed *ad libitum* state, where insulin and glucose driven signaling pathways are switched on and 6 hours fasted state, where insulin opposing glucagon signaling becomes predominant. Thus, RNA from livers of fed and fasted mice were collected and analyzed for expressions of 4 important gluconeogenic enzymes. As shown in figure 3.14, during the *ad libitum* fed states, genes of rate limiting enzymes *G6pc* [239] as well as *Pck1* were significantly downregulated in the *Pax6^{Leca2}* mice with normal levels of *Fbp1*, (fructose-1,6-bisphosphatase 1) and *Pcx* (Figure 3.14A-D). This is accordance to reduced HGP when effects of insulin signaling and glucose inhibit glycogen breakdown and gluconeogenesis. Interestingly, the opposite regulation of these genes was observed in the mutant mice during the 6 hour fasted state. Here the mRNA expressions of *G6pc*, *Pcx* and even *Fbp1* were significantly increased in the liver of *Pax6^{Leca2}* mice. The expression of *Pck1* was not significantly different, although a dramatic increase in its expression as compared to the *ad libitum* fed levels was evident. Nevertheless, this might be a compensatory mechanism to cope with the dramatic decrease in HGP during fed states which itself seems to be the predominant state, regardless of the time of day (Figure 3.11D).

One important revelation was made for wildtype that only *Pck1* showed a significant increase in its regulation and a modest, non-significant increase in *Pcx* (Figure 3.14A&C) as a consequence of 6 hour fasting period in the wildtype suggesting longer periods of fasting might be required to see changes in mRNA regulation of these enzymes. On the contrary, the transition from fed state to a 6 hours fasted state was able to elicit an increase in the mRNA levels of all the enzymes analyzed in the liver of *Pax6^{Leca2}* mice. This however, further potentiates that a mere 6 hour fasting period elicits glucagon driven effects in the liver to indeed cope with reduced blood glucose levels in the *Pax6^{Leca2}* mice.

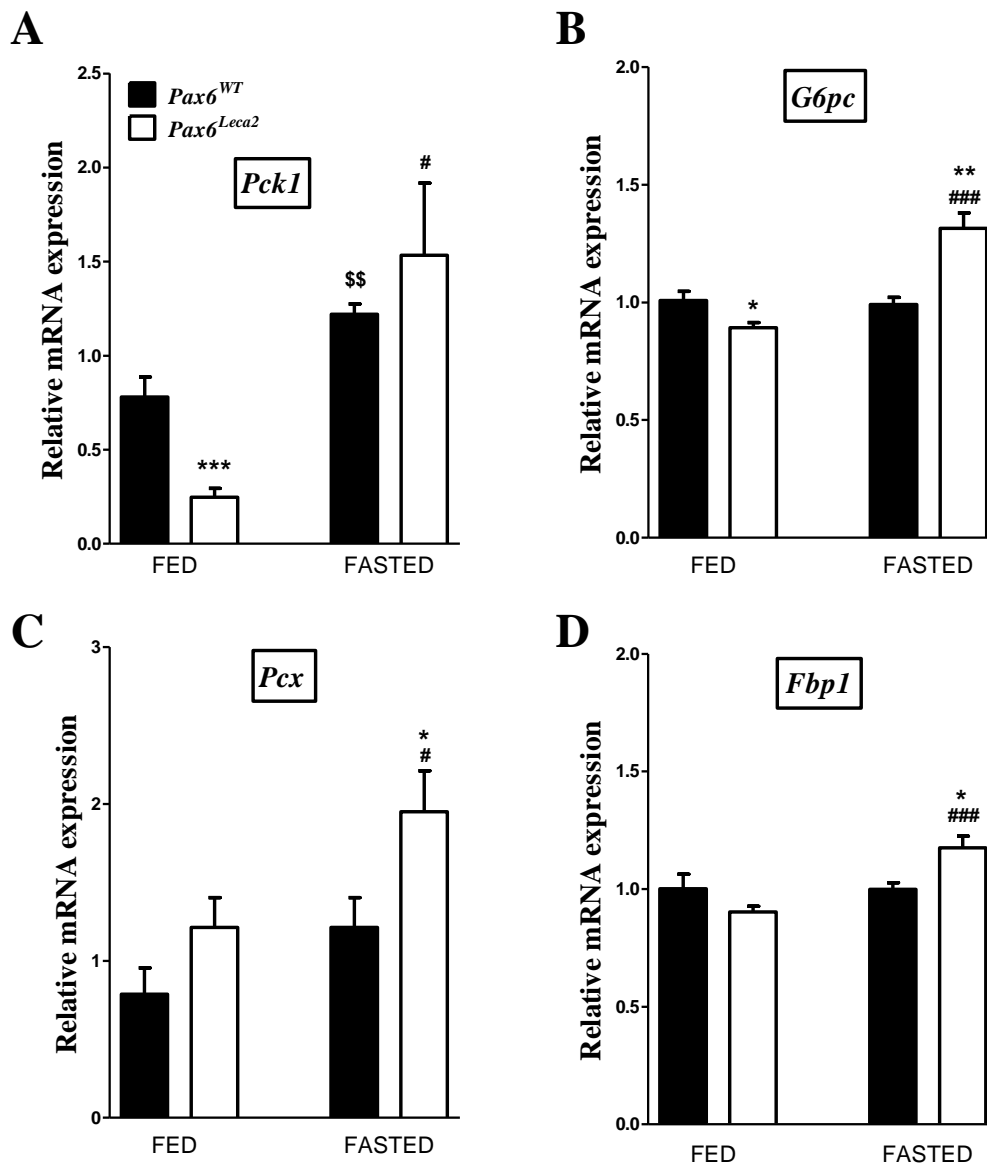


Figure 3.14: mRNA expressions of gluconeogenic enzymes

(A) mRNA expression of *Pck1*, (B) *G6pc*, (C) *Pcx* and (D) *Fbp1* in ad libitum fed and 6 hours fasted 14 week old male mice; n=5-6. Error bars display SEM values. Differences were considered statistically significant at $p < 0.05$ using a two tailed Student's t test - * = *Pax6*^{Leca2} vs *Pax6*^{WT}, \$ = fast vs fed *Pax6*^{WT}, # = vs fast vs fed *Pax6*^{Leca2} (*, # < 0.05, **, \$\$ < 0.01, ***, ### < 0.001).

To further demonstrate molecular changes contributing to this phenotype of mutant mice, 1 U/kg of insulin was administered to mice and their organs were rapidly excised after a brief period of 10 minutes. The insulin signaling pathway essentially targets phosphorylation of AKT at both residues Thr³⁰⁸ and Ser⁴⁷³ whereby it is activated [240], eventually causing nuclear exclusion of phosphorylated FOXO1 [153, 154] and affecting further downstream targets. Hence, protein from liver lysates was prepared and western blots were performed. Indeed, an increased expression of P-AKT^{Thr308} was clearly observed in the mutant mice (Figure 3.16A). AKT

inactivated FOXO1 in turn reduces the transcription of downstream targets such as enzymes glucose-6-phosphatase (G6PC) and phosphoenolpyruvate carboxykinase 1 (PEPCK) and thereby switching off gluconeogenesis in the liver in presence of insulin [241]. Expressions of PEPCK, G6PC and PCX, all showed a trend towards reduced protein amounts although only amounts for PEPCK were significantly reduced. The data here further affirms that livers of *Pax6^{Leca2}* mice have enhanced response to insulin and its subsequent effects.

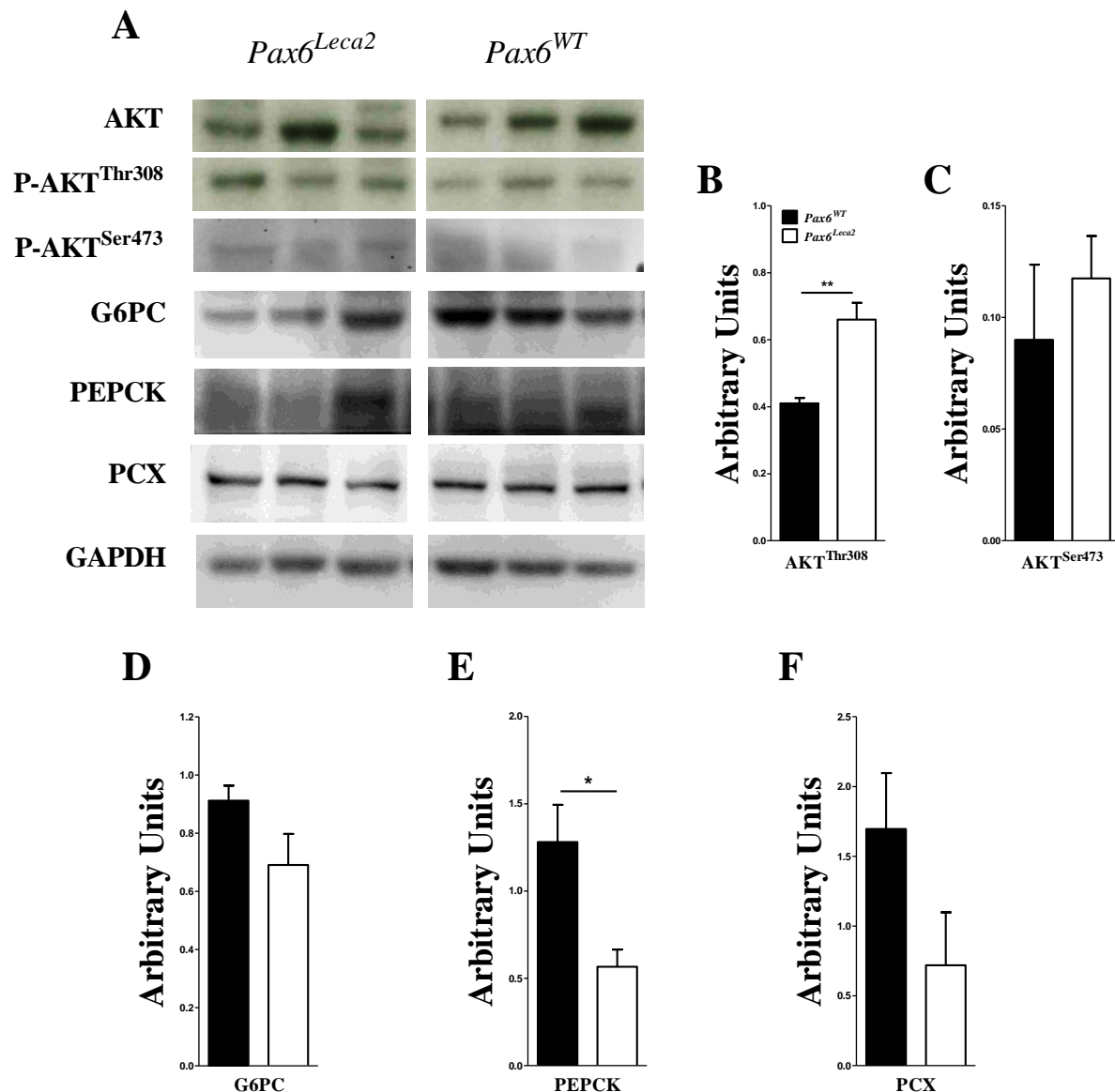


Figure 3.15: Protein expressions of gluconeogenic enzymes and insulin signaling intermediates

(A) Representative images of protein expressions of AKT and phosphorylated AKT (P-AKT) as well as that of gluconeogenic enzymes in 14 weeks old male mice. Quantification of protein bands for (B-C) P-AKT normalized to AKT and (D) G6PC, (E) PEPCK as well as (F) PCX normalized to GAPDH; n=3-4. Images were acquired using Bio-Rad ChemiDoc and quantification was done by using ImageLab® software (Bio-Rad). Error bars display SEM values. Differences were considered statistically significant at $p < 0.05$ using a two tailed Student's t test (** < 0.01).

The aforementioned experimental results clearly showed that liver glucose output was stunted in the *Pax6^{Leca2}* mice. To put the data into a physiological context, two separate challenge tests were performed to investigate the glycogenolytic and gluconeogenic pathway. After a 6 hour fasting period, the mice were either injected with an exogenous load of glucagon to demonstrate the state of the islet-liver axis or with sodium-pyruvate to address the gluconeogenic potential of the liver.

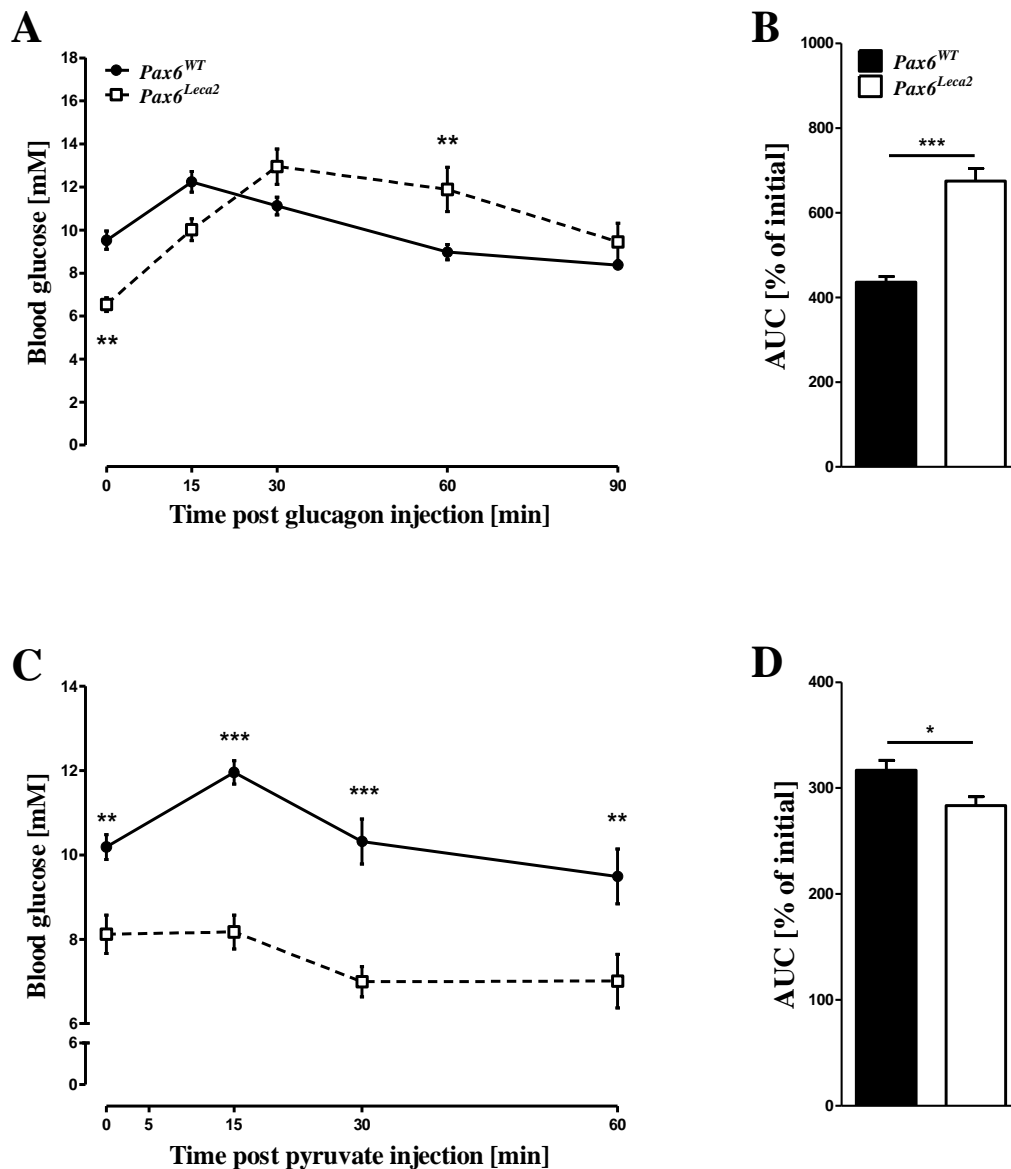


Figure 3.16: Glycogenolytic and gluconeogenic capacity

(A) 0.5 mg/kg of glucagon administration produces a rather dramatic change in blood glucose levels, (B) quantified as per basal values; n=11-15. (C) An opposite effect seems to be underway with an intraperitoneal injection of 2 g/kg of pyruvate which failed to elicit a strong response in the mutant mice (D) quantified as per basal values; n=15-17, 10-12 week old male mice. Error bars display SEM values. Differences were considered statistically significant at $p < 0.05$ using a two tailed Student's t test or two-way ANOVA (Bonferroni) (* < 0.05 , ** < 0.01 , *** < 0.001).

To our amazement, an ip administration of glucagon was able to elicit a strong response in mutant mice (Figure 3.16A). Results demonstrated a mild increase in glycaemia specifically at time point 60 minutes post glucagon administration, showing a significantly increased glucose levels as per basal values (Figure 3.16B). On the other hand, an ip pyruvate challenge modestly increased glucose levels in wildtype mice while in *Pax6^{Leca2}* mice, pyruvate failed to do the same (Figure 3.16C-D). Therefore, divergence in the liver function appears to be prevalent in *Pax6^{Leca2}* mice.

Insulin has a major effect in storage of glycogen in the liver ^[242] and the amount of insulin in the *Pax6^{Leca2}* mice is lower than in the wildtype (Figure 3.8A). Thus, we carried out Periodic acid-Schiff (PAS) staining to check whether differences in glycogen content may have a role to play in the reduced fasting blood glucose levels, specifically affecting glycogenolysis. As shown in Figure 17A-B, reduced glycogen storage was observed in livers of *Pax6^{Leca2}* mice during fed but not during fasted state compared to wildtype mice. Moreover, only mild and non-significant change was found in the blood glucose levels in mutant mice between 6 and 16 hour fasting periods as evidently seen in the wildtype mice (Figure 3.17B). However, 6 and 12 hours fasted mice did not show any significant changes in plasma glucagon between the groups as both showed similar increases in amount of the hormone between the fasting durations (Figure 3.17C). This is consistent with the *in vitro* assay and histological data (Figure 3.2D-F and Figure 3.8B-C) that do show a phenotype associated with glucagon or rather α -cell functionality.

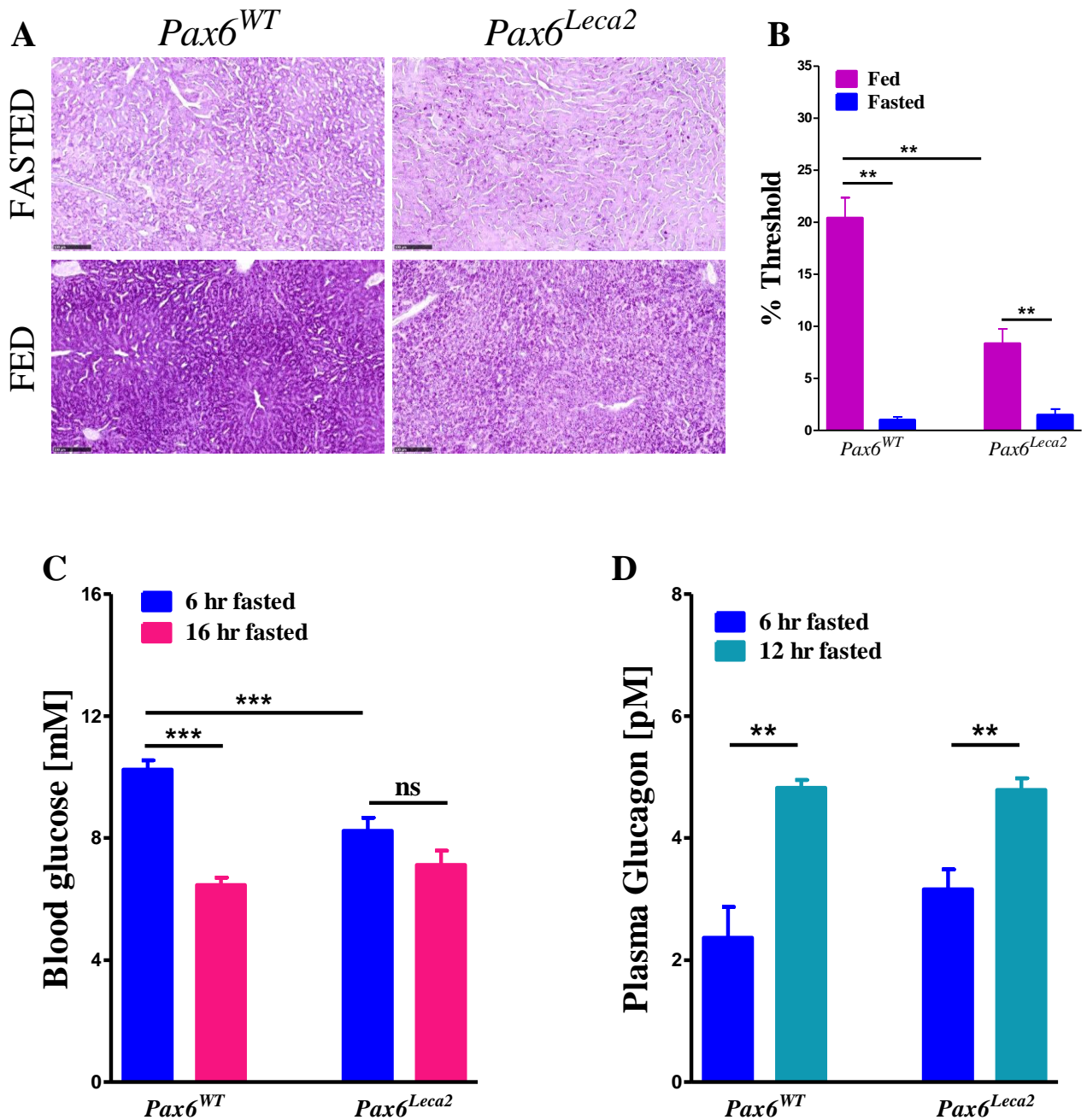


Figure 3.17: Evident change in fasting glycogen but normal glucagon levels in *Pax6*^{Leca2} mice

(A) Glycogen levels in 6 hour fasted and fed mice and (B) quantification of it using ImageJ as demonstrated by PAS staining; n=4-6, 14 week old male mice. Images were acquired using Nanozoomer (Hamamatsu). Scale bar (black) represents 50 μ m. (C) Mutant mice were able to maintain their blood glucose levels within the same range even after an overnight fast (16 hours); n=8-12, with similar changes in (D) plasma glucagon level; n=10-17; 10-12 week old male mice. Error bars display SEM values. Differences were considered statistically significant at $p < 0.05$ using a two tailed Student's t test or one-way ANOVA (Bonferroni) (** < 0.01 , *** < 0.001 , ns = non-significant).

Furthermore, biochemical analysis of plasma samples acquired from *vena cava* blood of mice fasted for 6 hours showed reduction in cholesterol, triglycerides and HDL (Table 3.2) in *Pax6^{Leca2}* mice, which is in accordance to their body composition (Figure 3.10H). However, no significant changes in gluconeogenic substrates glycerol and non-esterified fatty acids (NEFAs) (Table 3.2) were observed, ruling out any obvious lack of gluconeogenic substrates.

| Parameters | <i>Pax6^{WT}</i> | <i>Pax6^{Leca2}</i> |
|-----------------------|--------------------------|-----------------------------|
| Cholesterol [mg/dL] | 149.10 ± 19.08 | 129 ± 16.66* |
| Triglycerides [mg/dL] | 110.03 ± 25.66 | 64.46 ± 12.39*** |
| Lactate [mM] | 13.39 ± 9.73 | 7.48 ± 2.18 |
| LDL [mg/dL] | 13.85 ± 2.21 | 13.15 ± 2.43 |
| HDL [mg/dL] | 109.92 ± 11.50 | 94.86 ± 12.23* |
| Lipase [U/L] | 55.29 ± 6.80 | 57.80 ± 9.31 |
| Glycerol [mM] | 0.40 ± 0.04 | 0.37 ± 0.07 |
| NEFA [mM] | 0.77 ± 0.09 | 0.80 ± 0.11 |

Table 3.2: Biochemical parameters in chow fed mice

Table states average and standard deviation values of respective parameter in plasma obtained from 14 week old male mice after 6 hours fasting period; n=9-10. Differences were considered statistically significant at $p < 0.05$ using a two tailed Student's t test (* < 0.05 , *** < 0.001).

To demonstrate the aforementioned results in an *in vitro* setting, primary hepatocytes were isolated from 15 week old mice. The primary hepatocytes were allowed to polarize for 6 days in collagen sandwich culture medium [243]. Thereafter, cells were fasted for 10 hours before being stimulated to address their innate ability to secrete glucose at cell-culture day 6. As shown in Figure 3.18A, the primary hepatocytes from *Pax6^{Leca2}* mice showed lower, albeit non-significant basal glucose secretion and a similar non-significant, lower glucose secretion upon stimulation with dexamethasone and forskolin, thereby not completely recapitulating the *in vivo* pyruvate challenge test (Figure 3.16C-D). These outcomes indicate that hepatocytes, inherently, do not have decreased capacity to secrete glucose and that liver specific effects might be dictated by *in vivo* signals.

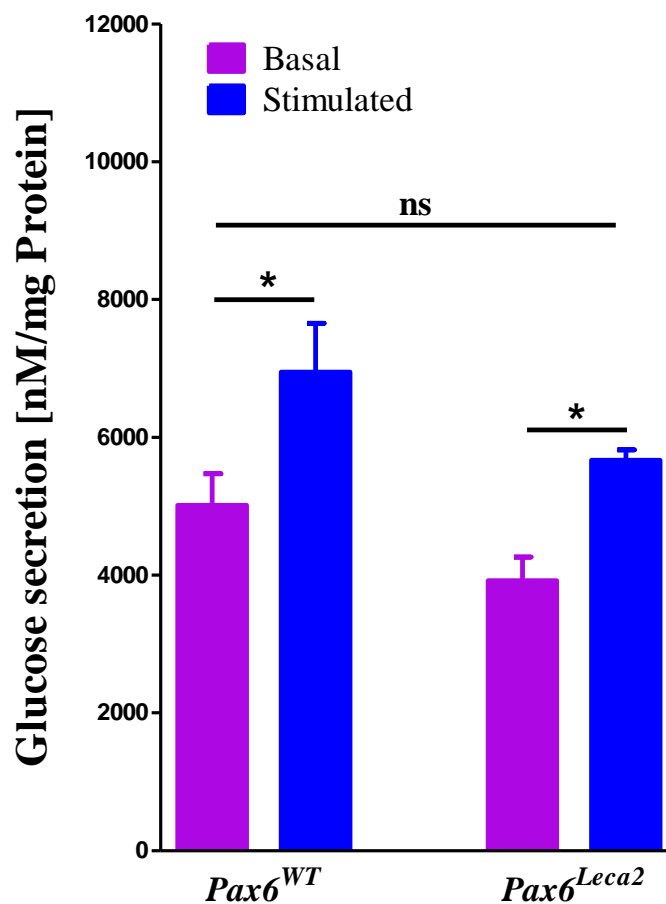


Figure 3.18: Glucose secretory capacity of primary hepatocytes

Primary hepatocytes were obtained from 15 week old male mice. Results were obtained in 4 technical replicates. Error bars display SEM values. Differences were considered statistically significant at $p < 0.05$ using a two tailed Student's t test (* < 0.05 , ns = non-significant).

Interestingly, one such signal, which is inherently a liver derived endocrine hormone, is FGF21 that has been shown to induce insulin sensitivity and protect mice from diet induced obesity perhaps by enhancing energy expenditure [166]. Indeed, *Pax6*^{Leca2} mice showed modest but significantly increased circulating levels of FGF21 at *ad libitum* fed state and dramatic increases in 6 hour fasted plasma levels (Figure 3.19A). Accordingly, liver mRNA expression levels of *Fgf21* were increased 2 fold and 5 fold at *ad libitum* fed and 6 hour fasted state, respectively (Figure 3.19B). Expression levels of liver *Ppara*, a regulator of FGF21 [163], did not seem to be significantly changed between the groups, suggesting other factors might be involved in its regulation (Figure 3.19C).

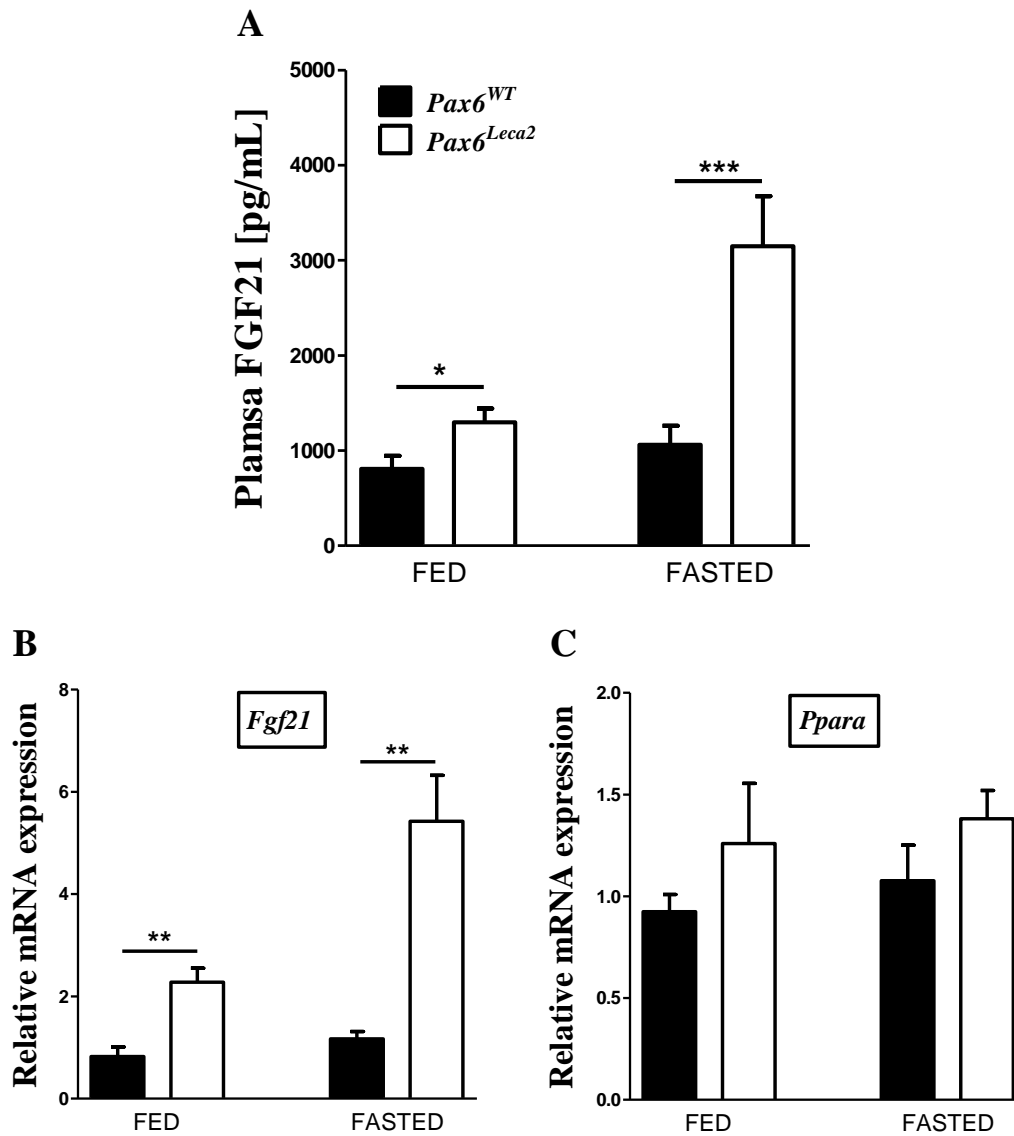


Figure 3.19: Increased FGF21 in *Pax6*^{Leca2} mice

(A) Plasma FGF21 levels, (B) mRNA expression of *Fgf21* and (C) *Ppara* in *ad libitum* fed and 6 hours fasted 14 week old male mice; n=5-6. Error bars display SEM values. Differences were considered statistically significant at $p < 0.05$ using a two tailed Student's t test (* < 0.05 , ** < 0.01 , *** < 0.001).

Furthermore, FGF21 has a particular effect on fat metabolism [165]. Indeed, several changes in key enzymes involved in lipogenic mechanism were observed. ATP citrate lyase (*Acly*) which drives acetyl CoA into fatty acid synthesis [244], acetyl-CoA carboxylase (*Acaca*), and fatty acid synthase (*Fasn*) which are required for long-chain fatty acid synthesis [245] were all downregulated in the *Pax6*^{Leca2} mice (Figure 3.20A-C). Moreover, sterol regulatory element-binding protein 1 (*Srebp1c*) which seems to regulate complete set of lipogenic genes [246] was also downregulated in the livers of *Pax6*^{Leca2} mice (Figure 3.20D). Interestingly, *Srebp1c* seems

to be inhibited by the induction FGF21 signaling ^[247] which is in accordance to changes seen in FGF21 levels.

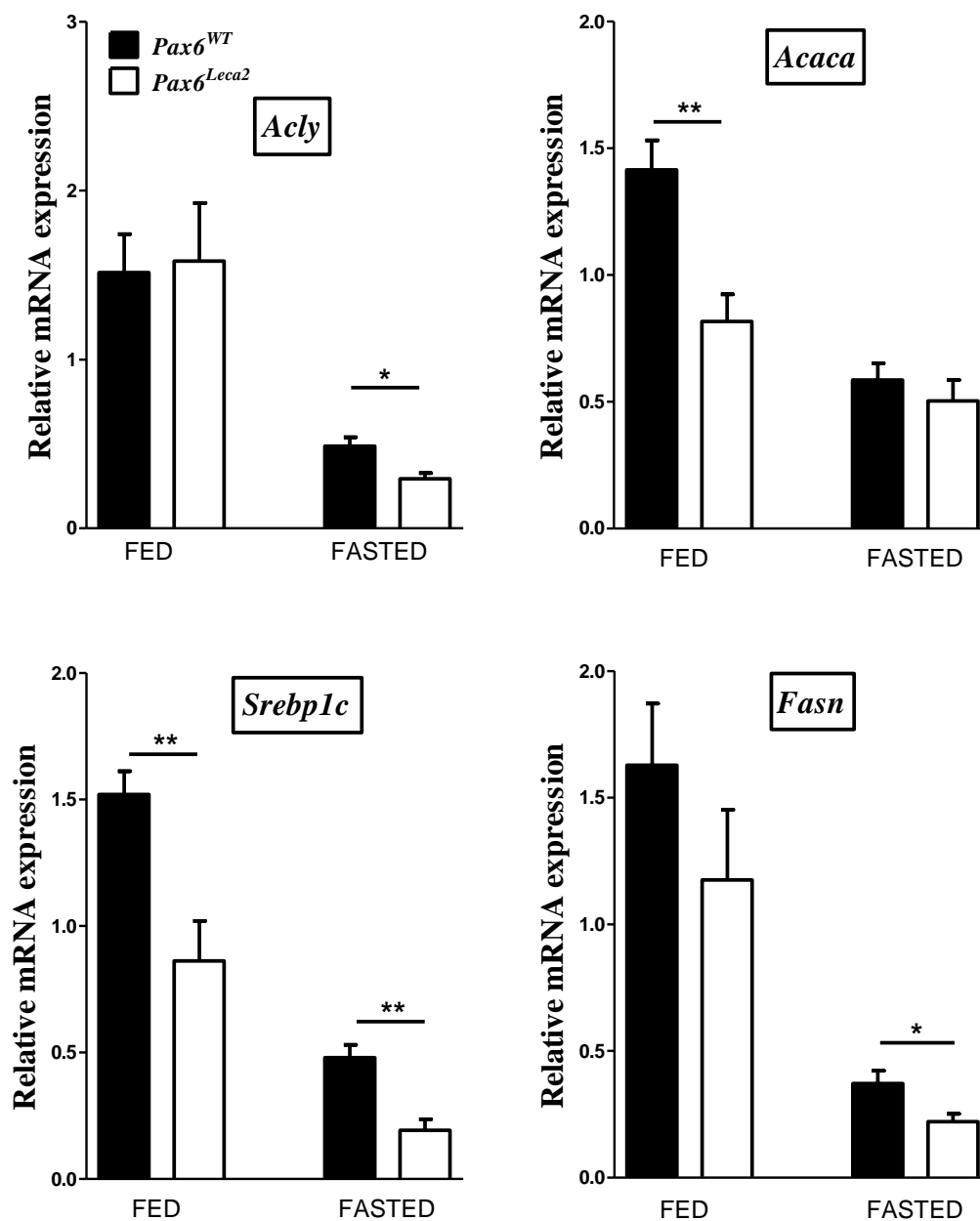


Figure 3.20: mRNA expression of liver genes involved in fat metabolism

Liver mRNA expression levels of (A) *Acly*, (B) *Acaca*, (C) *Srebp1c* and (D) *Fasn* in in fed *ad libitum* and 6 hours fasted 14 week old male mice; n=5-6. Error bars display SEM values. Differences were considered statistically significant at $p < 0.05$ using a two tailed Student's t test (* < 0.05 , ** < 0.01).

3.2.5 Resistance to diet induced obesity but not a hyperglycemic state

The glucagon challenge test revealed two important features. Firstly, glucagon secreted by pancreatic α -cells was able to induce glucose secretion in *Pax6*^{Leca2} mice (Figure 3.16A-B)

demonstrating a functional islet-liver axis. Secondly, increased insulin sensitivity is specific to liver and *Pax6^{Leca2}* mice are unable to compensate for the low amounts of insulin in presence of glucagon since no evidence for increased glucose uptake was shown by any tissue (Figure 3.13C). This is reflected in hyperglycemic state of the *Pax6^{Leca2}* mutants subsequent to glucagon administration. To further affirm this finding, mice were challenged with a high fat diet (HFD), containing about 60% fat and compared to a low fat control diet (LFCD), containing <10% fat. Dietary intervention in these mice was initiated one week after weaning, i.e. at 4 weeks of age. HFD and LFCD were fed to the mice for a period of 10 weeks in two independent cohorts. Weekly body weight and tail blood glucose was measured for the first 7 weeks prior to subjecting the mice to tolerance tests and other metabolic studies over the last 3 weeks.

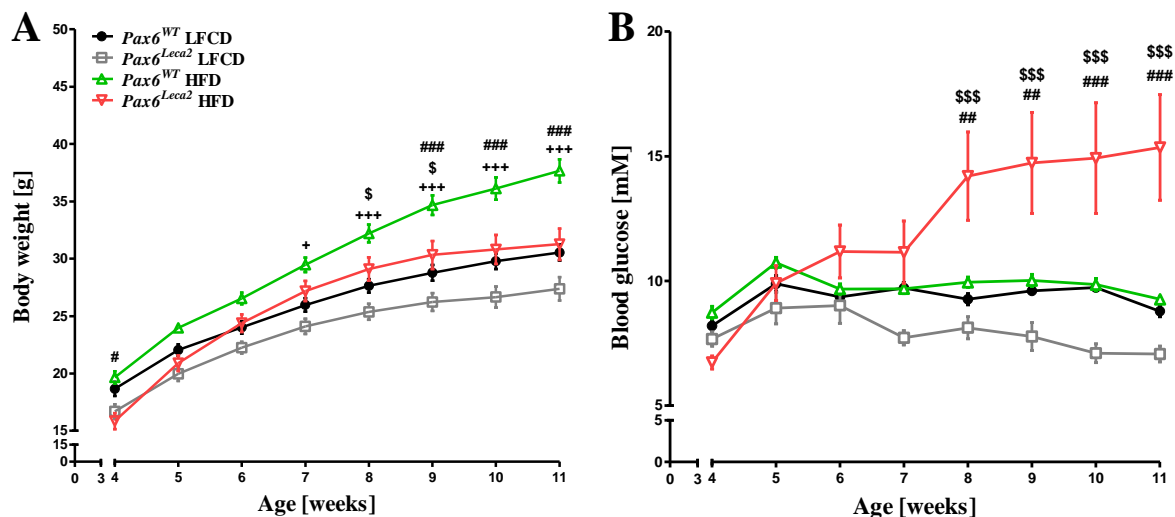


Figure 3.21: Weekly body weight and blood glucose of HFD fed mice

Changes in (A) body weight and (B) blood glucose levels show that HFD renders mutant mice hyperglycemic without major changes in body weight; $n=12-25$, male mice. Error bars display SEM values. Differences were considered statistically significant at $p < 0.05$ using a two-way ANOVA (Bonferroni). # = *Pax6^{WT}* HFD vs *Pax6^{Leca2}* HFD, + = *Pax6^{WT}* LFCD vs *Pax6^{WT}* HFD, \$ = *Pax6^{Leca2}* LFCD vs *Pax6^{Leca2}* HFD (\$, #, + < 0.05, ## < 0.01, \$\$\$, ###, +++ < 0.001).

Initially, mice fed with a HFD in both genotypes showed an increase in body weight, eliminating any significant difference between the groups up until 3 weeks of HFD, at 7 weeks of age (Figure 3.21A). Thereafter, the difference in weight gain between wildtype and *Pax6^{Leca2}* mice fed with HFD becomes greater. Whereas the weight difference between *Pax6^{Leca2}* mice from both dietary groups showed mild and only transient significant differences during the course of HFD, the differences between wildtype from HFD and LFCD groups was much greater and significant after merely 3 weeks of dietary challenge (Figure 3.21A). Simultaneously, *Pax6^{Leca2}* mice fed with HFD showed small increases in *ad libitum* glycaemia

and eventually entered into a hyperglycemic state at the age of 8 weeks, only 4 weeks after the advent of HFD challenge (Figure 3.21A-B). Hence, a HFD contributes to a hyperglycemic condition in the $Pax6^{Leca2}$ mice without overt obesity, which was further confirmed by NMR in these mice at the end of the HFD challenge. Indeed, $Pax6^{Leca2}$ mice fed with HFD displayed little change in body weight (Figure 3.22A) without any change in lean mass (Figure 3.22B) and only slight, albeit non-significant increase in fat mass as compared to $Pax6^{Leca2}$ mice fed with LFCD (Figure 3.22C). Therefore, regardless of the diet, $Pax6^{Leca2}$ mice are able to maintain similar differences in body composition as compared to wildtype mice indicating resistance to diet induced obesity (DIO).

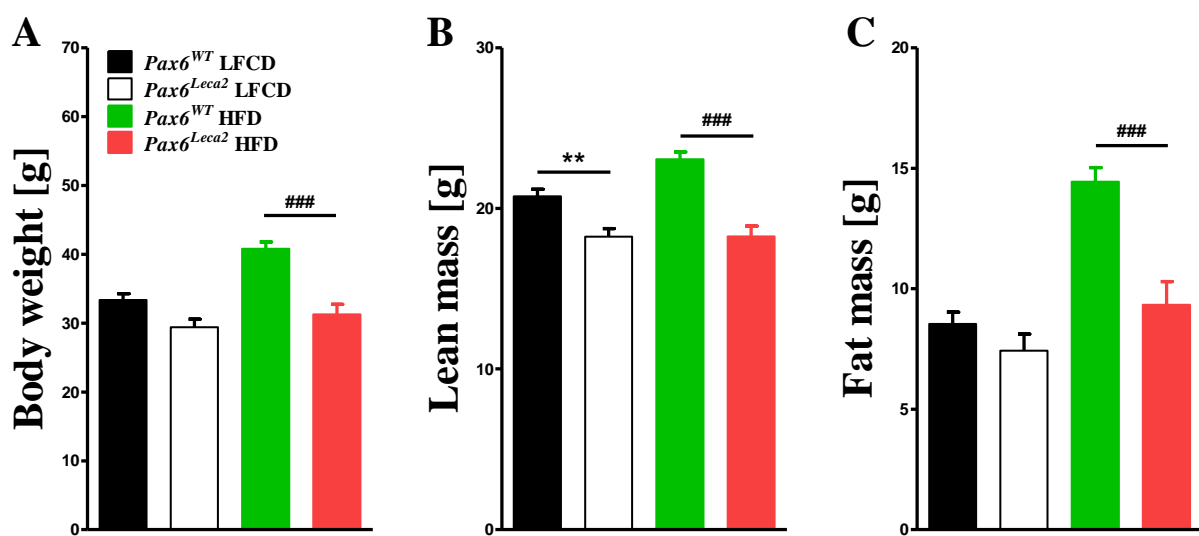


Figure 3.22: Resistance to DIO in HFD fed $Pax6^{Leca2}$ mice

Changes in (A) body weight, lean mass (B) and fat mass (C) showed that HFD fed mutant mice did not show significant changes in weight or fat gain; n=12-25, 14 week old male mice. Error bars display SEM values. Differences were considered statistically significant at $P < 0.05$ using a two-way ANOVA (Bonferroni). * = $Pax6^{WT}$ LFCD vs $Pax6^{Leca2}$ LFCD, # = $Pax6^{WT}$ HFD vs $Pax6^{Leca2}$ HFD (** < 0.01, ### < 0.001).

Additionally, glucose tolerance tests were carried out via two distinct forms of administration, intraperitoneally (ipGTT) and oral gavage (oGTT). In both experiments, strong glucose intolerance was observed in $Pax6^{Leca2}$ mice fed with HFD as compared to their LFCD counterparts (Figure 3.23A-D). This, however, was only mildly observed in the wildtype mice for glucose injected intraperitoneally and near-normal tolerance when given an oral gavage of glucose. HFD fed wildtype mice were therefore seem to be able to meet with the increased demands for insulin, unlike in the $Pax6^{Leca2}$ mice.

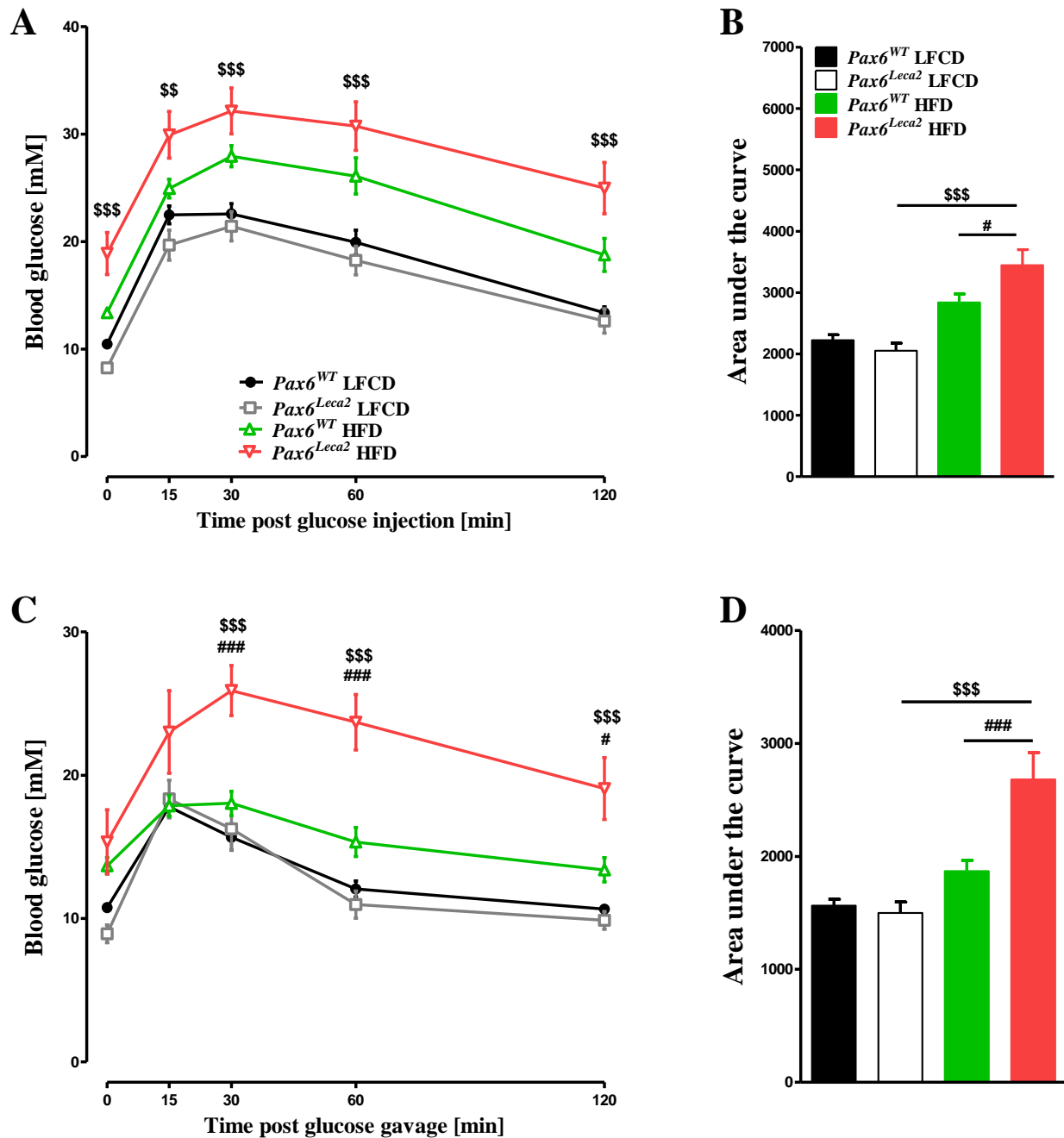


Figure 3.23: Glucose homeostasis of HFD fed mice

Both tests, (A-B) ipGTT (C-D) oGTT showed that HFD rendered 12 week old male mutant mice glucose intolerant; n=12-25. Error bars display SEM values. Differences were considered statistically significant at $p < 0.05$ using a two-way ANOVA (Bonferroni). # = *Pax6*^{WT} HFD vs *Pax6*^{Leca2} HFD, \$ = *Pax6*^{Leca2} LFCD vs *Pax6*^{Leca2} HFD (# < 0.05, \$\$ < 0.01, \$\$\$, ### < 0.001).

6 hour fasted plasma insulin levels were higher in HFD group as compared to the group on LFCD for wildtype mice and even *Pax6*^{Leca2} mice fed with HFD showed small increases in insulin levels (Figure 3.24A). However, during the course of the tolerance tests, HFD fed wildtype mice were able to elicit a substantial increase in insulin as per requirement unlike the

Pax6^{Leca2} mice, which showed lack of increment in both HFD and LFCD group (Figure 3.24A-B). This difference was particularly observable during an oGTT, where lack of sufficient incretin effect became evident.

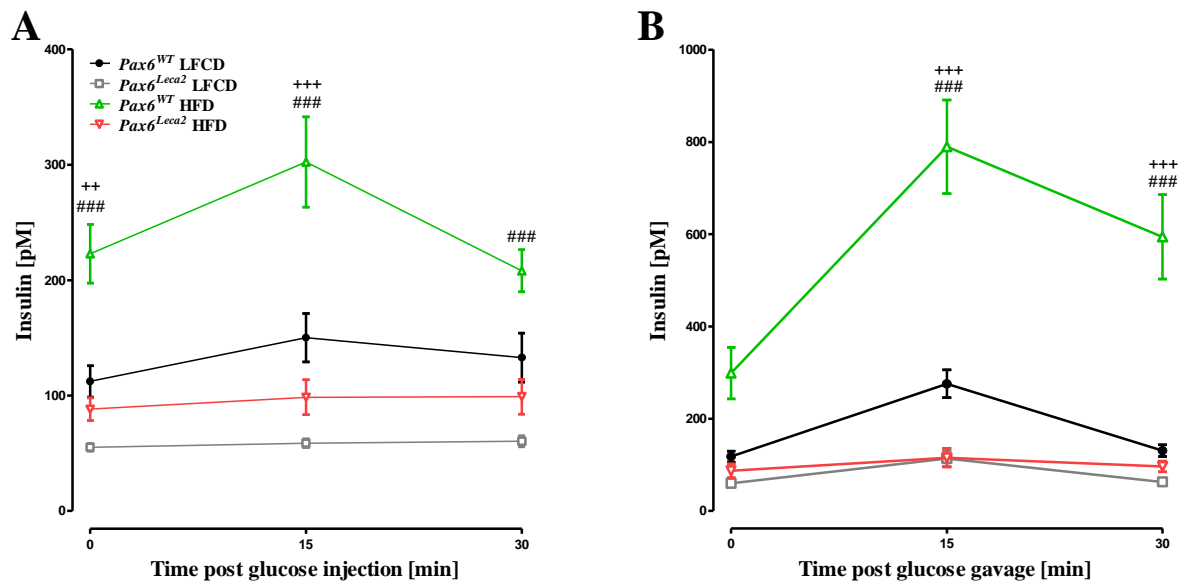


Figure 3.24: Absence of compensatory increase in insulin in HFD fed *Pax6^{Leca2}* mice

Insulin secretion during (A) ipGTT and (B) oGTT; Increased plasma insulin was observed in wildtype mice but was absent in mutant mice displaying similar levels of insulin increment regardless of diet; n=12-25. Error bars display SEM values. Differences were considered statistically significant at $p < 0.05$ using a two-way ANOVA (Bonferroni). # = *Pax6^{WT}* HFD vs *Pax6^{Leca2}* HFD, + = *Pax6^{WT}* LFCD vs *Pax6^{WT}* HFD (++ < 0.01, ###, +++ < 0.001).

Enhanced sensitivity to insulin in *Pax6^{Leca2}* mice fed with chow diet help these mice to evade hyperglycemia. Even though insulin levels were slightly higher in *Pax6^{Leca2}* mice fed with HFD as compared to *Pax6^{Leca2}* mice fed with LFCD, they still displayed hyperglycemia. Therefore, we wondered whether insulin sensitivity in *Pax6^{Leca2}* mice fed with HFD was affected. Thus, an insulin tolerance test was carried out. Whereas, a clear decrease of the acquired insulin sensitivity in *Pax6^{Leca2}* mice fed with HFD was observed, this feature was found to be intact in the LFCD group (Figure 3.25A-B), similar to what was observed in the chow fed group (Figure 3.12A-B). Remarkably, about 25% *Pax6^{Leca2}* mice fed with HFD died during the course of dietary intervention, recapitulating parts of *Pax6* β -cell knockout phenotype^[99] (Figure 3.25C). In summary, the inability to produce higher amounts of insulin when fed with HFD and subsequent loss of insulin sensitivity seem to have together contributed to the hyperglycemic state.

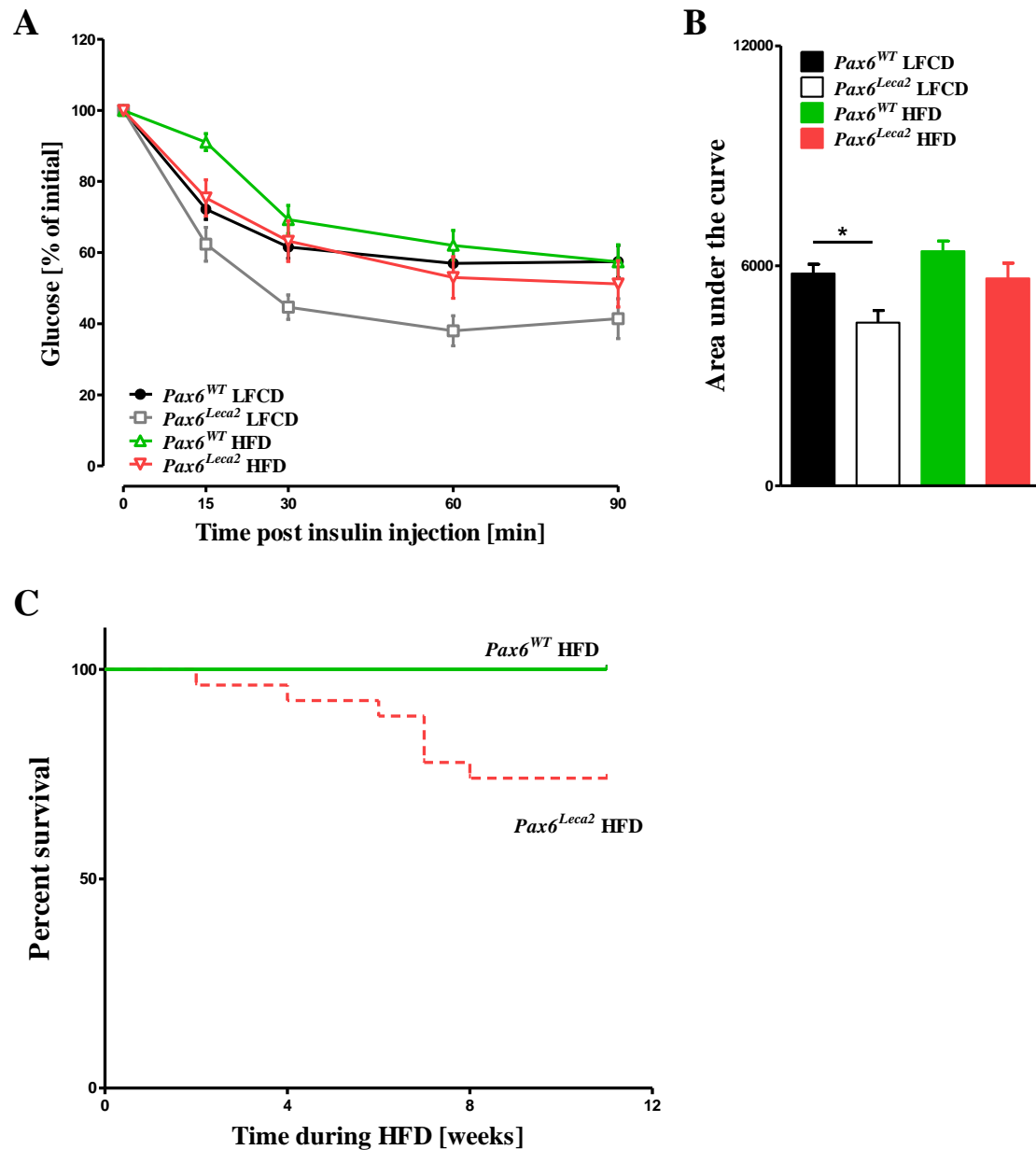


Figure 3.25: Loss of insulin sensitivity in *Pax6*^{Leca2} mice fed with HFD

(A, B) An intraperitoneal insulin administration (0.75 U/kg) showed that HFD fed 13 week old male mutant mice had similar insulin tolerance as that in wildtype mice fed with HFD; n=11-21. (C) Percent survival rate in mutant mice over 10 weeks of HFD. Error bars display SEM values. Differences were considered statistically significant at $p < 0.05$ using a one or two-way ANOVA (Bonferroni) ($* < 0.05$).

Furthermore, blood plasma collected from 6 hours fasted mice revealed little difference in biochemical profile between the HFD fed groups, which was in line with increased fat content of mice on HFD. However, *Pax6*^{Leca2} mice still showed a significant decrease in HDL as well as glycerol (Table 3.3).

| Parameters | <i>Pax6</i> ^{WT} HFD | <i>Pax6</i> ^{Leca2} HFD |
|-----------------------|-------------------------------|----------------------------------|
| Cholesterol [mg/dL] | 209.19 ± 32.93 | 195.47 ± 65.53 |
| Triglycerides [mg/dL] | 106.49 ± 45.53 | 105.65 ± 41.33 |
| Lactate [mM] | 8.09 ± 1.48 | 6.88 ± 2.64 |
| LDL [mg/dL] | 29.56 ± 8.62 | 29.34 ± 11.97 |
| HDL [mg/dL] | 150.96 ± 16.50 | 125.52 ± 19.12*** |
| Lipase [U/L] | 87.06 ± 30.15 | 83.36 ± 24.19 |
| Glycerol [mM] | 0.45 ± 0.13 | 0.35 ± 0.12* |
| NEFA [mM] | 0.94 ± 0.54 | 0.85 ± 0.51 |

Table 3.3: Biochemical parameters in HFD fed mice

Table states average and standard deviation values of respective parameter in plasma obtained from 14 week old male mice after 6 hours fasting period; n=13-16. Differences were considered statistically significant at P < 0.05 using a two tailed Student's t test (* < 0.05, *** < 0.001).

3.3 Possible contribution of hypothalamus to changes in the metabolic phenotype of *Pax6^{Leca2}* mice

3.3.1 Expression of *Pax6* in adult murine hypothalamus

Much of the aforementioned data rationally explains the absence of a hyperglycemic state in *Pax6^{Leca2}* mutants fed with a chow diet even though they have lost the capacity to secrete insulin in response to glucose. This, however, being a β -cell dependent phenotype, cannot completely explain as to why a point mutation in *Pax6* contributes to a phenotype that seems to protect the mouse from developing an overt diabetic phenotype as well as DIO. The hypothalamus is central to metabolic stability of rodents and humans and controls much of the feeding behavior and peripheral glycaemia [174, 248]. In the developing brain of mice, PAX6 has been observed to be scattered in hypothalamic tissue [220] and has been suggested to play an indirect role in metabolism [212] in both rodents and humans. Therefore, to check the presence of *Pax6* in the hypothalamus, RNA was extracted from hypothalamus and other metabolically important tissues such as liver and fat where the gene should not be expressed [249, 250] and mRNA expression levels of *Pax6* were revealed.

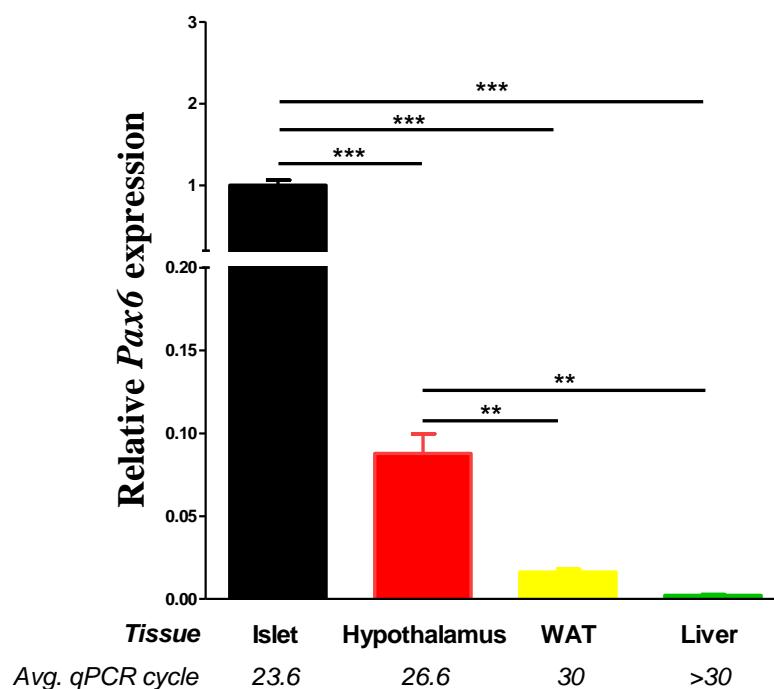


Figure 3.26: mRNA expression of *Pax6* in various tissues

mRNA expression and the average qPCR cycle at which the crossing point is achieved for the gene *Pax6* in different tissues of 10 week old male C3HeB/FeJ wildtype mice; n=4-6 Error bars display SEM values. Differences were considered statistically significant at $p < 0.05$ using a two tailed Student's t test (** < 0.01 , *** < 0.001).

An RT-qPCR was performed to check for the expression of *Pax6* in these tissues and as shown in Figure 3.26, islets display the highest expression of *Pax6* as compared to the other tissues. As expected, liver and fat showed little to no expression, while hypothalamus showed considerable amount of *Pax6* expression (Figure 3.26), confirming that *Pax6* gene is indeed expressed in the adult rodent hypothalamus. To check if the mRNA also translates to a detectable amount of protein, we stained hypothalamic sections from both groups with anti-PAX6 antibody to check the protein expression levels in the adult mice.

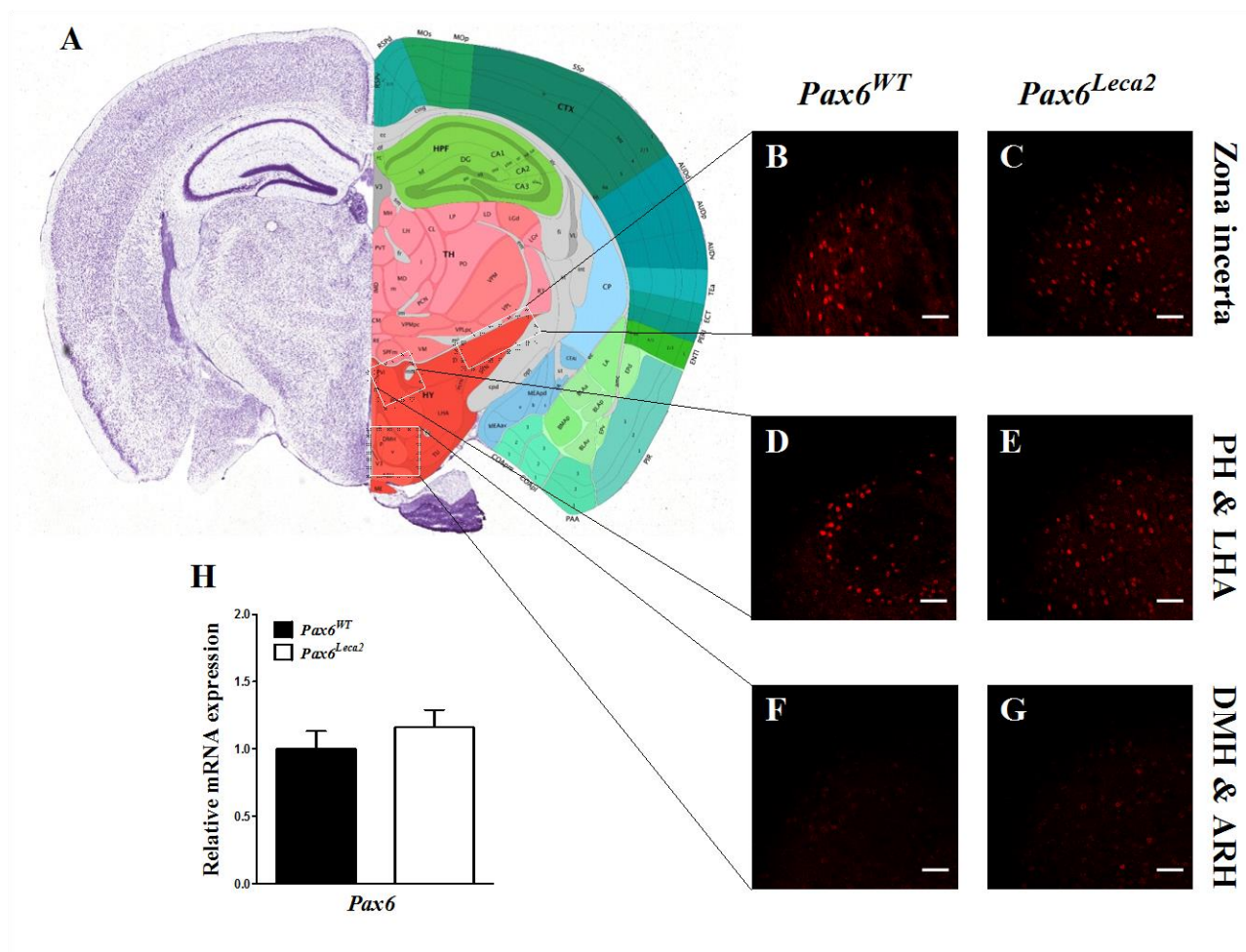


Figure 3.27: Expression and localization of PAX6 in hypothalamus

(A) Mouse brain section adapted from Allen brain atlas ^[251] displaying different parts of the brain including hypothalamus (RED). White boxes mark the 3 separate locations and the expression of PAX6 in each of these regions is shown in hypothalamic sections of 10-12 week old male mice; (B-C) zona incerta, (D-E) PH - posterior hypothalamic nucleus LHA – Lateral hypothalamic area, (F-G) DMH – Dorsomedial hypothalamus and ARH – Arcuate hypothalamic nucleus Scale bar (white) represents 50 μ m. Images were acquired using Leica TCS SP5 microscope. (H) mRNA expression level of *Pax6* in whole hypothalamus of 10-12 week old male mice; n=5. Error bars display SEM values. No significant differences were found using a two tailed Student's t test.

PAX6 expression was observed in many parts of the hypothalamus, most significantly in the ZI region (Figure 3.27B-C) as recently shown elsewhere ^[221]. Moreover, scattered PAX6 positive cells were also found in the dorsal parts of posterior hypothalamic nucleus (PH) and

parts of lateral hypothalamic area (LHA) (Figure 3.27D-H). Little to no expression was found in the dorsomedial hypothalamus (DMH) and the arcuate nucleus (ARH) (Figure 3.27F-G). To assess the regulation of certain important hypothalamic genes in the *Pax6^{Leca2}* mutants, RT-qPCR was carried out. As expected, expression of *Pax6* was found to be similar between the groups (Figure 3.27B). Intriguingly, *Pomc* and *Cartpt* were both downregulated whereas *Mc4r* was upregulated in the hypothalamic tissue (Figure 3.28A). This result seems to fit well with the evident increase in food intake in the mutant mice ^[252, 253] (Figure 3.11D).

Reduced HGP is one of the most prominent phenotypes of the *Pax6^{Leca2}* mice. The adipocyte derived hormone leptin affects the hypothalamus-pituitary-adrenal (HPA) axis and lowers HGP ^[254]. Moreover, it acts on the hypothalamus to induce anorexigenic effects ^[179]. Therefore, we explored the possibility that leptin signaling might have a role to play and may directly exert effects on liver. Hence, we first measured the plasma leptin levels, which are secreted in proportion to the amount of adipose tissue ^[177, 178]. *Pax6^{Leca2}* mice on chow diet, display about 15% reduction in absolute fat content as compared to the wildtype mice (Figure 3.11H). Therefore, lower levels of 6 hour fasting plasma leptin in *Pax6^{Leca2}* mice was expected (Figure 3.28B), however, such a dramatic reduction (~50%) was not. Therefore, we checked the expressions of leptin receptor and the corresponding intermediates of leptin signaling. We observed significant increase in the mRNA expression level of *Lepr* and significant though very modest increase in expressions of *Jak2* and *Pi3k* (Figure 3.28C) in the hypothalamus of *Pax6^{Leca2}* mice. The changes seen here were only modest and might be consequences of a compensatory increase due to reduced leptin levels. Nevertheless, physiological changes in energy metabolism in addition to reduced leptin levels presented some hints.

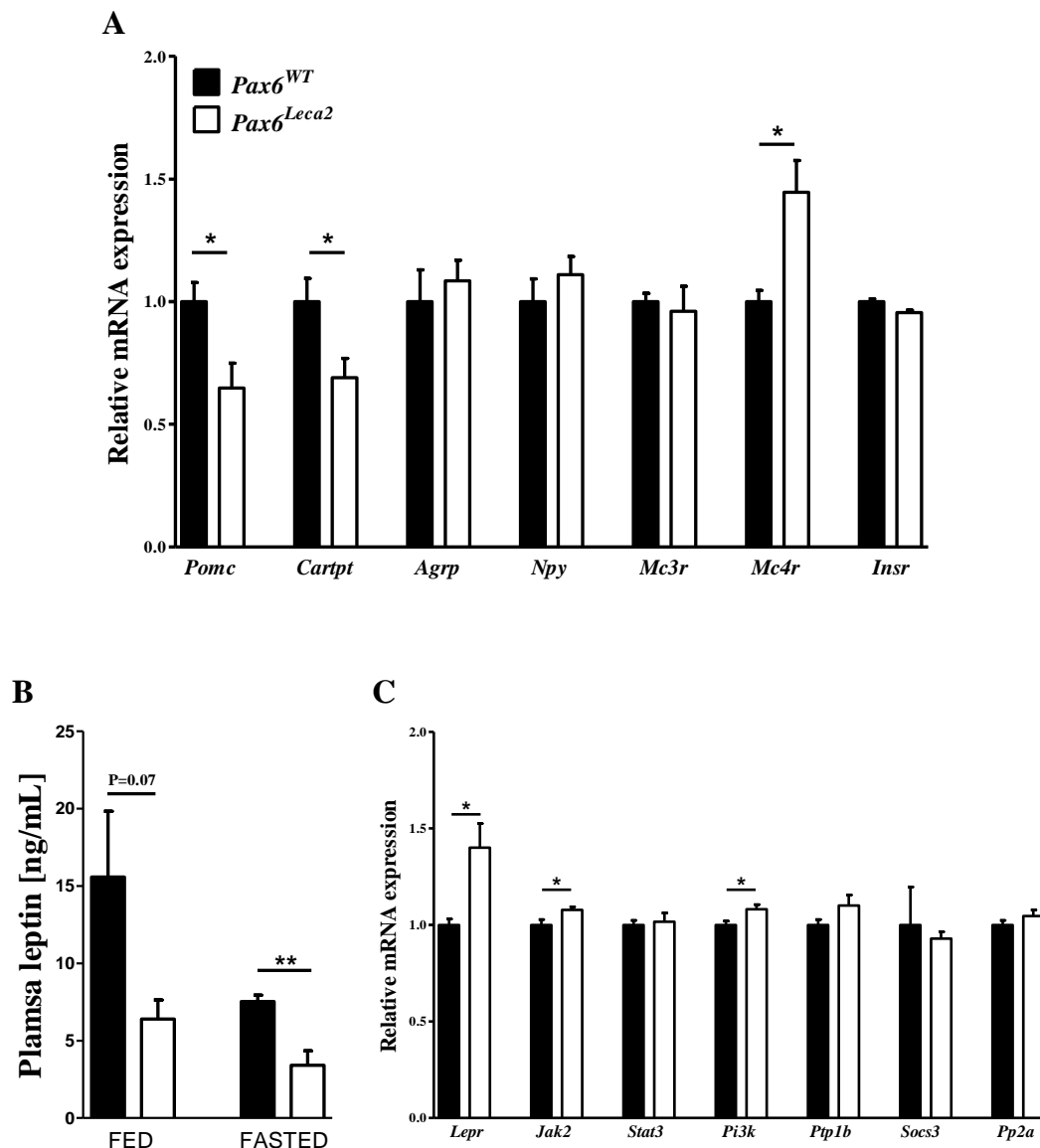


Figure 3.28: mRNA expressions of genes involved in feeding and leptin signaling in hypothalamus

(A) mRNA expressions of various genes involved in food intake and energy metabolism; n=4-5. (B) 6 hour fasted and fed plasma leptin level; n=8. (C) mRNA expression of several leptin signaling intermediates; n=4-5, 10-12 week old male mice. Error bars display SEM values. Differences were considered statistically significant at $p < 0.05$ using a two tailed Student's t test (* < 0.05 , ** < 0.01).

Hence, mice kept in metabolic cages (TSE systems) were injected either with vehicle or with 5 mg/kg of recombinant leptin. Wildtype mice showed an initial drop in food intake 2-8 hours [255, 256] after which their feeding was increased possibly to compensate for leptin effects (Figure 3.29A). *Pax6*^{Leca2} mice on the other hand showed similar feeding habits in the initial hours but showed a lower feeding trend thereafter (Figure 3.23B). However, differences in total food intake between vehicle and leptin treated groups for *Pax6*^{Leca2} mice failed to reach any significance (t test, $p=0.07$) which could have been in part due to much variability among the low sample number. Taken together, leptin effects, are at best only mildly enhanced, and hence

cannot fully explain the dramatic changes in energy metabolism. Although *Pax6* is expressed in the adult rodent hypothalamus, its specific role requires further investigations.

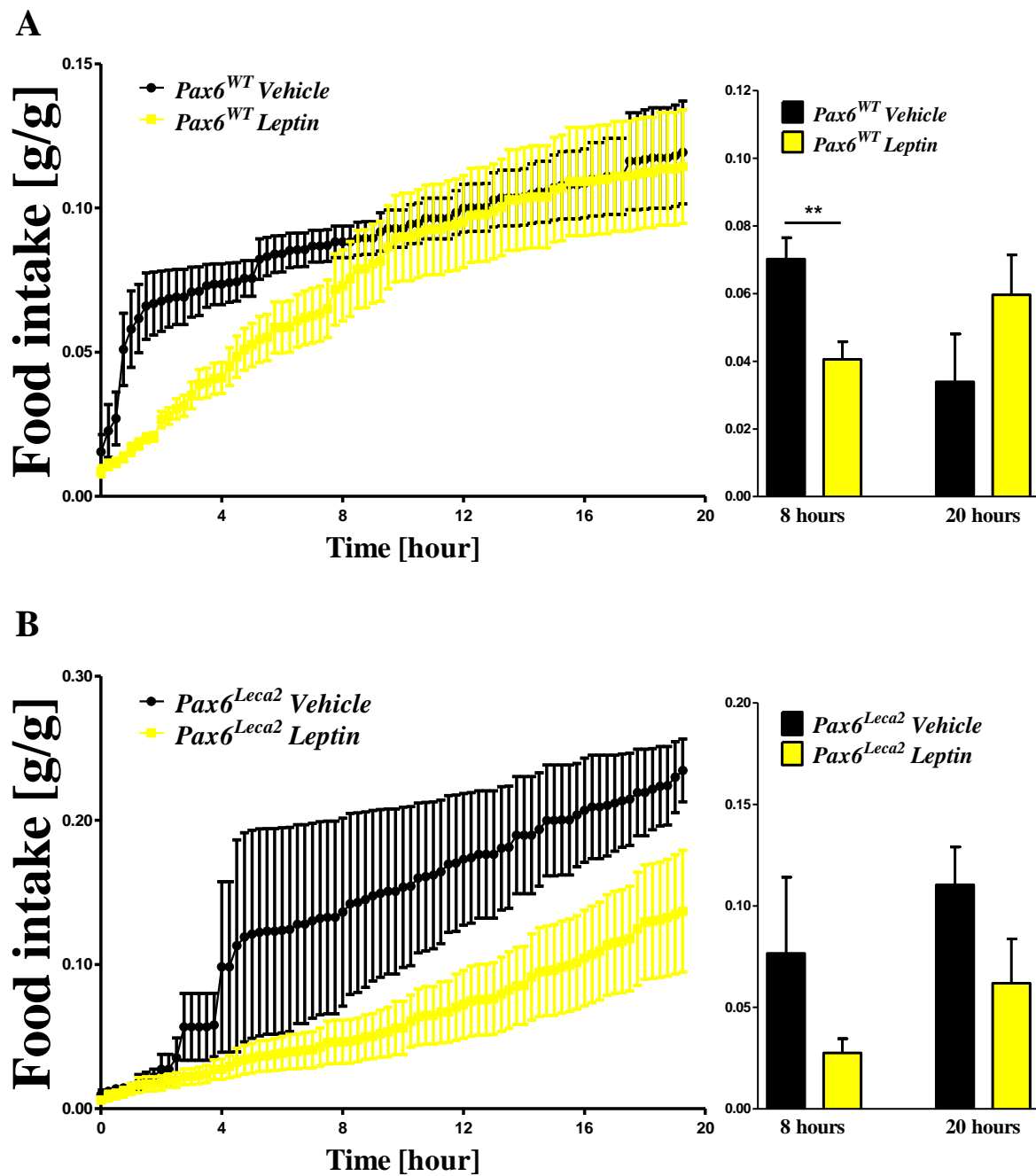


Figure 3.29: Leptin assay reveals a non-significant trend towards increased leptin sensitivity

13-14 week old male mice were injected with either vehicle or 5 mg/kg of recombinant leptin and food intake per gram body weight was measured in (A) wildtype; n=7-9 and (B) mutant mice; n=3-6, both groups kept in metabolic cages. Error bars display SEM values. Differences were considered statistically significant at $p < 0.05$ using a two tailed Student's t test (** < 0.01).

3.3.2 ChIP-sequencing reveals differentially bound targets of PAX6 in *Pax6^{Leca2}* mutants

To date, PAX6 has never been shown to have any specific function in adult hypothalamus of any organism and literature review revealed discovery of its presence in the ZI region of hypothalamus only recently [221], however, without any associated functional attributes. Since *Pax6* is present in both mRNA and protein form in hypothalamic tissue, it is safe to assume that it may have some function in the hypothalamus and hence important in the context of metabolism. Keeping up with this rationale, hypothalami of mice from both groups were excised and collected for storage at -80°C . These samples were then sent to the company Active Motif, Belgium for ChIP-sequencing analysis. 6 hypothalami from each genotype were pooled together and chromatin was prepared. Thereafter, next generation sequencing was carried out which revealed sequences of genomic sites bound by the transcription factor PAX6 in the hypothalamus. 3885 genomic sites were found to be associated with the wildtype sample while 3433 genomic sites in the *Pax6^{Leca2}* sample. Of these, 3826 genes in the wildtype and 3531 genes in the *Pax6^{Leca2}* hypothalamus were assigned to specific genomic sites. Distribution of peaks according to their locations shows a considerable amount of peaks that were present in promoter and gene body (exon and intron) regions in both groups.

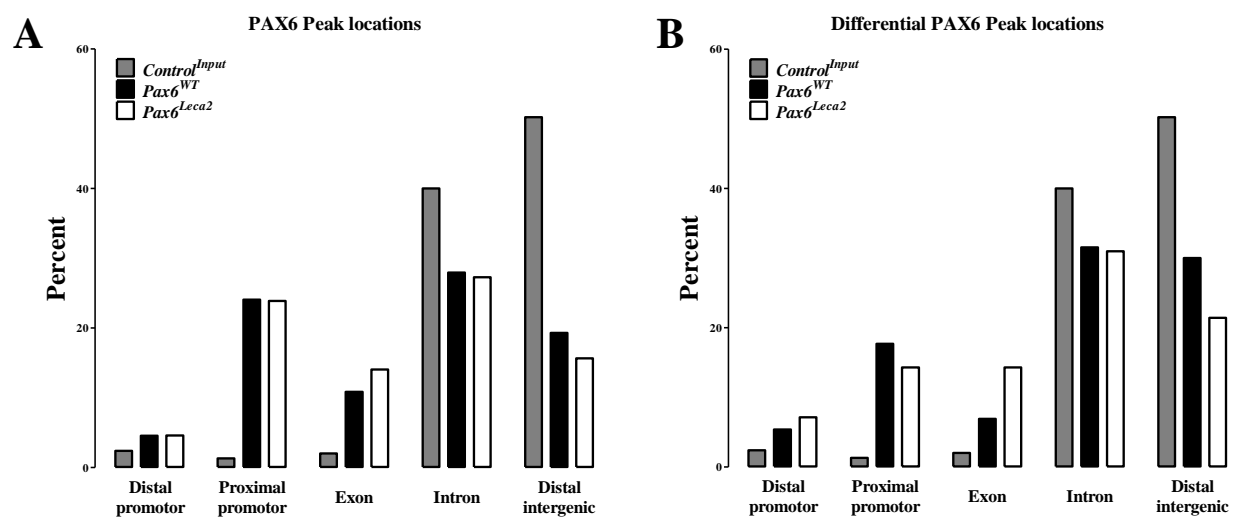


Figure 3.30: Peak locations in hypothalamus of PAX6 bound sites

(A) Peak locations in both samples as well as the control. (B) Locations of differentially bound peaks in wildtype and mutant hypothalami. Bar diagram represents percentage of distal promoter (1-3 kb relative to TSS), proximal promoter (0-1 kb relative to TSS), gene bodies (exon and intron) and intergenic regions.

However, PAX6 binding in distal intergenic regions was far less represented (Figure 3.30A). Furthermore, a similar trend was seen in differentially bound PAX6 regions, showing a considerable amount of representation in promoter and exon regions (Figure 3.30B). Moreover,

a clear high peak density was observed in both samples at ± 2 kb, a pattern expected with transcription factors.

Using MACS differential Peak calling ($p < 10^{-5}$) discovered site-assigned genes, 159 in the wildtype versus 41 in the *Pax6^{Leca2}* that were differentially bound in the hypothalamus (Supplementary table 4). In addition, Homer tool ^[257] was used for sequence analysis and motif discovery. Interestingly, the *Atf-1* motif was found to be the most enriched motif in both groups (Figure 3.31A). On the other hand, the *Pax6* motif was found to be highly enriched in the wildtype hypothalamus ($p = 10^{-19}$) compared to that in *Pax6^{Leca2}* ($p = 10^{-3}$). Moreover, *Pax6* motif was the most enriched motif in genes differentially bound in wildtype active regions while *Pax6* motif does not appear to be enriched in differentially bound regions, suggesting not only loss of binding but also gain of binding by the mutated PAX6 protein. Representative peak images are shown in Figure 3.31C, displaying *Foxo1* and *Pravg* (Parvin, gamma) with increased binding while decreased binding at *Eprs* and *Tstd2* promoter regions as compared to the wildtype. Therefore, some of the differentially bound genomic area-assigned genes, in which either the peak was placed close to the promoter region or the assigned genes have a known function in metabolism were analyzed for their expression levels in the hypothalamus using RT-qPCR. Increase in FOXO1 in the hypothalamus produces metabolic effects including increased food intake ^[183, 185]. Indeed, *Foxo1* expression seems to be increased in the *Pax6^{Leca2}* hypothalamus (Figure 3.31A), while most of the targets displaying loss of binding which were analyzed were found to be unaffected (Figure 3.31B).

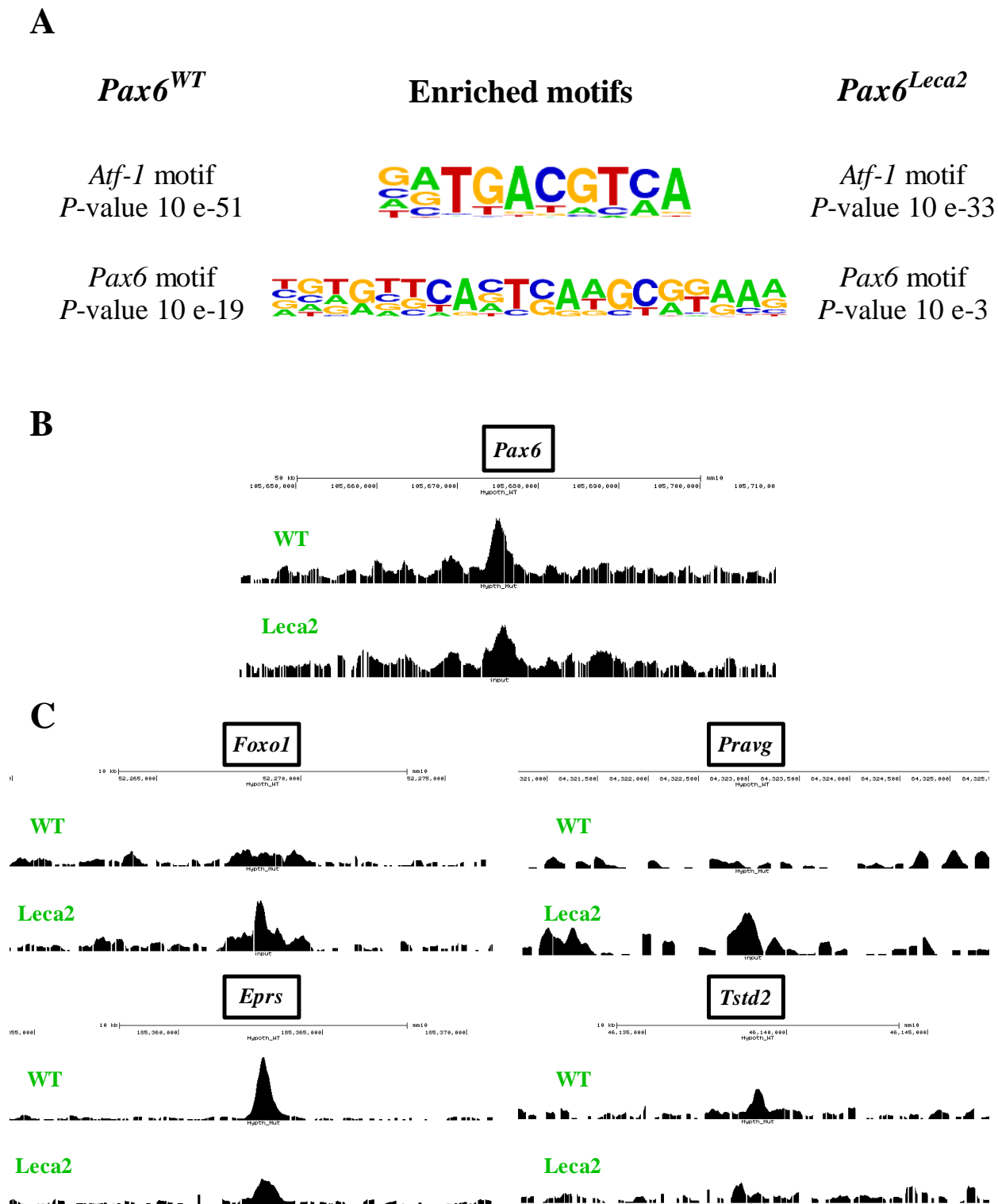


Figure 3.31: Motif enrichment in PAX6 bound regions

(A) Most enriched motif and enrichment of *Pax6* motif and their relative *P*-values in both groups using Homer software. (B) Peak density around the gene *Pax6*, top peak signifies that of the wildtype hypothalamus and the bottom peak of the mutant hypothalamus. (C) Examples of differential gain of binding in genomic regions assigned to genes *Foxo1* and *Pravg* and loss of binding at *Eprs* and *Tstd2* in the mutant hypothalamus; WT – wildtype, Leca2 – *Pax6*^{Leca2}.

Thus, changes in the regulation of the hypothalamic transcriptome may contribute to the prevailing phenotype of *Pax6^{Leca2}* mice. RNA expression profiling using microarray or RNA-sequencing should therefore be undertaken as a future experiment.

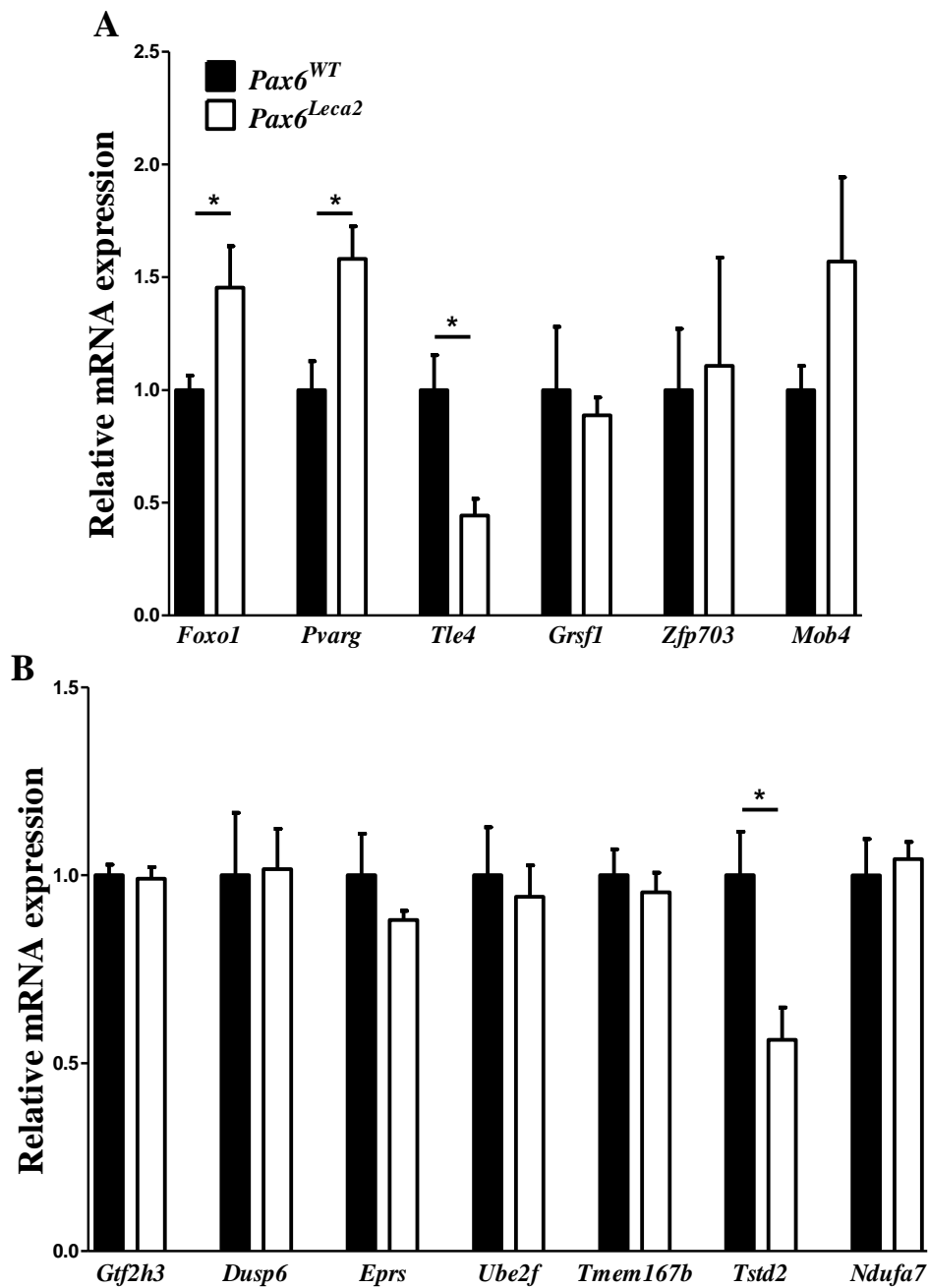


Figure 3.32: Comparison of bound and regulated gene targets

(A) mRNA expression of genes in the hypothalamus associated with peak regions displaying significantly increased PAX6 binding and (B) decreased binding in 10-12 week old mutant mice; n=5. Error bars display SEM values. Differences were considered statistically significant at $p < 0.05$ using a two tailed Student's t test (* < 0.05).

4. DISCUSSION

4.1 The islet story

4.1.1 Structural changes in the islets of homozygous *Pax6^{Leca2}* mice

A classical change in rodent islets upon disturbance in the transcriptome or in the secretory mechanism, especially that of β -cells results in a distortion of islet architecture [100, 105, 122, 130]. Several of these examples show a typical reduction in the number of insulin positive cells and an increase in centralized glucagon positive cells which may or may not arise from INS negative β -cells [104, 122, 130, 258]. Similarly, structural changes were observed in the *Pax6^{Leca2}* islets, wherein a reduced number of insulin positive β -cells was accompanied with centralized glucagon positive α -cells (Figure 3.1) although no change in the overall size of the islets was observed (Figure 3.2G-I). Somatostatin expression in the islets of the *Pax6^{Leca2}* mice did not seem to differ that from the wildtype although quantification was not carried out. Moreover, somatostatin and PP cells are affected to a lesser extent in other *Pax6* mutants [191], indicating that other TFs are involved in maintaining functional identity of these endocrinal cell types.

Previously, studies have reported the presence of cells expressing more than one hormone in β -cells of knockout mice [104, 105, 122]. Moreover, lineage-tracing experiments in β - and α -cell specific knockout of *Pax6* have clearly demonstrated that expression of ghrelin is found in cells expressing insulin or glucagon [101]. Although islets of the *Pax6^{Leca2}* mice display an increase in ghrelin positive cells (Figure 3.3A-C), no population of cells was found to be double-positive for hormonal expression. This is likely due to two important reasons. Firstly, lineage tracing was not undertaken, which is indispensable for identifying changes in hormone expression and localization in islet cells that are largely post-mitotic. Secondly, the increase in ghrelin positive cells is minute in this model compared to other reports [98-100], which is likely due to the fact that *Pax6^{Leca2}* mice harbor a point mutation that does not result in any obvious loss of PAX6 protein as shown in the islets of *Pax6^{Leca2}* mice (Figure 3.4G-H). This possibly also explains why α - and δ -cells are largely unaffected. The former is particularly astonishing since PAX6 has been proclaimed as the major TF required for α -cell identity [27, 28]. Interestingly, Dames et al. showed loss of glucagon positive α -cells was greater in mice with mutations in the PAI subdomain of the PD of PAX6 as compared to that in the HD [208] suggesting that the PAI subdomain may play an essential role in maintaining identity of α -cells. Indeed, the *Pax6^{Leca2}*

model, containing a R128C mutation in the RED subdomain of the PD is almost unique in that basically only β -cells seem to be affected and that no embryonic phenotype was found, even when examined at E18.5 [226]. Interestingly, the changes observed in hormone expression in the islets seem to remain similar throughout the ages that were analyzed (Figure 3.1 & 3.2) suggesting that the RED subdomain of the PD may play a role in the initial neonatal proliferation of β -cells. Therefore, investigation of islet cells during the maturation stages from birth, leading up to weaning, might be essential to mark the exact age at which first alterations appear.

4.1.2 R128C contributes to changes in gene expression pattern in isolated islets

4.1.2.1 Partial loss of β -cell identity

Previously in our lab, changes in global gene expression pattern was observed between isolated islets from 4 and 20 weeks old mice which was suggestive of a progressive degradation [226]. However, due to low sample number and the lack of gender separation [226], this part of the experiment was repeated with at least 3 samples per group and only male mice were taken under study (Figure 3.5A). Microarray analysis of isolated islets from mice aged 4, 6 and 10 week old was carried out. As expected, changes in gene expression were already evident at 4 weeks (Figure 3.5A). Moreover, the number of regulated genes was substantially increased at the age of 6 weeks, while further changes at week 10 were fewer (Figure 3.5B-C). PAX6 has previously been suggested to act as both a repressor and activator [259]. Changes in the transcriptome of *Pax6^{Leca2}* mice reflect this pattern; however, more genes were upregulated (~65%) in the data set especially at 6 and 10 weeks suggesting the RED subdomain may participate in a direct or indirect repressive role through possible protein-protein interaction and DNA binding properties.

The expression pattern in the microarray data set is essentially representative of a global change in the islet transcriptome. Various mature β -cells markers conferring identity as well as function were downregulated (Supplementary table 1, 2 & 3). The mRNA expression of both insulin gene isoforms *Ins1* and *Ins2* were reduced (Figure 3.6A) in the isolated islets of *Pax6^{Leca2}* mice, which is in accordance to the reduced insulin expression observed in histology (Figure 3.1 & 3.2). Moreover, the expression of the mutated *Pax6* itself was ~2 fold higher in the *Pax6^{Leca2}* mice similar to what was reported earlier [225] and might perhaps be a compensatory effect (Figure 3.6A). However, this may also indicate changes in auto-regulation [223] and/or negative feedback [260] due to loss of RED subdomain DNA binding on PAX6 itself.

RT-qPCR demonstrated non-significant decrease in the expressions of *Mafa* and *Pdx1*, although *Mafa* was found significantly downregulated in the islets of 6 and 10 week old *Pax6^{Leca2}* mice (Supplementary table 2 & 3). Both genes are highly expressed in mature β -cells and the transcription of both is driven by PAX6 [213, 261, 262]. This is particularly interesting since loss of β -cell maturation markers is frequently accompanied with an increase of neonatal or dedifferentiation markers, often termed “disallowed” or “forbidden” genes [96, 263]. Moreover, it was recently shown that PAX6 indirectly regulates the dedifferentiation marker *Neurog3* via FOXA2 [99]. Indeed, increased β -cell dedifferentiation and proliferation markers *Neurog3* and *Msln*, respectively were found in the islets of *Pax6^{Leca2}* mice (Figure 3.6B) concurrently with the increase in the expressions of neuronal genes such as *Cnr1*, which might be indicative of a reversion to a premature state [264]. Moreover, GO term analysis revealed several genes involved in regulation of neurogenesis to be dysregulated (Table 1). Remarkably, expression of the apoptotic marker genes *Ddit3* (encoding CHOP) was downregulated and that of the splice variant of X-box binding protein 1, encoded by *sXbp1*, was found to be similar between the groups, strongly hinting at the lack of evident cell death in the islets of *Pax6^{Leca2}* mice (Figure 3.6C, supplementary table 2 & 3).

Here, an intriguing pile of evidence points to a partial loss of β -cell identity without any obvious loss of islet cells by apoptosis. Recent advances in single cell transcriptomics and increasing evidence for β -cell heterogeneity point to an alternative perspective for the present study. In this context, the expression of *Ucn3*, a marker for mature β -cells [233] is of particular significance. Recently, UCN3 negative β -cells were shown to reside in the periphery of the islet and which, although expressing insulin, are functionally immature [265]. Additionally, UCN3 negative, immature β -cells also showed a significant downregulation in the expression of *Mafa*, *Ins1*, *Ins2*, *G6pc2* and *Styl4* [265], all of which are also significantly downregulated in *Pax6^{Leca2}* mice at all ages (Supplementary table 1, 2 & 3). Moreover, *Neurog3* was also found to be specifically enriched in the immature β -cells [265]. Taking into consideration that only mild increase in the number of ghrelin positive cells observed in islets of *Pax6^{Leca2}* mice excludes transdifferentiation, immaturity driven loss of mature β -cell markers and loss of insulin secretory mechanism presents itself as a plausible explanation for the predominant phenotype. However, it was not possible to provide evidence of NEUROG3 on the protein level in islets of *Pax6^{Leca2}* mice. Somewhat similar result was reported by Brereton et al, wherein hyperglycemia induced glucagon and insulin, double positive β -cells showed an increase in *Neurog3* expression without any change of it at the protein level [130]. The authors suggested

that the mutation might not have been strong enough to produce an overt increase in *Neurog3*, which may in part be true for the *Leca2* mutation [130, 258].

4.1.2.2 Loss of insulin secretory mechanism

GO term analysis using GeneRanker® tool showed a plethora of dysregulated genes involved in important functional aspects of the β -cell. In this regard, genes involved in insulin secretion and glucose homeostasis (Table 3.1), appeared as the most relevant and important dysregulated set in the *Pax6^{Leca2}* mice. Studies have found a direct effect of *Pax6* on insulin secretion *in vitro* and *in vivo* [100, 212, 213]. Expectantly, isolated islets of *Pax6^{Leca2}* mice displayed reduced total islet insulin content at all ages (Figure 3.8A, supplementary figure 1 & 2), a feature observed in other *Pax6* mutant mice demonstrating, undoubtedly, the importance of a fully functional PAX6 in the maintenance of functional adult pancreatic islets [99, 100, 208, 212]. Additionally, the glucagon content of islets as well as its secretion at low glucose concentration (2.8 mM) was similar between the homozygous mutants and wildtypes (Figure 3.8B-C). The same was not found to be true for β -cells and this capacity of the β -cells to secrete insulin was dissected at 3 separate junctures in the pathway.

Firstly, glucose sensing does not seem to be negatively affected as the expression of *Gck* was found to be similar between the groups (Figure 3.7A). This conclusion is in some measure supported by a recent study that demonstrated an increase in glucokinase activity in a β -cell specific knockout of *Pax6* [100]. Furthermore, *G6pc2*, a negative regulator of GSIS [266], was found to be downregulated, which may in turn enhance glycolytic flux [267]. *Slc2a2* (encoding GLUT2) is a direct PAX6 target, as it was shown in mice and human β -cell lines [99] its expression was found to be downregulated in β -cell specific *Pax6* knockout mouse models [99, 100]. In our data set, *Slc2a2* in 10 weeks old *Pax6^{Leca2}* mice showed a non-significant trend towards reduced expression when measured by qRT-PCR (Figure 3.7A) but was found significantly regulated in the microarray data (FC -1.80, supplementary table 3). Nevertheless, glucose uptake and glucose sensing seem largely unaffected in β -cells of *Pax6^{Leca2}* mice.

Secondly, isolated islets of *Pax6^{Leca2}* upon glucose stimulation showed no significant change in insulin output at low glucose (2.8 mM) but significantly reduced insulin secretion at high glucose (12 mM) (Figure 3.8D). Moreover, addition of various insulin secretagogues did not rescue the phenotype completely. The transcriptomics data set of isolated islets from *Pax6^{Leca2}* mice showed reduction in several genes necessary for insulin secretion such as *Pfkfb2* via GCK activity [268], vesicle-associated protein *Syt14* [269], *Ucn3* [270] and *Igfr1* [271] including GPCRs

such *Gcgr*, *Ffar1* and *Glp1r* (Figure 3.7B), which specifically grants the incretin effect to β -cells and are direct targets of PAX6 [213]. Notably, inactivation of these receptors in β -cells results in a reduced competence for insulin secretion as the fundamental consequence [78, 272, 273]. Likewise, when the islets were stimulated with 12 mM glucose in addition to exendin-4, a GLP-1 analog, only small but significant increases in insulin secretion were observed in mutant islets (Figure 3.8D). A similar effect was observed when islets were stimulated with KCl, which is a potent insulin secretagogue as it depolarizes the membrane, releasing all readily available insulin vesicles (Figure 3.8D). Interestingly, stimulating islets with forskolin, which bypasses the receptors and directly activates adenylyl cyclase [274], significantly increased insulin secretion in mutant islets. In fact, up to the age of 10 weeks, the release of insulin per content did not show any significant differences between the groups (Figure 3.9C). This suggests that although a trend of lower secretion was observed at all ages, the insulin content of *Pax6^{Leca2}* islets seems to be the primary reason behind the lack of a significant insulin secretion at earlier stages (Figure 3.9). Thereafter, secretory capacity adds to the faulty mechanism as additional downstream targets such as EPAC2 [71] (encoded by *Rapgef4*) are down-regulated (FC -1.81, supplementary table 3). For further affirmation, measurements of cAMP in islet samples under various stimulatory conditions should be undertaken.

Finally, several genes involved in the TCA cycle were regulated in isolated islets of *Pax6^{Leca2}* mice. More precisely, *Pcx* was downregulated (FC -2.74, supplementary table 3) and *Pdk2*, which has been implicated in reduced insulin secretion [275], showed an increased expression (FC 1.96, supplementary table 3). The TCA cycle intermediates ultimately feed into the mitochondrial machinery to induce production of ATP that eventually triggers insulin secretion. Upregulation of mitochondrial genes such as *Ucp2* (uncoupling protein 2, FC 1.70, supplementary table 3) and downregulation of *Pck2* (phosphoenolpyruvate carboxykinase 2, FC -1.69, supplementary table 3) also indicated faulty mitochondrial activity [276, 277]. Therefore, a measurement of the ATP:ADP ratio, in addition to mitochondrial respiration, is further required to demonstrate a potential mitochondrial dysfunction in *Pax6^{Leca2}* islets.

As stated earlier, the insulin gene is under direct control of PAX6 [28] and indirectly via its downstream processing by regulating expressions of *Pcsk1* and *Pcsk2* [213, 214, 216] to ultimately generate mature and functional insulin. Intriguingly, mRNA expressions of *Pcsk1* and *Pcsk2* were similar between the groups in our data. Consistently, it was rather puzzling to find that β -cell specific knockout of *Pax6* did not show downregulation of *Pcsk1* and *Pcsk2* [99, 100]. Results from studies that showed a concomitant decrease in *Pcsk1*, *Pcsk2* and *Pax6* were drawn from

either mouse and human global point mutations or murine β -cell lines [212-214, 216]. This discrepancy could either be explained by the fact that other factors are involved in the control and regulation of the pro-hormone convertases, or that important phenotypic difference between global point mutations and tissue specific knockout mouse models might exist. Nevertheless, considering human patients that carry a *Pax6* mutation, *Pcsk1* seems to be strongly associated with PAX6 [212, 215] and may therefore be taken into consideration as a potential therapeutic target.

Of note, the expression of several genes encoding glycolytic enzymes have been shown to be increased in neonatal islets or in mutants displaying dedifferentiation of β -cells [97, 278]. This essential lack of increase in glycolytic genes further potentiates the notion that loss of β -cell identity cannot fully explain the faulty GSIS of *Pax6^{Leca2}* islets, and instead points to an immature, non-functional state.

Importantly, one significant aspect of PAX6, which was not studied here, is its direct control of the proglucagon gene (*Gcg*), not only in the islet but also in intestinal cells [219]. In this context, GLP-1, a product of the proglucagon gene, has previously been shown to be reduced in *Pax6* mutants [131, 218]. GLP-1 is a major incretin and recently the importance of the islet derived GLP-1 as opposed to intestinal GLP-1 on glucose metabolism, was demonstrated [77]. In regards to the present study, no evidence for a change in the expression of the proglucagon gene was found in isolated islets (Supplementary table 1, 2 & 3). Nonetheless, if we assume that amount of circulating GLP-1 was altered in the *Pax6^{Leca2}* mice, neither an oral gavage nor the direct stimulation of islets with GLP-1 analog exendin-4 (Figure 3.24B & 3.8D) caused a sufficient increase in insulin, which is likely due to the downregulation of the *Glp1r* gene encoding the GLP-1 receptor. Therefore, we considered the investigation of GLP-1 at this point as irrelevant.

4.1.2.3 Changes in RED subdomain DNA binding: A speculation

In the *Pax6^{Aey18}* mutant, the absence of a splice acceptor site leads to the exclusion of exons 5a and 6, eventually rendering the PAI subdomain of the paired domain inactive [279]. Phenotypic differences between *Pax6^{Leca2}* and this model, then, suggest a divergent role for the PAI and RED subdomains of PAX6 in islet endocrine cells. This is in accordance with previous biochemical studies that reported distinct DNA-binding activities for the PAI and RED subdomain [198, 223]. The PAI subdomain directs DNA binding of the PAX6 isoform 1 to the P6CON site, whereas the RED subdomain is responsible for binding of the isoform 5a to the

5aCON site [198]. Confirming this view, biochemical analyses showed that the R128C substitution (precisely the missense mutation of the *Pax6^{Leca2}* model) abolishes binding to 5aCON but has only minor effects on P6CON binding [223]. Hence, with regards to the islets, a model emerges in which the PAI subdomain seems to exert its transcriptional activity during development, specifically for α -cells as recapitulated in the *Pax6^{Aey18}* model [208]. On the other hand, the RED subdomain displays little effect at the developmental stage but seems crucial in adult islets, specifically for β -cells, as demonstrated by our results. Furthermore, a study has shown that the mutation in one subdomain not only renders the other subdomain functional but also causes hyper-activation of it [223]. More recently, Walcher et al. [225] showed similar *in vitro* transactivation activities and demonstrated super-activation of the P6CON motif in the *Pax6^{Leca2}* model. Therefore, it is plausible that lack of an α -cell phenotype in the *Pax6^{Leca2}* model might be the consequence of a hyperactive PAI subdomain function that protects α -cell identity and function. To support this, further hints are derived from studies carried out on *Pax6^{Sey-Neu}*, which lacks the PST transactivation domain and shows diminished β - and α -cell area although to a lesser degree than that as observed in the islets of *Pax6^{Aey18}* mice, wherein the PAI subdomain of the PD is rendered non-functional [208]. This, however, requires further molecular and biochemical validation.

4.2 The metabolic story

4.2.1 *Pax6^{Leca2}* mice maintain normoglycemia with low insulin levels

Most mouse models carrying either a point mutation in *Pax6* or a knockout of the gene show a relatively strong diabetic phenotype [191]. *Pax6* is therefore considered indispensable and required to modulate glucose levels. In fact, other than the non-phenotypic *Pax6^{14Neu}* mice, which carry a point mutation in the HD, no homozygous *Pax6* mutant studied to date survived past a few days postnatally [208]. Moreover, 50% of mice in which *Pax6* is specifically inactivated in the adult β -cell die due to reasons other than hyperglycemia [99]. On the contrary to prior studies, *Pax6^{Leca2}* mice are unique in that they survive to adulthood and the male homozygous *Pax6^{Leca2}* mice can even reproduce. Therefore, to further illustrate changes in blood glucose, weekly measurements at *ad libitum* fed state were carried out. To our surprise, the mice not only showed an absence of hyperglycemia but significantly lower blood glucose levels throughout the measurement period (Figure 3.10B). The differences were obvious from weaning and the blood glucose levels from both groups were maintained within a narrow range. This suggests that overall modulation of blood glucose levels in the *Pax6^{Leca2}* mice is normal considering low insulin levels. Indeed, during an ipGTT in 6 hours fasted mice, both groups

showed similar disposal of glucose, although *Pax6^{Leca2}* mice showed a clear trend towards lower glucose levels (Figure 3.10C). As expected, only low basal insulin levels were found in *Pax6^{Leca2}* mice compared to the increment of insulin levels in the wildtype during GTT (Figure 3.10D). This confirms the *in vitro* data where no increase of insulin secretion was observed in isolated islets of *Pax6^{Leca2}* mice when stimulated with high glucose concentrations (Figure 3.8D). Therefore, at this interval, we hypothesized that the available insulin in *Pax6^{Leca2}* mice must suffice and that other factors might be involved in this apparent increased insulin stimulated glucose utilization.

4.2.2 Changes in the metabolic state of *Pax6^{Leca2}* mice

4.2.2.1 Increased energy expenditure and food intake

Indirect calorimetry is a powerful tool to measure energy flux and it helps to understand changes in metabolic states. Hence, to investigate alterations in fuel consumption and food intake, the mice were transferred in metabolic cages and various parameters were measured over a period of 5 days. A typical response in healthy mice is an increase in locomotor activity as they enter into the active phase around 18:00 hours and consume food (mainly carbohydrates). This inherently increases RER, which subsequently drops as the mice slowly reduce their physical activity around 06:00 hours and enter the inactive phase (predominantly fasting). Therefore, an increase in lipid oxidation is observed as the mice utilize endogenous sources for energy production until they enter into the active phase again thus completing the diurnal cycle. This shift from fasting lipid oxidation to carbohydrate oxidation under insulin stimulation is termed as metabolic flexibility ^[237]. *Pax6^{Leca2}* mice showed a slight increase in oxygen consumption and surprisingly, a significant increase in RER in the inactive phase whereas oxygen consumption was significantly decreased in the active phase (Figure 3.11A-B). However, this significant decrease in oxygen consumption of *Pax6^{Leca2}* mice was only evident because of the adjacent increase in oxygen consumption of wildtype mice, which is a normal response during the active phase. The oxygen consumption of *Pax6^{Leca2}* mice remained similar between the active and inactive phases, as did the RER, suggesting an overall change in metabolic fuel utilization. Indeed, when fuel preference was calculated from the aforementioned information ^[236] an increase in carbohydrate oxidation was observed concurrently with a decrease in lipid oxidation during the inactive phase (Figure 3.11E-F). Again, there was no inherent change in lipid oxidation of *Pax6^{Leca2}* mice between the two phases. By the same token, no significant change in food intake of *Pax6^{Leca2}* mice was observed between the phases (Figure 3.11D). This is reflected in increased food intake during the inactive

phase and comparable food consumption during the active phase as compared to wildtype mice. Diabetic and obese mouse models as well as human diabetic patients exhibit classical metabolic inflexibility, when in the presence of insulin resistance and consequently lower glucose uptake, lipid oxidation continues even under insulin stimulation [280]. Although it was clearly demonstrated that *Pax6^{Leca2}* mice have reduced insulin islet content and secretion *in vivo* and *in vitro*, low lipid oxidation was not an unexpected outcome. In fact, absence of a hyperglycemic state suggests that peripheral tissues respond to insulin and that because *Pax6^{Leca2}* mice show increased food intake, in particular during the inactive phase, carbohydrate oxidation is increased. Moreover, increased locomotor activity supports the notion that the increases in energy expenditure are prevalent, as the mice have significantly reduced body weight, lean mass and fat mass (Figure 3.11G-I). Constant hunger and continuous consumption of food and therefore increased locomotion, seems to be the trigger for increased energy expenditure. Additionally, peripheral tissues in the *Pax6^{Leca2}* mice seem to be able respond to insulin normally, even at very low levels.

The evident loss of metabolic flexibility and lack of diurnal change in energy metabolism during a 24 hour period strongly indicates altered circadian rhythm. Indeed, PAX6 is not only involved in the development of the pineal gland [281], the main regulator of diurnal rhythm [282], but several patients presenting *Pax6* mutations show hypoplasia or absence of the pineal gland [210, 283]. However, these studies do not report metabolic features of patients. Moreover, disruption of clock genes, *Clock* and *Bmal1*, results in a classical diabetic phenotype, reduction in circulating insulin and predisposition to diet-induced obesity [284-286]. Interestingly, liver-specific deletion of *Bmal1* results in better glucose tolerance possibly due to a reduced daily rhythm of hepatic glucose output [287]. Although the circadian status of tissues in *Pax6^{Leca2}* mice was not tested, most of these physiological traits do not fit with the *Pax6^{Leca2}* model. Moreover, presence of the pineal gland was detected in *Pax6^{Leca2}* mice and comparable values of plasma serotonin (data not shown) between the mutant and wildtype groups suggest that any changes, if present, are possibly downstream of serotonin signaling and would require further investigation.

4.2.2.2 Increased insulin sensitivity and reduced hepatic glucose production

The next rational step was to verify whether *Pax6^{Leca2}* mice were hyper-responsive to insulin. Indeed, an insulin tolerance test clearly demonstrated that a higher decrement in blood glucose levels upon insulin administration in the *Pax6^{Leca2}* mice was evident (Figure 3.12A). This was further affirmed by undertaking hyperinsulinemic-euglycaemic clamp wherein the amount of

glucose infused in the mice to maintain glycemic levels were significantly increased in the *Pax6^{Leca2}* mice (Figure 3.12D). The liver is responsible for about 30% of glucose disposal as estimated in human and canine studies [288], but in addition, liver also curtails its own glucose output under the influence of insulin. Hence, the amount of glucose released from the liver was calculated and *Pax6^{Leca2}* mice showed a highly significant suppression of HGP during the clamp (Figure 3.13A-B). Furthermore, skeletal muscle accounts for about 65% of the postprandial glucose uptake, while white adipose tissue (WAT) accounts for less than 10% of glucose disposal in humans [289, 290]. Therefore, these tissues among others were collected after the clamp and glucose uptake was measured. Interestingly, no tissue showed any significant increase in glucose uptake in *Pax6^{Leca2}* mice while only non-significant trends towards increased uptake were observed for WAT and liver (Figure 3.13C). This was also reflected in non-significant trends towards increased total glucose disposal (Figure 3.13D). Additionally, urine was collected at the end of the experiment to correct for any loss of glucose via micturition, also termed glycosuria, and no significant difference was found between the groups excluding the possibility of loss of glucose via urine (Figure 3.13E) to contribute to increased GIR. Therefore, reduced blood glucose values after 6 hours fasting and at the *ad libitum* fed state in *Pax6^{Leca2}* mice were mostly attributed to decreased HGP or to increased response of the liver to insulin.

Insulin signaling in the liver activates the AKT pathway that ultimately shuts down transcription of key gluconeogenic enzymes [291]. Therefore, to further affirm the aforementioned conclusions, RNA was extracted from livers of fed and 6 hours fasted mice and the expression levels of 4 major gluconeogenic enzymes were analyzed. As expected, *Pck1* and *G6pc* were both significantly downregulated in the livers of *Pax6^{Leca2}* mice during the fed state (Figure 3.14A-B). Conversely, the regulation of these enzymes was significantly increased in *Pax6^{Leca2}* mice during the fasted state. This data hints directly towards a decrease in the HGP pathway during fed states when insulin signaling suppresses gluconeogenesis. In light of this, livers of mice were collected shortly after being injected with insulin to directly assess effects on this pathway. A significant decrease in PEPCCK and a non-significant trend towards decreased expressions of G6PC and PCX was observed in *Pax6^{Leca2}* mice (Figure 3.15D-F). This was concurrently observed with a significant increase in phosphorylated AKT at Thr308 (Figure 3.15B). Taken together, these results reveal a potential hyper-activation of insulin signaling, which may be responsible for reduced HGP in *Pax6^{Leca2}* mice.

To put these effects into a physiological context, we injected mice with either pyruvate to target gluconeogenesis or glucagon to allow breakdown of glycogen and thereby promote HGP. Interestingly, though pyruvate administration did not produce a strong response in *Pax6^{Leca2}* mice, glucagon injection brought the blood glucose values in these mice significantly higher than that in the wildtype (Figure 3.16). Of note, *Pck1* seems to be the most affected gene in the liver during fed states of *Pax6^{Leca2}* mice and liver specific *Pck1*-null mice respond poorly to pyruvate as a gluconeogenic substrate [292]. Therefore, a distinction between these 2 pathways was observed and several revelations were made;

- i. Directly providing substrate for gluconeogenesis produced little effect on blood glucose levels in the *Pax6^{Leca2}* mice, thereby confirming suppression of gluconeogenesis
- ii. Liver responded to glucagon normally and increased blood glucose levels in the *Pax6^{Leca2}* mice, displaying an intact connection between pancreatic α -cells and the liver
- iii. In presence of glucagon, enhanced glucose lowering effects exerted by insulin diminished and these mice become hyperglycemic

In mice lacking the glucagon receptor, insulin levels drop due to a failure of the secretory mechanism although these mice display higher insulin sensitivity and hyperglucagonemia due to a distorted islet-liver interaction [272, 293]. However, in *Pax6^{Leca2}* mice, the islet-liver axis seems to be intact and no change was observed in the levels of circulating glucagon (Figure 3.17D). Moreover, no evidence exists in literature to suggest that PAX6 is involved in translation of glucagon and its related products such as GLP-1 and GIP and neither does it play a role in post-translational modification. Therefore, the significant increase in blood glucose of *Pax6^{Leca2}* mice as a response to exogenous administration of glucagon mirrors a lack of insulin action when glucagon signaling is predominantly present. Although *ad libitum* fed glucagon levels were not measured, it is conceivable that by consuming food and maintaining a fed state, glucose itself could be a major factor behind inhibition of glucagon action on liver [148] and in doing so, prevent an increase in glycemia via HGP in presence of low insulin levels.

Glucagon stimulates the breakdown of glycogen in the liver. To investigate whether the glycogen stores were affected, PAS staining was carried out. The results showed lower amounts of glycogen storage in livers of fed *Pax6^{Leca2}* mice (Figure 3.17A), suggesting that these mice store less glucose, possibly as a consequence of lower amounts of circulating insulin. However, this may also reflect an increase in glycogenolysis in order to compensate for the decreased gluconeogenic output [147]. Of note, glycogen levels were similar between the groups after a 6

hour fasting period (Figure 3.17B). This indicates that the increase in $Pax6^{Leca2}$ glycemia levels post glucagon administration is independent of the glycogen content, which additionally supports the fact that absence of insulin signaling is primarily the cause behind increase in blood glucose levels.

Intriguingly, little change in blood glucose levels was observed when $Pax6^{Leca2}$ mice fasted for 6 and 16 hours (Figure 3.17C). Moreover, simultaneous increment in circulating glucagon levels after 6 or 12 hours fasted time points were similar between the groups (Figure 3.17D), again demonstrating normal pancreatic α -cell function. Therefore, $Pax6^{Leca2}$ mice in presence of glucagon continue to maintain their blood glucose levels wherein the absence of predominant insulin signaling and its effects on liver are absent. It is noteworthy that mice, unlike humans, utilize glycogen rapidly during the first few hours of fasting and the lowest amounts are detected after about 12 hours of fasting [294]. Therefore, absence of change in circulating glucose levels between 6 and 16 hours of fasting in $Pax6^{Leca2}$ mice suggests that other sources such as intestine and kidney may compensate for the reduced HGP [137].

However, $Pax6^{Leca2}$ mice do not enter a prolonged fasting state or maintain glucagon signaling as shown by their increase in locomotor activity as well as food intake regardless of the time (Figure 11C-D). Hence, these mice consume food and consequently maintain their blood glucose levels and in turn keep HGP suppressed. Another clue that can be added to support the inherent reduction in HGP machinery emanates from normal lipolytic substrate availability. Circulating FFAs and glycerol, which feed into the HGP cycle without changing the regulation of PEPCK and G6PC [144] were similar between the groups (Table 3.2). Thus, availability of substrates does not seem to contribute to the reduction of HGP in the $Pax6^{Leca2}$ mice.

An additional effect might come from FGF21, another *in vivo* endocrine signal, which is specific to peripheral metabolism. The circulating level of FGF21 was found to be altered in $Pax6^{Leca2}$ mice. Most of the circulating FGF21 comes from liver and has been shown to be a gluconeogenic activator [167]. However, exogenous administration of FGF21 has shown to increase insulin sensitivity and reduce triglycerides to ultimately reduce blood glucose levels [295] and protect mice from DIO [296]. Expression of *Fgf21* was significantly regulated in the livers of $Pax6^{Leca2}$ mice during both fed and fasted states (Figure 3.19B). Concomitantly, circulating FGF21 levels were also increased during both fasting and fed states (Figure 3.19A). This finding proposes two different possibilities. Firstly, this increase may simply be an added factor to the increased regulation of gluconeogenic enzymes as a compensatory mechanism to

the reduced blood glucose levels. Secondly, and perhaps a more likely scenario is that FGF21, which increases after prolonged fasting, might reflect a constant fasting state being overcome by *Pax6^{Leca2}* mice. Indeed, FGF21 induces food intake and simultaneously protect the mice from obesity, possibly by inducing energy expenditure [296]. A major regulator of FGF21 is *Ppara* [163-166] which, however, does not seem to be regulated in either group. Furthermore, additional evidences are presented, as FGF21 also decreases enzymes related to fatty acid synthesis in the liver of mice [247]. In *Pax6^{Leca2}* mice, *Srebp1c*, *Fasn* and *Acaca* were all downregulated during the fasting state (Figure 3.20). Increased *Srebp1c* levels have been associated with a fatty liver phenotype with corresponding increases in expressions of FASN and ACC in *ob/ob* mice [297]. Likewise, ATP-citrate lyase (ACLY) was downregulated in *Pax6^{Leca2}* mice and mice lacking hepatic ACLY have a reduced glycemic index and are protected from developing a fatty liver [298]. The data together provides indications for reduced fat in the liver of *Pax6^{Leca2}* mice. However, it is difficult to explain what triggers this evident increase in FGF21 although its effects seem to be in accordance to the prevailing phenotype of the *Pax6^{Leca2}* mouse model. *Pax6^{Leca2}* mice appear to circumvent hyperglycemia due to the lack of insulin via enhanced action of insulin on the liver, increased food intake and thereby glucose induced inhibition of HGP as well as by increasing energy expenditure, which may in part be driven via increased levels of FGF21. Isolated hepatocytes from mice were used to investigate the capacity to release glucose in absence of any *in vivo* stimuli after 6 days in culture medium. Hepatocytes from both groups neither showed any significant difference in basal glucose release nor after stimulation with glucagon, dexamethasone and forskolin (Figure 3.18). Hence, a lack of external stimuli could explain why no change was observed between glucose release from the hepatocytes of *Pax6^{Leca2}* and wildtype mice.

In summary, although breakdown of glycogen via glucagon appears to be normal, glycogen itself is reduced thereby limiting its availability to contribute to HGP during fasted states in the *Pax6^{Leca2}* mice. On the other hand, in presence of abundant lipolytic substrates, the innate gluconeogenic mechanism itself seems to be distorted, which is indicated to be under the influence of enhanced effects of insulin and/or FGF21. Hence, both pathways of HGP seem to be negatively affected in *Pax6^{Leca2}* mice, conclusively demonstrating a liver-specific enhanced insulin action, despite low amounts of circulating insulin.

4.2.2.3 HFD fed *Pax6^{Leca2}* mice are resistant to DIO but not to hyperglycemia

Feeding high fat diet in animal studies has become an essential part of the experimental design as it recapitulates parts of modern life style in humans and at the same time, exacerbates

metabolic phenotypes. In the present study, mice carrying a mutation in the *Pax6* gene have shown a plethora of metabolic features, some of which seem counterintuitive. To investigate their response to a higher fat content in their diet, *Pax6^{Leca2}* and wildtype mice were challenged with 10 weeks of HFD together with control from both genotypes being fed a low fat diet. Interestingly, *Pax6^{Leca2}* mice showed signs of increased glycemia just one week after replacing chow food with HFD (Figure 3.21B). Subsequently, *Pax6^{Leca2}* mice became significantly hyperglycemic after another 3 weeks of HFD and continued to increase their blood glucose levels. It is worth mentioning that much variation existed within the HFD group of *Pax6^{Leca2}* mice as seen by the large error bars. About 15% of the mice from this group tended to be resistant to HFD induced hyperglycemia during the course of the dietary challenge. However, the majority of them displayed blood glucose levels similar to (40%) or higher (45%) than that found in the wildtypes. Surprisingly, *Pax6^{Leca2}* mice showed small but significant increases in weight gain during the HFD challenge compared to low fat diet *Pax6^{Leca2}* controls. However, their weight gain remained significantly less than that in the wildtype HFD group showing signs of resistance to obesity conferred by higher fat contents in the diet (Figure 3.21A). After 10 weeks of high fat or low fat diet, measurements concerning body composition were made. *Pax6^{Leca2}* mice fed with HFD showed only mild and non-significant increases in fat mass as compared to *Pax6^{Leca2}* mice fed with LFCD (Figure 3.22C). Moreover, body weight and lean mass remained significantly lower than in wildtype mice fed with HFD (Figure 3.22A-B).

To test the capacity of HFD mice to metabolize glucose, we challenged the mice with an ipGTT and oGTT. In accordance to the weekly blood glucose measurements, HFD mice from both genotypes showed significantly increased glycemia although *Pax6^{Leca2}* mice showed a higher area under the curve suggesting intolerance to glucose (Figure 3.23). Interestingly, blood plasma collected during ipGTT clearly showed an increase in fasting insulin levels in both groups fed with HFD as a consequence of increased β -cell mass in response to higher demands [299]. However, only the wildtype mice were able to elicit a response to increased glucose regardless of the diet (Figure 3.24A). This difference is further accentuated when glucose was given orally and the incretin driven amplification of insulin was missing in *Pax6^{Leca2}* mice but evidently present in the wildtype (Figure 3.24B), supporting the lack of increase in *ad libitum* fed blood glucose values. This is of utmost significance as the failure of β -cell expansion in response to increased requirements is the hallmark of obesity induced diabetes [299]. Disruption of insulin receptor substrate 1 (*Irs1*), produces glucose intolerance without diabetes because enhanced insulin secretion is able to compensate for insulin resistance [300, 301]. This, however,

is not the case for *Irs2*-null mice wherein lack of β -cell compensation renders the mice diabetic [302, 303]. Likewise, wildtype mice in the present study were able to metabolize glucose with a similar rate regardless of the diet as HFD potentiated the increase in insulin content and secretion, hence allowing meeting the increased demands. On the other hand, *Pax6*^{Leca2} mice on HFD showed small but ultimately insufficient increases in insulin content and the lack of a working secretory mechanism as discussed before paved the way for hyperglycemia and subsequently diabetes.

Of note, this particular *Pax6* model is on a C3HeB/FeJ background, which is genetically predisposed to quicker glucose disposal as compared to mice on C57BL/6J background [304]. It is vital to mention this because some metabolic studies carried out to elucidate functional aspects of *Pax6* mutations have used C57BL/6J [131, 212]. In the present study, wildtype C3HeB/FeJ mice are able to maintain normoglycemia even with dietary intervention, hence the effects observed due to the interaction between the *Pax6* mutation and the diet must be independent from the genetic background of the mice. However, for further confirmation, *Pax6*^{Leca2} mice need to be backcrossed to the C57BL/6J background and investigated for a similar metabolic phenotype.

In spite of the fact that the reduction in circulating insulin levels in *Pax6*^{Leca2} mice fed with HFD is certainly an important contributor to increased blood glucose levels, we wondered whether the diet may have also affected fat metabolism and subsequently whole body insulin sensitivity. Blood collected from the mice fed with HFD was analyzed for various parameters. Interestingly, no difference between plasma cholesterol and triglycerides was observed between the groups as that seen in the chow fed diet, which may reflect the increase in lipid oxidation as a normal response to increased fat content in the food (Table 3.3). This was in accordance to reduction in RER in both groups on HFD as compared to those on LFCD (Supplementary figure 4). An insulin tolerance test further revealed loss of the acquired insulin sensitivity, which can be seen intact in *Pax6*^{Leca2} mice fed with LFCD (Figure 3.25A-B). Another aspect of the dietary intervention was that about 25% of *Pax6*^{Leca2} mice died during the course of HFD (Figure 3.25C). A similar observation was made recently in β -cell specific knockout of *Pax6* where almost 50% mice died due to lack of PAX6 and hyperglycemia [99]. The authors however, hypothesized that hyperglycemia may not been the lone factor since other mouse models of diabetes show similar increases in blood glucose levels and still survive. Ketoacidosis is known to cause death in acute diabetes and *Pax6* inactivation in neonatal and adult mice have both shown increased ketone, which in addition to hyperglycemia may have

contributed to death in these animals [99, 207]. Moreover, pancreatic α -cell secreted glucagon is a major contributor to ketone formation [305-307] and it was suggested to be involved in death of β -cell specific *Pax6*-null mice [99]. Although signatures for ketone formation were not investigated, no signs of increased circulating plasma glucagon were observed in *Pax6^{Leca2}* mice fed with HFD (Supplementary figure 5). Another endocrine hormone implicated in this regard is FGF21. Knockdown of FGF21 in mice has shown to evidently reduce serum ketones thereby suggesting promotion of ketogenesis [165]. This finding underlies the temporal link between late induction of FGF21 during prolonged fasting [163, 164] wherein ketogenesis takes precedence as a major source of energy. Therefore, the increased FGF21 levels in *Pax6^{Leca2}* mice may have exacerbated ketogenic processes and in turn cause diabetic ketoacidosis resulting in the death of mice during the HFD challenge test.

4.2.2.4 Contribution of the hypothalamus to the metabolic phenotype of *Pax6^{Leca2}* mice

The complexity in the whole body mutant model has warranted investigations of several tissues. The data acquired thus far has determined major changes in metabolism, which seem to primarily involve the liver. A key conundrum arises here as *Pax6*, which is highly expressed in the islets, cannot explain changes in the liver directly as very low to no expression of the TF was detected in the metabolic tissue [249] including fat (Figure 3.26). Considering the lack of obvious changes in lipolytic substrates and glucose uptake in muscle and adipose tissue, metabolic changes in these tissues, such as decrease in fat content, must be secondary to an islet and liver phenotype. Moreover, changes in liver might echo a peripheral reaction to centrally controlled food intake and energy expenditure. *Pax6* expression was observed in some scattered population of cells in the hypothalamus during development [220]. More recently, the presence of *Pax6* was found in the ZI region of the hypothalamus [221]. Therefore, we extracted the hypothalamus from mice of both genotypes and confirmed *Pax6* to be expressed in high amounts (Figure 3.26). Moreover, immunostaining revealed PAX6 protein to be present with high expression in the ZI and dorsal parts of lateral and posterior hypothalamic areas (Figure 3.27B-E) as well as sporadically lower expression in some other parts while very low to no expression in the arcuate nucleus (Figure 3.27F-G).

Considering the phenotypic changes in energy expenditure and food intake, we determined whether any changes in hypothalamic expression of genes involved in energy balancing and regulation were present. qRT-PCR results showed a significant decrease in expression of *Pomc* and *Cartpt* (cocaine- and amphetamine-regulated transcript) in the hypothalami of *Pax6^{Leca2}* mice (Figure 3.28A). POMC/CART neurons are anorexigenic, which upon stimulation by

insulin and leptin pathways, reduce food intake^[179]. Therefore, the decrease in their expression is in accordance to the increased food consumption of *Pax6^{Leca2}* mice. On the contrary, transcripts for orexigenic *Npy* (Neuropeptide Y) and *Agrp* seem unaffected (Figure 3.28A). We also measured the mRNA levels of two melanocortin receptors *Mc3r* and *Mc4r*, both of which are involved in feeding mechanisms^[308, 309]. Although *Mc3r* expression was similar between the groups, *Mc4r* expression was significantly increased in *Pax6^{Leca2}* mice. MC4R is a seven-transmembrane GPCR, which has high affinity for the POMC product^[310], α -melanocortin stimulating hormone (α MSH)^[311]. Studies have shown that *Mc4r*-null mice display increased food intake, obesity and hyperglycemia^[312], which are paralleled with cases of morbid obesity in humans carrying *Mc4r* mutations^[313]. As observed, *Pax6^{Leca2}* mice have an increased food intake but display lower body weight, which is reflected in increased energy expenditure. Incidentally, divergent roles of the melanocortin pathway have elucidated that MC4R in the paraventricular hypothalamus (PVH) controls food intake while in the other regions of the hypothalamus; MC4R is involved in regulating energy expenditure^[314]. These effects, however, are likely to be mutually exclusive^[315] and since the location of the increase of *Mc4r* in the hypothalamus is unknown, it is uncertain whether its effects contribute to food intake or energy expenditure since both were significantly increased in *Pax6^{Leca2}* mice.

Furthermore, leptin and insulin are the two major hormones that stimulate and control hypothalamic regulation of metabolism. Circulating insulin levels are low in *Pax6^{Leca2}* mice and no change in hypothalamic *Insr* was observed in these mice (Figure 3.28A). Likewise, we also found low levels of circulating leptin amounts in *Pax6^{Leca2}* mice (Figure 3.28B), which was unsurprising considering the lower absolute fat content. Leptin acts as an indicator of the energy stores, which increases after feeding and reduces only hours after fasting in rodents^[316] and is directly proportional to the fat mass^[177]. In addition, insulin stimulates leptin production and its secretion^[317, 318] and therefore, low levels of leptin correlate with low insulin levels^[316]. The relative decrease in fasted and fed plasma samples from both groups was similar (2.07 fold decrease in wildtype and 1.80 fold decrease in *Pax6^{Leca2}*), suggesting normal response of adipose tissue to insulin as indicated during the clamp study. However, mRNA expressions of leptin receptor (*Lepr*) and some intermediates in its pathway in *ad libitum* fed hypothalamus samples of *Pax6^{Leca2}* mice showed small but significant increases (Figure 3.28C). This increase in expression may have been a compensatory effect in response to low leptin amounts or an actual increase in the activation of the leptin pathway to counter food intake and increase energy expenditure. To determine whether leptin exerts an increased effect on energy

metabolism, mice were either injected ip with leptin or vehicle and their food intake was monitored. Interestingly, the wildtype mice showed a decrease in food intake for the first 2-8 hours post leptin administration but later increase their food intake (Figure 3.29A) as the effects of leptin decreased [255, 256]. Conversely, the *Pax6^{Leca2}* mice from the leptin and vehicle groups initially showed similar food intake but leptin treated mice seem to decline slowly in their food uptake although the differences could not reach significance (Figure 3.29B). Therefore, the effects of leptin are largely unable to significantly reduce food intake in *Pax6^{Leca2}* mice and it is therefore likely that the increased expressions of leptin pathway intermediates are a compensatory response to the reduced quantity of circulating leptin.

At this juncture, it is still highly likely that the hypothalamus plays a role in shaping the metabolic phenotype of *Pax6^{Leca2}* mice as features such as food intake, energy expenditure and even effects derived from the liver are to a large extent centrally controlled. A genome-wide study of DNA-binding properties unravels the most basic of molecular interactions and provides a global view on the possible functions of a particular protein. Since we established the presence of PAX6 expression in the hypothalamus but its function is as yet unknown, chromatin immunoprecipitation and subsequent sequencing of the protein bound DNA was used to determine direct PAX6 targets in the whole hypothalamus. Moreover, a comparative study was conducted in order to determine changes in the DNA binding properties of the mutated PAX6 protein. The ChIP-seq experiment revealed 3,885 genomic sites associated with PAX6 binding in the wildtype and 3,433 genomic sites in the *Pax6^{Leca2}* sample. These genomic sites were assigned to 3,826 and 3,531 genes depending on the proximity in the wildtype and *Pax6^{Leca2}* hypothalamus respectively (data available on request). Therefore, this displays that PAX6 is not only expressed in the hypothalamus but also binds to various sites on the hypothalamus and in turn indicates unknown functional aspect. The overall binding pattern was similar between the groups. To take a closer look into the genes that were associated with the genomic regions and present in both samples, GO term analysis was carried out. It was interesting to note that several hundred of these genes are involved in various metabolic processes among which were *Igfr1*, *Pcx*, *Pdk2*, *Vldlr*, *Cbp2* and *Pax6* itself, all of which are dysregulated in the islets of 10 week old *Pax6^{Leca2}* mice hinting that PAX6 directs their regulation in the islets. Furthermore, *Irs1* was found to be a direct target of PAX6, which prompts further investigations into the role of *Pax6* as an intrinsic player in the insulin-signaling cascade. These results from ChIP-sequencing provide a first insight into the whole spectrum of possible roles of PAX6 in the hypothalamus. One recent study revealed its

presence in the ZI region of the hypothalamus where it specifically marks a subpopulation of GABAergic neurons [221]. GABAergic neurons essentially release gamma-aminobutyric acid (GABA) and are present in various parts of the hypothalamus [319]. The importance of GABA has previously been highlighted in central regulation of feeding and energy balance via AGRP neurons [320,321]. Moreover, GABAergic neurons have also been shown to mediate leptin driven anti-obesity effects via POMC neurons [319]. Chen et al, elegantly separated gene markers to define certain neuronal subtype population in the hypothalamus and their findings showed that a *Pax6* positive cell cluster lies in GABAergic neurons in the ZI [221]. Therefore, we compared their RNA-sequencing data with our whole hypothalamus ChIP-sequencing data from both sets of samples and found that Protocadherin 8 (*Pcdh8*) and *Pax6* as direct targets within *Pax6* positive neuronal cluster. Interestingly, certain genes were regulated in their study as a consequence of a 24 hours food deprivation [221], of which four other genes were found to be direct targets of PAX6 demonstrated in our data; namely, *Pura* (Purine Rich Element Binding Protein A), *Lsm2* (Small Nuclear Ribonuclear Protein D Homolog), *Tubg2* (Tubulin Gamma 2) and *Miat* (Myocardial Infarction Associated Transcript). Despite the fact that none of these genes have any specific reported function in the hypothalamus regarding metabolism, it sets the stage for further exploration into the possible functions of PAX6 in the adult mouse hypothalamus.

Bound regions from both samples displayed the ATF-1 motif was found to be the most enriched one (Figure 3.31A). PAX6 may indirectly regulate ATF-1 as upregulation of *Pax6* (via *Pax6*(con) as in the case of *Pax6^{Leca2}* mice) also upregulated *Atf-1* and might therefore act in union and share similar binding sites [322]. *Pax6* motif however, was highly enriched in the wildtype unlike in the *Pax6^{Leca2}* hypothalamus (wildtype $p=10^{-19}$ and *Pax6^{Leca2}* $p=10^{-3}$). Furthermore, several genes assigned to genomic sites seem to be associated with a differential binding property of the PAX6 when compared between the wildtype and *Pax6^{Leca2}* hypothalamus. Using MACS differential Peak calling, 124 genomic sites in the wildtype and 38 in *Pax6^{Leca2}* were found to be differentially bound (Supplementary table 4). Of these, 159 site-associated genes that showed reduced binding in *Pax6^{Leca2}* mice, the *Pax6* motif was found to be the most enriched while the 41 site-associated genes that displayed increased binding in the *Pax6^{Leca2}* mice did not show any enrichment. This indicates that the mutated PAX6 protein may have acquired the ability to bind on different sites and therefore to genes not usually bound by the TF in the hypothalamus. RT-qPCR carried out to verify the regulation of transcripts of the bound genes revealed differential expression in some. In this regard, *Foxo1* appeared as an

important target, which was differentially bound (Figure 3.31C) and upregulated in the *Pax6^{Leca2}* hypothalamus (Figure 3.32A). This TF mediates actions of leptin and insulin via POMC and AGRP neurons in the hypothalamus [179, 183, 184]. Although small amounts of *Pomc* and *Agrp* appear to be expressed in the *Pax6* positive neuronal cell cluster in the ZI [221], it is uncertain and highly speculative at this point whether a small population of cells with presumed altered actions could modulate the energy metabolism for the whole body. Nonetheless, it is noteworthy that an increase in the transcript levels of *Foxo1* (Figure 3.32A) is in accordance to a decrease in *Pomc* and an increase in the food intake [183] of *Pax6^{Leca2}* mice. Thus, *Foxo1* appears to be under direct control of the mutated PAX6 protein.

One of the most remarkable effects in *Pax6^{Leca2}* mice is the reduced HGP. Hypothalamic pathways directly affecting this peripheral mechanism have been studied previously [172-174, 254] and although much needs to be further validated, a liver-hypothalamus axis seems to be an important regulator to HGP. In the context of the *Pax6^{Leca2}* mouse model, FGF21 may be of importance. FGF21 has shown to be able to cross the blood brain barrier [323] and was recently shown to directly affect brain-liver interaction via the HPA axis [324]. Moreover, FGF21 acts via FGFR1-3 [325], all of which are broadly distributed across the hypothalamus [326]. Hence, it would be interesting to investigate the extent to which FGF21 modulates energy metabolism in the *Pax6^{Leca2}* mice.

A key issue in relation with changes in the hypothalamus in this model has to be underlined. Even though alterations in mRNA levels of important genes reflect the current state of *Pax6^{Leca2}* mice as a whole, direct involvement of *Pax6* has to be put under question. In this regard, MC4R positive neurons are not GABAergic and are present in the PVH [327], where little to no expression of *Pax6* was found. In addition, absence of *Pax6* expression in ARH and PVH, where large number of POMC neurons reside [328, 329], suggests that effects on *Pomc* too, are likely to be indirect. Nonetheless, FOXO1 is an intrinsic player in the insulin signaling pathway, and the insulin receptor is found in many parts of the brain and hypothalamus including the ZI region [330]. Moreover, rodents with lesions in the ZI region show alterations in feeding [331, 332]. Additionally, melanin-concentrating hormone (MCH), an important player in regulation of energy metabolism [333], is specifically expressed in LHA and ZI regions [334, 335] of the hypothalamus where PAX6 positive neurons can be found. Consequently, blocking MCH signaling results in changes in activity and feeding behavior of mice [336]. Therefore, the inclusion of PAX6 in feeding mechanism and energy metabolism as a whole by means of

alternative pathways, such as that of MCH via unknown mechanisms might be plausible although much remains to be explored in the role of PAX6 in these neurons.

In summary, the *Leca2* mutation of the PAX6 protein seems to be sufficient for inducing physiologic abnormalities in the islet, which seem specific to the functional identity of β -cells. *In vivo* studies displayed dramatically reduced insulin secretion in *Pax6^{Leca2}* mice. This was supported by *in vitro* insulin secretion assay, wherein islets of *Pax6^{Leca2}* mice secrete less insulin even after incretin stimulation. This decrease is driven by changes in gene expression of several GPCRs (*Glp1r*, *Ffar1* and *Gcgr*) and TCA cycle intermediates (*Pcx* and *Pdk2*) among others, therefore hinting at a possible mitochondrial dysfunction. However, these mice are able to evade a hyperglycemic state due to enhanced insulin action in the liver. *Pax6^{Leca2}* mice displayed reduced expressions of gluconeogenic enzymes such as PEPCK, therefore attenuating gluconeogenesis and have lower glycogen storage thereby negatively affecting contribution to HGP via glycogenolysis. The metabolic phenotype of *Pax6^{Leca2}* mice reflects a constant orexigenic phase and increased feeding, however, with reduced body weight possibly due to increased energy expenditure and locomotor activity. Accordingly, decreased gene expression of *Pomc* and *Cartpt*, while increased gene expression of *Foxo1* in the hypothalamus of *Pax6^{Leca2}* mice support this notion. Remarkably, *Pax6^{Leca2}* mice displayed increased binding to *Foxo1* in the hypothalamus, which suggests direct involvement of PAX6 and calls for further investigations of its function in hypothalamus. Although phenotypic characteristics related to β -cell dysfunction of *Pax6^{Leca2}* mice are similar to other *Pax6* mutants, the absence of hyperglycemia and increased liver insulin sensitivity is specific to this model. Therefore, this *Pax6* model demonstrates the importance of studying individual DNA binding domains of TFs as opposed to whole gene deletions especially for mutations relevant for human population. A graphical summary of the present study is shown in Figure 4.1, highlighting the most important findings.

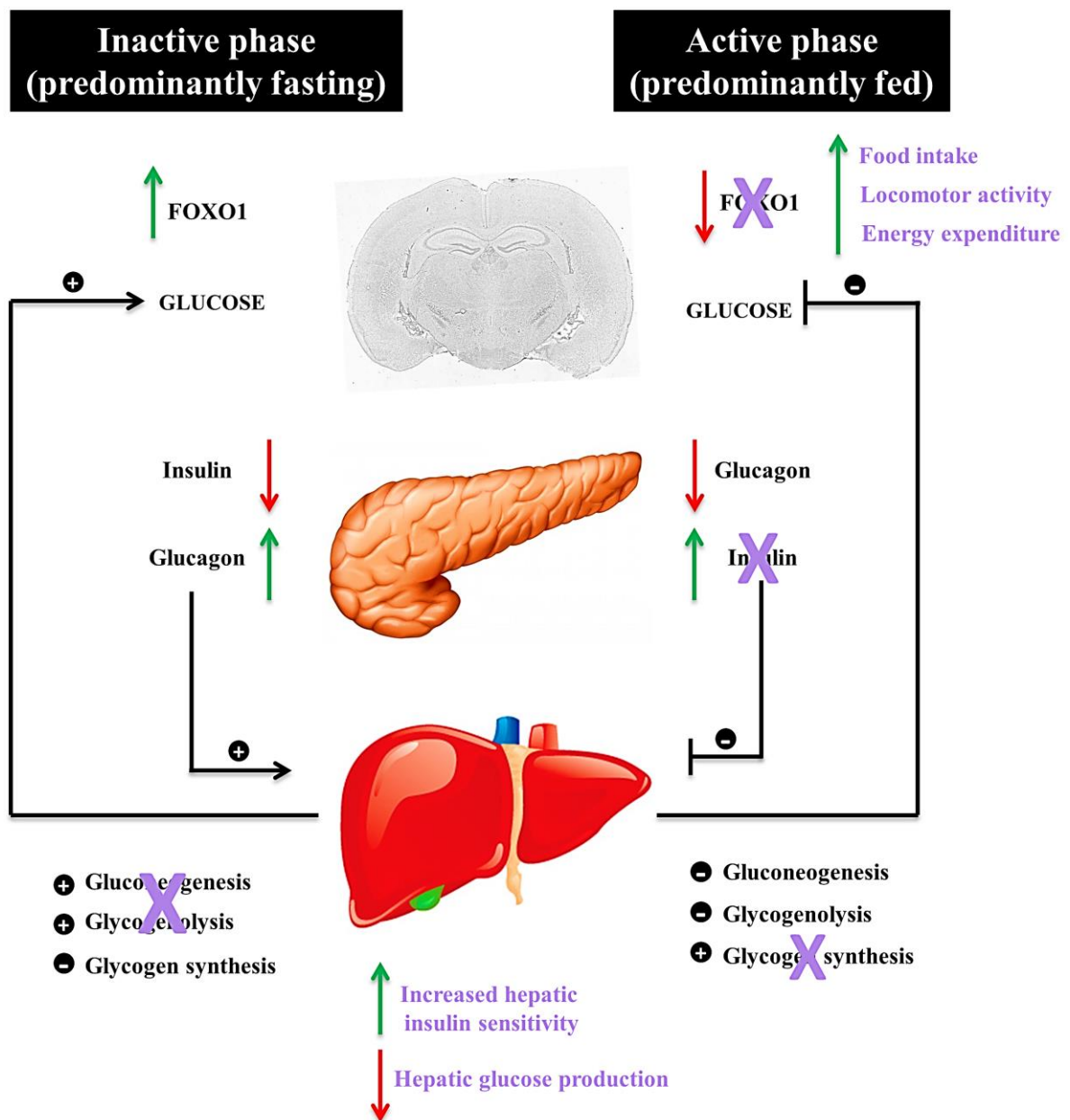


Figure 4.1: Graphical summary of *Pax6^{Leca2}* mouse model

Schematic diagram displays normal metabolic changes during fed and fasted state in wildtype mice. Representative symbols: green arrows and plus signs – positive regulation; red arrows and minus signs – negative regulation; black lines – direction of physiological effect. Purple crosses and text – negative regulation and phenotypic changes in *Pax6^{Leca2}* mice, respectively. Images of organs were adapted from [251, 337, 338].

4.3 General remarks and future perspectives

From *Pax6^{Leca2}*, being a homozygous whole body mutant, several organs and organ systems were brought into study to investigate the existence of a non-diabetic phenotype. Unlike tissue specific knockout models, this could complicate certain conclusions since various indirect factors may be at play. The well-established role of PAX6 in the development of the pancreas and certain parts of the brain further add to the complexity of the model. In the present study, insulin and glucagon positive cells at E18.5 showed no difference between the groups.

Therefore, it is safe to assume that changes in β -cells in *Pax6^{Leca2}* mice are mostly postnatal. Similarly, functional variations in the liver of these mice must be postnatal, since liver and pancreas are specified into individual tissues at the same time without any overlap^[339, 340], just before the emergence of *Pax6* expression^[27]. In the developing hypothalamus, PAX6 has not been shown to play a role although presence of *Pax6* expression in ZI indicates a pending investigation.

Even though ChIP-sequencing data was recently made available to demonstrate PAX6 binding sites in the pancreatic β -cell line Min6^[99], binding sites in the whole islet would elucidate a more global functional view. For this purpose, either islet chromatin or sorted primary islet cells, should be collected and subjected to ChIP-sequencing to elucidate DNA binding in the whole set of islet cells or individual islet populations. Furthermore, the recent advances in illuminating β -cell heterogeneity^[128, 341] would warrant sorting of different β -cell subpopulations and investigating functions of PAX6 and other TFs. Similarly, the recent discovery of PAX6 positive cells in the ZI region of the hypothalamus^[221], which supports the findings of the present study, opens new questions regarding the function of a PAX6 positive neuronal population in the hypothalamus. Although the data presented here gives an overview of possible functions of PAX6, a complimentary analysis of the transcriptome in the hypothalamus is certainly essential. Therefore, either RNA-sequencing or microarray analysis should be carried out. Moreover, different regions of the hypothalamus in which PAX6 expression was found should be investigated individually. This would reveal *Pax6* expression levels for each region and subsequently help to expose the extent to which the hypothalamus might be involved in the metabolic phenotype of the *Pax6^{Leca2}* model. Additionally, any possible distortions in circadian rhythm should be investigated, which may in part explain the prevailing liver-associated phenotype in *Pax6^{Leca2}* mice.

Lastly, the degree to which the liver function in the *Pax6^{Leca2}* mice was altered was somehow surprising. Perhaps a more in-depth understanding of the liver function is required. A detailed *in vitro* experiment to elucidate mitochondrial function in isolated hepatocytes could be undertaken, including assays to demonstrate glucose secretory capacity under various conditions. Moreover, inducing a tissue-specific R128C mutation in adult mice could help indicate the origins of the evident enhanced insulin action on the liver. This in turn will also help to understand the role of individual tissue and organ systems contributing to the prevailing metabolic characteristics of *Pax6^{Leca2}* mice.

4.4 Closing remarks

The complexity of the *Pax6*^{Leca2} mouse model is as fascinating as its unexpected metabolic features. Despite a β -cell dysfunction, *Pax6*^{Leca2} mice show the absence of an expected hyperglycemic state due to increased hepatic insulin activity. The present study is the first report of such a feature associated with *Pax6*. Moreover, the R128C mutation was previously discovered in human patients with aniridia. Therefore, a point mutation captures a much closer and more global outlook thereby laying out questions for investigations in altered rather than abolished gene regulatory network. Furthermore, this study brings to light, that different and even opposing effects can be exerted by the same gene with different mutations, emphasizing that the changes in DNA binding may precede loss of protein. Additionally, the hypothalamus seems to be included in the PAX6 regulatory network, which leaves room for much needed inquiries and examinations of its precise function in the central control of metabolism.

5. APPENDIX

5.1 Supplementary methods

Supplementary method 1: Chromatin Immunoprecipitation

Hypothalamus tissue was submersed in PBS + 1% formaldehyde, cut into small pieces and incubated at room temperature for 15 minutes. Fixation was stopped by the addition of 0.125 M glycine (final concentration). The tissue pieces were then treated with a TissueTearer and finally spun down and washed 2x in PBS. Chromatin was isolated by the addition of lysis buffer, followed by disruption with a Dounce homogenizer. Lysates were sonicated and the DNA sheared to an average length of 300-500 bp. Genomic DNA (Input) was prepared by treating aliquots of chromatin with RNase, proteinase K and heat for de-crosslinking, followed by ethanol precipitation. Pellets were re-suspended and the resulting DNA was quantified on a NanoDrop spectrophotometer. Extrapolation to the original chromatin volume allowed quantitation of the total chromatin yield.

An aliquot of chromatin (30 µg) was precleared with protein A agarose beads (Invitrogen). Genomic DNA regions of interest were isolated using 4 µg of antibody against PAX6. Complexes were washed, eluted from the beads with SDS buffer, and subjected to RNase and proteinase K treatment. Crosslinks were reversed by incubation overnight at 65 °C, and ChIP DNA was purified by phenol-chloroform extraction and ethanol precipitation.

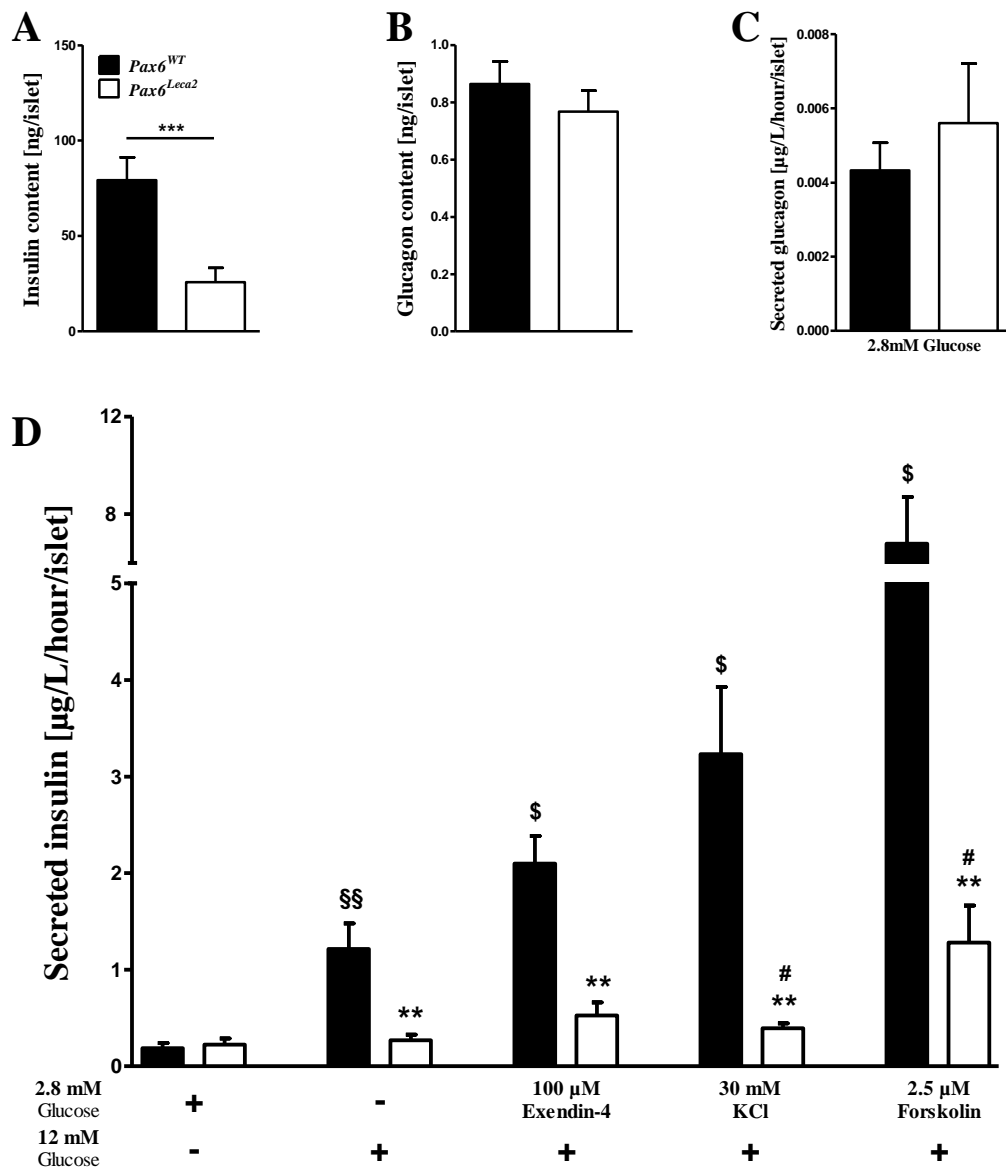
Quantitative PCR (QPCR) reactions were carried out in triplicate on specific genomic regions using SYBR Green Supermix (Bio-Rad). The resulting signals were normalized for primer efficiency by carrying out QPCR for each primer pair using Input DNA.

Supplementary method 2: ChIP Sequencing (Illumina)

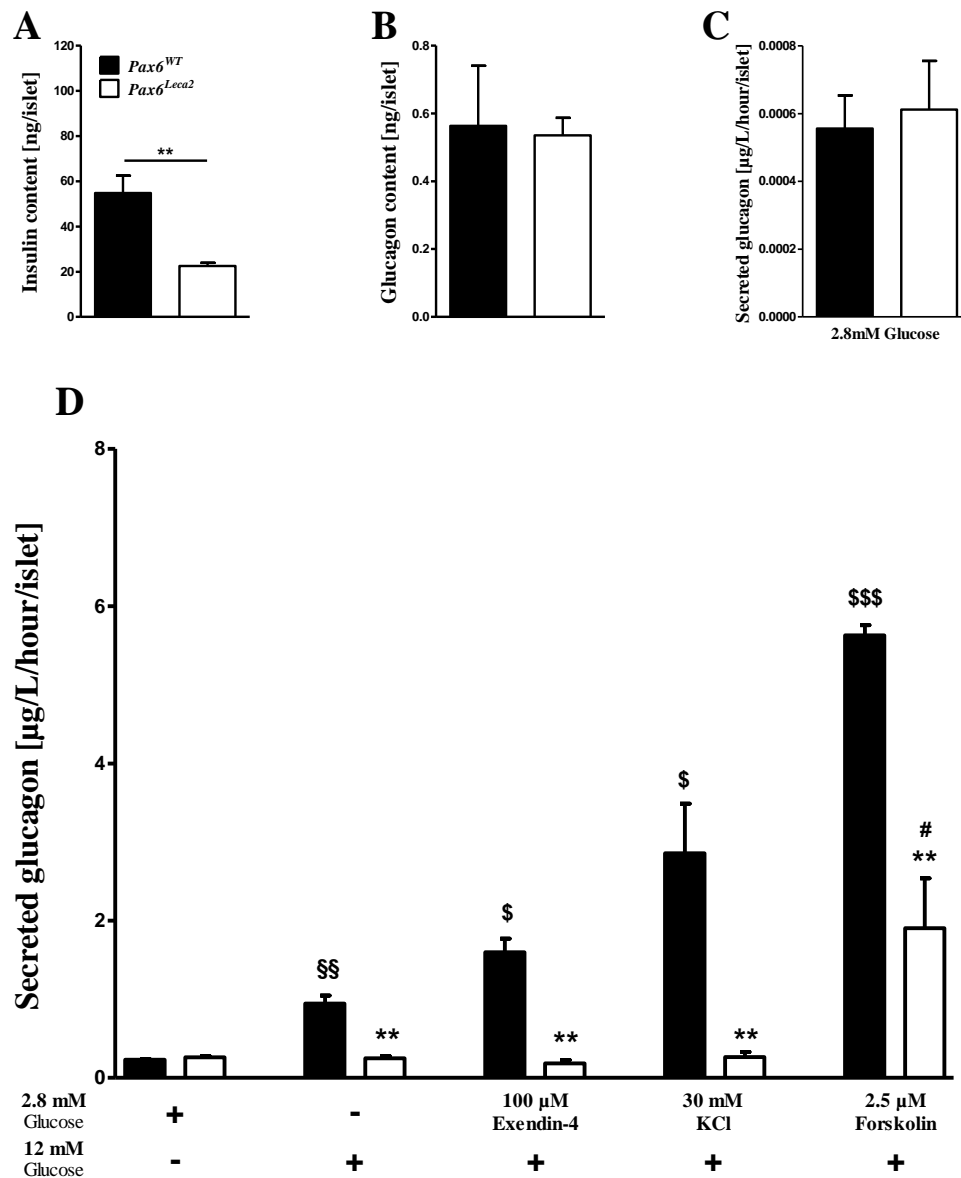
Illumina sequencing libraries were prepared from the ChIP and Input DNAs by the standard consecutive enzymatic steps of end-polishing, dA-addition, and adaptor ligation. After a final PCR amplification step, the resulting DNA libraries were quantified and sequenced on Illumina's NextSeq 500 (75 nt reads, single end). Reads were aligned to the mouse genome (mm10) using the BWA algorithm^[342] (default settings). Duplicate reads were removed and only uniquely mapped reads (mapping quality \geq 25) were used for further analysis. Alignments were extended *in silico* at their 3'-ends to a length of 200 bp, which is the average genomic fragment length in the size-selected library, and assigned to 32-nt bins along the genome. The resulting histograms (genomic "signal maps") were stored in bigWig files. Peak

locations were determined using the MACS ^[343] algorithm (v2.1.0) with a cutoff of p-value = 1e-5. Signal maps and peak locations were used as input data to Active Motifs proprietary analysis program, which creates Excel tables containing detailed information on sample comparison, peak metrics, peak locations and gene annotations.

5.2 Supplementary figures

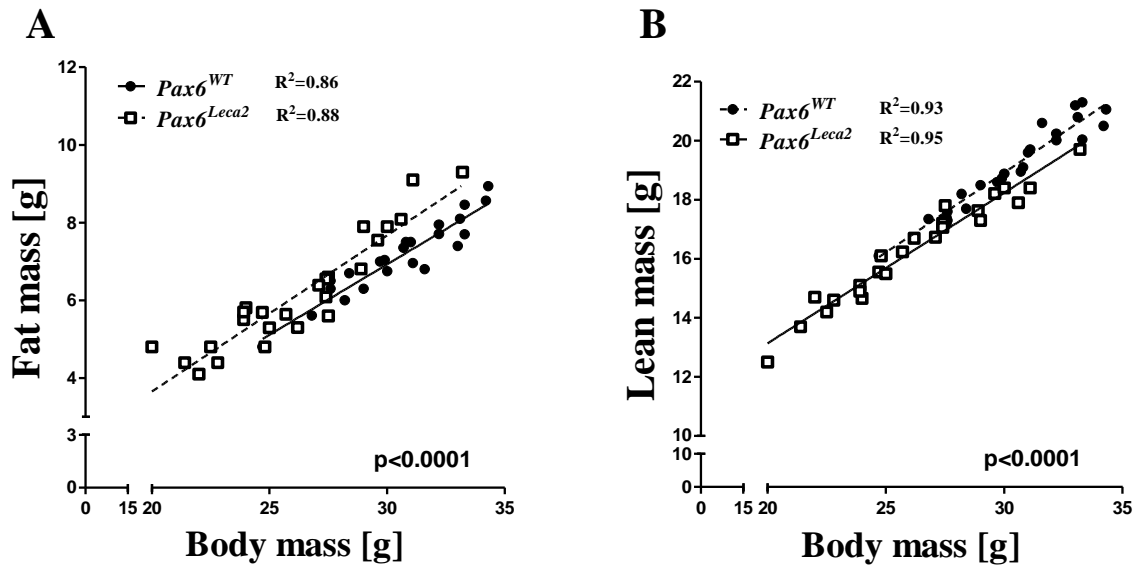
Supplementary figure 1: *In vitro* analysis of hormonal content and secretory capacity in 4 weeks old mice

(A) Reduced amount of insulin in isolated islets of 4 weeks old male mice as identified by insulin ELISA. (B) Glucagon content and (C) glucagon secretion seem to be normal in mutants. (D) Beta cells in the islet mutants have dramatically reduced capacity to secrete insulin following stimulation with several secretagogues, $n=4-8$. Error bars display SEM values. Differences were considered statistically significant at $P < 0.05$ using a two tailed Student's t test. * = *Pax6^{Leca2}* vs *Pax6^{WT}*, § = vs 2.8mM *Pax6^{WT}*, \$ = vs 12mM *Pax6^{WT}*, # = vs 12mM *Pax6^{Leca2}* (§, #, < 0.05, §§, ** < 0.01, *** < 0.001).



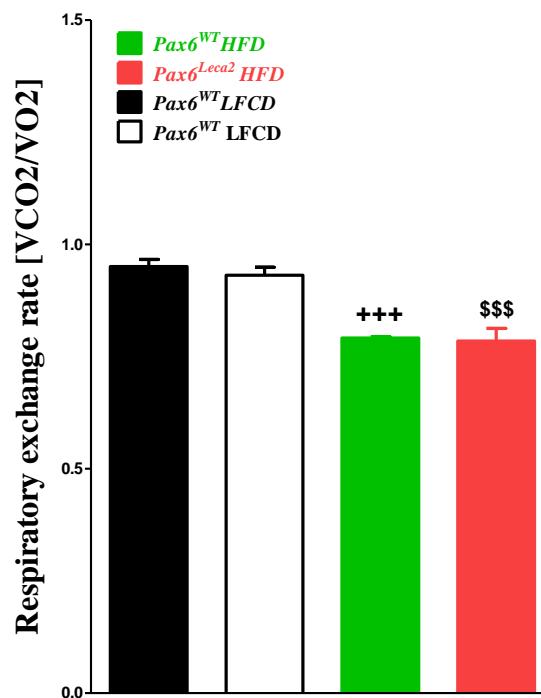
Supplementary figure 2: *In vitro* analysis of hormonal content and secretory capacity in 6 weeks old mice

(A) Reduced amount of insulin in isolated islets of 6 weeks old male mice as identified by insulin ELISA. (B) Glucagon content and (C) glucagon secretion seem to be normal in mutants. (D) Beta cells in the islet mutants have dramatically reduced capacity to secrete insulin following stimulation with several secretagogues, $n=4-6$. Error bars display SEM values. Differences were considered statistically significant at $P < 0.05$ using a two tailed Student's t test. * = *Pax6*^{Leca2} vs *Pax6*^{WT}, § = vs 2.8mM *Pax6*^{WT}, \$ = vs 12mM *Pax6*^{WT}, # = vs 12mM *Pax6*^{Leca2} (§, #, < 0.05, §§, ** < 0.01, §§§ < 0.001).



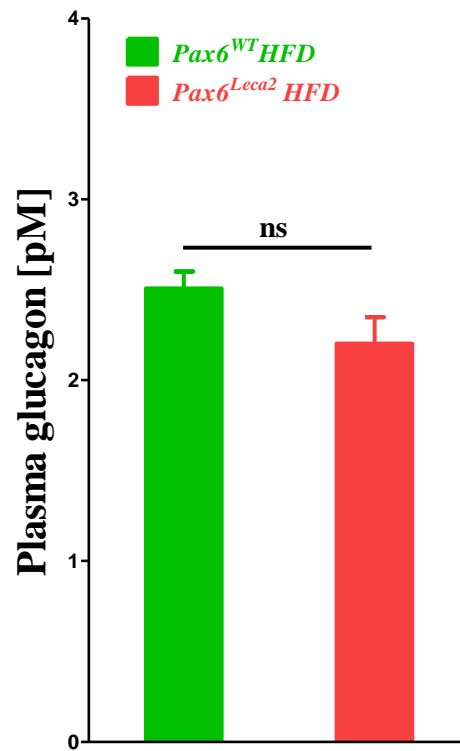
Supplementary figure 3: Linear regression model for analysis of body composition

Linear regression model displaying (A) fat mass and (B) lean mass plotted against body mass shows increased fat mass and reduced lean mass in 14 week old male mutant mice; n=23-25.



Supplementary figure 4: RER of mice fed with HFD and LFCD

Indirect calorimetry, averaged over 21 hours in metabolic cages, demonstrated a decrease of RER in mice from both genotypes, fed with HFD, n=8-12. Error bars display SEM values. Differences were considered statistically significant at $p < 0.05$ using a two-way ANOVA (Bonferroni). += *Pax6*^{WT} LFCD vs *Pax6*^{WT} HFD, \$ = *Pax6*^{Leca2} LFCD vs *Pax6*^{Leca2} HFD (\$\$\$, +++ < 0.001).



Supplementary figure 5: Plasma glucagon levels in mice fed with HFD

No difference in 6 hour fasting plasma glucagon levels were found between the groups, n=10-14. Error bars display SEM values. No statistically significant differences were found using a two tailed Student's t test (ns = non-significant).

5.3 Supplementary tables

Supplementary table 1: Differential expression of genes in isolated islets of 4 weeks old male *Pax6^{Leca2}* (*Leca2*) and wildtype (WT) mice filtered for a minimum FC 1.5 and <10% FDR

| Gene symbol | Gene name | <i>Leca2</i> / WT |
|----------------------|---|----------------------|
| <i>Cpb2</i> | carboxypeptidase B2 (plasma) | 12.78 |
| <i>Lyz2</i> | lysozyme 2 | 11.99 |
| <i>Vwde</i> | von Willebrand factor D and EGF domains | 8.50 |
| <i>Gm22506</i> | predicted gene, 22506 | 8.18 |
| <i>Tcrb-J</i> | T cell receptor beta, joining region | 8.17 |
| <i>6330403K07Rik</i> | RIKEN cDNA 6330403K07 gene | 7.94 |
| <i>Cnr1</i> | cannabinoid receptor 1 (brain) | 7.21 |
| <i>Slc35f4</i> | solute carrier family 35, member F4 | 5.74 |
| <i>Clec7a</i> | C-type lectin domain family 7, member a | 5.60 |
| <i>Cd52</i> | CD52 antigen | 5.44 |
| <i>Rbp1</i> | retinol binding protein 1, cellular | 5.34 |
| <i>Msr1</i> | macrophage scavenger receptor 1 | 5.26 |
| <i>Gast</i> | gastrin | 5.03 |
| <i>Wfdc18</i> | WAP four-disulfide core domain 18 | 4.80 |
| <i>Guca2a</i> | guanylate cyclase activator 2a (guanylin) | 4.56 |
| <i>Nrip3</i> | nuclear receptor interacting protein 3 | 4.40 |
| <i>Gm23553</i> | predicted gene, 23553 | 4.39 |
| <i>Plet1</i> | placenta expressed transcript 1 | 4.37 |
| <i>Socs2</i> | suppressor of cytokine signaling 2 | 4.24 |
| <i>Cd53</i> | CD53 antigen | 4.14 |
| <i>Dynlrb2</i> | dynein light chain roadblock-type 2 | 4.13 |
| <i>Clec4n</i> | C-type lectin domain family 4, member n | 4.10 |
| <i>Chst8</i> | carbohydrate (N-acetylgalactosamine 4-0) sulfotransferase 8 | 4.10 |
| <i>Dpp10</i> | dipeptidylpeptidase 10 | 4.05 |
| <i>Ccl6</i> | chemokine (C-C motif) ligand 6 | 3.95 |
| <i>Lrch2</i> | leucine-rich repeats and calponin homology (CH) domain containing 2 | 3.95 |
| <i>n-R5s26</i> | nuclear encoded rRNA 5S 26 | 3.93 |
| <i>Ly6a</i> | lymphocyte antigen 6 complex, locus A | 3.80 |
| <i>Vcam1</i> | vascular cell adhesion molecule 1 | 3.77 |
| <i>Gchfr</i> | GTP cyclohydrolase I feedback regulator | 3.67 |
| <i>DQ267100</i> | snoRNA DQ267100 | 3.66 |
| <i>C3</i> | complement component 3 | 3.66 |
| <i>Pgf</i> | placental growth factor | 3.60 |
| <i>Fxyd3</i> | FXYD domain-containing ion transport regulator 3 | 3.39 |
| <i>Gpr119</i> | G-protein coupled receptor 119 | 3.39 |
| <i>Mir15a</i> | microRNA 15a | 3.39 |
| <i>Marco</i> | macrophage receptor with collagenous structure | 3.34 |
| <i>Arhgap36</i> | Rho GTPase activating protein 36 | 3.30 |

| | | |
|----------------------|---|------|
| <i>Syt17</i> | synaptotagmin XVII | 3.28 |
| <i>Ffar4</i> | free fatty acid receptor 4 | 3.24 |
| <i>Eef1a2</i> | eukaryotic translation elongation factor 1 alpha 2 | 3.24 |
| <i>Parm1</i> | prostate androgen-regulated mucin-like protein 1 | 3.24 |
| <i>Tmprss2</i> | transmembrane protease, serine 2 | 3.21 |
| <i>Cd55</i> | CD55 molecule, decay accelerating factor for complement | 3.19 |
| <i>Ifi2712a</i> | interferon, alpha-inducible protein 27 like 2A | 3.14 |
| <i>Csn3</i> | casein kappa | 3.13 |
| <i>Gpnmb</i> | glycoprotein (transmembrane) nmb | 3.09 |
| <i>Plet1os</i> | placenta expressed transcript 1, opposite strand | 3.05 |
| <i>Stat4</i> | signal transducer and activator of transcription 4 | 3.03 |
| <i>Gm22962</i> | predicted gene, 22962 | 2.92 |
| <i>NONMMUT017874</i> | <i>No associated gene</i> | 2.92 |
| <i>Enpep</i> | glutamyl aminopeptidase | 2.92 |
| <i>Snord118</i> | small nucleolar RNA, C/D box 118 | 2.91 |
| <i>F2</i> | coagulation factor II | 2.90 |
| <i>Krt27</i> | keratin 27 | 2.89 |
| <i>C630016N16Rik</i> | <i>No associated gene</i> | 2.88 |
| <i>Dapl1</i> | death associated protein-like 1 | 2.88 |
| <i>Bst2</i> | bone marrow stromal cell antigen 2 | 2.85 |
| <i>17238912</i> | <i>No associated gene</i> | 2.85 |
| <i>Msln</i> | mesothelin | 2.79 |
| <i>Lrrn3</i> | leucine rich repeat protein 3, neuronal | 2.79 |
| <i>Cped1</i> | cadherin-like and PC-esterase domain containing 1 | 2.78 |
| <i>Apof</i> | apolipoprotein F | 2.78 |
| <i>Gucy2c</i> | guanylate cyclase 2c | 2.76 |
| <i>Mfge8</i> | milk fat globule-EGF factor 8 protein | 2.76 |
| <i>Enpp3</i> | ectonucleotide pyrophosphatase/phosphodiesterase 3 | 2.76 |
| <i>Fhl2</i> | four and a half LIM domains 2 | 2.73 |
| <i>Tyrobp</i> | TYRO protein tyrosine kinase binding protein | 2.73 |
| <i>Cyba</i> | cytochrome b-245, alpha polypeptide | 2.68 |
| <i>Gm25930</i> | predicted gene, 25930 | 2.68 |
| <i>Nsg1</i> | neuron specific gene family member 1 | 2.65 |
| <i>4632427E13Rik</i> | RIKEN cDNA 4632427E13 gene | 2.65 |
| <i>Mustn1</i> | musculoskeletal, embryonic nuclear protein 1 | 2.63 |
| <i>Lgi1</i> | leucine-rich repeat LGI family, member 1 | 2.62 |
| <i>Mir669n</i> | microRNA 669n | 2.62 |
| <i>Gfra3</i> | glial cell line derived neurotrophic factor family receptor alpha 3 | 2.59 |
| <i>Wfdc16</i> | WAP four-disulfide core domain 16 | 2.59 |
| <i>Tekt2</i> | tektin 2 | 2.59 |
| <i>Dlk1</i> | delta-like 1 homolog (Drosophila) | 2.58 |
| <i>Npl</i> | N-acetylneuraminic acid pyruvate lyase | 2.58 |
| <i>Fam105a</i> | family with sequence similarity 105, member A | 2.57 |
| <i>Fxyd6</i> | FXD domain-containing ion transport regulator 6 | 2.56 |
| <i>Gm24568</i> | predicted gene, 24568 | 2.54 |
| <i>Ifi44</i> | interferon-induced protein 44 | 2.51 |

| | | |
|-----------------|---|------|
| Arap2 | ArfGAP with RhoGAP domain, ankyrin repeat and PH domain 2 | 2.51 |
| Crim1 | cysteine rich transmembrane BMP regulator 1 (chordin like) | 2.48 |
| 17548166 | <i>No associated gene</i> | 2.47 |
| Gbp9 | guanylate-binding protein 9 | 2.46 |
| Rbp4 | retinol binding protein 4, plasma | 2.44 |
| Vstm2a | V-set and transmembrane domain containing 2A | 2.43 |
| AW551984 | expressed sequence AW551984 | 2.43 |
| Ascl1 | achaete-scute family bHLH transcription factor 1 | 2.42 |
| Tmem132b | transmembrane protein 132B | 2.42 |
| Far2 | fatty acyl CoA reductase 2 | 2.38 |
| Cntn3 | contactin 3 | 2.37 |
| Il1rn | interleukin 1 receptor antagonist | 2.35 |
| Bambi | BMP and activin membrane-bound inhibitor | 2.33 |
| Ddc | dopa decarboxylase | 2.32 |
| Slamf7 | SLAM family member 7 | 2.31 |
| A4galt | alpha 1,4-galactosyltransferase | 2.31 |
| Plac8 | placenta-specific 8 | 2.30 |
| Foxp2 | forkhead box P2 | 2.29 |
| Cpne2 | copine II | 2.29 |
| Gcnt3 | glucosaminyl (N-acetyl) transferase 3, mucin type | 2.28 |
| Rerg | RAS-like, estrogen-regulated, growth-inhibitor | 2.27 |
| Cd38 | CD38 antigen | 2.26 |
| Sncb | synuclein, beta | 2.25 |
| Ccl19 | chemokine (C-C motif) ligand 19 | 2.25 |
| Rarres2 | retinoic acid receptor responder (tazarotene induced) 2 | 2.25 |
| Fcer1g | Fc receptor, IgE, high affinity I, gamma polypeptide | 2.25 |
| St3gal4 | ST3 beta-galactoside alpha-2,3-sialyltransferase 4 | 2.24 |
| Rpl23a | ribosomal protein L23A | 2.22 |
| Aqp4 | aquaporin 4 | 2.21 |
| Mmp7 | matrix metalloproteinase 7 | 2.20 |
| Nebl | nebulin | 2.20 |
| Gm20559 | predicted gene, 20559 | 2.18 |
| Ly6c2 | lymphocyte antigen 6 complex, locus C2 | 2.18 |
| Ctss | cathepsin S | 2.18 |
| Cd74 | CD74 antigen (invariant polypeptide of major histocompatibility complex, class II antigen-associated) | 2.17 |
| 17550454 | <i>No associated gene</i> | 2.17 |
| C1ql3 | C1q-like 3 | 2.17 |
| Iglv1 | immunoglobulin lambda variable 1 | 2.17 |
| Galnt13 | UDP-N-acetyl-alpha-D-galactosamine:polypeptide N-acetylgalactosaminyltransferase 13 | 2.17 |
| 17404073 | <i>No associated gene</i> | 2.16 |
| Kl | klotho | 2.16 |
| Gm22805 | predicted gene, 22805 | 2.16 |
| Ifit1 | interferon-induced protein with tetratricopeptide repeats 1 | 2.13 |
| Sez6 | seizure related gene 6 | 2.13 |
| Vsig2 | V-set and immunoglobulin domain containing 2 | 2.12 |

| | | |
|----------------------|--|------|
| Lgmn | legumain | 2.12 |
| H2-Ab1 | histocompatibility 2, class II antigen A, beta 1 | 2.11 |
| Cyp39a1 | cytochrome P450, family 39, subfamily a, polypeptide 1 | 2.09 |
| Lgals3 | lectin, galactose binding, soluble 3 | 2.09 |
| Nid1 | nidogen 1 | 2.08 |
| Cpne8 | copine VIII | 2.07 |
| Mpeg1 | macrophage expressed gene 1 | 2.07 |
| Gc | group specific component | 2.06 |
| Zbp1 | Z-DNA binding protein 1 | 2.06 |
| LOC102632786 | <i>No associated gene</i> | 2.06 |
| Pde3a | phosphodiesterase 3A, cGMP inhibited | 2.04 |
| Isg15 | ISG15 ubiquitin-like modifier | 2.04 |
| Cdh9 | cadherin 9 | 2.03 |
| Gm23119 | predicted gene, 23119 | 2.03 |
| Gm26804 | predicted gene, 26804 | 2.03 |
| Snora81 | small nucleolar RNA, H/ACA box 81 | 2.03 |
| Fam159b | family with sequence similarity 159, member B | 2.03 |
| Trit1 | tRNA isopentenyltransferase 1 | 2.02 |
| Pigr | polymeric immunoglobulin receptor | 2.02 |
| Ptprg | protein tyrosine phosphatase, receptor type, G | 2.02 |
| Abcg2 | ATP-binding cassette, sub-family G (WHITE), member 2 | 2.02 |
| Uchl1 | ubiquitin carboxy-terminal hydrolase L1 | 2.01 |
| 17548315 | <i>No associated gene</i> | 2.00 |
| Tmem86a | transmembrane protein 86A | 1.99 |
| LOC100862024 | <i>No associated gene</i> | 1.98 |
| n-R5s82 | nuclear encoded rRNA 5S 82 | 1.97 |
| Necab2 | N-terminal EF-hand calcium binding protein 2 | 1.96 |
| H2-T23 | histocompatibility 2, T region locus 23 | 1.96 |
| 17214729 | <i>No associated gene</i> | 1.95 |
| Cd83 | CD83 antigen | 1.95 |
| 1810026B05Rik | RIKEN cDNA 1810026B05 gene | 1.94 |
| 17547541 | <i>No associated gene</i> | 1.94 |
| Gm25770 | predicted gene, 25770 | 1.93 |
| Lfng | LFNG O-fucosylpeptide 3-beta-N-acetylglucosaminyltransferase | 1.92 |
| Blnk | B cell linker | 1.92 |
| Rab8b | RAB8B, member RAS oncogene family | 1.91 |
| Wipf1 | WAS/WASL interacting protein family, member 1 | 1.91 |
| Ang | angiogenin, ribonuclease, RNase A family, 5 | 1.91 |
| Igsf1 | immunoglobulin superfamily, member 1 | 1.91 |
| Sepp1 | selenoprotein P, plasma, 1 | 1.90 |
| Sgce | sarcoglycan, epsilon | 1.89 |
| Slc35b3 | solute carrier family 35, member B3 | 1.89 |
| Cyp4v3 | cytochrome P450, family 4, subfamily v, polypeptide 3 | 1.88 |
| Stxbp5l | syntaxin binding protein 5-like | 1.88 |
| Ptchd1 | patched domain containing 1 | 1.88 |
| Ntn4 | netrin 4 | 1.87 |

| | | |
|----------------------|---|------|
| 17389048 | <i>No associated gene</i> | 1.87 |
| DQ267102 | snoRNA DQ267102 | 1.85 |
| Kcnh8 | potassium voltage-gated channel, subfamily H (eag-related), member 8 | 1.85 |
| Mfi2 | <i>No associated gene</i> | 1.84 |
| Cd274 | CD274 antigen | 1.84 |
| Timp2 | tissue inhibitor of metalloproteinase 2 | 1.84 |
| Nespas | neuroendocrine secretory protein antisense | 1.83 |
| Cd44 | CD44 antigen | 1.83 |
| Map3k15 | mitogen-activated protein kinase kinase kinase 15 | 1.83 |
| Gm14964 | predicted gene 14964 | 1.83 |
| Zdhhc13 | zinc finger, DHHC domain containing 13 | 1.83 |
| Pphln1 | periphilin 1 | 1.83 |
| 1700109K24Rik | RIKEN cDNA 1700109K24 gene | 1.81 |
| Igkv4-73 | immunoglobulin kappa variable 4-73 | 1.81 |
| Nr1h3 | nuclear receptor subfamily 1, group H, member 3 | 1.80 |
| Gm13420 | predicted gene 13420 | 1.80 |
| Fcgrt | Fc receptor, IgG, alpha chain transporter | 1.80 |
| Rasgrf2 | RAS protein-specific guanine nucleotide-releasing factor 2 | 1.80 |
| AI662270 | expressed sequence AI662270 | 1.79 |
| Ccng2 | cyclin G2 | 1.78 |
| Asah2 | N-acylsphingosine amidohydrolase 2 | 1.78 |
| Tiparp | TCDD-inducible poly(ADP-ribose) polymerase | 1.77 |
| Klhl24 | kelch-like 24 | 1.76 |
| Pkia | protein kinase inhibitor, alpha | 1.76 |
| Arhgef28 | Rho guanine nucleotide exchange factor (GEF) 28 | 1.76 |
| Trpm3 | transient receptor potential cation channel, subfamily M, member 3 | 1.76 |
| Gm10139 | predicted gene 10139 | 1.75 |
| Tox | thymocyte selection-associated high mobility group box | 1.75 |
| 17290695 | <i>No associated gene</i> | 1.74 |
| 17548477 | <i>No associated gene</i> | 1.74 |
| Serinc2 | serine incorporator 2 | 1.74 |
| Pon2 | paraoxonase 2 | 1.74 |
| Dct | dopachrome tautomerase | 1.74 |
| 17333402 | <i>No associated gene</i> | 1.73 |
| 6430503K07Rik | RIKEN cDNA 6430503K07 gene | 1.73 |
| Crmp1 | collapsin response mediator protein 1 | 1.73 |
| Adamts6 | a disintegrin-like and metallopeptidase (reprolysin type) with thrombospondin type 1 motif, 6 | 1.73 |
| Dcdc2a | doublecortin domain containing 2a | 1.71 |
| Nfkbie | nuclear factor of kappa light polypeptide gene enhancer in B cells inhibitor, epsilon | 1.71 |
| Gls | glutaminase | 1.70 |
| C4bp | complement component 4 binding protein | 1.70 |
| Thrb | thyroid hormone receptor beta | 1.70 |
| Wbscr27 | Williams Beuren syndrome chromosome region 27 (human) | 1.70 |
| Tctn1 | tectonic family member 1 | 1.70 |
| 1500012F01Rik | <i>No associated gene</i> | 1.70 |

| | | |
|-------------------------|---|-------|
| <i>Igkv4-69</i> | immunoglobulin kappa variable 4-69 | 1.69 |
| <i>Snap91</i> | synaptosomal-associated protein 91 | 1.69 |
| <i>Cd200</i> | CD200 antigen | 1.69 |
| <i>Tanc1</i> | tetratricopeptide repeat, ankyrin repeat and coiled-coil containing 1 | 1.68 |
| <i>Gm996</i> | predicted gene 996 | 1.67 |
| <i>Grn</i> | granulin | 1.66 |
| <i>Snhg4</i> | small nucleolar RNA host gene 4 | 1.66 |
| <i>Clec12a</i> | C-type lectin domain family 12, member a | 1.66 |
| <i>17358825</i> | <i>No associated gene</i> | 1.65 |
| <i>Itga6</i> | integrin alpha 6 | 1.65 |
| <i>Itih1</i> | inter-alpha trypsin inhibitor, heavy chain 1 | 1.64 |
| <i>Cd81</i> | CD81 antigen | 1.64 |
| <i>Gcnt2</i> | glucosaminyl (N-acetyl) transferase 2, I-branching enzyme | 1.63 |
| <i>Ctsd</i> | cathepsin D | 1.63 |
| <i>Gng2</i> | guanine nucleotide binding protein (G protein), gamma 2 | 1.63 |
| <i>Rfx6</i> | regulatory factor X, 6 | 1.62 |
| <i>Mef2a</i> | myocyte enhancer factor 2A | 1.61 |
| <i>Zdhhc20</i> | zinc finger, DHHC domain containing 20 | 1.61 |
| <i>Herc6</i> | hect domain and RLD 6 | 1.61 |
| <i>Trav9d-3</i> | T cell receptor alpha variable 9D-3 | 1.61 |
| <i>Clec1b</i> | C-type lectin domain family 1, member b | 1.59 |
| <i>Mtif3</i> | mitochondrial translational initiation factor 3 | 1.59 |
| <i>Cntn1</i> | contactin 1 | 1.58 |
| <i>Scarb1</i> | scavenger receptor class B, member 1 | 1.58 |
| <i>17410612</i> | <i>No associated gene</i> | 1.56 |
| <i>Zfand1</i> | zinc finger, AN1-type domain 1 | 1.56 |
| <i>Capg</i> | capping protein (actin filament), gelsolin-like | 1.56 |
| <i>Dram1</i> | DNA-damage regulated autophagy modulator 1 | 1.56 |
| <i>Ralgds</i> | ral guanine nucleotide dissociation stimulator | 1.56 |
| <i>Tmem123</i> | transmembrane protein 123 | 1.54 |
| <i>Galnt7</i> | UDP-N-acetyl-alpha-D-galactosamine: polypeptide N-acetylgalactosaminyltransferase 7 | 1.54 |
| <i>Zwint</i> | ZW10 interactor | 1.54 |
| <i>Fam43a</i> | family with sequence similarity 43, member A | 1.53 |
| <i>Tnfrsf13c</i> | tumor necrosis factor receptor superfamily, member 13c | 1.52 |
| <i>Sec14l1</i> | SEC14-like lipid binding 1 | -1.51 |
| <i>Gnat2</i> | guanine nucleotide binding protein, alpha transducing 2 | -1.51 |
| <i>Gosr2</i> | golgi SNAP receptor complex member 2 | -1.51 |
| <i>Aox1</i> | aldehyde oxidase 1 | -1.52 |
| <i>Elov15</i> | ELOVL family member 5, elongation of long chain fatty acids (yeast) | -1.52 |
| <i>Tle3</i> | transducin-like enhancer of split 3 | -1.52 |
| <i>Rwdd1</i> | RWD domain containing 1 | -1.53 |
| <i>BB557941</i> | expressed sequence BB557941 | -1.53 |
| <i>Gm2897</i> | predicted gene 2897 | -1.54 |
| <i>17441949</i> | <i>No associated gene</i> | -1.54 |
| <i>Cope</i> | coatomer protein complex, subunit epsilon | -1.55 |

| | | |
|----------------------|---|-------|
| Lrrc59 | leucine rich repeat containing 59 | -1.55 |
| Ufm1 | ubiquitin-fold modifier 1 | -1.55 |
| Ccdc47 | coiled-coil domain containing 47 | -1.55 |
| Scfd1 | Sec1 family domain containing 1 | -1.57 |
| A830010M20Rik | RIKEN cDNA A830010M20 gene | -1.57 |
| Tsfm | Ts translation elongation factor, mitochondrial | -1.57 |
| Nelfb | negative elongation factor complex member B | -1.57 |
| Sec16a | SEC16 homolog A, endoplasmic reticulum export factor | -1.58 |
| Abcc4 | ATP-binding cassette, sub-family C (CFTR/MRP), member 4 | -1.58 |
| Tmem206 | transmembrane protein 206 | -1.58 |
| Sympk | symplekin | -1.58 |
| Disp2 | dispatched RND transporter family member 2 | -1.58 |
| Copg1 | coatomer protein complex, subunit gamma 1 | -1.58 |
| Mad1l1 | MAD1 mitotic arrest deficient 1-like 1 | -1.58 |
| Pprc1 | peroxisome proliferative activated receptor, gamma, coactivator-related 1 | -1.59 |
| Srm | spermidine synthase | -1.59 |
| Iars | isoleucine-tRNA synthetase | -1.60 |
| Ccdc25 | coiled-coil domain containing 25 | -1.62 |
| 1810008I18Rik | RIKEN cDNA 1810008I18 gene | -1.62 |
| Comt | catechol-O-methyltransferase | -1.62 |
| Ero1lb | ERO1-like beta (<i>S. cerevisiae</i>) | -1.63 |
| Pxk | PX domain containing serine/threonine kinase | -1.63 |
| Sec23b | SEC23 homolog B, COPII coat complex component | -1.63 |
| Itpa | inosine triphosphatase (nucleoside triphosphate pyrophosphatase) | -1.63 |
| Per2 | period circadian clock 2 | -1.63 |
| Tdrkh | tudor and KH domain containing protein | -1.63 |
| Tshz1 | teashirt zinc finger family member 1 | -1.64 |
| Shc1 | src homology 2 domain-containing transforming protein C1 | -1.64 |
| LOC102638330 | <i>No associated gene</i> | -1.64 |
| Ptpn21 | protein tyrosine phosphatase, non-receptor type 21 | -1.64 |
| Abca5 | ATP-binding cassette, sub-family A (ABC1), member 5 | -1.65 |
| 17548174 | <i>No associated gene</i> | -1.65 |
| Abat | 4-aminobutyrate aminotransferase | -1.65 |
| Ppp1r15a | protein phosphatase 1, regulatory (inhibitor) subunit 15A | -1.65 |
| Spn | SPEN homolog, transcriptional regulator (<i>Drosophila</i>) | -1.66 |
| Xrcc1 | X-ray repair complementing defective repair in Chinese hamster cells 1 | -1.66 |
| 2310022B05Rik | RIKEN cDNA 2310022B05 gene | -1.66 |
| Gm3558 | predicted gene 3558 | -1.67 |
| Mia3 | melanoma inhibitory activity 3 | -1.67 |
| Dennd4c | DENN/MADD domain containing 4C | -1.67 |
| Npas2 | neuronal PAS domain protein 2 | -1.67 |
| 17549652 | <i>No associated gene</i> | -1.68 |
| Arhgap23 | Rho GTPase activating protein 23 | -1.68 |
| Rassf4 | Ras association (RalGDS/AF-6) domain family member 4 | -1.68 |
| Prkar2b | protein kinase, cAMP dependent regulatory, type II beta | -1.68 |
| Map10 | microtubule-associated protein 10 | -1.68 |

| | | |
|-----------------------------|---|-------|
| <i>Celsr1</i> | cadherin, EGF LAG seven-pass G-type receptor 1 | -1.68 |
| <i>Rab3gap2</i> | RAB3 GTPase activating protein subunit 2 | -1.69 |
| <i>LOC102638434</i> | <i>No associated gene</i> | -1.69 |
| <i>Reps2</i> | RALBP1 associated Eps domain containing protein 2 | -1.69 |
| <i>Thap2</i> | THAP domain containing, apoptosis associated protein 2 | -1.70 |
| <i>Farp2</i> | FERM, RhoGEF and pleckstrin domain protein 2 | -1.70 |
| <i>Hykk</i> | hydroxylysine kinase 1 | -1.70 |
| <i>Igfbp5</i> | insulin-like growth factor binding protein 5 | -1.70 |
| <i>Oacyl</i> | O-acyltransferase like | -1.70 |
| <i>Akap12</i> | A kinase (PRKA) anchor protein (gravin) 12 | -1.70 |
| <i>Fbxo27</i> | F-box protein 27 | -1.70 |
| <i>Trappc9</i> | trafficking protein particle complex 9 | -1.70 |
| <i>Ergic1</i> | endoplasmic reticulum-golgi intermediate compartment (ERGIC) 1 | -1.70 |
| <i>Atp4a</i> | ATPase, H ⁺ /K ⁺ exchanging, gastric, alpha polypeptide | -1.71 |
| <i>Atf5</i> | activating transcription factor 5 | -1.71 |
| <i>Camta2</i> | calmodulin binding transcription activator 2 | -1.71 |
| <i>Hfe</i> | hemochromatosis | -1.72 |
| <i>Cdh4</i> | cadherin 4 | -1.72 |
| <i>1700019G17Rik</i> | <i>No associated gene</i> | -1.72 |
| <i>Cttnbp2</i> | cortactin binding protein 2 | -1.72 |
| <i>Hs3st6</i> | heparan sulfate (glucosamine) 3-O-sulfotransferase 6 | -1.73 |
| <i>Tars</i> | threonyl-tRNA synthetase | -1.73 |
| <i>Helq</i> | helicase, POLQ-like | -1.74 |
| <i>Ero1l</i> | ERO1-like (<i>S. cerevisiae</i>) | -1.75 |
| <i>Gne</i> | glucosamine (UDP-N-acetyl)-2-epimerase/N-acetylmannosamine kinase | -1.76 |
| <i>Bicc1</i> | BicC family RNA binding protein 1 | -1.76 |
| <i>17547596</i> | <i>No associated gene</i> | -1.76 |
| <i>Proser3</i> | proline and serine rich 3 | -1.76 |
| <i>Ptpn2</i> | protein tyrosine phosphatase, non-receptor type 2 | -1.76 |
| <i>Armc5</i> | armadillo repeat containing 5 | -1.77 |
| <i>Prkcb</i> | protein kinase C, beta | -1.78 |
| <i>Mpp3</i> | membrane protein, palmitoylated 3 (MAGUK p55 subfamily member 3) | -1.78 |
| <i>Skap1</i> | src family associated phosphoprotein 1 | -1.78 |
| <i>Vstm2l</i> | V-set and transmembrane domain containing 2-like | -1.78 |
| <i>4930550C14Rik</i> | RIKEN cDNA 4930550C14 gene | -1.78 |
| <i>Hdac4</i> | histone deacetylase 4 | -1.78 |
| <i>Tmem209</i> | transmembrane protein 209 | -1.78 |
| <i>B830017H08Rik</i> | RIKEN cDNA B830017H08 gene | -1.79 |
| <i>Hist2h3c1</i> | histone cluster 2, H3c1 | -1.79 |
| <i>Zfx2os</i> | zinc finger homeobox 2, opposite strand | -1.79 |
| <i>Rif1</i> | replication timing regulatory factor 1 | -1.79 |
| <i>Dennd2d</i> | DENN/MADD domain containing 2D | -1.79 |
| <i>Kcnip1</i> | Kv channel-interacting protein 1 | -1.79 |
| <i>Anks1</i> | ankyrin repeat and SAM domain containing 1 | -1.80 |
| <i>17299196</i> | <i>No associated gene</i> | -1.80 |
| <i>Dhx29</i> | DEAH (Asp-Glu-Ala-His) box polypeptide 29 | -1.80 |

| | | |
|------------------------|--|-------|
| <i>Plcb1</i> | phospholipase C, beta 1 | -1.80 |
| 17286496 | <i>No associated gene</i> | -1.81 |
| <i>Madd</i> | MAP-kinase activating death domain | -1.81 |
| <i>Ltv1</i> | LTV1 ribosome biogenesis factor | -1.81 |
| <i>Zfp462</i> | zinc finger protein 462 | -1.82 |
| <i>Srebfl</i> | sterol regulatory element binding transcription factor 1 | -1.82 |
| <i>Fh1</i> | fumarate hydratase 1 | -1.82 |
| <i>D8Ert82e</i> | <i>No associated gene</i> | -1.83 |
| <i>Glce</i> | glucuronyl C5-epimerase | -1.83 |
| <i>Esrp2</i> | epithelial splicing regulatory protein 2 | -1.84 |
| <i>Mest</i> | mesoderm specific transcript | -1.84 |
| <i>Cdr2</i> | cerebellar degeneration-related 2 | -1.85 |
| <i>Hyo1</i> | hypoxia up-regulated 1 | -1.85 |
| <i>Cpeb1</i> | cytoplasmic polyadenylation element binding protein 1 | -1.85 |
| <i>Cpm</i> | carboxypeptidase M | -1.86 |
| 7530414M10Rik | RIKEN cDNA 7530414M10 gene | -1.87 |
| <i>Cad</i> | carbamoyl-phosphate synthetase 2, aspartate transcarbamylase, and dihydroorotase | -1.87 |
| <i>Gdf15</i> | growth differentiation factor 15 | -1.88 |
| <i>Dvl3</i> | dishevelled segment polarity protein 3 | -1.88 |
| 6430548M08Rik | RIKEN cDNA 6430548M08 gene | -1.88 |
| <i>Tpcn1</i> | two pore channel 1 | -1.88 |
| <i>Sdf2l1</i> | stromal cell-derived factor 2-like 1 | -1.89 |
| <i>Cyb5b</i> | cytochrome b5 type B | -1.89 |
| <i>Aldh5a1</i> | aldehyde dehydrogenase family 5, subfamily A1 | -1.89 |
| <i>Gnl2</i> | guanine nucleotide binding protein-like 2 (nucleolar) | -1.89 |
| <i>Tnfrsf21</i> | tumor necrosis factor receptor superfamily, member 21 | -1.89 |
| <i>Egfr</i> | epidermal growth factor receptor | -1.90 |
| <i>Chst11</i> | carbohydrate sulfotransferase 11 | -1.90 |
| <i>Ptprt</i> | protein tyrosine phosphatase, receptor type, T | -1.90 |
| <i>Urb2</i> | URB2 ribosome biogenesis 2 homolog (<i>S. cerevisiae</i>) | -1.91 |
| <i>Mafa</i> | v-maf musculoaponeurotic fibrosarcoma oncogene family, protein A (avian) | -1.92 |
| <i>Areg</i> | amphiregulin | -1.92 |
| <i>Sdk2</i> | sidekick cell adhesion molecule 2 | -1.93 |
| <i>Bhlha15</i> | basic helix-loop-helix family, member a15 | -1.93 |
| <i>Fermt1</i> | fermitin family member 1 | -1.93 |
| <i>Gm3159</i> | predicted gene 3159 | -1.93 |
| <i>Rhd</i> | Rh blood group, D antigen | -1.93 |
| 17537713 | <i>No associated gene</i> | -1.94 |
| <i>Erich3</i> | glutamate rich 3 | -1.95 |
| <i>Dnajc21</i> | DnaJ heat shock protein family (Hsp40) member C21 | -1.95 |
| <i>Wars</i> | tryptophanyl-tRNA synthetase | -1.97 |
| 1700020N18Rik | RIKEN cDNA 1700020N18 gene | -1.97 |
| <i>Wfs1</i> | wolframin ER transmembrane glycoprotein | -1.97 |
| 17549460 | <i>No associated gene</i> | -1.97 |
| <i>Cdhr1</i> | cadherin-related family member 1 | -1.98 |

| | | |
|----------------------|---|-------|
| Pitrm1 | pitrilysin metallepetidase 1 | -1.98 |
| Ramp2 | receptor (calcitonin) activity modifying protein 2 | -1.98 |
| Gale | galactose-4-epimerase, UDP | -1.98 |
| Fam101b | <i>No associated gene</i> | -1.99 |
| Rwdd4a | RWD domain containing 4A | -1.99 |
| Psph | phosphoserine phosphatase | -1.99 |
| X61497 | <i>No associated gene</i> | -1.99 |
| Trib3 | tribbles pseudokinase 3 | -1.99 |
| Eprs | glutamyl-prolyl-tRNA synthetase | -1.99 |
| Gabbr2 | gamma-aminobutyric acid (GABA) B receptor, 2 | -1.99 |
| Rny3 | RNA, Y3 small cytoplasmic (associated with Ro protein) | -2.00 |
| Rapgef4 | Rap guanine nucleotide exchange factor (GEF) 4 | -2.00 |
| Serpina3n | serine (or cysteine) peptidase inhibitor, clade A, member 3N | -2.00 |
| Gm10406 | predicted gene 10406 | -2.02 |
| Wipi1 | WD repeat domain, phosphoinositide interacting 1 | -2.03 |
| F2r11 | coagulation factor II (thrombin) receptor-like 1 | -2.03 |
| Psat1 | phosphoserine aminotransferase 1 | -2.03 |
| AI182371 | expressed sequence AI182371 | -2.03 |
| 9130023H24Rik | RIKEN cDNA 9130023H24 gene | -2.05 |
| Reep6 | receptor accessory protein 6 | -2.07 |
| 1810011O10Rik | RIKEN cDNA 1810011O10 gene | -2.07 |
| Dach2 | dachshund 2 (Drosophila) | -2.07 |
| Rad51ap2 | RAD51 associated protein 2 | -2.07 |
| Glp1r | glucagon-like peptide 1 receptor | -2.08 |
| Ttc28 | tetratricopeptide repeat domain 28 | -2.08 |
| 17549462 | <i>No associated gene</i> | -2.09 |
| Ntrk2 | neurotrophic tyrosine kinase, receptor, type 2 | -2.09 |
| D630039A03Rik | RIKEN cDNA D630039A03 gene | -2.09 |
| 17549252 | <i>No associated gene</i> | -2.09 |
| Elov16 | ELOVL family member 6, elongation of long chain fatty acids (yeast) | -2.11 |
| Ccdc6 | coiled-coil domain containing 6 | -2.12 |
| Pgm3 | phosphoglucomutase 3 | -2.12 |
| Galns | galactosamine (N-acetyl)-6-sulfate sulfatase | -2.12 |
| Lonp1 | lon peptidase 1, mitochondrial | -2.12 |
| Gcnt1 | glucosaminyl (N-acetyl) transferase 1, core 2 | -2.14 |
| 17549848 | <i>No associated gene</i> | -2.14 |
| Gm10734 | predicted gene 10734 | -2.14 |
| Sdk1 | sidekick cell adhesion molecule 1 | -2.16 |
| Mns1 | meiosis-specific nuclear structural protein 1 | -2.16 |
| Vdr | vitamin D receptor | -2.17 |
| Tssc4 | tumor-suppressing subchromosomal transferable fragment 4 | -2.17 |
| Swsap1 | SWIM type zinc finger 7 associated protein 1 | -2.18 |
| Armc10 | armadillo repeat containing 10 | -2.18 |
| Heg1 | heart development protein with EGF-like domains 1 | -2.18 |
| Golga3 | golgi autoantigen, golgin subfamily a, 3 | -2.18 |
| Adm2 | adrenomedullin 2 | -2.18 |

| | | |
|----------------------|---|-------|
| Fbp1 | fructose biphosphatase 1 | -2.19 |
| Abcb4 | ATP-binding cassette, sub-family B (MDR/TAP), member 4 | -2.19 |
| Papss2 | 3'-phosphoadenosine 5'-phosphosulfate synthase 2 | -2.21 |
| Fmo4 | flavin containing monooxygenase 4 | -2.22 |
| Coro2b | coronin, actin binding protein, 2B | -2.23 |
| Edn3 | endothelin 3 | -2.24 |
| LOC102637131 | <i>No associated gene</i> | -2.24 |
| Ubr4 | ubiquitin protein ligase E3 component n-recognin 4 | -2.25 |
| Gm20400 | predicted gene 20400 | -2.25 |
| Tmem8 | transmembrane protein 8 (five membrane-spanning domains) | -2.25 |
| Cryl1 | crystallin, lambda 1 | -2.25 |
| Lrp5 | low density lipoprotein receptor-related protein 5 | -2.27 |
| B3galt5 | UDP-Gal:betaGlcNAc beta 1,3-galactosyltransferase, polypeptide 5 | -2.28 |
| Matn2 | matrilin 2 | -2.29 |
| Irak1bp1 | interleukin-1 receptor-associated kinase 1 binding protein 1 | -2.30 |
| Gdap2 | ganglioside-induced differentiation-associated-protein 2 | -2.30 |
| Stk32b | serine/threonine kinase 32B | -2.30 |
| Pfkfb2 | 6-phosphofructo-2-kinase/fructose-2,6-biphosphatase 2 | -2.30 |
| Gm7457 | predicted gene 7457 | -2.31 |
| Grin1os | glutamate receptor, ionotropic, NMDA1 (zeta 1), opposite strand | -2.31 |
| Kcnh5 | potassium voltage-gated channel, subfamily H (eag-related), member 5 | -2.32 |
| Palmd | palmdelphin | -2.32 |
| Slc4a10 | solute carrier family 4, sodium bicarbonate cotransporter-like, member 10 | -2.33 |
| Scd2 | stearoyl-Coenzyme A desaturase 2 | -2.35 |
| 1700016K19Rik | RIKEN cDNA 1700016K19 gene | -2.40 |
| Kcnh1 | potassium voltage-gated channel, subfamily H (eag-related), member 1 | -2.40 |
| Stc1 | stanniocalcin 1 | -2.41 |
| Ereg | epiregulin | -2.42 |
| Lrrtm2 | leucine rich repeat transmembrane neuronal 2 | -2.42 |
| Cbx4 | chromobox 4 | -2.46 |
| Spock1 | sparc/osteonectin, cwcv and kazal-like domains proteoglycan 1 | -2.49 |
| 17530231 | <i>No associated gene</i> | -2.50 |
| C2cd4b | C2 calcium-dependent domain containing 4B | -2.50 |
| Rtkn2 | rhotekin 2 | -2.51 |
| Tat | tyrosine aminotransferase | -2.51 |
| Phactr1 | phosphatase and actin regulator 1 | -2.53 |
| Pde5a | phosphodiesterase 5A, cGMP-specific | -2.54 |
| Rab6b | RAB6B, member RAS oncogene family | -2.54 |
| Nostrin | nitric oxide synthase trafficker | -2.55 |
| Dlgap1 | discs, large (Drosophila) homolog-associated protein 1 | -2.56 |
| Adora1 | adenosine A1 receptor | -2.56 |
| Fhdc1 | FH2 domain containing 1 | -2.59 |
| Gsdma | gasdermin A | -2.60 |
| Dock5 | dedicator of cytokinesis 5 | -2.62 |
| Gm23134 | predicted gene, 23134 | -2.64 |
| Sytl4 | synaptotagmin-like 4 | -2.64 |

| | | |
|---------------------|--|-------|
| LOC102632360 | <i>No associated gene</i> | -2.70 |
| Slco1a6 | solute carrier organic anion transporter family, member 1a6 | -2.72 |
| Gpr158 | G protein-coupled receptor 158 | -2.72 |
| Inhba | inhibin beta-A | -2.75 |
| Gcgr | glucagon receptor | -2.76 |
| Slc25a35 | solute carrier family 25, member 35 | -2.77 |
| Gpm6a | glycoprotein m6a | -2.79 |
| Maob | monoamine oxidase B | -2.79 |
| Pdyn | prodynorphin | -2.79 |
| 17547971 | <i>No associated gene</i> | -2.79 |
| Itpkb | inositol 1,4,5-trisphosphate 3-kinase B | -2.79 |
| Gm10941 | predicted gene 10941 | -2.80 |
| Rbmy | RNA binding motif protein, Y chromosome | -2.81 |
| Olfm4 | olfactomedin 4 | -2.82 |
| St8sia1 | ST8 alpha-N-acetyl-neuraminide alpha-2,8-sialyltransferase 1 | -2.84 |
| Nme4 | NME/NM23 nucleoside diphosphate kinase 4 | -2.84 |
| Sv2b | synaptic vesicle glycoprotein 2 b | -2.85 |
| Gm11454 | predicted gene 11454 | -2.85 |
| Dyrk3 | dual-specificity tyrosine-(Y)-phosphorylation regulated kinase 3 | -2.86 |
| Itgb8 | integrin beta 8 | -2.88 |
| Hist2h3c2 | histone cluster 2, H3c2 | -2.95 |
| Prss53 | protease, serine 53 | -3.14 |
| Nrcam | neuronal cell adhesion molecule | -3.17 |
| Adh1 | alcohol dehydrogenase 1 (class I) | -3.17 |
| Aldh1l2 | aldehyde dehydrogenase 1 family, member L2 | -3.17 |
| Car15 | carbonic anhydrase 15 | -3.18 |
| Grin1 | glutamate receptor, ionotropic, NMDA1 (zeta 1) | -3.20 |
| Ptprz1 | protein tyrosine phosphatase, receptor type Z, polypeptide 1 | -3.21 |
| Tnfrsf23 | tumor necrosis factor receptor superfamily, member 23 | -3.21 |
| Il11 | interleukin 11 | -3.22 |
| Ttyh1 | tweety family member 1 | -3.29 |
| Dsp | desmoplakin | -3.30 |
| Gm4791 | predicted gene 4791 | -3.31 |
| Cntfr | ciliary neurotrophic factor receptor | -3.32 |
| Prlr | prolactin receptor | -3.34 |
| Pcx | pyruvate carboxylase | -3.40 |
| Ipcef1 | interaction protein for cytohesin exchange factors 1 | -3.44 |
| Ucn3 | urocortin 3 | -3.45 |
| Gm5069 | predicted pseudogene 5069 | -3.66 |
| Elovl4 | elongation of very long chain fatty acids (FEN1/Elo2, SUR4/Elo3, yeast)-like 4 | -3.78 |
| Nnat | neuronatin | -3.82 |
| 17529381 | <i>No associated gene</i> | -3.87 |
| Rasgrf1 | RAS protein-specific guanine nucleotide-releasing factor 1 | -3.93 |
| Angptl7 | angiopoietin-like 7 | -3.94 |
| Asb4 | ankyrin repeat and SOCS box-containing 4 | -4.07 |

| | | |
|---------------------|---|--------|
| <i>Rab3c</i> | RAB3C, member RAS oncogene family | -4.19 |
| <i>Ptgs2</i> | prostaglandin-endoperoxide synthase 2 | -4.35 |
| <i>Dgkg</i> | diacylglycerol kinase, gamma | -4.36 |
| <i>Cbln4</i> | cerebellin 4 precursor protein | -4.45 |
| <i>Ceacam1</i> | carcinoembryonic antigen-related cell adhesion molecule 1 | -4.55 |
| <i>LOC102633833</i> | <i>No associated gene</i> | -4.56 |
| <i>Spc25</i> | SPC25, NDC80 kinetochore complex component, homolog (S. cerevisiae) | -4.60 |
| <i>Vrk1</i> | vaccinia related kinase 1 | -4.69 |
| <i>Gm14692</i> | predicted gene 14692 | -4.70 |
| <i>Crybb3</i> | crystallin, beta B3 | -4.93 |
| <i>Gm11789</i> | predicted gene 11789 | -4.97 |
| <i>P2ry12</i> | purinergic receptor P2Y, G-protein coupled 12 | -5.01 |
| <i>G6pc2</i> | glucose-6-phosphatase, catalytic, 2 | -5.06 |
| <i>Igf1r</i> | insulin-like growth factor I receptor | -5.16 |
| <i>Ppp1r1a</i> | protein phosphatase 1, regulatory (inhibitor) subunit 1A | -5.23 |
| <i>Slitrk6</i> | SLIT and NTRK-like family, member 6 | -5.67 |
| <i>Cdh8</i> | cadherin 8 | -5.92 |
| <i>Cbs</i> | cystathionine beta-synthase | -6.00 |
| <i>Robo1</i> | roundabout guidance receptor 1 | -6.18 |
| <i>Nell1</i> | NEL-like 1 | -6.35 |
| <i>17547793</i> | <i>No associated gene</i> | -6.61 |
| <i>Ffar3</i> | free fatty acid receptor 3 | -6.92 |
| <i>Hspa12a</i> | heat shock protein 12A | -7.31 |
| <i>Cox6a2</i> | cytochrome c oxidase subunit VIa polypeptide 2 | -7.55 |
| <i>Tmem215</i> | transmembrane protein 215 | -12.91 |
| <i>Ffar1</i> | free fatty acid receptor 1 | -15.02 |

Supplementary table 2: Differential expression of genes in isolated islets of 6 weeks old male *Pax6^{Leca2}* (*Leca2*) and wildtype (WT) mice filtered for a minimum FC 1.5 and <10% FDR

| Gene symbol | Gene name | <i>Leca2</i> / WT |
|---------------------|--|----------------------|
| <i>Cd79b</i> | CD79B antigen | 13.05 |
| <i>Gbp8</i> | guanylate-binding protein 8 | 10.96 |
| <i>Iigp1</i> | interferon inducible GTPase 1 | 10.59 |
| <i>Ifi204</i> | interferon activated gene 204 | 10.51 |
| <i>LOC102641542</i> | immunoglobulin omega chain-like | 10.41 |
| <i>Cnr1</i> | cannabinoid receptor 1 (brain) | 9.22 |
| <i>Cxcl10</i> | chemokine (C-X-C motif) ligand 10 | 8.60 |
| <i>Ptprc</i> | protein tyrosine phosphatase, receptor type, C | 8.42 |
| <i>Igkv4-68</i> | immunoglobulin kappa variable 4-68 | 8.27 |
| <i>Prss1</i> | protease, serine 1 (trypsin 1) | 7.95 |
| <i>Pou2af1</i> | POU domain, class 2, associating factor 1 | 7.81 |
| <i>Igkv8-30</i> | immunoglobulin kappa chain variable 8-30 | 7.79 |
| <i>H2-Ea-ps</i> | histocompatibility 2, class II antigen E alpha, pseudogene | 7.65 |

| | | |
|----------------------|--|------|
| <i>Slfn2</i> | schlafen 2 | 7.63 |
| <i>Ms4a1</i> | membrane-spanning 4-domains, subfamily A, member 1 | 7.51 |
| <i>Cpb2</i> | carboxypeptidase B2 (plasma) | 7.50 |
| <i>C3</i> | complement component 3 | 7.40 |
| <i>Cd52</i> | CD52 antigen | 7.39 |
| <i>LOC101055672</i> | nuclear autoantigen Sp-100-like | 7.37 |
| <i>Ly6a</i> | lymphocyte antigen 6 complex, locus A | 7.31 |
| <i>17536665</i> | <i>No associated gene</i> | 7.28 |
| <i>Igkv4-50</i> | immunoglobulin kappa variable 4-50 | 7.23 |
| <i>Ly6c2</i> | lymphocyte antigen 6 complex, locus C2 | 7.20 |
| <i>Il2rg</i> | interleukin 2 receptor, gamma chain | 7.18 |
| <i>Sp100</i> | nuclear antigen Sp100 | 7.03 |
| <i>Ifi2712a</i> | interferon, alpha-inducible protein 27 like 2A | 7.00 |
| <i>Cxcl11</i> | chemokine (C-X-C motif) ligand 11 | 6.86 |
| <i>Plet1</i> | placenta expressed transcript 1 | 6.86 |
| <i>Igkj5</i> | immunoglobulin kappa joining 5 | 6.82 |
| <i>Zbp1</i> | Z-DNA binding protein 1 | 6.59 |
| <i>Ifi205</i> | interferon activated gene 205 | 6.41 |
| <i>Ighv1-62-3</i> | immunoglobulin heavy variable 1-62-3 | 6.35 |
| <i>Igkv4-62</i> | immunoglobulin kappa variable 4-62 | 6.27 |
| <i>6330403K07Rik</i> | RIKEN cDNA 6330403K07 gene | 6.23 |
| <i>Mndal</i> | myeloid nuclear differentiation antigen like | 6.18 |
| <i>Mnda</i> | myeloid cell nuclear differentiation antigen interferon activated gene 204 | 6.17 |
| <i>Lyz2</i> | lysozyme 2 | 6.13 |
| <i>Ifi44</i> | interferon-induced protein 44 | 5.85 |
| <i>Ifi202b</i> | interferon activated gene 202B | 5.76 |
| <i>Cyp1b1</i> | cytochrome P450, family 1, subfamily b, polypeptide 1 | 5.72 |
| <i>Pyhin1</i> | pyrin and HIN domain family, member 1 | 5.55 |
| <i>Isg15</i> | ISG15 ubiquitin-like modifier | 5.52 |
| <i>Lilrb4</i> | leukocyte immunoglobulin-like receptor, subfamily B, member 4 | 5.46 |
| <i>Ccl11</i> | chemokine (C-C motif) ligand 11 | 5.34 |
| <i>Trav9d-3</i> | T cell receptor alpha variable 9D-3 | 5.19 |
| <i>Gm5431</i> | predicted gene 5431 | 5.04 |
| <i>Plac8</i> | placenta-specific 8 | 5.02 |
| <i>Ccl7</i> | chemokine (C-C motif) ligand 7 | 5.00 |
| <i>Cd53</i> | CD53 antigen | 4.98 |
| <i>Gm10334</i> | predicted gene 10334 | 4.94 |
| <i>17533223</i> | <i>No associated gene</i> | 4.81 |
| <i>Cybb</i> | cytochrome b-245, beta polypeptide | 4.72 |
| <i>Saa3</i> | serum amyloid A 3 | 4.72 |
| <i>Dynlrb2</i> | dynein light chain roadblock-type 2 | 4.71 |
| <i>Bst2</i> | bone marrow stromal cell antigen 2 | 4.68 |
| <i>Msr1</i> | macrophage scavenger receptor 1 | 4.61 |
| <i>Tnfsf10</i> | tumor necrosis factor (ligand) superfamily, member 10 | 4.58 |
| <i>Apof</i> | apolipoprotein F | 4.56 |
| <i>Enpp1</i> | ectonucleotide pyrophosphatase/phosphodiesterase 1 | 4.54 |

| | | |
|----------------------|---|------|
| 9130208D14Rik | RIKEN cDNA 9130208D14 gene | 4.51 |
| Ms4a6b | membrane-spanning 4-domains, subfamily A, member 6B | 4.47 |
| Ifit1 | interferon-induced protein with tetratricopeptide repeats 1 | 4.45 |
| 17242306 | <i>No associated gene</i> | 4.43 |
| Mx2 | MX dynamin-like GTPase 2 | 4.42 |
| Gm22506 | predicted gene, 22506 | 4.41 |
| Phf11b | PHD finger protein 11B | 4.40 |
| Ms4a4d | membrane-spanning 4-domains, subfamily A, member 4D | 4.38 |
| 17238868 | <i>No associated gene</i> | 4.38 |
| Oasl2 | 2'-5' oligoadenylate synthetase-like 2 | 4.36 |
| Parm1 | prostate androgen-regulated mucin-like protein 1 | 4.36 |
| 17549388 | <i>No associated gene</i> | 4.33 |
| 17238920 | <i>No associated gene</i> | 4.32 |
| Cd180 | CD180 antigen | 4.31 |
| Gcnt3 | glucosaminyl (N-acetyl) transferase 3, mucin type | 4.30 |
| 17549772 | <i>No associated gene</i> | 4.30 |
| Chrn4 | cholinergic receptor, nicotinic, beta polypeptide 4 | 4.29 |
| Gm8369 | predicted gene 8369 | 4.28 |
| AW112010 | expressed sequence AW112010 | 4.24 |
| Aqp4 | aquaporin 4 | 4.19 |
| Cidea | cell death-inducing DNA fragmentation factor, alpha subunit-like effector A | 4.18 |
| Enpp3 | ectonucleotide pyrophosphatase/phosphodiesterase 3 | 4.18 |
| Dnase1l3 | deoxyribonuclease 1-like 3 | 4.16 |
| Gast | gastrin | 4.11 |
| Arhgap36 | Rho GTPase activating protein 36 | 4.10 |
| Sell | selectin, lymphocyte | 4.02 |
| Epsti1 | epithelial stromal interaction 1 (breast) | 3.98 |
| Ms4a6c | membrane-spanning 4-domains, subfamily A, member 6C | 3.94 |
| 17398176 | <i>No associated gene</i> | 3.93 |
| AU020206 | expressed sequence AU020206 | 3.91 |
| LOC102642603 | <i>No associated gene</i> | 3.91 |
| Rbp1 | retinol binding protein 1, cellular | 3.91 |
| Colec12 | collectin sub-family member 12 | 3.91 |
| Irf7 | interferon regulatory factor 7 | 3.87 |
| Rab38 | RAB38, member RAS oncogene family | 3.86 |
| Igkv4-73 | immunoglobulin kappa variable 4-73 | 3.84 |
| Aif1 | allograft inflammatory factor 1 | 3.83 |
| Rarres2 | retinoic acid receptor responder (tazarotene induced) 2 | 3.82 |
| Msln | mesothelin | 3.81 |
| Rtp4 | receptor transporter protein 4 | 3.78 |
| Ms4a4c | membrane-spanning 4-domains, subfamily A, member 4C | 3.75 |
| Ctla2b | cytotoxic T lymphocyte-associated protein 2 beta | 3.75 |
| Gpr65 | G-protein coupled receptor 65 | 3.75 |
| Gbp3 | guanylate binding protein 3 | 3.74 |
| Dlk1 | delta-like 1 homolog (Drosophila) | 3.74 |
| H2-T22 | histocompatibility 2, T region locus 22 | 3.73 |

| | | |
|--------------------------------|---|------|
| Try4 | trypsin 4 | 3.72 |
| Ly6d | lymphocyte antigen 6 complex, locus D | 3.72 |
| 4931429I11Rik | RIKEN cDNA 4931429I11 gene | 3.71 |
| 17238916 | <i>No associated gene</i> | 3.71 |
| Scimp | SLP adaptor and CSK interacting membrane protein | 3.69 |
| Vwde | von Willebrand factor D and EGF domains | 3.68 |
| Gbp9 | guanylate-binding protein 9 | 3.66 |
| Serpinb6b | serine (or cysteine) peptidase inhibitor, clade B, member 6b | 3.64 |
| GENSCAN0000003983 2 | <i>No associated gene</i> | 3.63 |
| Enpep | glutamyl aminopeptidase | 3.58 |
| Gm22888 | predicted gene, 22888 | 3.56 |
| Mmp3 | matrix metalloproteinase 3 | 3.55 |
| 17238878 | <i>No associated gene</i> | 3.55 |
| 17238846 | <i>No associated gene</i> | 3.54 |
| Ifi203 | interferon activated gene 203 | 3.53 |
| 17238880 | <i>No associated gene</i> | 3.53 |
| Gm17757 | GTPase, very large interferon inducible 1 pseudogen | 3.50 |
| Phf11d | PHD finger protein 11D | 3.47 |
| Ly86 | lymphocyte antigen 86 | 3.45 |
| 17238866 | <i>No associated gene</i> | 3.44 |
| Faim3 | Fas apoptotic inhibitory molecule 3 | 3.44 |
| 17238844 | <i>No associated gene</i> | 3.42 |
| Gbp2b | guanylate binding protein 2b | 3.42 |
| Clec4n | C-type lectin domain family 4, member n | 3.38 |
| Slc35f4 | solute carrier family 35, member F4 | 3.36 |
| Tcrb-J | T cell receptor beta, joining region | 3.36 |
| Tlr1 | toll-like receptor 1 | 3.36 |
| Bcl2a1b | B cell leukemia/lymphoma 2 related protein A1b | 3.36 |
| Flrt2 | fibronectin leucine rich transmembrane protein 2 | 3.36 |
| Marco | macrophage receptor with collagenous structure | 3.35 |
| 17548315 | <i>No associated gene</i> | 3.34 |
| Neurog3 | neurogenin 3 | 3.33 |
| Calca | calcitonin/calcitonin-related polypeptide, alpha | 3.32 |
| Xaf1 | XIAP associated factor 1 | 3.31 |
| Dpt | dermatopontin | 3.30 |
| Casp1 | caspase 1 | 3.29 |
| P2ry13 | purinergic receptor P2Y, G-protein coupled 13 | 3.28 |
| Gimap4 | GTPase, IMAF family member 4 | 3.26 |
| Cd74 | CD74 antigen (invariant polypeptide of major histocompatibility complex, class II antigen-associated) | 3.25 |
| Osmr | oncostatin M receptor | 3.23 |
| Clip4 | CAP-GLY domain containing linker protein family, member 4 | 3.23 |
| Lcp1 | lymphocyte cytosolic protein 1 | 3.21 |
| Ccl2 | chemokine (C-C motif) ligand 2 | 3.20 |
| Gm5409 | predicted pseudogene 5409 | 3.20 |
| H2-Ab1 | histocompatibility 2, class II antigen A, beta 1 | 3.20 |

| | | |
|----------------------|---|------|
| Gbp2 | guanylate binding protein 2 | 3.18 |
| Slc43a3 | solute carrier family 43, member 3 | 3.18 |
| Ttc25 | tetratricopeptide repeat domain 25 | 3.17 |
| Syncn | syncollin | 3.17 |
| Chst8 | carbohydrate (N-acetylgalactosamine 4-0) sulfotransferase 8 | 3.15 |
| Ffar4 | free fatty acid receptor 4 | 3.15 |
| Vsig2 | V-set and immunoglobulin domain containing 2 | 3.15 |
| Arhgdib | Rho, GDP dissociation inhibitor (GDI) beta | 3.15 |
| Nckap1l | NCK associated protein 1 like | 3.13 |
| NONMMUT004543 | <i>No associated gene</i> | 3.13 |
| Wfdc18 | WAP four-disulfide core domain 18 | 3.12 |
| Igh-V10 | immunoglobulin heavy chain (V10 family) | 3.11 |
| Bambi | BMP and activin membrane-bound inhibitor | 3.10 |
| Pdgfra | platelet derived growth factor receptor, alpha polypeptide | 3.10 |
| 17238858 | <i>No associated gene</i> | 3.10 |
| Fhl2 | four and a half LIM domains 2 | 3.08 |
| Laptm5 | lysosomal-associated protein transmembrane 5 | 3.07 |
| NONMMUT004538 | <i>No associated gene</i> | 3.06 |
| Arap2 | ArfGAP with RhoGAP domain, ankyrin repeat and PH domain 2 | 3.05 |
| Ifi3 | interferon-induced protein with tetratricopeptide repeats 3 | 3.04 |
| Ighv8-8 | immunoglobulin heavy variable 8-8 | 3.03 |
| Gpr133 | G protein-coupled receptor 133 | 3.03 |
| Fcgr1 | Fc receptor, IgG, high affinity I | 3.02 |
| Cd48 | CD48 antigen | 3.01 |
| Bcl2a1a | B cell leukemia/lymphoma 2 related protein A1a | 3.00 |
| Gm14446 | predicted gene 14446 | 3.00 |
| Iglv1 | immunoglobulin lambda variable 1 | 2.99 |
| Ceacam10 | carcinoembryonic antigen-related cell adhesion molecule 10 | 2.99 |
| Gvin1 | GTPase, very large interferon inducible 1 | 2.98 |
| Slc15a3 | solute carrier family 15, member 3 | 2.98 |
| Stk17b | serine/threonine kinase 17b (apoptosis-inducing) | 2.97 |
| Taf1d | TATA-box binding protein associated factor, RNA polymerase I, D | 2.94 |
| Jam2 | junction adhesion molecule 2 | 2.94 |
| 17238842 | <i>No associated gene</i> | 2.93 |
| Eef1a2 | eukaryotic translation elongation factor 1 alpha 2 | 2.93 |
| Cd38 | CD38 antigen | 2.93 |
| Cped1 | cadherin-like and PC-esterase domain containing 1 | 2.92 |
| Gm5150 | predicted gene 5150 | 2.91 |
| 17238870 | <i>No associated gene</i> | 2.90 |
| Ccl8 | chemokine (C-C motif) ligand 8 | 2.90 |
| Igsf6 | immunoglobulin superfamily, member 6 | 2.89 |
| 17238832 | <i>No associated gene</i> | 2.89 |
| LOC102632976 | predicted gene 15247 | 2.89 |
| 17366275 | <i>No associated gene</i> | 2.88 |
| Gbp10 | guanylate-binding protein 10 | 2.88 |
| H2-Eb1 | histocompatibility 2, class II antigen E beta | 2.88 |

| | | |
|-----------------------|--|------|
| Rasgrp1 | RAS guanyl releasing protein 1 | 2.87 |
| Cxcl5 | chemokine (C-X-C motif) ligand 5 | 2.87 |
| Ccl5 | chemokine (C-C motif) ligand 5 | 2.87 |
| Aspn | asporin | 2.87 |
| Pgf | placental growth factor | 2.87 |
| Pde3a | phosphodiesterase 3A, cGMP inhibited | 2.87 |
| Casp4 | caspase 4, apoptosis-related cysteine peptidase | 2.85 |
| Mustn1 | musculoskeletal, embryonic nuclear protein 1 | 2.85 |
| Mpeg1 | macrophage expressed gene 1 | 2.84 |
| Bank1 | B cell scaffold protein with ankyrin repeats 1 | 2.83 |
| Apol9a | apolipoprotein L 9a | 2.83 |
| 9930111J21Rik2 | RIKEN cDNA 9930111J21 gene 2 | 2.82 |
| 17549290 | <i>No associated gene</i> | 2.82 |
| Gbp5 | guanylate binding protein 5 | 2.82 |
| Fcer1g | Fc receptor, IgE, high affinity I, gamma polypeptide | 2.82 |
| Syt17 | synaptotagmin XVII | 2.82 |
| 17547505 | <i>No associated gene</i> | 2.81 |
| Ifi47 | interferon gamma inducible protein 47 | 2.80 |
| Igtp | interferon gamma induced GTPase | 2.80 |
| Rasd2 | RASD family, member 2 | 2.80 |
| Gm7609 | predicted pseudogene 7609 | 2.79 |
| Cdh11 | cadherin 11 | 2.79 |
| Pfkfb3 | 6-phosphofructo-2-kinase/fructose-2,6-biphosphatase 3 | 2.79 |
| Lsp1 | lymphocyte specific 1 | 2.78 |
| Pigr | polymeric immunoglobulin receptor | 2.77 |
| Apol9b | apolipoprotein L 9b | 2.77 |
| Il1a | interleukin 1 alpha | 2.77 |
| BC048594 | cDNA sequence BC048594, doublecortin domain containing 5 | 2.77 |
| Gm20412 | predicted gene 20412 | 2.77 |
| Vcam1 | vascular cell adhesion molecule 1 | 2.77 |
| Sez6 | seizure related gene 6 | 2.76 |
| Cfb | complement factor B | 2.76 |
| 17548709 | <i>No associated gene</i> | 2.76 |
| Tyrobp | TYRO protein tyrosine kinase binding protein | 2.75 |
| Tekt2 | tektin 2 | 2.74 |
| Igkv4-69 | immunoglobulin kappa variable 4-69 | 2.74 |
| Des | desmin | 2.73 |
| Igh-V11 | immunoglobulin heavy chain (V11 family) | 2.73 |
| C1qb | complement component 1, q subcomponent, beta polypeptide | 2.73 |
| Ddx60 | DEAD (Asp-Glu-Ala-Asp) box polypeptide 60 | 2.72 |
| Tmem173 | transmembrane protein 173 | 2.71 |
| Depdc7 | DEP domain containing 7 | 2.70 |
| Gpx8 | glutathione peroxidase 8 (putative) | 2.69 |
| Slfn1 | schlafen 1 | 2.69 |
| Slc7a7 | solute carrier family 7 (cationic amino acid transporter, y+ system), member 7 | 2.69 |

| | | |
|----------------------|--|------|
| Gpr165 | G protein-coupled receptor 165 | 2.69 |
| Npnt | nephronectin | 2.69 |
| Slc38a1 | solute carrier family 38, member 1 | 2.68 |
| Gm12840 | predicted gene 12840 | 2.68 |
| 17238892 | <i>No associated gene</i> | 2.68 |
| Rnase6 | ribonuclease, RNase A family, 6 | 2.68 |
| Gbp11 | guanylate binding protein 11 | 2.68 |
| NONMMUT004548 | <i>No associated gene</i> | 2.68 |
| Cd86 | CD86 antigen | 2.67 |
| Slamf7 | SLAM family member 7 | 2.67 |
| Acp5 | acid phosphatase 5, tartrate resistant | 2.67 |
| F2 | coagulation factor II | 2.67 |
| Gpnmb | glycoprotein (transmembrane) nmb | 2.67 |
| Selplg | selectin, platelet (p-selectin) ligand | 2.67 |
| 17238860 | <i>No associated gene</i> | 2.67 |
| Gm12250 | predicted gene 12250 | 2.67 |
| Cdh9 | cadherin 9 | 2.63 |
| Gm19980 | predicted gene, 19980 | 2.63 |
| Zfp361l | zinc finger protein 36, C3H type-like 1 | 2.63 |
| Cd44 | CD44 antigen | 2.62 |
| Anxa3 | annexin A3 | 2.61 |
| 17238848 | <i>No associated gene</i> | 2.61 |
| Tmem132b | transmembrane protein 132B | 2.61 |
| Cp | ceruloplasmin | 2.60 |
| Tspan1 | tetraspanin 1 | 2.60 |
| 17238896 | <i>No associated gene</i> | 2.60 |
| Loxl3 | lysyl oxidase-like 3 | 2.59 |
| Spic | Spi-C transcription factor (Spi-1/PU.1 related) | 2.59 |
| Ctss | cathepsin S | 2.58 |
| Blnk | B cell linker | 2.58 |
| Stat4 | signal transducer and activator of transcription 4 | 2.57 |
| Cxcl12 | chemokine (C-X-C motif) ligand 12 | 2.57 |
| 17358825 | <i>No associated gene</i> | 2.57 |
| 17318967 | <i>No associated gene</i> | 2.57 |
| Syne1 | spectrin repeat containing, nuclear envelope 1 | 2.56 |
| Vstm2a | V-set and transmembrane domain containing 2A | 2.55 |
| H2-T23 | histocompatibility 2, T region locus 23 | 2.55 |
| Ccl12 | chemokine (C-C motif) ligand 12 | 2.53 |
| Cygb | cytoglobin | 2.53 |
| Rac2 | RAS-related C3 botulinum substrate 2 | 2.53 |
| Cyba | cytochrome b-245, alpha polypeptide | 2.53 |
| Mmp7 | matrix metalloproteinase 7 | 2.53 |
| Rerg | RAS-like, estrogen-regulated, growth-inhibitor | 2.53 |
| 17549384 | <i>No associated gene</i> | 2.52 |
| Lgi1 | leucine-rich repeat LGI family, member 1 | 2.52 |
| Cldn4 | claudin 4 | 2.52 |

| | | |
|----------------------|---|------|
| 17548532 | <i>No associated gene</i> | 2.51 |
| Far2 | fatty acyl CoA reductase 2 | 2.51 |
| Emp3 | epithelial membrane protein 3 | 2.49 |
| Xdh | xanthine dehydrogenase | 2.49 |
| Gfra2 | glial cell line derived neurotrophic factor family receptor alpha 2 | 2.48 |
| Ddc | dopa decarboxylase | 2.48 |
| Fam49a | family with sequence similarity 49, member A | 2.48 |
| G530011O06Rik | RIKEN cDNA G530011O06 gene | 2.48 |
| Gchfr | GTP cyclohydrolase I feedback regulator | 2.46 |
| Krt19 | keratin 19 | 2.46 |
| 17294682 | <i>No associated gene</i> | 2.45 |
| Oas1g | 2'-5' oligoadenylate synthetase 1G | 2.45 |
| Mfge8 | milk fat globule-EGF factor 8 protein | 2.44 |
| Cd2 | CD2 antigen | 2.44 |
| Tle4 | transducin-like enhancer of split 4 | 2.43 |
| Bmp3 | bone morphogenetic protein 3 | 2.42 |
| Aebp1 | AE binding protein 1 | 2.41 |
| Tmprss2 | transmembrane protease, serine 2 | 2.40 |
| 17238918 | <i>No associated gene</i> | 2.40 |
| Plxdc2 | plexin domain containing 2 | 2.40 |
| Plet1os | placenta expressed transcript 1, opposite strand | 2.40 |
| Cdr1 | cerebellar degeneration related antigen 1 | 2.40 |
| Rsad2 | radical S-adenosyl methionine domain containing 2 | 2.39 |
| Epas1 | endothelial PAS domain protein 1 | 2.39 |
| Car13 | carbonic anhydrase 13 | 2.39 |
| Srgn | serglycin | 2.39 |
| 17238856 | <i>No associated gene</i> | 2.38 |
| Oas1l | 2'-5' oligoadenylate synthetase-like 1 | 2.38 |
| Nrip3 | nuclear receptor interacting protein 3 | 2.37 |
| Csn3 | casein kappa | 2.37 |
| Lrch2 | leucine-rich repeats and calponin homology (CH) domain containing 2 | 2.37 |
| Slc5a10 | solute carrier family 5 (sodium/glucose cotransporter), member 10 | 2.37 |
| Themis2 | thymocyte selection associated family member 2 | 2.36 |
| Gpr119 | G-protein coupled receptor 119 | 2.36 |
| Arhgap10 | Rho GTPase activating protein 10 | 2.35 |
| Sulf1 | sulfatase 1 | 2.35 |
| 17238912 | <i>No associated gene</i> | 2.34 |
| H2-T24 | histocompatibility 2, T region locus 24 | 2.34 |
| Ifit2 | interferon-induced protein with tetratricopeptide repeats 2 | 2.33 |
| Swap70 | SWA-70 protein | 2.33 |
| Ighg3 | Immunoglobulin heavy constant gamma 3 | 2.33 |
| Elmod1 | ELMO/CED-12 domain containing 1 | 2.32 |
| Col3a1 | collagen, type III, alpha 1 | 2.32 |
| Neurl3 | neuralized E3 ubiquitin protein ligase 3 | 2.32 |
| Clqc | complement component 1, q subcomponent, C chain | 2.31 |
| 17238924 | <i>No associated gene</i> | 2.31 |

| | | |
|----------------------|---|------|
| AB124611 | cDNA sequence AB124611 | 2.31 |
| AW551984 | expressed sequence AW551984 | 2.31 |
| 17238834 | <i>No associated gene</i> | 2.31 |
| Dpp10 | dipeptidylpeptidase 10 | 2.31 |
| Timp2 | tissue inhibitor of metalloproteinase 2 | 2.31 |
| Uba7 | ubiquitin-like modifier activating enzyme 7 | 2.30 |
| Gbp4 | guanylate binding protein 4 | 2.29 |
| Fli1 | Friend leukemia integration 1 | 2.28 |
| Gbp7 | guanylate binding protein 7 | 2.28 |
| Tnfaip8l3 | tumor necrosis factor, alpha-induced protein 8-like 3 | 2.28 |
| Lcp2 | lymphocyte cytosolic protein 2 | 2.27 |
| Ppp1r3c | protein phosphatase 1, regulatory (inhibitor) subunit 3C | 2.27 |
| Ccdc80 | coiled-coil domain containing 80 | 2.27 |
| Fam179a | family with sequence similarity 179, member A | 2.27 |
| Tap1 | transporter 1, ATP-binding cassette, sub-family B (MDR/TAP) | 2.26 |
| Gucy2c | guanylate cyclase 2c | 2.26 |
| Cntnap5b | contactin associated protein-like 5B | 2.26 |
| Gm11640 | predicted gene 11640 | 2.25 |
| Il1rn | interleukin 1 receptor antagonist | 2.25 |
| Parp14 | poly (ADP-ribose) polymerase family, member 14 | 2.25 |
| Prrg3 | proline rich Gla (G-carboxyglutamic acid) 3 (transmembrane) | 2.25 |
| Gm25761 | predicted gene, 25761 | 2.25 |
| Gfra3 | glial cell line derived neurotrophic factor family receptor alpha 3 | 2.25 |
| Usp18 | ubiquitin specific peptidase 18 | 2.23 |
| Brinp1 | bone morphogenic protein/retinoic acid inducible neural specific 1 | 2.22 |
| Lrrn3 | leucine rich repeat protein 3, neuronal | 2.22 |
| Pamr1 | peptidase domain containing associated with muscle regeneration 1 | 2.22 |
| 17238876 | <i>No associated gene</i> | 2.22 |
| BC028528 | cDNA sequence BC028528 | 2.21 |
| Oas2 | 2'-5' oligoadenylate synthetase 2 | 2.21 |
| Fam159b | family with sequence similarity 159, member B | 2.21 |
| 17548703 | <i>No associated gene</i> | 2.21 |
| Irgm2 | immunity-related GTPase family M member 2 | 2.21 |
| S1pr3 | sphingosine-1-phosphate receptor 3 | 2.20 |
| Itgb2 | integrin beta 2 | 2.20 |
| Il4ra | interleukin 4 receptor, alpha | 2.20 |
| Ptafr | platelet-activating factor receptor | 2.20 |
| Ptgs1 | prostaglandin-endoperoxide synthase 1 | 2.20 |
| Il33 | interleukin 33 | 2.19 |
| Mmp14 | matrix metalloproteinase 14 (membrane-inserted) | 2.19 |
| C2 | complement component 2 (within H-2S) | 2.19 |
| Ccl22 | chemokine (C-C motif) ligand 22 | 2.19 |
| NONMMUT017874 | <i>No associated gene</i> | 2.19 |
| Trim9 | tripartite motif-containing 9 | 2.19 |
| Grem2 | gremlin 2, DAN family BMP antagonist | 2.18 |
| Serpine2 | serine (or cysteine) peptidase inhibitor, clade E, member 2 | 2.18 |

| | | |
|----------------------|---|------|
| Rgs5 | regulator of G-protein signaling 5 | 2.18 |
| Gm26719 | predicted gene, 26719 | 2.18 |
| Tnfrsf1b | tumor necrosis factor receptor superfamily, member 1b | 2.18 |
| Rorc | RAR-related orphan receptor gamma | 2.17 |
| Igk | immunoglobulin kappa chain complex | 2.17 |
| Iqsec3 | IQ motif and Sec7 domain 3 | 2.17 |
| Stat2 | signal transducer and activator of transcription 2 | 2.17 |
| Fxyd6 | FXDY domain-containing ion transport regulator 6 | 2.17 |
| Scarf2 | scavenger receptor class F, member 2 | 2.16 |
| Crim1 | cysteine rich transmembrane BMP regulator 1 (chordin like) | 2.16 |
| Samhd1 | SAM domain and HD domain, 1 | 2.15 |
| C330006A16Rik | RIKEN cDNA C330006A16 gene | 2.15 |
| Gm25506 | predicted gene, 25506 | 2.15 |
| 17549570 | <i>No associated gene</i> | 2.15 |
| Fcgrt | Fc receptor, IgG, alpha chain transporter | 2.15 |
| 17462872 | <i>No associated gene</i> | 2.15 |
| Asic1 | acid-sensing (proton-gated) ion channel 1 | 2.15 |
| Rab32 | RAB32, member RAS oncogene family | 2.15 |
| Gm26669 | predicted gene, 26669 | 2.14 |
| Mmp2 | matrix metalloproteinase 2 | 2.14 |
| Epb4.1l2 | erythrocyte protein band 4.1-like 2 | 2.14 |
| Cd37 | CD37 antigen | 2.14 |
| Cd97 | CD97 antigen | 2.14 |
| Cpne2 | copine II | 2.14 |
| Bgn | biglycan | 2.14 |
| Erdr1 | erythroid differentiation regulator 1 | 2.13 |
| Plbd1 | phospholipase B domain containing 1 | 2.13 |
| Peak1 | pseudopodium-enriched atypical kinase 1 | 2.12 |
| 17510770 | <i>No associated gene</i> | 2.12 |
| Racgap1 | Rac GTPase-activating protein 1 | 2.12 |
| Cyp1a1 | cytochrome P450, family 1, subfamily a, polypeptide 1 | 2.11 |
| Il34 | interleukin 34 | 2.11 |
| Apbb1ip | amyloid beta (A4) precursor protein-binding, family B, member 1 interacting protein | 2.10 |
| Lypd8 | LY6/PLAUR domain containing 8 | 2.10 |
| Rspo3 | R-spondin 3 | 2.10 |
| Car8 | carbonic anhydrase 8 | 2.09 |
| Gpr126 | G protein-coupled receptor 126 | 2.09 |
| Gadd45b | growth arrest and DNA-damage-inducible 45 beta | 2.09 |
| Ptprg | protein tyrosine phosphatase, receptor type, G | 2.09 |
| Anxa2 | annexin A2 | 2.09 |
| Guca2a | guanylate cyclase activator 2a (guanylin) | 2.09 |
| Igh-VJ558 | immunoglobulin heavy chain (J558 family) | 2.08 |
| Htra1 | HtrA serine peptidase 1 | 2.08 |
| Pcolce | procollagen C-endopeptidase enhancer protein | 2.08 |
| Rbm11 | RNA binding motif protein 11 | 2.08 |

| | | |
|----------------------|--|------|
| 17238874 | <i>No associated gene</i> | 2.08 |
| Ust | uronyl-2-sulfotransferase | 2.07 |
| Tnfrsf13c | tumor necrosis factor receptor superfamily, member 13c | 2.07 |
| Tmem255a | transmembrane protein 255A | 2.06 |
| Fstl1 | follistatin-like 1 | 2.06 |
| 17214729 | <i>No associated gene</i> | 2.05 |
| Sla | src-like adaptor | 2.05 |
| Tspo | translocator protein | 2.05 |
| Tpd52l1 | tumor protein D52-like 1 | 2.05 |
| Tgm2 | transglutaminase 2, C polypeptide | 2.05 |
| Lxn | latexin | 2.04 |
| Ephb2 | Eph receptor B2 | 2.04 |
| S100a2 | S100 calcium binding protein A2 | 2.04 |
| Angptl2 | angiopoietin-like 2 | 2.03 |
| Tusc5 | tumor suppressor candidate 5 | 2.03 |
| 17486956 | <i>No associated gene</i> | 2.03 |
| Prrx1 | paired related homeobox 1 | 2.03 |
| Ddr2 | discoidin domain receptor family, member 2 | 2.03 |
| Dcdc2a | doublecortin domain containing 2a | 2.03 |
| Ednra | endothelin receptor type A | 2.02 |
| Ccl19 | chemokine (C-C motif) ligand 19 | 2.02 |
| LOC101056250 | sp110 nuclear body protein-like | 2.02 |
| AI662270 | expressed sequence AI662270 | 2.02 |
| Arhgef6 | Rac/Cdc42 guanine nucleotide exchange factor (GEF) 6 | 2.02 |
| Col6a3 | collagen, type VI, alpha 3 | 2.01 |
| Hcls1 | hematopoietic cell specific Lyn substrate 1 | 2.01 |
| Msn | moesin | 2.01 |
| 1700020114Rik | RIKEN cDNA 1700020114 gene | 2.01 |
| Socs2 | suppressor of cytokine signaling 2 | 2.01 |
| Arrdc4 | arrestin domain containing 4 | 2.00 |
| Mfap5 | microfibrillar associated protein 5 | 2.00 |
| Csf1r | colony stimulating factor 1 receptor | 2.00 |
| H2-M2 | histocompatibility 2, M region locus 2 | 2.00 |
| Unc93b1 | unc-93 homolog B1 (C. elegans) | 2.00 |
| 1700006F04Rik | RIKEN cDNA 1700006F04 gene | 2.00 |
| Gm8995 | predicted gene 8995 | 2.00 |
| Nebl | nebulette | 2.00 |
| Tlr9 | toll-like receptor 9 | 2.00 |
| Rab8b | RAB8B, member RAS oncogene family | 1.99 |
| Tgfb1 | transforming growth factor, beta induced | 1.99 |
| Oas1a | 2'-5' oligoadenylate synthetase 1A | 1.99 |
| Acta2 | actin, alpha 2, smooth muscle, aorta | 1.99 |
| Fam105a | family with sequence similarity 105, member A | 1.99 |
| Cd19 | CD19 antigen | 1.99 |
| 17542364 | <i>No associated gene</i> | 1.98 |
| Uchl1 | ubiquitin carboxy-terminal hydrolase L1 | 1.98 |

| | | |
|-----------------------------|--|------|
| <i>Pros1</i> | protein S (alpha) | 1.98 |
| <i>A4galt</i> | alpha 1,4-galactosyltransferase | 1.98 |
| <i>Itpr1l2</i> | inositol 1,4,5-triphosphate receptor interacting protein-like 2 | 1.98 |
| <i>Gimap6</i> | GTPase, IMAP family member 6 | 1.97 |
| <i>Ptgfrn</i> | prostaglandin F2 receptor negative regulator | 1.97 |
| <i>Cd14</i> | CD14 antigen | 1.97 |
| <i>Fbn1</i> | fibrillin 1 | 1.96 |
| <i>Sparcl1</i> | SPARC-like 1 | 1.96 |
| <i>Il18bp</i> | interleukin 18 binding protein | 1.96 |
| <i>Kcnab3</i> | potassium voltage-gated channel, shaker-related subfamily, beta member 3 | 1.96 |
| <i>Dbn1</i> | drebrin 1 | 1.96 |
| <i>Gpr171</i> | G protein-coupled receptor 171 | 1.96 |
| <i>Cmtm7</i> | CKLF-like MARVEL transmembrane domain containing 7 | 1.95 |
| <i>Plscr2</i> | phospholipid scramblase 2 | 1.95 |
| <i>Stat1</i> | signal transducer and activator of transcription 1 | 1.94 |
| <i>17547680</i> | <i>No associated gene</i> | 1.94 |
| <i>Tpbg</i> | trophoblast glycoprotein | 1.94 |
| <i>Usp25</i> | ubiquitin specific peptidase 25 | 1.94 |
| <i>17549588</i> | <i>No associated gene</i> | 1.94 |
| <i>Procr</i> | protein C receptor, endothelial | 1.94 |
| <i>Cald1</i> | caldesmon 1 | 1.94 |
| <i>Rnf213</i> | ring finger protein 213 | 1.94 |
| <i>Scn3a</i> | sodium channel, voltage-gated, type III, alpha | 1.94 |
| <i>Plekho1</i> | pleckstrin homology domain containing, family O member 1 | 1.93 |
| <i>Lyn</i> | LYN proto-oncogene, Src family tyrosine kinase | 1.93 |
| <i>Slamf9</i> | SLAM family member 9 | 1.92 |
| <i>Ceacam1</i> | carcinoembryonic antigen-related cell adhesion molecule 1 | 1.92 |
| <i>Dapl1</i> | death associated protein-like 1 | 1.92 |
| <i>Necab2</i> | N-terminal EF-hand calcium binding protein 2 | 1.92 |
| <i>Ccng2</i> | cyclin G2 | 1.91 |
| <i>BC023105</i> | cDNA sequence BC023105 | 1.91 |
| <i>17229451</i> | <i>No associated gene</i> | 1.91 |
| <i>H2-Q5</i> | histocompatibility 2, Q region locus 5 | 1.90 |
| <i>Nr1h4</i> | nuclear receptor subfamily 1, group H, member 4 | 1.90 |
| <i>Tmem86a</i> | transmembrane protein 86A | 1.90 |
| <i>Shisa5</i> | shisa family member 5 | 1.90 |
| <i>Tk2</i> | thymidine kinase 2, mitochondrial | 1.90 |
| <i>Irgm1</i> | immunity-related GTPase family M member 1 | 1.90 |
| <i>Sorcs2</i> | sortilin-related VPS10 domain containing receptor 2 | 1.90 |
| <i>Txnip</i> | thioredoxin interacting protein | 1.90 |
| <i>B430306N03Rik</i> | RIKEN cDNA B430306N03 gene | 1.89 |
| <i>Prcp</i> | prolylcarboxypeptidase (angiotensinase C) | 1.89 |
| <i>Ltbp1</i> | latent transforming growth factor beta binding protein 1 | 1.89 |
| <i>Parp12</i> | poly (ADP-ribose) polymerase family, member 12 | 1.89 |
| <i>Cd248</i> | CD248 antigen, endosialin | 1.89 |
| <i>Csf1</i> | colony stimulating factor 1 (macrophage) | 1.89 |

| | | |
|----------------------|--|------|
| C4b | complement component 4B (Chido blood group) | 1.89 |
| Pltp | phospholipid transfer protein | 1.89 |
| Tmem59l | transmembrane protein 59-like | 1.88 |
| Terc | telomerase RNA component | 1.88 |
| Arhgef28 | Rho guanine nucleotide exchange factor (GEF) 28 | 1.88 |
| Rbp4 | retinol binding protein 4, plasma | 1.88 |
| Il18 | interleukin 18 | 1.88 |
| Gbe1 | glucan (1,4-alpha-), branching enzyme 1 | 1.88 |
| Cyth4 | cytohesin 4 | 1.88 |
| Kl | klotho | 1.87 |
| Sdc3 | syndecan 3 | 1.87 |
| Lamb2 | laminin, beta 2 | 1.87 |
| Mcm6 | minichromosome maintenance complex component 6 | 1.87 |
| Penk | preproenkephalin | 1.87 |
| Nrgn | neurogranin | 1.87 |
| Lrig1 | leucine-rich repeats and immunoglobulin-like domains 1 | 1.87 |
| Rsph4a | radial spoke head 4 homolog A (Chlamydomonas) | 1.86 |
| Heyl | hairly/enhancer-of-split related with YRPW motif-like | 1.86 |
| Flna | filamin, alpha | 1.86 |
| Tfpi2 | tissue factor pathway inhibitor 2 | 1.86 |
| Fxyd3 | FXDY domain-containing ion transport regulator 3 | 1.86 |
| Fam84a | family with sequence similarity 84, member A | 1.86 |
| Traf1 | TRAF type zinc finger domain containing 1 | 1.86 |
| Antxr1 | anthrax toxin receptor 1 | 1.86 |
| Klf10 | Kruppel-like factor 10 | 1.86 |
| Cd83 | CD83 antigen | 1.85 |
| Prelp | proline arginine-rich end leucine-rich repeat | 1.85 |
| Tox | thymocyte selection-associated high mobility group box | 1.85 |
| Tspan33 | tetraspanin 33 | 1.85 |
| Mov10 | Moloney leukemia virus 10 | 1.85 |
| Large | like-glycosyltransferase | 1.85 |
| Lrrk2 | leucine-rich repeat kinase 2 | 1.85 |
| 17548908 | <i>No associated gene</i> | 1.85 |
| Plod2 | procollagen lysine, 2-oxoglutarate 5-dioxygenase 2 | 1.85 |
| Clcn5 | chloride channel, voltage-sensitive 5 | 1.84 |
| Naip2 | NLR family, apoptosis inhibitory protein 2 | 1.84 |
| Parp9 | poly (ADP-ribose) polymerase family, member 9 | 1.84 |
| Pon2 | paraoxonase 2 | 1.84 |
| NONMMUT004544 | <i>No associated gene</i> | 1.84 |
| Pdlim7 | PDZ and LIM domain 7 | 1.83 |
| Itga6 | integrin alpha 6 | 1.83 |
| Icam1 | intercellular adhesion molecule 1 | 1.83 |
| Slfn5 | schlafen 5 | 1.83 |
| 17549810 | <i>No associated gene</i> | 1.83 |
| Eng | endoglin | 1.83 |
| Ube2l6 | ubiquitin-conjugating enzyme E2L 6 | 1.83 |

| | | |
|----------------------|--|------|
| Cfi | complement component factor i | 1.83 |
| Cpne8 | copine VIII | 1.83 |
| Rasa3 | RAS p21 protein activator 3 | 1.83 |
| Lipa | lysosomal acid lipase A | 1.83 |
| Itga2 | integrin alpha 2 | 1.83 |
| Lgmn | legumain | 1.82 |
| 17238922 | <i>No associated gene</i> | 1.82 |
| Ehf | ets homologous factor | 1.82 |
| Lrrc32 | leucine rich repeat containing 32 | 1.82 |
| Dram1 | DNA-damage regulated autophagy modulator 1 | 1.82 |
| Gm20559 | predicted gene, 20559 | 1.82 |
| Anpep | alanyl (membrane) aminopeptidase | 1.82 |
| Cacnb3 | calcium channel, voltage-dependent, beta 3 subunit | 1.82 |
| Ly6e | lymphocyte antigen 6 complex, locus E | 1.82 |
| Tlr7 | toll-like receptor 7 | 1.81 |
| Ndufa4l2 | NADH dehydrogenase (ubiquinone) 1 alpha subcomplex, 4-like 2 | 1.81 |
| Fas | Fas (TNF receptor superfamily member 6) | 1.81 |
| Gm12945 | predicted gene 12945 | 1.81 |
| Hist1h4i | histone cluster 1, H4i | 1.81 |
| LOC100862024 | spleen focus forming virus (SFFV) proviral integration oncogene | 1.81 |
| Mmp19 | matrix metalloproteinase 19 | 1.80 |
| 17247155 | <i>No associated gene</i> | 1.80 |
| Axl | AXL receptor tyrosine kinase | 1.80 |
| Ifi30 | interferon gamma inducible protein 30 | 1.80 |
| Cd84 | CD84 antigen | 1.80 |
| H2-Aa | histocompatibility 2, class II antigen A, alpha | 1.80 |
| Itga5 | integrin alpha 5 (fibronectin receptor alpha) | 1.79 |
| 17548750 | <i>No associated gene</i> | 1.79 |
| Slc35b3 | solute carrier family 35, member B3 | 1.79 |
| 17480528 | <i>No associated gene</i> | 1.79 |
| Ighm | immunoglobulin heavy constant mu | 1.79 |
| Snx20 | sorting nexin 20 | 1.79 |
| Mpp2 | membrane protein, palmitoylated 2 (MAGUK p55 subfamily member 2) | 1.79 |
| Rftn1 | raftlin lipid raft linker 1 | 1.79 |
| Rem2 | rad and gem related GTP binding protein 2 | 1.79 |
| 17547541 | <i>No associated gene</i> | 1.78 |
| Cd274 | CD274 antigen | 1.78 |
| Abcg2 | ATP-binding cassette, sub-family G (WHITE), member 2 | 1.78 |
| Timp3 | tissue inhibitor of metalloproteinase 3 | 1.78 |
| Cd3d | CD3 antigen, delta polypeptide | 1.78 |
| 2810455O05Rik | RIKEN cDNA 2810455O05 gene | 1.78 |
| Fbln2 | fibulin 2 | 1.78 |
| Chrm4 | cholinergic receptor, muscarinic 4 | 1.78 |
| Slc39a8 | solute carrier family 39 (metal ion transporter), member 8 | 1.78 |
| Xpa | xeroderma pigmentosum, complementation group A | 1.78 |
| Cblb | Casitas B-lineage lymphoma b | 1.78 |

| | | |
|-----------------------------|--|------|
| <i>Tmem178b</i> | transmembrane protein 178B | 1.77 |
| <i>Tm4sf20</i> | transmembrane 4 L six family member 20 | 1.77 |
| <i>Sh3bgrl2</i> | SH3 domain binding glutamic acid-rich protein like 2 | 1.77 |
| <i>Col6a2</i> | collagen, type VI, alpha 2 | 1.77 |
| <i>Gda</i> | guanine deaminase | 1.77 |
| <i>Scn9a</i> | sodium channel, voltage-gated, type IX, alpha | 1.77 |
| <i>Rgs16</i> | regulator of G-protein signaling 16 | 1.77 |
| <i>Fap</i> | fibroblast activation protein | 1.77 |
| <i>Cyp39a1</i> | cytochrome P450, family 39, subfamily a, polypeptide 1 | 1.77 |
| <i>Cat</i> | catalase | 1.77 |
| <i>Egr2</i> | early growth response 2 | 1.77 |
| <i>17264338</i> | <i>No associated gene</i> | 1.77 |
| <i>Pilrb1</i> | paired immunoglobulin-like type 2 receptor beta 1 | 1.77 |
| <i>Elf4</i> | E74-like factor 4 (ets domain transcription factor) | 1.77 |
| <i>Vim</i> | vimentin | 1.77 |
| <i>Nfatc1</i> | nuclear factor of activated T cells, cytoplasmic, calcineurin dependent 1 | 1.77 |
| <i>Sdc1</i> | syndecan 1 | 1.76 |
| <i>Hspb1</i> | heat shock protein 1 | 1.76 |
| <i>Cd81</i> | CD81 antigen | 1.76 |
| <i>2200002D01Rik</i> | RIKEN cDNA 2200002D01 gene | 1.76 |
| <i>Mpp1</i> | membrane protein, palmitoylated | 1.76 |
| <i>17547589</i> | <i>No associated gene</i> | 1.76 |
| <i>Tspan17</i> | tetraspanin 17 | 1.75 |
| <i>Ecm1</i> | extracellular matrix protein 1 | 1.75 |
| <i>Fgf14</i> | fibroblast growth factor 14 | 1.75 |
| <i>Galnt7</i> | UDP-N-acetyl-alpha-D-galactosamine: polypeptide N-acetylgalactosaminyltransferase 7 | 1.75 |
| <i>Gm26735</i> | predicted gene, 26735 | 1.75 |
| <i>Gip</i> | gastric inhibitory polypeptide | 1.75 |
| <i>Magi2</i> | membrane associated guanylate kinase, WW and PDZ domain containing 2 | 1.75 |
| <i>Frrs11</i> | ferric-chelate reductase 1 like | 1.75 |
| <i>Dock3</i> | dedicator of cyto-kinesis 3 | 1.75 |
| <i>Foxp2</i> | forkhead box P2 | 1.75 |
| <i>Spc24</i> | SPC24, NDC80 kinetochore complex component, homolog (<i>S. cerevisiae</i>) | 1.75 |
| <i>Irf9</i> | interferon regulatory factor 9 | 1.75 |
| <i>17548193</i> | <i>No associated gene</i> | 1.74 |
| <i>17389048</i> | <i>No associated gene</i> | 1.74 |
| <i>Panx1</i> | pannexin 1 | 1.74 |
| <i>Calcr1</i> | calcitonin receptor-like | 1.74 |
| <i>Bmp2</i> | bone morphogenetic protein 2 | 1.74 |
| <i>Abi3bp</i> | ABI gene family, member 3 (NESH) binding protein | 1.74 |
| <i>Atp10d</i> | ATPase, class V, type 10D | 1.74 |
| <i>Tcirg1</i> | T cell, immune regulator 1, ATPase, H ⁺ transporting, lysosomal V0 protein A3 | 1.74 |
| <i>Ak7</i> | adenylate kinase 7 | 1.73 |
| <i>4930562F07Rik</i> | RIKEN cDNA 4930562F07 gene | 1.73 |
| <i>Gprin3</i> | GPRIN family member 3 | 1.73 |

| | | |
|----------------------|--|------|
| 17238826 | <i>No associated gene</i> | 1.73 |
| P2rx4 | purinergic receptor P2X, ligand-gated ion channel 4 | 1.73 |
| Emr1 | EGF-like module containing, mucin-like, hormone receptor-like sequence 1 | 1.73 |
| Thbs3 | thrombospondin 3 | 1.73 |
| Jmjd7-pla2g4b | jumonji domain containing 7 | 1.73 |
| Negr1 | neuronal growth regulator 1 | 1.73 |
| Fam43a | family with sequence similarity 43, member A | 1.73 |
| Kctd12 | potassium channel tetramerisation domain containing 12 | 1.72 |
| Mlkl | mixed lineage kinase domain-like | 1.72 |
| Serpinh1 | serine (or cysteine) peptidase inhibitor, clade H, member 1 | 1.72 |
| Fmo2 | flavin containing monooxygenase 2 | 1.72 |
| Cd151 | CD151 antigen | 1.72 |
| Rgs4 | regulator of G-protein signaling 4 | 1.72 |
| Sepp1 | selenoprotein P, plasma, 1 | 1.72 |
| Scgn | secretagogin, EF-hand calcium binding protein | 1.72 |
| Gucy1a2 | guanylate cyclase 1, soluble, alpha 2 | 1.72 |
| Tmem243 | transmembrane protein 243, mitochondrial | 1.72 |
| Igsf1 | immunoglobulin superfamily, member 1 | 1.72 |
| Ppap2c | phosphatidic acid phosphatase type 2C | 1.71 |
| Ankrd50 | ankyrin repeat domain 50 | 1.71 |
| Ddx58 | DEAD (Asp-Glu-Ala-Asp) box polypeptide 58 | 1.71 |
| Abcc9 | ATP-binding cassette, sub-family C (CFTR/MRP), member 9 | 1.71 |
| Lst1 | leukocyte specific transcript 1 | 1.71 |
| 17548153 | <i>No associated gene</i> | 1.71 |
| Cnn2 | calponin 2 | 1.71 |
| 17548317 | <i>No associated gene</i> | 1.71 |
| Rasgrf2 | RAS protein-specific guanine nucleotide-releasing factor 2 | 1.71 |
| Hist1h4a | histone cluster 1, H4a | 1.70 |
| Tmem229a | transmembrane protein 229A | 1.70 |
| Man2b1 | mannosidase 2, alpha B1 | 1.70 |
| D330045A20Rik | RIKEN cDNA D330045A20 gene | 1.70 |
| Ptgis | prostaglandin I2 (prostacyclin) synthase | 1.70 |
| Aldh1a3 | aldehyde dehydrogenase family 1, subfamily A3 | 1.70 |
| Irf8 | interferon regulatory factor 8 | 1.70 |
| Zfp521 | zinc finger protein 521 | 1.70 |
| Layn | layilin | 1.70 |
| 17261333 | <i>No associated gene</i> | 1.70 |
| Gc | group specific component | 1.69 |
| Lair1 | leukocyte-associated Ig-like receptor 1 | 1.69 |
| Pla2g2d | phospholipase A2, group IID | 1.69 |
| Tmem140 | transmembrane protein 140 | 1.69 |
| Gngt2 | guanine nucleotide binding protein (G protein), gamma transducing activity polypeptide 2 | 1.69 |
| Fzd1 | frizzled class receptor 1 | 1.69 |
| Sox18 | SRY (sex determining region Y)-box 18 | 1.69 |
| Thy1 | thymus cell antigen 1, theta | 1.69 |

| | | |
|----------------------|--|------|
| Fam26f | family with sequence similarity 26, member F | 1.69 |
| 4933412E12Rik | RIKEN cDNA 4933412E12 gene | 1.69 |
| Nid1 | nidogen 1 | 1.69 |
| Zdhhc14 | zinc finger, DHHC domain containing 14 | 1.69 |
| Coll1a1 | collagen, type I, alpha 1 | 1.68 |
| Grn | granulin | 1.68 |
| Scarb1 | scavenger receptor class B, member 1 | 1.68 |
| Sorbs3 | sorbin and SH3 domain containing 3 | 1.68 |
| Zfp366 | zinc finger protein 366 | 1.68 |
| Chmp4c | charged multivesicular body protein 4C | 1.68 |
| Dab2 | disabled 2, mitogen-responsive phosphoprotein | 1.68 |
| Dapk1 | death associated protein kinase 1 | 1.68 |
| Cd3e | CD3 antigen, epsilon polypeptide | 1.67 |
| Mfi2 | <i>No associated gene</i> | 1.67 |
| D630023F18Rik | RIKEN cDNA D630023F18 gene | 1.67 |
| Dopey2 | dopey family member 2 | 1.67 |
| Tmlhe | trimethyllysine hydroxylase, epsilon | 1.67 |
| Arl4c | ADP-ribosylation factor-like 4C | 1.67 |
| Pak1 | p21 protein (Cdc42/Rac)-activated kinase 1 | 1.67 |
| Psmb9 | proteasome (prosome, macropain) subunit, beta type 9 (large multifunctional peptidase 2) | 1.67 |
| LOC102635076 | serine/arginine repetitive matrix protein 2-like | 1.67 |
| Ncf2 | neutrophil cytosolic factor 2 | 1.67 |
| Cd200 | CD200 antigen | 1.67 |
| Amica1 | adhesion molecule, interacts with CXADR antigen 1 | 1.67 |
| Itp1 | inositol 1,4,5-trisphosphate receptor 1 | 1.67 |
| Gsap | gamma-secretase activating protein | 1.67 |
| Tns1 | tensin 1 | 1.67 |
| Rgma | repulsive guidance molecule family member A | 1.67 |
| Epha7 | Eph receptor A7 | 1.67 |
| Sox4 | SRY (sex determining region Y)-box 4 | 1.67 |
| Lynx1 | Ly6/neurotoxin 1 | 1.66 |
| Rest | RE1-silencing transcription factor | 1.66 |
| Mvb12b | multivesicular body subunit 12B | 1.66 |
| Cit | citron | 1.66 |
| Igfbp4 | insulin-like growth factor binding protein 4 | 1.66 |
| Rbms1 | RNA binding motif, single stranded interacting protein 1 | 1.66 |
| Nap1l5 | nucleosome assembly protein 1-like 5 | 1.66 |
| Gprc5b | G protein-coupled receptor, family C, group 5, member B | 1.66 |
| 4930570G19Rik | RIKEN cDNA 4930570G19 gene | 1.66 |
| Tcf7 | transcription factor 7, T cell specific | 1.66 |
| Plaur | plasminogen activator, urokinase receptor | 1.66 |
| 1810044D09Rik | RIKEN cDNA 1810044D09 gene | 1.66 |
| Cpxm1 | carboxypeptidase X 1 (M14 family) | 1.66 |
| Cd34 | CD34 antigen | 1.66 |
| Crp | C-reactive protein, pentraxin-related | 1.66 |

| | | |
|---------------------|---|------|
| LOC102638481 | <i>No associated gene</i> | 1.65 |
| Dnm1 | dynamain 1 | 1.65 |
| Rin2 | Ras and Rab interactor 2 | 1.65 |
| Lox11 | lysyl oxidase-like 1 | 1.65 |
| Pld1 | phospholipase D1 | 1.65 |
| Esam | endothelial cell-specific adhesion molecule | 1.65 |
| Rnf138rt1 | ring finger protein 138, retrogene 1 | 1.65 |
| 17539649 | <i>No associated gene</i> | 1.65 |
| Trim21 | tripartite motif-containing 21 | 1.65 |
| Uaca | uveal autoantigen with coiled-coil domains and ankyrin repeats | 1.65 |
| Preli2 | PRELI domain containing 2 | 1.65 |
| Rfx6 | regulatory factor X, 6 | 1.65 |
| Ppap2b | phosphatidic acid phosphatase type 2B | 1.65 |
| Tmem14a | transmembrane protein 14A | 1.65 |
| Bcl2l11 | BCL2-like 11 (apoptosis facilitator) | 1.64 |
| Lrrtm3 | leucine rich repeat transmembrane neuronal 3 | 1.64 |
| Ifi35 | interferon-induced protein 35 | 1.64 |
| 17225046 | <i>No associated gene</i> | 1.64 |
| Serpib9 | serine (or cysteine) peptidase inhibitor, clade B, member 9 | 1.64 |
| Ctla2a | cytotoxic T lymphocyte-associated protein 2 alpha | 1.64 |
| Snhg18 | small nucleolar RNA host gene 18 | 1.64 |
| Gm16984 | predicted gene, 16984 | 1.64 |
| Gprasp2 | G protein-coupled receptor associated sorting protein 2 | 1.64 |
| Rps6ka6 | ribosomal protein S6 kinase polypeptide 6 | 1.64 |
| Dcp2 | decapping mRNA 2 | 1.64 |
| Tmem98 | transmembrane protein 98 | 1.64 |
| Ninl | ninein-like | 1.64 |
| Inpp4b | inositol polyphosphate-4-phosphatase, type II | 1.63 |
| Arhgap29 | Rho GTPase activating protein 29 | 1.63 |
| Shisa4 | shisa family member 4 | 1.63 |
| Nfkbia | nuclear factor of kappa light polypeptide gene enhancer in B cells inhibitor, alpha | 1.63 |
| Oprl1 | opioid receptor-like 1 | 1.63 |
| Traf4 | TNF receptor associated factor 4 | 1.63 |
| Cxcl14 | chemokine (C-X-C motif) ligand 14 | 1.63 |
| Ctsk | cathepsin K | 1.63 |
| Tram2 | translocating chain-associating membrane protein 2 | 1.63 |
| Col4a1 | collagen, type IV, alpha 1 | 1.63 |
| Pgm2l1 | phosphoglucomutase 2-like 1 | 1.63 |
| Ifngr2 | interferon gamma receptor 2 | 1.63 |
| Hspb8 | heat shock protein 8 | 1.63 |
| Unc5a | unc-5 netrin receptor A | 1.63 |
| 17548808 | <i>No associated gene</i> | 1.62 |
| Ralgds | ral guanine nucleotide dissociation stimulator | 1.62 |
| Pdk2 | pyruvate dehydrogenase kinase, isoenzyme 2 | 1.62 |
| Ascl1 | achaete-scute family bHLH transcription factor 1 | 1.62 |

| | | |
|-----------------------------|--|------|
| <i>Stxbp5l</i> | syntaxin binding protein 5-like | 1.62 |
| <i>Cxcl16</i> | chemokine (C-X-C motif) ligand 16 | 1.62 |
| <i>Rspo4</i> | R-spondin 4 | 1.62 |
| <i>Tm4sf1</i> | transmembrane 4 superfamily member 1 | 1.62 |
| <i>Itga1</i> | integrin alpha 1 | 1.62 |
| <i>Sparc</i> | secreted acidic cysteine rich glycoprotein | 1.62 |
| <i>Fermt1</i> | fermitin family member 1 | 1.62 |
| <i>Spsb1</i> | splA/ryanodine receptor domain and SOCS box containing 1 | 1.62 |
| <i>Suds3</i> | suppressor of defective silencing 3 homolog (<i>S. cerevisiae</i>) | 1.62 |
| <i>Lgals3</i> | lectin, galactose binding, soluble 3 | 1.62 |
| <i>Leprot</i> | leptin receptor overlapping transcript | 1.62 |
| <i>Gm17071</i> | predicted gene 17071 | 1.62 |
| <i>Dusp26</i> | dual specificity phosphatase 26 (putative) | 1.62 |
| <i>Mapkapk3</i> | mitogen-activated protein kinase-activated protein kinase 3 | 1.62 |
| <i>Adora2a</i> | adenosine A2a receptor | 1.61 |
| <i>Herc3</i> | hect domain and RLD 3 | 1.61 |
| <i>Dtx3l</i> | deltex 3-like, E3 ubiquitin ligase | 1.61 |
| <i>Tnfaip2</i> | tumor necrosis factor, alpha-induced protein 2 | 1.61 |
| <i>Myo1g</i> | myosin IG | 1.61 |
| <i>17238852</i> | <i>No associated gene</i> | 1.61 |
| <i>Slc44a2</i> | solute carrier family 44, member 2 | 1.61 |
| <i>Rtn1</i> | reticulon 1 | 1.61 |
| <i>Rbms3</i> | RNA binding motif, single stranded interacting protein | 1.61 |
| <i>Gm15441</i> | predicted gene 15441 | 1.61 |
| <i>Eif2ak2</i> | eukaryotic translation initiation factor 2-alpha kinase 2 | 1.61 |
| <i>Gm13889</i> | predicted gene 13889 | 1.60 |
| <i>Gm2a</i> | GM2 ganglioside activator protein | 1.60 |
| <i>Cnih2</i> | cornichon family AMPA receptor auxiliary protein 2 | 1.60 |
| <i>B4galt5</i> | UDP-Gal:betaGlcNAc beta 1,4-galactosyltransferase, polypeptide 5 | 1.60 |
| <i>Plvap</i> | plasmalemma vesicle associated protein | 1.60 |
| <i>P2rx7</i> | purinergic receptor P2X, ligand-gated ion channel, 7 | 1.60 |
| <i>Adcy2</i> | adenylate cyclase 2 | 1.60 |
| <i>Gm11626</i> | predicted gene 11626 | 1.60 |
| <i>Mir382</i> | microRNA 382 | 1.60 |
| <i>Esrrg</i> | estrogen-related receptor gamma | 1.60 |
| <i>Gm10499</i> | predicted gene 10499 | 1.60 |
| <i>Psmb8</i> | proteasome (prosome, macropain) subunit, beta type 8 (large multifunctional peptidase 7) | 1.60 |
| <i>Ahr</i> | aryl-hydrocarbon receptor | 1.60 |
| <i>Tmem246</i> | transmembrane protein 246 | 1.60 |
| <i>Wwc2</i> | WW, C2 and coiled-coil domain containing 2 | 1.60 |
| <i>17548713</i> | <i>No associated gene</i> | 1.60 |
| <i>Il6ra</i> | interleukin 6 receptor, alpha | 1.59 |
| <i>Rnf122</i> | ring finger protein 122 | 1.59 |
| <i>Serpine1</i> | serine (or cysteine) peptidase inhibitor, clade E, member 1 | 1.59 |
| <i>4833427G06Rik</i> | RIKEN cDNA 4833427G06 gene | 1.59 |

| | | |
|---------------------------|---|------|
| Rnasel | ribonuclease L (2', 5'-oligoadenylate synthetase-dependent) | 1.59 |
| Zdhhc20 | zinc finger, DHHC domain containing 20 | 1.59 |
| Pik3ip1 | phosphoinositide-3-kinase interacting protein 1 | 1.59 |
| Nek5 | NIMA (never in mitosis gene a)-related expressed kinase 5 | 1.59 |
| St8sia4 | ST8 alpha-N-acetyl-neuraminide alpha-2,8-sialyltransferase 4 | 1.59 |
| Pla1a | phospholipase A1 member A | 1.59 |
| GENSCAN00000019044 | <i>No associated gene</i> | 1.59 |
| Cemip | cell migration inducing protein, hyaluronan binding | 1.59 |
| Oas3 | 2'-5' oligoadenylate synthetase 3 | 1.59 |
| Fnbp1 | formin binding protein 1 | 1.59 |
| Wisp1 | WNT1 inducible signaling pathway protein 1 | 1.59 |
| A730011C13Rik | RIKEN cDNA A730011C13 gene | 1.59 |
| Tnr | tenascin R | 1.59 |
| Emilin2 | elastin microfibril interfacier 2 | 1.59 |
| Dnm3 | dynamamin 3 | 1.59 |
| Pmp22 | peripheral myelin protein 22 | 1.58 |
| Sat1 | spermidine/spermine N1-acetyl transferase 1 | 1.58 |
| Hist1h4h | histone cluster 1, H4h | 1.58 |
| Kcnj10 | potassium inwardly-rectifying channel, subfamily J, member 10 | 1.58 |
| Serping1 | serine (or cysteine) peptidase inhibitor, clade G, member 1 | 1.58 |
| 1110017D15Rik | RIKEN cDNA 1110017D15 gene | 1.58 |
| Abhd4 | abhydrolase domain containing 4 | 1.58 |
| Mgp | matrix Gla protein | 1.58 |
| Ptprd | protein tyrosine phosphatase, receptor type, D | 1.58 |
| Cadps | Ca ²⁺ -dependent secretion activator | 1.58 |
| Mgst3 | microsomal glutathione S-transferase 3 | 1.58 |
| Baiap2 | brain-specific angiogenesis inhibitor 1-associated protein 2 | 1.58 |
| Tgfbr2 | transforming growth factor, beta receptor II | 1.58 |
| Limch1 | LIM and calponin homology domains 1 | 1.58 |
| Elovl7 | ELOVL family member 7, elongation of long chain fatty acids (yeast) | 1.58 |
| Heca | hdc homolog, cell cycle regulator | 1.58 |
| Dock11 | dedicator of cytokinesis 11 | 1.58 |
| Fam221a | family with sequence similarity 221, member A | 1.58 |
| Arhgef3 | Rho guanine nucleotide exchange factor (GEF) 3 | 1.58 |
| Cyp26b1 | cytochrome P450, family 26, subfamily b, polypeptide 1 | 1.57 |
| Lrch1 | leucine-rich repeats and calponin homology (CH) domain containing 1 | 1.57 |
| Tiparp | TCDD-inducible poly(ADP-ribose) polymerase | 1.57 |
| Tgfbr3 | transforming growth factor, beta receptor III | 1.57 |
| Hist1h1c | histone cluster 1, H1c | 1.57 |
| Kcnk16 | potassium channel, subfamily K, member 16 | 1.57 |
| Fat1 | FAT atypical cadherin 1 | 1.57 |
| 17373937 | <i>No associated gene</i> | 1.57 |
| 17499394 | <i>No associated gene</i> | 1.57 |
| Ppp1r18 | protein phosphatase 1, regulatory subunit 18 | 1.57 |
| Sim1 | single-minded homolog 1 (Drosophila) | 1.57 |

| | | |
|-----------------------------|--|------|
| <i>Tpm1</i> | tropomyosin 1, alpha | 1.57 |
| <i>Entpd1</i> | ectonucleoside triphosphate diphosphohydrolase 1 | 1.57 |
| <i>Snora5c</i> | small nucleolar RNA, H/ACA box 5C | 1.57 |
| <i>17238850</i> | <i>No associated gene</i> | 1.57 |
| <i>Igkv12-41</i> | immunoglobulin kappa chain variable 12-41 | 1.57 |
| <i>Siglec1</i> | sialic acid binding Ig-like lectin 1, sialoadhesin | 1.57 |
| <i>Gm9780</i> | predicted gene 9780 | 1.57 |
| <i>1700042O10Rik</i> | RIKEN cDNA 1700042O10 gene | 1.56 |
| <i>Igkv9-120</i> | immunoglobulin kappa chain variable 9-120 | 1.56 |
| <i>17249829</i> | <i>No associated gene</i> | 1.56 |
| <i>Sft2d1</i> | SFT2 domain containing 1 | 1.56 |
| <i>Col5a1</i> | collagen, type V, alpha 1 | 1.56 |
| <i>Arid5b</i> | AT rich interactive domain 5B (MRF1-like) | 1.56 |
| <i>Lcn2</i> | lipocalin 2 | 1.56 |
| <i>Apoc1</i> | apolipoprotein C-I | 1.56 |
| <i>Il17re</i> | interleukin 17 receptor E | 1.56 |
| <i>Adora2b</i> | adenosine A2b receptor | 1.56 |
| <i>Cdh2</i> | cadherin 2 | 1.56 |
| <i>Clic5</i> | chloride intracellular channel 5 | 1.56 |
| <i>Rab3b</i> | RAB3B, member RAS oncogene family | 1.56 |
| <i>St3gal4</i> | ST3 beta-galactoside alpha-2,3-sialyltransferase 4 | 1.55 |
| <i>Disp1</i> | dispatched RND transporter family member 1 | 1.55 |
| <i>Rras</i> | related RAS viral (r-ras) oncogene | 1.55 |
| <i>Frmd4b</i> | FERM domain containing 4B | 1.55 |
| <i>Per3</i> | period circadian clock 3 | 1.55 |
| <i>Inpp5d</i> | inositol polyphosphate-5-phosphatase D | 1.55 |
| <i>Cyrr1</i> | cysteine and tyrosine-rich protein 1 | 1.55 |
| <i>Ang</i> | angiogenin, ribonuclease, RNase A family, 5 | 1.55 |
| <i>Cst6</i> | cystatin E/M | 1.55 |
| <i>Capg</i> | capping protein (actin filament), gelsolin-like | 1.55 |
| <i>Sgk3</i> | serum/glucocorticoid regulated kinase 3 | 1.55 |
| <i>Ehd2</i> | EH-domain containing 2 | 1.55 |
| <i>Cdk1</i> | cyclin-dependent kinase 1 | 1.55 |
| <i>Slco2a1</i> | solute carrier organic anion transporter family, member 2a1 | 1.55 |
| <i>Foxm1</i> | forkhead box M1 | 1.55 |
| <i>Acer2</i> | alkaline ceramidase 2 | 1.55 |
| <i>St8sia6</i> | ST8 alpha-N-acetyl-neuraminide alpha-2,8-sialyltransferase 6 | 1.55 |
| <i>Tbc1d4</i> | TBC1 domain family, member 4 | 1.55 |
| <i>Stat6</i> | signal transducer and activator of transcription 6 | 1.55 |
| <i>Aplp1</i> | amyloid beta (A4) precursor-like protein 1 | 1.54 |
| <i>Pphln1</i> | periphilin 1 | 1.54 |
| <i>Plxnb2</i> | plexin B2 | 1.54 |
| <i>Nsg1</i> | neuron specific gene family member 1 | 1.54 |
| <i>Tfpi</i> | tissue factor pathway inhibitor | 1.54 |
| <i>Map3k15</i> | mitogen-activated protein kinase kinase kinase 15 | 1.54 |
| <i>Nespas</i> | neuroendocrine secretory protein antisense | 1.54 |

| | | |
|----------------------|--|------|
| <i>Mical2</i> | microtubule associated monooxygenase, calponin and LIM domain containing 2 | 1.54 |
| <i>Myt1</i> | myelin transcription factor 1 | 1.54 |
| <i>Zfp937</i> | zinc finger protein 937 | 1.54 |
| <i>A330050F15Rik</i> | RIKEN cDNA A330050F15 gene | 1.54 |
| <i>17549370</i> | <i>No associated gene</i> | 1.54 |
| <i>Gfod1</i> | glucose-fructose oxidoreductase domain containing 1 | 1.53 |
| <i>Ptchd1</i> | patched domain containing 1 | 1.53 |
| <i>F2r</i> | coagulation factor II (thrombin) receptor | 1.53 |
| <i>Trim47</i> | tripartite motif-containing 47 | 1.53 |
| <i>Rnf19b</i> | ring finger protein 19B | 1.53 |
| <i>Gng2</i> | guanine nucleotide binding protein (G protein), gamma 2 | 1.53 |
| <i>B4galt1</i> | UDP-Gal:betaGlcNAc beta 1,4- galactosyltransferase, polypeptide 1 | 1.53 |
| <i>Tspan15</i> | tetraspanin 15 | 1.53 |
| <i>Slc4a4</i> | solute carrier family 4 (anion exchanger), member 4 | 1.53 |
| <i>Pex5l</i> | peroxisomal biogenesis factor 5-like | 1.53 |
| <i>LOC102639005</i> | predicted gene 16096 | 1.53 |
| <i>Rnf145</i> | ring finger protein 145 | 1.53 |
| <i>Prdx4</i> | peroxiredoxin 4 | 1.53 |
| <i>Cyr61</i> | cysteine rich protein 61 | 1.53 |
| <i>1700017B05Rik</i> | RIKEN cDNA 1700017B05 gene | 1.53 |
| <i>Tcp11l2</i> | t-complex 11 (mouse) like 2 | 1.53 |
| <i>Klhl24</i> | kelch-like 24 | 1.53 |
| <i>Lrp1</i> | low density lipoprotein receptor-related protein 1 | 1.53 |
| <i>Mrap2</i> | melanocortin 2 receptor accessory protein 2 | 1.53 |
| <i>LOC68395</i> | histocompatibility 2, Q region locus 6-like | 1.53 |
| <i>Akap2</i> | A kinase (PRKA) anchor protein 2 | 1.52 |
| <i>Gcnt2</i> | glucosaminyl (N-acetyl) transferase 2, I-branching enzyme | 1.52 |
| <i>Sh3pxd2b</i> | SH3 and PX domains 2B | 1.52 |
| <i>Zdhhc1</i> | zinc finger, DHHC domain containing 1 | 1.52 |
| <i>Cep70</i> | centrosomal protein 70 | 1.52 |
| <i>Nin</i> | ninein | 1.52 |
| <i>Tgfb1</i> | transforming growth factor, beta 1 | 1.52 |
| <i>Me2</i> | malic enzyme 2, NAD(+)-dependent, mitochondrial | 1.52 |
| <i>Il13ra1</i> | interleukin 13 receptor, alpha 1 | 1.52 |
| <i>Cilp</i> | cartilage intermediate layer protein, nucleotide pyrophosphohydrolase | 1.52 |
| <i>Cds1</i> | CDP-diacylglycerol synthase 1 | 1.52 |
| <i>Gfpt2</i> | glutamine fructose-6-phosphate transaminase 2 | 1.52 |
| <i>Lamc1</i> | laminin, gamma 1 | 1.52 |
| <i>Pvrl2</i> | poliovirus receptor-related 2 | 1.52 |
| <i>Trpm3</i> | transient receptor potential cation channel, subfamily M, member 3 | 1.52 |
| <i>Gm5424</i> | predicted gene 5424 | 1.52 |
| <i>Kctd12b</i> | potassium channel tetramerisation domain containing 12b | 1.52 |
| <i>Plcb4</i> | phospholipase C, beta 4 | 1.52 |
| <i>0610043K17Rik</i> | RIKEN cDNA 0610043K17 gene | 1.51 |
| <i>Erap1</i> | endoplasmic reticulum aminopeptidase 1 | 1.51 |

| | | |
|----------------------|--|-------|
| Zbtb7c | zinc finger and BTB domain containing 7C | 1.51 |
| Fscn1 | fascin actin-bundling protein 1 | 1.51 |
| Ephx1 | epoxide hydrolase 1, microsomal | 1.51 |
| Nbl1 | neuroblastoma, suppression of tumorigenicity 1 | 1.51 |
| Hdx | highly divergent homeobox | 1.51 |
| Nr1h3 | nuclear receptor subfamily 1, group H, member 3 | 1.51 |
| Kdr | kinase insert domain protein receptor | 1.51 |
| LOC101056100 | centrin-4-like | 1.51 |
| Egr1 | early growth response 1 | 1.51 |
| Cdc42ep2 | CDC42 effector protein (Rho GTPase binding) 2 | 1.51 |
| Sipa1 | signal-induced proliferation associated gene 1 | 1.51 |
| Malt1 | MALT1 paracaspase | 1.51 |
| Rab12 | RAB12, member RAS oncogene family | 1.51 |
| Cort | cortistatin | 1.51 |
| Tubb5 | tubulin, beta 5 class I | 1.51 |
| Cyp4v3 | cytochrome P450, family 4, subfamily v, polypeptide 3 | 1.51 |
| Blvrb | biliverdin reductase B (flavin reductase (NADPH)) | 1.51 |
| Wipf1 | WAS/WASL interacting protein family, member 1 | 1.51 |
| Myo1d | myosin ID | 1.51 |
| Hs6st1 | heparan sulfate 6-O-sulfotransferase 1 | 1.51 |
| Anks1b | ankyrin repeat and sterile alpha motif domain containing 1B | 1.51 |
| Kitl | kit ligand | 1.51 |
| Cntn3 | contactin 3 | 1.51 |
| Triqk | triple QxxK/R motif containing | -1.51 |
| Bex4 | brain expressed X-linked 4 | -1.51 |
| Zfp131 | zinc finger protein 131 | -1.51 |
| Dcaf11 | DDB1 and CUL4 associated factor 11 | -1.51 |
| Exosc6 | exosome component 6 | -1.51 |
| Gnl2 | guanine nucleotide binding protein-like 2 (nucleolar) | -1.51 |
| Mafg | v-maf musculoaponeurotic fibrosarcoma oncogene family, protein G (avian) | -1.51 |
| Myl6b | myosin, light polypeptide 6B | -1.51 |
| Sra1 | steroid receptor RNA activator 1 | -1.51 |
| Fa2h | fatty acid 2-hydroxylase | -1.51 |
| Gcdh | glutaryl-Coenzyme A dehydrogenase | -1.51 |
| LOC102636661 | protein transport protein Sec61 subunit beta-like | -1.51 |
| Ppm1b | protein phosphatase 1B, magnesium dependent, beta isoform | -1.51 |
| Gm7551 | predicted gene 7551 | -1.51 |
| Dgkg | diacylglycerol kinase, gamma | -1.52 |
| 17548953 | <i>No associated gene</i> | -1.52 |
| Hdac4 | histone deacetylase 4 | -1.52 |
| Sept11 | septin 11 | -1.52 |
| Tenc1 | tensin like C1 domain-containing phosphatase | -1.52 |
| NONMMUT015156 | <i>No associated gene</i> | -1.52 |
| Crybg3 | beta-gamma crystallin domain containing 3 | -1.52 |
| Elovl6 | ELOVL family member 6, elongation of long chain fatty acids (yeast) | -1.52 |
| LOC102641857 | RIKEN cDNA D630024D03 gene | -1.52 |

| | | |
|-------------------|--|-------|
| Nat10 | N-acetyltransferase 10 | -1.52 |
| E2f4 | E2F transcription factor 4 | -1.52 |
| Pwp1 | PWP1 homolog, endonuclease | -1.52 |
| Taf1a | TATA-box binding protein associated factor, RNA polymerase I, A | -1.52 |
| Scly | selenocysteine lyase | -1.52 |
| Clpb | ClpB caseinolytic peptidase B | -1.52 |
| 17540486 | <i>No associated gene</i> | -1.52 |
| 17547879 | <i>No associated gene</i> | -1.52 |
| DIERtd448e | DNA segment, Chr 1, ERATO Doi 448, expressed | -1.52 |
| Ubap1l | ubiquitin-associated protein 1-like | -1.52 |
| Mir1938 | microRNA 1938 | -1.52 |
| Zfyve19 | zinc finger, FYVE domain containing 19 | -1.52 |
| Mrps31 | mitochondrial ribosomal protein S31 | -1.52 |
| Ttf1 | transcription termination factor, RNA polymerase I | -1.52 |
| Pak3 | p21 protein (Cdc42/Rac)-activated kinase 3 | -1.52 |
| Gm16536 | predicted gene 16536 | -1.52 |
| Gm25804 | predicted gene, 25804 | -1.53 |
| Cad | carbamoyl-phosphate synthetase 2, aspartate transcarbamylase, and dihydroorotase | -1.53 |
| Angpt2 | angiopoietin 2 | -1.53 |
| Rgs2 | regulator of G-protein signaling 2 | -1.53 |
| Mfsd3 | major facilitator superfamily domain containing 3 | -1.53 |
| Gm17364 | predicted gene, 17364 | -1.53 |
| Abcd2 | ATP-binding cassette, sub-family D (ALD), member 2 | -1.53 |
| Mpp6 | membrane protein, palmitoylated 6 (MAGUK p55 subfamily member 6) | -1.53 |
| 17512413 | <i>No associated gene</i> | -1.53 |
| Gm10406 | predicted gene 10406 | -1.53 |
| Tmod2 | tropomodulin 2 | -1.53 |
| BC026585 | cDNA sequence BC026585 | -1.53 |
| Syt5 | synaptotagmin V | -1.53 |
| Extl1 | exostoses (multiple)-like 1 | -1.53 |
| Mkln1os | muskelin 1, intracellular mediator containing kelch motifs, opposite strand | -1.53 |
| Nr4a2 | nuclear receptor subfamily 4, group A, member 2 | -1.53 |
| Rbm20 | RNA binding motif protein 20 | -1.53 |
| T2 | brachyury 2 | -1.53 |
| 17311649 | <i>No associated gene</i> | -1.53 |
| Atp2a2 | ATPase, Ca ⁺⁺ transporting, cardiac muscle, slow twitch 2 | -1.54 |
| Tnfrsf21 | tumor necrosis factor receptor superfamily, member 21 | -1.54 |
| Gp5 | glycoprotein 5 (platelet) | -1.54 |
| Trim37 | tripartite motif-containing 37 | -1.54 |
| Ppp1r14d | protein phosphatase 1, regulatory (inhibitor) subunit 14D | -1.54 |
| AK129341 | cDNA sequence AK129341 | -1.54 |
| Nme4 | NME/NM23 nucleoside diphosphate kinase 4 | -1.54 |
| Erich3 | glutamate rich 3 | -1.54 |
| Eif3c | eukaryotic translation initiation factor 3, subunit C | -1.54 |
| Sdk2 | sidekick cell adhesion molecule 2 | -1.54 |

| | | |
|----------------------|---|-------|
| Agap1 | ArfGAP with GTPase domain, ankyrin repeat and PH domain 1 | -1.54 |
| 17549548 | <i>No associated gene</i> | -1.54 |
| Zfp930 | zinc finger protein 930 | -1.55 |
| Arntl | aryl hydrocarbon receptor nuclear translocator-like | -1.55 |
| Fmn2 | formin 2 | -1.55 |
| Bag2 | BCL2-associated athanogene 2 | -1.55 |
| Mlh3 | mutL homolog 3 | -1.55 |
| Sepsecs | Sep (O-phosphoserine) tRNA:Sec (selenocysteine) tRNA synthase | -1.55 |
| mt-Tf | mitochondrially encoded tRNA phenylalanine | -1.55 |
| 17216244 | <i>No associated gene</i> | -1.55 |
| Edaradd | EDAR (ectodysplasin-A receptor)-associated death domain | -1.55 |
| P2ry6 | pyrimidinergic receptor P2Y, G-protein coupled, 6 | -1.55 |
| 17455673 | <i>No associated gene</i> | -1.55 |
| Tfb2m | transcription factor B2, mitochondrial | -1.55 |
| Gm12524 | predicted gene 12524 | -1.55 |
| Ypel2 | yippee-like 2 (Drosophila) | -1.55 |
| Nup160 | nucleoporin 160 | -1.55 |
| Scg3 | secretogranin III | -1.55 |
| Gm7665 | predicted pseudogene 7665 | -1.55 |
| Fkbp5 | FK506 binding protein 5 | -1.56 |
| Dhcr24 | 24-dehydrocholesterol reductase | -1.56 |
| 17548746 | <i>No associated gene</i> | -1.56 |
| Glp1r | glucagon-like peptide 1 receptor | -1.56 |
| Timm8a1 | translocase of inner mitochondrial membrane 8A1 | -1.56 |
| Dennd4c | DENN/MADD domain containing 4C | -1.56 |
| Eif2s2 | eukaryotic translation initiation factor 2, subunit 2 (beta) | -1.56 |
| Lrguk | leucine-rich repeats and guanylate kinase domain containing | -1.56 |
| Vstm2l | V-set and transmembrane domain containing 2-like | -1.56 |
| Bhlha15 | basic helix-loop-helix family, member a15 | -1.56 |
| Gm26695 | predicted gene, 26695 | -1.56 |
| Slc2a5 | solute carrier family 2 (facilitated glucose transporter), member 5 | -1.56 |
| Gm17035 | predicted gene 17035 | -1.56 |
| Ndrp1 | N-myc downstream regulated gene 1 | -1.56 |
| Wfs1 | wolframin ER transmembrane glycoprotein | -1.57 |
| Prim1 | DNA primase, p49 subunit | -1.57 |
| Srsf1 | serine/arginine-rich splicing factor 1 | -1.57 |
| Daam1 | dishevelled associated activator of morphogenesis 1 | -1.57 |
| Il6st | interleukin 6 signal transducer | -1.57 |
| Fmo4 | flavin containing monooxygenase 4 | -1.57 |
| Efcab1 | EF hand calcium binding domain 1 | -1.57 |
| Alg3 | asparagine-linked glycosylation 3 (alpha-1,3-mannosyltransferase) | -1.57 |
| Sec16b | SEC16 homolog B (S. cerevisiae) | -1.57 |
| Tnfrsf9 | tumor necrosis factor receptor superfamily, member 9 | -1.57 |
| 9430065F17Rik | RIKEN cDNA 9430065F17 gene | -1.57 |
| Pth2 | peptidyl-tRNA hydrolase 2 | -1.57 |
| Dnaja3 | DnaJ heat shock protein family (Hsp40) member A3 | -1.57 |

| | | |
|-----------------------------|---|-------|
| <i>Folr1</i> | folate receptor 1 (adult) | -1.57 |
| <i>Nacad</i> | NAC alpha domain containing | -1.57 |
| <i>Gm24930</i> | predicted gene, 24930 | -1.58 |
| <i>Trappc11</i> | trafficking protein particle complex 11 | -1.58 |
| <i>Gramd3</i> | GRAM domain containing 3 | -1.58 |
| <i>LOC102632394</i> | predicted gene, 26910 | -1.58 |
| <i>Fdps</i> | farnesyl diphosphate synthetase | -1.58 |
| <i>Ivd</i> | isovaleryl coenzyme A dehydrogenase | -1.58 |
| <i>Hs3st6</i> | heparan sulfate (glucosamine) 3-O-sulfotransferase 6 | -1.58 |
| <i>Lrrc6</i> | leucine rich repeat containing 6 (testis) | -1.58 |
| <i>Mdm1</i> | transformed mouse 3T3 cell double minute 1 | -1.58 |
| <i>Gm10129</i> | predicted gene 10129 | -1.58 |
| <i>Gap43</i> | growth associated protein 43 | -1.58 |
| <i>Fam208b</i> | family with sequence similarity 208, member B | -1.58 |
| <i>Gm16494</i> | predicted gene 16494 | -1.58 |
| <i>Diras2</i> | DIRAS family, GTP-binding RAS-like 2 | -1.58 |
| <i>Hip1</i> | huntingtin interacting protein 1 | -1.58 |
| <i>Gm26215</i> | predicted gene, 26215 | -1.58 |
| <i>Brpf1</i> | bromodomain and PHD finger containing, 1 | -1.59 |
| <i>Cend1</i> | cell cycle exit and neuronal differentiation 1 | -1.59 |
| <i>Atf6b</i> | activating transcription factor 6 beta | -1.59 |
| <i>Ptprt</i> | protein tyrosine phosphatase, receptor type, T | -1.59 |
| <i>5430416N02Rik</i> | RIKEN cDNA 5430416N02 gene | -1.59 |
| <i>Idh3a</i> | isocitrate dehydrogenase 3 (NAD+) alpha | -1.59 |
| <i>Prdm15</i> | PR domain containing 15 | -1.59 |
| <i>Pcdhb21</i> | protocadherin beta 21 | -1.59 |
| <i>Arpc5l</i> | actin related protein 2/3 complex, subunit 5-like | -1.59 |
| <i>Gfra4</i> | glial cell line derived neurotrophic factor family receptor alpha 4 | -1.59 |
| <i>Sdk1</i> | sidekick cell adhesion molecule 1 | -1.59 |
| <i>Tsfn</i> | Ts translation elongation factor, mitochondrial | -1.59 |
| <i>Ankrd10</i> | ankyrin repeat domain 10 | -1.59 |
| <i>Gm8281</i> | predicted gene, 8281 | -1.59 |
| <i>Rab39b</i> | RAB39B, member RAS oncogene family | -1.59 |
| <i>Rnf185</i> | ring finger protein 185 | -1.59 |
| <i>0610009E02Rik</i> | RIKEN cDNA 0610009E02 gene | -1.59 |
| <i>Zfp422</i> | zinc finger protein 422 | -1.59 |
| <i>1700013F07Rik</i> | RIKEN cDNA 1700013F07 gene | -1.60 |
| <i>Ica1l</i> | islet cell autoantigen 1-like | -1.60 |
| <i>2810025M15Rik</i> | RIKEN cDNA 2810025M15 gene | -1.60 |
| <i>Hmox1</i> | heme oxygenase 1 | -1.60 |
| <i>17264469</i> | <i>No associated gene</i> | -1.60 |
| <i>Nars</i> | asparaginyl-tRNA synthetase | -1.60 |
| <i>LOC102635342</i> | predicted gene 15415 | -1.60 |
| <i>Gm3594</i> | predicted gene 3594 | -1.60 |
| <i>Cog6</i> | component of oligomeric golgi complex 6 | -1.60 |
| <i>Gm20071</i> | predicted gene, 20071 | -1.60 |

| | | |
|----------------------|--|-------|
| Lactb2 | lactamase, beta 2 | -1.60 |
| Sema3c | sema domain, immunoglobulin domain (Ig), short basic domain, secreted, (semaphorin) 3C | -1.60 |
| Ltv1 | LTV1 ribosome biogenesis factor | -1.60 |
| Vdac3 | voltage-dependent anion channel 3 | -1.60 |
| Fabp3-ps1 | fatty acid binding protein 3, muscle and heart, pseudogene 1 | -1.60 |
| Ccdc173 | coiled-coil domain containing 173 | -1.60 |
| Rnf157 | ring finger protein 157 | -1.61 |
| Arl14ep | ADP-ribosylation factor-like 14 effector protein | -1.61 |
| St8sia1 | ST8 alpha-N-acetyl-neuraminide alpha-2,8-sialyltransferase 1 | -1.61 |
| Jade1 | jade family PHD finger 1 | -1.61 |
| Sdf2ll | stromal cell-derived factor 2-like 1 | -1.61 |
| 1700096K18Rik | RIKEN cDNA 1700096K18 gene | -1.61 |
| Madd | MAP-kinase activating death domain | -1.62 |
| LOC101056195 | <i>No associated gene</i> | -1.62 |
| LOC102641835 | | -1.62 |
| Tmem8 | transmembrane protein 8 (five membrane-spanning domains) | -1.62 |
| Gm14295 | predicted gene 14295 | -1.62 |
| Morn4 | MORN repeat containing 4 | -1.62 |
| Matn2 | matrilin 2 | -1.62 |
| Rab11b | RAB11B, member RAS oncogene family | -1.62 |
| Abca5 | ATP-binding cassette, sub-family A (ABC1), member 5 | -1.62 |
| 17391329 | <i>No associated gene</i> | -1.62 |
| Ascc2 | activating signal cointegrator 1 complex subunit 2 | -1.63 |
| Sv2a | synaptic vesicle glycoprotein 2 a | -1.63 |
| Slc2a2 | solute carrier family 2 (facilitated glucose transporter), member 2 | -1.63 |
| Sec22c | SEC22 homolog C, vesicle trafficking protein | -1.63 |
| Fah | fumarylacetoacetate hydrolase | -1.63 |
| Gins3 | GINS complex subunit 3 (Psf3 homolog) | -1.63 |
| mt-Tm | mitochondrially encoded tRNA methionine | -1.63 |
| Mphosph9 | M-phase phosphoprotein 9 | -1.63 |
| Adora3 | adenosine A3 receptor | -1.64 |
| 17550016 | <i>No associated gene</i> | -1.64 |
| Fzd7 | frizzled class receptor 7 | -1.64 |
| Abhd17c | abhydrolase domain containing 17C | -1.64 |
| Mpp3 | membrane protein, palmitoylated 3 (MAGUK p55 subfamily member 3) | -1.64 |
| Arhgef2 | rho/rac guanine nucleotide exchange factor (GEF) 2 | -1.64 |
| Oxct1 | 3-oxoacid CoA transferase 1 | -1.64 |
| Flnb | filamin, beta | -1.64 |
| 17548508 | <i>No associated gene</i> | -1.64 |
| Grb10 | growth factor receptor bound protein 10 | -1.65 |
| Pitrm1 | pitrilysin metallopeptidase 1 | -1.65 |
| 2210408F21Rik | RIKEN cDNA 2210408F21 gene | -1.65 |
| Gpm6a | glycoprotein m6a | -1.65 |
| Adra2a | adrenergic receptor, alpha 2a | -1.65 |
| Tcea1 | transcription elongation factor A (SII) 1 | -1.65 |

| | | |
|----------------------|--|-------|
| <i>Tcte3</i> | t-complex-associated testis expressed 3 | -1.65 |
| <i>Bpnt1</i> | bisphosphate 3'-nucleotidase 1 | -1.65 |
| <i>Asns</i> | asparagine synthetase | -1.65 |
| <i>2610042L04Rik</i> | RIKEN cDNA 2610042L04 gene | -1.65 |
| <i>Cars</i> | cysteinyl-tRNA synthetase | -1.66 |
| <i>Rundc3b</i> | RUN domain containing 3B | -1.66 |
| <i>Dnajc21</i> | DnaJ heat shock protein family (Hsp40) member C21 | -1.66 |
| <i>Pi4k2a</i> | phosphatidylinositol 4-kinase type 2 alpha | -1.66 |
| <i>Rassf4</i> | Ras association (RalGDS/AF-6) domain family member 4 | -1.66 |
| <i>Ubr4</i> | ubiquitin protein ligase E3 component n-recogin 4 | -1.66 |
| <i>Ttc8</i> | tetratricopeptide repeat domain 8 | -1.66 |
| <i>Ghsr</i> | growth hormone secretagogue receptor | -1.66 |
| <i>Ift172</i> | intraflagellar transport 172 | -1.66 |
| <i>LOC102637737</i> | predicted gene 10010 | -1.66 |
| <i>Ins1</i> | insulin I | -1.67 |
| <i>Lrrc16b</i> | leucine rich repeat containing 16B | -1.67 |
| <i>17489508</i> | <i>No associated gene</i> | -1.67 |
| <i>Tmco6</i> | transmembrane and coiled-coil domains 6 | -1.67 |
| <i>Tenm4</i> | teneurin transmembrane protein 4 | -1.67 |
| <i>Slc7a1</i> | solute carrier family 7 (cationic amino acid transporter, y+ system), member 1 | -1.67 |
| <i>Suox</i> | sulfite oxidase | -1.67 |
| <i>Gmpr</i> | guanosine monophosphate reductase | -1.67 |
| <i>Tmem150c</i> | transmembrane protein 150C | -1.67 |
| <i>Slc6a17</i> | solute carrier family 6 (neurotransmitter transporter), member 17 | -1.67 |
| <i>Rbp3</i> | retinol binding protein 3, interstitial | -1.68 |
| <i>LOC102639184</i> | <i>No associated gene</i> | -1.68 |
| <i>Lrrc10b</i> | leucine rich repeat containing 10B | -1.68 |
| <i>Nid2</i> | nidogen 2 | -1.68 |
| <i>Smpd2</i> | sphingomyelin phosphodiesterase 2, neutral | -1.68 |
| <i>A830010M20Rik</i> | RIKEN cDNA A830010M20 gene | -1.68 |
| <i>Tcf24</i> | transcription factor 24 | -1.69 |
| <i>Trav7-3</i> | T cell receptor alpha variable 7-3 | -1.69 |
| <i>Hax1</i> | HCLS1 associated X-1 | -1.69 |
| <i>Dus4l</i> | dihydrouridine synthase 4-like (<i>S. cerevisiae</i>) | -1.69 |
| <i>Ttc32</i> | tetratricopeptide repeat domain 32 | -1.69 |
| <i>Gm22120</i> | predicted gene, 22120 | -1.69 |
| <i>Avil</i> | advillin | -1.69 |
| <i>Gm15972</i> | predicted gene 15972 | -1.69 |
| <i>Pik3c2g</i> | phosphatidylinositol 3-kinase, C2 domain containing, gamma polypeptide | -1.69 |
| <i>4921536K21Rik</i> | RIKEN cDNA 4921536K21 gene | -1.69 |
| <i>Syt4</i> | synaptotagmin IV | -1.69 |
| <i>Map10</i> | microtubule-associated protein 10 | -1.69 |
| <i>Cryba2</i> | crystallin, beta A2 | -1.69 |
| <i>Tmem206</i> | transmembrane protein 206 | -1.70 |
| <i>Lss</i> | lanosterol synthase | -1.70 |

| | | |
|----------------------|---|-------|
| M5C1000I18Rik | RIKEN cDNA M5C1000I18 gene | -1.70 |
| Cth | cystathionase (cystathionine gamma-lyase) | -1.70 |
| Lgals6 | lectin, galactose binding, soluble 6 | -1.70 |
| Mars | methionine-tRNA synthetase | -1.70 |
| Deb1 | <i>No associated gene</i> | -1.70 |
| Ttc28 | tetratricopeptide repeat domain 28 | -1.70 |
| Tra2a | transformer 2 alpha homolog (Drosophila) | -1.70 |
| Rny1 | RNA, Y1 small cytoplasmic, Ro-associated | -1.70 |
| Vbp1 | von Hippel-Lindau binding protein 1 | -1.71 |
| Cpeb1 | cytoplasmic polyadenylation element binding protein 1 | -1.71 |
| Fam129a | family with sequence similarity 129, member A | -1.71 |
| Ccdc47 | coiled-coil domain containing 47 | -1.71 |
| Lrp5 | low density lipoprotein receptor-related protein 5 | -1.71 |
| 2310040G24Rik | RIKEN cDNA 2310040G24 gene | -1.71 |
| Tsacc | TSSK6 activating co-chaperone | -1.71 |
| Sgcz | sarcoglycan zeta | -1.71 |
| Star | steroidogenic acute regulatory protein | -1.71 |
| Ift81 | intraflagellar transport 81 | -1.72 |
| Gm14817 | predicted gene 14817 | -1.72 |
| LOC102641079 | Ras association (RalGDS/AF-6) domain family (N-terminal) member 8 | -1.72 |
| 6430548M08Rik | RIKEN cDNA 6430548M08 gene | -1.72 |
| Prkcb | protein kinase C, beta | -1.72 |
| Kif5b | kinesin family member 5B | -1.72 |
| Tbc1d19 | TBC1 domain family, member 19 | -1.72 |
| Nrf1 | nuclear respiratory factor 1 | -1.73 |
| Ing2 | inhibitor of growth family, member 2 | -1.73 |
| Rps4l | ribosomal protein S4-like | -1.73 |
| Tmtc1 | transmembrane and tetratricopeptide repeat containing 1 | -1.73 |
| Helq | helicase, POLQ-like | -1.73 |
| 17421797 | <i>No associated gene</i> | -1.73 |
| LOC102635457 | predicted gene 15418 | -1.74 |
| Naaa | N-acylethanolamine acid amidase | -1.74 |
| Ndst4 | N-deacetylase/N-sulfotransferase (heparin glucosaminyl) 4 | -1.74 |
| Hspb6 | heat shock protein, alpha-crystallin-related, B6 | -1.74 |
| C2cd4a | C2 calcium-dependent domain containing 4A | -1.74 |
| BC048403 | cDNA sequence BC048403 | -1.74 |
| L1cam | L1 cell adhesion molecule | -1.74 |
| Yars | tyrosyl-tRNA synthetase | -1.75 |
| Fdft1 | farnesyl diphosphate farnesyl transferase 1 | -1.75 |
| LOC102638408 | predicted gene 16174 | -1.75 |
| Ap3b2 | adaptor-related protein complex 3, beta 2 subunit | -1.75 |
| Kbtbd7 | kelch repeat and BTB (POZ) domain containing 7 | -1.75 |
| Got1 | glutamic-oxaloacetic transaminase 1, soluble | -1.75 |
| Zfp420 | zinc finger protein 420 | -1.75 |
| Gm6356 | predicted gene 6356 | -1.75 |
| Rhbdd1 | rhomboid domain containing 1 | -1.75 |

| | | |
|----------------------|--|-------|
| Gm26508 | predicted gene, 26508 | -1.75 |
| Gm5327 | predicted pseudogene 5327 | -1.76 |
| Atf5 | activating transcription factor 5 | -1.76 |
| Cyp51 | cytochrome P450, family 51 | -1.76 |
| 9130023H24Rik | RIKEN cDNA 9130023H24 gene | -1.76 |
| Amd2 | S-adenosylmethionine decarboxylase 2 | -1.76 |
| Eml5 | echinoderm microtubule associated protein like 5 | -1.76 |
| X61497 | <i>No associated gene</i> | -1.77 |
| Taar1 | trace amine-associated receptor 1 | -1.77 |
| 17408273 | <i>No associated gene</i> | -1.77 |
| 17299196 | <i>No associated gene</i> | -1.77 |
| Endou | endonuclease, polyU-specific | -1.77 |
| Mtpb | Mdm2, transformed 3T3 cell double minute p53 binding protein | -1.77 |
| 17355228 | <i>No associated gene</i> | -1.77 |
| 4932702P03Rik | RIKEN cDNA 4932702P03 gene | -1.77 |
| 4930550C14Rik | RIKEN cDNA 4930550C14 gene | -1.77 |
| A830039N20Rik | RIKEN cDNA A830039N20 gene | -1.77 |
| Rtkn2 | rhotekin 2 | -1.78 |
| Mthfd1l | methylenetetrahydrofolate dehydrogenase (NADP+ dependent) 1-like | -1.78 |
| AI182371 | expressed sequence AI182371 | -1.78 |
| Gm10340 | predicted gene 10340 | -1.78 |
| Hspa9 | heat shock protein 9 | -1.78 |
| Pecr | peroxisomal trans-2-enoyl-CoA reductase | -1.78 |
| Eaf1 | ELL associated factor 1 | -1.78 |
| Pappa2 | pappalysin 2 | -1.78 |
| Fmn1 | formin 1 | -1.79 |
| Tmem212 | transmembrane protein 212 | -1.79 |
| Fbln5 | fibulin 5 | -1.79 |
| Atp4a | ATPase, H+/K+ exchanging, gastric, alpha polypeptide | -1.79 |
| Olfr617 | olfactory receptor 617 | -1.79 |
| Nedd1 | neural precursor cell expressed, developmentally down-regulated gene 1 | -1.80 |
| Tmem97 | transmembrane protein 97 | -1.80 |
| Grip1 | glutamate receptor interacting protein 1 | -1.80 |
| 17549566 | <i>No associated gene</i> | -1.80 |
| Tspyl4 | TSPY-like 4 | -1.80 |
| Snai2 | snail family zinc finger 2 | -1.80 |
| Snapc5 | small nuclear RNA activating complex, polypeptide 5 | -1.80 |
| Erlin1 | ER lipid raft associated 1 | -1.80 |
| Pitpnm3 | PITPNM family member 3 | -1.80 |
| Iars | isoleucine-tRNA synthetase | -1.81 |
| Stk32b | serine/threonine kinase 32B | -1.81 |
| Stk32a | serine/threonine kinase 32A | -1.81 |
| 17286496 | <i>No associated gene</i> | -1.81 |
| Rps11 | ribosomal protein S11 | -1.82 |
| Mettl5os | methyltransferase like 5, opposite strand | -1.82 |
| Zyg11b | zyg-11 family member B, cell cycle regulator | -1.82 |

| | | |
|----------------------|---|-------|
| <i>Slc7a5</i> | solute carrier family 7 (cationic amino acid transporter, y+ system), member 5 | -1.82 |
| <i>NONMMUT012630</i> | <i>No associated gene</i> | -1.83 |
| <i>Gars</i> | glycyl-tRNA synthetase | -1.83 |
| <i>1700113A16Rik</i> | RIKEN cDNA 1700113A16 gene | -1.83 |
| <i>Reps2</i> | RALBP1 associated Eps domain containing protein 2 | -1.83 |
| <i>Shmt2</i> | serine hydroxymethyltransferase 2 (mitochondrial) | -1.84 |
| <i>Pofut2</i> | protein O-fucosyltransferase 2 | -1.84 |
| <i>Gm4791</i> | predicted gene 4791 | -1.85 |
| <i>Ramp2</i> | receptor (calcitonin) activity modifying protein 2 | -1.85 |
| <i>Napb</i> | N-ethylmaleimide sensitive fusion protein attachment protein beta | -1.85 |
| <i>Gdf15</i> | growth differentiation factor 15 | -1.85 |
| <i>Idi1</i> | isopentenyl-diphosphate delta isomerase | -1.86 |
| <i>Atp7a</i> | ATPase, Cu ⁺⁺ transporting, alpha polypeptide | -1.86 |
| <i>Ero1l</i> | ERO1-like (<i>S. cerevisiae</i>) | -1.86 |
| <i>mt-Tr</i> | mitochondrially encoded tRNA arginine | -1.86 |
| <i>Cenpq</i> | centromere protein Q | -1.86 |
| <i>Mthfd2</i> | methylenetetrahydrofolate dehydrogenase (NAD ⁺ dependent), methenyltetrahydrofolate cyclohydrolase | -1.86 |
| <i>Lars</i> | leucyl-tRNA synthetase | -1.86 |
| <i>Gm6999</i> | predicted gene 6999 | -1.86 |
| <i>Trpm5</i> | transient receptor potential cation channel, subfamily M, member 5 | -1.87 |
| <i>Gcat</i> | glycine C-acetyltransferase (2-amino-3-ketobutyrate-coenzyme A ligase) | -1.87 |
| <i>Odc1</i> | ornithine decarboxylase, structural 1 | -1.87 |
| <i>Cldn6</i> | claudin 6 | -1.87 |
| <i>Lmo1</i> | LIM domain only 1 | -1.87 |
| <i>17547596</i> | <i>No associated gene</i> | -1.88 |
| <i>Zc3h3</i> | zinc finger CCCH type containing 3 | -1.88 |
| <i>Mettl1</i> | methyltransferase like 1 | -1.88 |
| <i>Ero1lb</i> | ERO1-like beta (<i>S. cerevisiae</i>) | -1.88 |
| <i>Clstn2</i> | calsyntenin 2 | -1.88 |
| <i>Vdr</i> | vitamin D receptor | -1.89 |
| <i>Entpd3</i> | ectonucleoside triphosphate diphosphohydrolase 3 | -1.89 |
| <i>Sfrp5</i> | secreted frizzled-related sequence protein 5 | -1.89 |
| <i>Rapgef4</i> | Rap guanine nucleotide exchange factor (GEF) 4 | -1.90 |
| <i>Vipr1</i> | vasoactive intestinal peptide receptor 1 | -1.90 |
| <i>Pck2</i> | phosphoenolpyruvate carboxykinase 2 (mitochondrial) | -1.90 |
| <i>Nfil3</i> | nuclear factor, interleukin 3, regulated | -1.90 |
| <i>Camk1g</i> | calcium/calmodulin-dependent protein kinase I gamma | -1.91 |
| <i>Gulo</i> | gulonolactone (L-) oxidase | -1.91 |
| <i>Ghitm</i> | growth hormone inducible transmembrane protein | -1.92 |
| <i>LOC102637131</i> | predicted gene 12976 | -1.92 |
| <i>Dph6</i> | diphthamine biosynthesis 6 | -1.93 |
| <i>Pstpip2</i> | proline-serine-threonine phosphatase-interacting protein 2 | -1.93 |
| <i>Taf15</i> | TATA-box binding protein associated factor 15 | -1.93 |
| <i>Abcb4</i> | ATP-binding cassette, sub-family B (MDR/TAP), member 4 | -1.93 |
| <i>Xpot</i> | exportin, tRNA (nuclear export receptor for tRNAs) | -1.94 |

| | | |
|----------------------|--|-------|
| Fbp1 | fructose bisphosphatase 1 | -1.94 |
| Lrrfip2 | leucine rich repeat (in FLII) interacting protein 2 | -1.94 |
| Gm25998 | predicted gene, 25998 | -1.95 |
| Cebpg | CCAAT/enhancer binding protein (C/EBP), gamma | -1.95 |
| 2310081O03Rik | RIKEN cDNA 2310081O03 gene | -1.96 |
| F2rl1 | coagulation factor II (thrombin) receptor-like 1 | -1.96 |
| Mest | mesoderm specific transcript | -1.96 |
| Tbc1d31 | TBC1 domain family, member 31 | -1.97 |
| Fam135a | family with sequence similarity 135, member A | -1.98 |
| Serpina3n | serine (or cysteine) peptidase inhibitor, clade A, member 3N | -1.98 |
| 17547897 | <i>No associated gene</i> | -1.98 |
| 1500002C15Rik | RIKEN cDNA 1500002C15 gene | -1.98 |
| Mlph | melanophilin | -1.99 |
| Tssc4 | tumor-suppressing subchromosomal transferable fragment 4 | -1.99 |
| Slc25a35 | solute carrier family 25, member 35 | -1.99 |
| Dlgap1 | discs, large (Drosophila) homolog-associated protein 1 | -1.99 |
| Adora1 | adenosine A1 receptor | -2.00 |
| 0610040F04Rik | RIKEN cDNA 0610040F04 gene | -2.00 |
| Itpkb | inositol 1,4,5-trisphosphate 3-kinase B | -2.00 |
| Gm7241 | predicted pseudogene 7241 | -2.00 |
| Dusp10 | dual specificity phosphatase 10 | -2.00 |
| Mafa | v-maf musculoaponeurotic fibrosarcoma oncogene family, protein A (avian) | -2.00 |
| Gm15559 | predicted gene 15559 | -2.01 |
| Gm6484 | predicted gene 6484 | -2.03 |
| Muc4 | mucin 4 | -2.03 |
| Galns | galactosamine (N-acetyl)-6-sulfate sulfatase | -2.03 |
| Snora62 | small nucleolar RNA, H/ACA box 62 | -2.04 |
| 17548422 | <i>No associated gene</i> | -2.04 |
| Gm2115 | predicted gene 2115 | -2.04 |
| Esrp1 | epithelial splicing regulatory protein 1 | -2.05 |
| Wls | wntless homolog (Drosophila) | -2.05 |
| Tfrc | transferrin receptor | -2.06 |
| Rny3 | RNA, Y3 small cytoplasmic (associated with Ro protein) | -2.06 |
| Lrrtm2 | leucine rich repeat transmembrane neuronal 2 | -2.06 |
| Tmem65 | transmembrane protein 65 | -2.06 |
| Reep6 | receptor accessory protein 6 | -2.07 |
| Cbx4 | chromobox 4 | -2.07 |
| 17549460 | <i>No associated gene</i> | -2.07 |
| Dusp4 | dual specificity phosphatase 4 | -2.07 |
| Car15 | carbonic anhydrase 15 | -2.07 |
| Scpep1 | serine carboxypeptidase 1 | -2.07 |
| Gm15810 | predicted gene 15810 | -2.07 |
| Gcgr | glucagon receptor | -2.08 |
| LOC102632986 | predicted gene 16035 | -2.08 |
| Lgals12 | lectin, galactose binding, soluble 12 | -2.08 |
| Wipi1 | WD repeat domain, phosphoinositide interacting 1 | -2.09 |

| | | |
|----------------------|--|-------|
| Ccdc6 | coiled-coil domain containing 6 | -2.10 |
| Cabp1 | calcium binding protein 1 | -2.10 |
| Mum11l | melanoma associated antigen (mutated) 1-like 1 | -2.11 |
| 17549252 | <i>No associated gene</i> | -2.11 |
| Msmo1 | methylsterol monooxygenase 1 | -2.11 |
| Sqle | squalene epoxidase | -2.11 |
| Cyb5b | cytochrome b5 type B | -2.11 |
| LOC106740 | PHD finger protein 10 | -2.11 |
| Fgg | fibrinogen gamma chain | -2.11 |
| Cdh7 | cadherin 7, type 2 | -2.11 |
| Th | tyrosine hydroxylase | -2.12 |
| Fmo1 | flavin containing monooxygenase 1 | -2.12 |
| Armc10 | armadillo repeat containing 10 | -2.12 |
| Gcnt1 | glucosaminyl (N-acetyl) transferase 1, core 2 | -2.13 |
| Pgm3 | phosphoglucomutase 3 | -2.13 |
| 17549848 | <i>No associated gene</i> | -2.13 |
| Igsf11 | immunoglobulin superfamily, member 11 | -2.14 |
| Dach2 | dachshund 2 (Drosophila) | -2.14 |
| Aldh5a1 | aldehyde dehydrogenase family 5, subfamily A1 | -2.15 |
| Tars | threonyl-tRNA synthetase | -2.16 |
| Npas2 | neuronal PAS domain protein 2 | -2.16 |
| Sult1c2 | sulfotransferase family, cytosolic, 1C, member 2 | -2.17 |
| 17549462 | <i>No associated gene</i> | -2.17 |
| Uck2 | uridine-cytidine kinase 2 | -2.18 |
| Wars | tryptophanyl-tRNA synthetase | -2.18 |
| Gale | galactose-4-epimerase, UDP | -2.19 |
| Dsp | desmoplakin | -2.19 |
| Glce | glucuronyl C5-epimerase | -2.20 |
| Aldh18a1 | aldehyde dehydrogenase 18 family, member A1 | -2.20 |
| Rwdd4a | RWD domain containing 4A | -2.21 |
| Angptl6 | angiopoietin-like 6 | -2.22 |
| Stom | stomatin | -2.23 |
| Scd2 | stearoyl-Coenzyme A desaturase 2 | -2.23 |
| Coro2b | coronin, actin binding protein, 2B | -2.24 |
| Spock1 | sparc/osteonectin, cwcv and kazal-like domains proteoglycan 1 | -2.24 |
| 2210019I11Rik | RIKEN cDNA 2210019I11 gene | -2.25 |
| 17548723 | <i>No associated gene</i> | -2.25 |
| Gm3325 | predicted gene 3325 | -2.25 |
| Eprs | glutamyl-prolyl-tRNA synthetase | -2.26 |
| Gpr158 | G protein-coupled receptor 158 | -2.28 |
| Ciart | circadian associated repressor of transcription | -2.28 |
| Fh1 | fumarate hydratase 1 | -2.28 |
| Kcnh1 | potassium voltage-gated channel, subfamily H (eag-related), member 1 | -2.30 |
| Hist2h3c2 | histone cluster 2, H3c2 | -2.30 |
| 1700084E18Rik | RIKEN cDNA 1700084E18 gene | -2.31 |
| Akr1c13 | aldo-keto reductase family 1, member C13 | -2.32 |

| | | |
|----------------------|--|-------|
| Vldlr | very low density lipoprotein receptor | -2.32 |
| Gm4419 | predicted gene 4419 | -2.32 |
| Skap1 | src family associated phosphoprotein 1 | -2.33 |
| 17547971 | <i>No associated gene</i> | -2.33 |
| Eif4ebp1 | eukaryotic translation initiation factor 4E binding protein 1 | -2.34 |
| 17529381 | <i>No associated gene</i> | -2.37 |
| Mns1 | meiosis-specific nuclear structural protein 1 | -2.37 |
| Ky | kyphoscoliosis peptidase | -2.38 |
| Gpt2 | glutamic pyruvate transaminase (alanine aminotransferase) 2 | -2.38 |
| Fam107a | family with sequence similarity 107, member A | -2.39 |
| Grin1os | glutamate receptor, ionotropic, NMDA1 (zeta 1), opposite strand | -2.39 |
| Papss2 | 3'-phosphoadenosine 5'-phosphosulfate synthase 2 | -2.39 |
| Edn3 | endothelin 3 | -2.41 |
| Chac1 | ChaC, cation transport regulator 1 | -2.41 |
| LOC102633910 | predicted gene 16315 | -2.42 |
| Avp1l | arginine vasopressin-induced 1 | -2.42 |
| 17549652 | <i>No associated gene</i> | -2.44 |
| Pde5a | phosphodiesterase 5A, cGMP-specific | -2.45 |
| Cdh4 | cadherin 4 | -2.46 |
| Dyrk3 | dual-specificity tyrosine-(Y)-phosphorylation regulated kinase 3 | -2.46 |
| Ntrk2 | neurotrophic tyrosine kinase, receptor, type 2 | -2.46 |
| Pfkfb2 | 6-phosphofructo-2-kinase/fructose-2,6-biphosphatase 2 | -2.48 |
| Cntfr | ciliary neurotrophic factor receptor | -2.51 |
| Gm15407 | predicted gene 15407 | -2.51 |
| Slc1a4 | solute carrier family 1 (glutamate/neutral amino acid transporter), member 4 | -2.51 |
| Etv5 | ets variant 5 | -2.53 |
| Tnfrsf23 | tumor necrosis factor receptor superfamily, member 23 | -2.54 |
| Adh1 | alcohol dehydrogenase 1 (class I) | -2.54 |
| Cyb5r2 | cytochrome b5 reductase 2 | -2.55 |
| A530058N18Rik | RIKEN cDNA A530058N18 gene | -2.56 |
| 17307425 | <i>No associated gene</i> | -2.56 |
| Jph3 | junctophilin 3 | -2.57 |
| Scel | sciellin | -2.59 |
| Ppp1r15a | protein phosphatase 1, regulatory (inhibitor) subunit 15A | -2.60 |
| P2ry12 | purinergic receptor P2Y, G-protein coupled 12 | -2.60 |
| Spp1 | secreted phosphoprotein 1 | -2.65 |
| Cyb5r1 | cytochrome b5 reductase 1 | -2.66 |
| Nostrin | nitric oxide synthase trafficker | -2.67 |
| Hfe | hemochromatosis | -2.67 |
| Kcnip1 | Kv channel-interacting protein 1 | -2.68 |
| Phactr1 | phosphatase and actin regulator 1 | -2.68 |
| Sytl4 | synaptotagmin-like 4 | -2.69 |
| Maob | monoamine oxidase B | -2.69 |
| Gdap2 | ganglioside-induced differentiation-associated-protein 2 | -2.69 |
| Defb1 | defensin beta 1 | -2.70 |
| Itgb8 | integrin beta 8 | -2.71 |

| | | |
|----------------------|--|-------|
| <i>Sv2b</i> | synaptic vesicle glycoprotein 2 b | -2.71 |
| <i>LOC102632360</i> | predicted gene 14616 | -2.71 |
| <i>Plk3</i> | polo-like kinase 3 | -2.74 |
| <i>Dock5</i> | dedicator of cytokinesis 5 | -2.74 |
| <i>Gm14412</i> | predicted gene 14412 | -2.81 |
| <i>C2cd4b</i> | C2 calcium-dependent domain containing 4B | -2.87 |
| <i>Spag1</i> | sperm associated antigen 1 | -2.87 |
| <i>Gnpnat1</i> | glucosamine-phosphate N-acetyltransferase 1 | -2.88 |
| <i>Grin1</i> | glutamate receptor, ionotropic, NMDA1 (zeta 1) | -2.91 |
| <i>Gsdma</i> | gasdermin A | -2.91 |
| <i>Psph</i> | phosphoserine phosphatase | -2.92 |
| <i>Cbln4</i> | cerebellin 4 precursor protein | -2.92 |
| <i>BB557941</i> | expressed sequence BB557941 | -2.92 |
| <i>Pycr1</i> | pyrroline-5-carboxylate reductase 1 | -2.93 |
| <i>Irak1bp1</i> | interleukin-1 receptor-associated kinase 1 binding protein 1 | -2.95 |
| <i>Steap1</i> | six transmembrane epithelial antigen of the prostate 1 | -2.95 |
| <i>Pcx</i> | pyruvate carboxylase | -2.97 |
| <i>Lonp1</i> | lon peptidase 1, mitochondrial | -2.97 |
| <i>Asb4</i> | ankyrin repeat and SOCS box-containing 4 | -2.97 |
| <i>Olf330</i> | olfactory receptor 330 | -2.98 |
| <i>Olfm4</i> | olfactomedin 4 | -2.99 |
| <i>Gm10941</i> | predicted gene 10941 | -3.03 |
| <i>Slc7a3</i> | solute carrier family 7 (cationic amino acid transporter, y+ system), member 3 | -3.11 |
| <i>Fhdc1</i> | FH2 domain containing 1 | -3.11 |
| <i>Hamp</i> | hepcidin antimicrobial peptide | -3.13 |
| <i>Ddit3</i> | DNA-damage inducible transcript 3 | -3.14 |
| <i>Yae1d1</i> | Yae1 domain containing 1 | -3.15 |
| <i>Nnat</i> | neuronatin | -3.16 |
| <i>Ucn3</i> | urocortin 3 | -3.18 |
| <i>Adm2</i> | adrenomedullin 2 | -3.24 |
| <i>1700016K19Rik</i> | RIKEN cDNA 1700016K19 gene | -3.28 |
| <i>Vgf</i> | VGF nerve growth factor inducible | -3.43 |
| <i>Rasgrf1</i> | RAS protein-specific guanine nucleotide-releasing factor 1 | -3.47 |
| <i>Ipcef1</i> | interaction protein for cytohesin exchange factors 1 | -3.47 |
| <i>17547943</i> | <i>No associated gene</i> | -3.48 |
| <i>1700056E22Rik</i> | RIKEN cDNA 1700056E22 gene | -3.59 |
| <i>Tat</i> | tyrosine aminotransferase | -3.64 |
| <i>Gpr137b-ps</i> | G protein-coupled receptor 137B, pseudogene | -3.71 |
| <i>Vrk1</i> | vaccinia related kinase 1 | -3.72 |
| <i>Prss53</i> | protease, serine 53 | -3.75 |
| <i>Psat1</i> | phosphoserine aminotransferase 1 | -3.81 |
| <i>Gm11789</i> | predicted gene 11789 | -3.93 |
| <i>Nrcam</i> | neuronal cell adhesion molecule | -3.96 |
| <i>Slco1a6</i> | solute carrier organic anion transporter family, member 1a6 | -3.97 |
| <i>Trib3</i> | tribbles pseudokinase 3 | -4.13 |

| | | |
|-----------------|---|--------|
| <i>Angptl7</i> | angiopoietin-like 7 | -4.18 |
| <i>Elovl4</i> | elongation of very long chain fatty acids (FEN1/Elo2, SUR4/Elo3, yeast)-like 4 | -4.23 |
| <i>Aldh1l2</i> | aldehyde dehydrogenase 1 family, member L2 | -4.31 |
| <i>Kcnh5</i> | potassium voltage-gated channel, subfamily H (eag-related), member 5 | -4.34 |
| <i>Ptprz1</i> | protein tyrosine phosphatase, receptor type Z, polypeptide 1 | -4.35 |
| <i>Rab3c</i> | RAB3C, member RAS oncogene family | -4.43 |
| <i>Igf1r</i> | insulin-like growth factor I receptor | -4.49 |
| <i>Prlr</i> | prolactin receptor | -4.49 |
| <i>Slc4a10</i> | solute carrier family 4, sodium bicarbonate cotransporter-like, member 10 | -4.58 |
| <i>Slitrk6</i> | SLIT and NTRK-like family, member 6 | -4.61 |
| <i>17547793</i> | <i>No associated gene</i> | -4.80 |
| <i>Gm23134</i> | predicted gene, 23134 | -5.00 |
| <i>Crybb3</i> | crystallin, beta B3 | -5.36 |
| <i>Serpina7</i> | serine (or cysteine) peptidase inhibitor, clade A (alpha-1 antiproteinase, antitrypsin), member 7 | -5.39 |
| <i>Robo1</i> | roundabout guidance receptor 1 | -5.41 |
| <i>Ffar3</i> | free fatty acid receptor 3 | -5.61 |
| <i>Hspa12a</i> | heat shock protein 12A | -5.92 |
| <i>Gm11454</i> | predicted gene 11454 | -6.15 |
| <i>Ttyh1</i> | tweety family member 1 | -6.37 |
| <i>Ppp1r1a</i> | protein phosphatase 1, regulatory (inhibitor) subunit 1A | -6.60 |
| <i>Pdyn</i> | prodynorphin | -6.63 |
| <i>Cdh8</i> | cadherin 8 | -6.68 |
| <i>Spc25</i> | SPC25, NDC80 kinetochore complex component, homolog (<i>S. cerevisiae</i>) | -6.83 |
| <i>Cbs</i> | cystathionine beta-synthase | -7.42 |
| <i>Nell1</i> | NEL-like 1 | -7.94 |
| <i>Tmem215</i> | transmembrane protein 215 | -10.71 |
| <i>G6pc2</i> | glucose-6-phosphatase, catalytic, 2 | -10.84 |
| <i>Ffar1</i> | free fatty acid receptor 1 | -13.29 |
| <i>Cox6a2</i> | cytochrome c oxidase subunit VIa polypeptide 2 | -13.78 |

Supplementary table 3: Differential expression of genes in isolated islets of 10 weeks old male *Pax6^{Leca2}* (*Leca2*) and wildtype (WT) mice filtered for a minimum FC 1.5 and <10% FDR

| Gene symbol | Gene name | <i>Leca2</i> / WT |
|----------------------|--|----------------------|
| <i>Gbp8</i> | guanylate-binding protein 8 | 14.09 |
| <i>6330403K07Rik</i> | RIKEN cDNA 6330403K07 gene | 11.05 |
| <i>Cnr1</i> | cannabinoid receptor 1 (brain) | 9.70 |
| <i>Cpb2</i> | carboxypeptidase B2 (plasma) | 9.15 |
| <i>Ifi204</i> | interferon activated gene 204 | 7.24 |
| <i>Rbp1</i> | retinol binding protein 1, cellular | 6.81 |
| <i>Depdc7</i> | DEP domain containing 7 | 6.10 |
| <i>Calca</i> | calcitonin/calcitonin-related polypeptide, alpha | 5.92 |
| <i>Il6</i> | interleukin 6 | 5.69 |

| | | |
|----------------------|--|------|
| Ifi2712a | interferon, alpha-inducible protein 27 like 2A | 5.52 |
| Arhgap36 | Rho GTPase activating protein 36 | 5.46 |
| Ccl11 | chemokine (C-C motif) ligand 11 | 5.37 |
| 17238880 | <i>No associated gene</i> | 5.33 |
| Apof | apolipoprotein F | 5.19 |
| Jam2 | junction adhesion molecule 2 | 5.13 |
| Ly6a | lymphocyte antigen 6 complex, locus A | 5.10 |
| Iigp1 | interferon inducible GTPase 1 | 5.08 |
| Mnda | myeloid cell nuclear differentiation antigen /// interferon activated gene 204 | 5.05 |
| Tnfsf10 | tumor necrosis factor (ligand) superfamily, member 10 | 5.02 |
| Slc35f4 | solute carrier family 35, member F4 | 5.01 |
| Enpp1 | ectonucleotide pyrophosphatase/phosphodiesterase 1 | 4.97 |
| Rasgrp1 | RAS guanyl releasing protein 1 | 4.92 |
| Neurog3 | neurogenin 3 | 4.91 |
| 17238846 | <i>No associated gene</i> | 4.91 |
| Gcnt3 | glucosaminyl (N-acetyl) transferase 3, mucin type | 4.84 |
| Snora73b | small nucleolar RNA, H/ACA box 73b | 4.84 |
| 17238896 | <i>No associated gene</i> | 4.84 |
| Gm5431 | predicted gene 5431 | 4.83 |
| Dynlrb2 | dynein light chain roadblock-type 2 | 4.78 |
| Zbp1 | Z-DNA binding protein 1 | 4.66 |
| Mndal | myeloid nuclear differentiation antigen like | 4.64 |
| Gbp3 | guanylate binding protein 3 | 4.64 |
| Cxcl14 | chemokine (C-X-C motif) ligand 14 | 4.58 |
| Chrn4 | cholinergic receptor, nicotinic, beta polypeptide 4 | 4.58 |
| Aqp4 | aquaporin 4 | 4.57 |
| Cxcl10 | chemokine (C-X-C motif) ligand 10 | 4.57 |
| 4931429I11Rik | RIKEN cDNA 4931429I11 gene | 4.54 |
| Sp100 | nuclear antigen Sp100 | 4.51 |
| 17238920 | <i>No associated gene</i> | 4.43 |
| Bambi | BMP and activin membrane-bound inhibitor | 4.43 |
| Parm1 | prostate androgen-regulated mucin-like protein 1 | 4.40 |
| Enpep | glutamyl aminopeptidase | 4.40 |
| Rab38 | RAB38, member RAS oncogene family | 4.33 |
| Mmp3 | matrix metalloproteinase 3 | 4.31 |
| 17549772 | <i>No associated gene</i> | 4.30 |
| 17549388 | <i>No associated gene</i> | 4.19 |
| LOC101056250 | sp110 nuclear body protein-like | 4.17 |
| Slfn2 | schlafen 2 | 4.17 |
| Dpp10 | dipeptidylpeptidase 10 | 4.08 |
| Fhl2 | four and a half LIM domains 2 | 4.08 |
| 17238922 | <i>No associated gene</i> | 4.07 |
| Vwde | von Willebrand factor D and EGF domains | 4.07 |
| 17238866 | <i>No associated gene</i> | 4.06 |

| | | |
|----------------------|---|------|
| Plet1 | placenta expressed transcript 1 | 4.04 |
| Ifi1 | interferon-induced protein with tetratricopeptide repeats 1 | 3.99 |
| Oasl2 | 2'-5' oligoadenylate synthetase-like 2 | 3.97 |
| Clip4 | CAP-GLY domain containing linker protein family, member 4 | 3.96 |
| NONMMUT004543 | <i>No associated gene</i> | 3.96 |
| C3 | complement component 3 | 3.94 |
| Bmp3 | bone morphogenetic protein 3 | 3.93 |
| Ifi44 | interferon-induced protein 44 | 3.92 |
| Ffar4 | free fatty acid receptor 4 | 3.92 |
| AW112010 | expressed sequence AW112010 | 3.92 |
| Cxcl11 | chemokine (C-X-C motif) ligand 11 | 3.83 |
| 17238870 | <i>No associated gene</i> | 3.81 |
| Vip | vasoactive intestinal polypeptide | 3.81 |
| Rtp4 | receptor transporter protein 4 | 3.78 |
| Ms4a4d | membrane-spanning 4-domains, subfamily A, member 4D | 3.73 |
| Eef1a2 | eukaryotic translation elongation factor 1 alpha 2 | 3.69 |
| Isg15 | ISG15 ubiquitin-like modifier | 3.69 |
| Ccl2 | chemokine (C-C motif) ligand 2 | 3.69 |
| 17238860 | <i>No associated gene</i> | 3.68 |
| 17238848 | <i>No associated gene</i> | 3.67 |
| Serpine2 | serine (or cysteine) peptidase inhibitor, clade E, member 2 | 3.65 |
| Brinp1 | bone morphogenic protein/retinoic acid inducible neural specific 1 | 3.61 |
| Gm11640 | predicted gene 11640 | 3.61 |
| 17238878 | <i>No associated gene</i> | 3.59 |
| Chst8 | carbohydrate (N-acetylgalactosamine 4-0) sulfotransferase 8 | 3.57 |
| Gucy2c | guanylate cyclase 2c | 3.57 |
| 17238874 | <i>No associated gene</i> | 3.57 |
| Cygb | cytoglobin | 3.56 |
| Lrch2 | leucine-rich repeats and calponin homology (CH) domain containing 2 | 3.56 |
| Hist1h4m | histone cluster 1, H4m | 3.55 |
| Ttc25 | tetratricopeptide repeat domain 25 | 3.55 |
| 17238854 | <i>No associated gene</i> | 3.54 |
| 17238916 | <i>No associated gene</i> | 3.53 |
| Gm12840 | predicted gene 12840 | 3.53 |
| Ifi202b | interferon activated gene 202B | 3.51 |
| Bgn | biglycan | 3.51 |
| Wfdc16 | WAP four-disulfide core domain 16 | 3.47 |
| 17238856 | <i>No associated gene</i> | 3.46 |
| Gbp9 | guanylate-binding protein 9 | 3.45 |
| 17238918 | <i>No associated gene</i> | 3.43 |
| Plac8 | placenta-specific 8 | 3.42 |
| 17238868 | <i>No associated gene</i> | 3.40 |
| 17238876 | <i>No associated gene</i> | 3.38 |
| 17548532 | <i>No associated gene</i> | 3.38 |

| | | |
|----------------------|---|------|
| 17238832 | <i>No associated gene</i> | 3.38 |
| Gm24497 | predicted gene, 24497 | 3.37 |
| Vsig2 | V-set and immunoglobulin domain containing 2 | 3.36 |
| Enpp3 | ectonucleotide pyrophosphatase/phosphodiesterase 3 | 3.35 |
| Gbp2 | guanylate binding protein 2 | 3.35 |
| Timp1 | tissue inhibitor of metalloproteinase 1 | 3.32 |
| Cped1 | cadherin-like and PC-esterase domain containing 1 | 3.30 |
| Pde3a | phosphodiesterase 3A, cGMP inhibited | 3.30 |
| 17366275 | <i>No associated gene</i> | 3.29 |
| NONMMUT004544 | <i>No associated gene</i> | 3.29 |
| Uchl1 | ubiquitin carboxy-terminal hydrolase L1 | 3.25 |
| Il2rg | interleukin 2 receptor, gamma chain | 3.25 |
| Gm25813 | predicted gene, 25813 | 3.22 |
| Pfkfb3 | 6-phosphofructo-2-kinase/fructose-2,6-biphosphatase 3 | 3.21 |
| 17536665 | <i>No associated gene</i> | 3.20 |
| Npnt | nephronectin | 3.19 |
| Dapl1 | death associated protein-like 1 | 3.19 |
| Syt17 | synaptotagmin XVII | 3.15 |
| 17238858 | <i>No associated gene</i> | 3.14 |
| Gpr119 | G-protein coupled receptor 119 | 3.12 |
| Sparcl1 | SPARC-like 1 | 3.09 |
| Sez6 | seizure related gene 6 | 3.08 |
| 17238892 | <i>No associated gene</i> | 3.07 |
| Bst2 | bone marrow stromal cell antigen 2 | 3.06 |
| Gbp11 | guanylate binding protein 11 | 3.06 |
| Vstm2a | V-set and transmembrane domain containing 2A | 3.06 |
| Postn | periostin, osteoblast specific factor | 3.06 |
| Far2 | fatty acyl CoA reductase 2 | 3.04 |
| 17542364 | <i>No associated gene</i> | 3.03 |
| Cfh | complement component factor h | 3.03 |
| Gpr165 | G protein-coupled receptor 165 | 3.02 |
| Gpx8 | glutathione peroxidase 8 (putative) | 3.02 |
| Pdpn | podoplanin | 3.02 |
| Epsti1 | epithelial stromal interaction 1 (breast) | 3.02 |
| Ctla2a | cytotoxic T lymphocyte-associated protein 2 alpha | 3.00 |
| 17238826 | <i>No associated gene</i> | 3.00 |
| Ly6c2 | lymphocyte antigen 6 complex, locus C2 | 2.99 |
| Aebp1 | AE binding protein 1 | 2.97 |
| Phf11b | PHD finger protein 11B | 2.97 |
| 9130208D14Rik | RIKEN cDNA 9130208D14 gene | 2.97 |
| Gfra2 | glial cell line derived neurotrophic factor family receptor alpha 2 | 2.96 |
| Slc43a3 | solute carrier family 43, member 3 | 2.96 |
| Tnc | tenascin C | 2.95 |
| Cartpt | CART prepropeptide | 2.94 |

| | | |
|----------------------|---|------|
| Ddc | dopa decarboxylase | 2.93 |
| Ifi205 | interferon activated gene 205 | 2.92 |
| AW551984 | expressed sequence AW551984 | 2.92 |
| Rorc | RAR-related orphan receptor gamma | 2.91 |
| Ifi203 | interferon activated gene 203 | 2.91 |
| 17238862 | <i>No associated gene</i> | 2.91 |
| Mx2 | MX dynamin-like GTPase 2 | 2.90 |
| BC048594 | cDNA sequence BC048594 /// doublecortin domain containing 5 | 2.90 |
| Cyp39a1 | cytochrome P450, family 39, subfamily a, polypeptide 1 | 2.90 |
| Arrdc4 | arrestin domain containing 4 | 2.89 |
| Ddx60 | DEAD (Asp-Glu-Ala-Asp) box polypeptide 60 | 2.89 |
| Gbp10 | guanylate-binding protein 10 | 2.89 |
| 17549570 | <i>No associated gene</i> | 2.87 |
| 17238912 | <i>No associated gene</i> | 2.87 |
| Rarres2 | retinoic acid receptor responder (tazarotene induced) 2 | 2.87 |
| Rgs4 | regulator of G-protein signaling 4 | 2.86 |
| Ctsk | cathepsin K | 2.86 |
| Ptprg | protein tyrosine phosphatase, receptor type, G | 2.85 |
| Mkx | mohawk homeobox | 2.84 |
| Ifit2 | interferon-induced protein with tetratricopeptide repeats 2 | 2.84 |
| Fam179a | family with sequence similarity 179, member A | 2.83 |
| Gsta4 | glutathione S-transferase, alpha 4 | 2.83 |
| Iqsec3 | IQ motif and Sec7 domain 3 | 2.83 |
| Ccl7 | chemokine (C-C motif) ligand 7 | 2.83 |
| Epas1 | endothelial PAS domain protein 1 | 2.82 |
| NONMMUT017874 | <i>No associated gene</i> | 2.81 |
| Dlk1 | delta-like 1 homolog (Drosophila) | 2.81 |
| Gm22506 | predicted gene, 22506 | 2.80 |
| Osmr | oncostatin M receptor | 2.79 |
| Nrgn | neurogranin | 2.79 |
| Elmod1 | ELMO/CED-12 domain containing 1 | 2.77 |
| Colgalt2 | collagen beta(1-O)galactosyltransferase 2 | 2.77 |
| NONMMUT004548 | <i>No associated gene</i> | 2.77 |
| Inhba | inhibin beta-A | 2.76 |
| Nr1h4 | nuclear receptor subfamily 1, group H, member 4 | 2.76 |
| Cd52 | CD52 antigen | 2.75 |
| Pgf | placental growth factor | 2.75 |
| Ifi47 | interferon gamma inducible protein 47 | 2.75 |
| 17238924 | <i>No associated gene</i> | 2.75 |
| Rerg | RAS-like, estrogen-regulated, growth-inhibitor | 2.74 |
| Guca2a | guanylate cyclase activator 2a (guanylin) | 2.74 |
| Vcam1 | vascular cell adhesion molecule 1 | 2.74 |
| Fam159b | family with sequence similarity 159, member B | 2.73 |
| 17549290 | <i>No associated gene</i> | 2.72 |

| | | |
|----------------------|---|------|
| Lgi1 | leucine-rich repeat LGI family, member 1 | 2.72 |
| Timp3 | tissue inhibitor of metalloproteinase 3 | 2.71 |
| Irf7 | interferon regulatory factor 7 | 2.71 |
| Pigr | polymeric immunoglobulin receptor | 2.71 |
| NONMMUT004542 | <i>No associated gene</i> | 2.70 |
| Ms4a4c | membrane-spanning 4-domains, subfamily A, member 4C | 2.70 |
| Gbp7 | guanylate binding protein 7 | 2.69 |
| 17549588 | <i>No associated gene</i> | 2.69 |
| 17214729 | <i>No associated gene</i> | 2.68 |
| Colec12 | collectin sub-family member 12 | 2.68 |
| 17238842 | <i>No associated gene</i> | 2.68 |
| Pyhin1 | pyrin and HIN domain family, member 1 | 2.68 |
| Msln | mesothelin | 2.68 |
| 17358825 | <i>No associated gene</i> | 2.68 |
| Plod2 | procollagen lysine, 2-oxoglutarate 5-dioxygenase 2 | 2.67 |
| 4930539E08Rik | RIKEN cDNA 4930539E08 gene | 2.66 |
| Spic | Spi-C transcription factor (Spi-1/PU.1 related) | 2.65 |
| Cfi | complement component factor i | 2.65 |
| Tmem132b | transmembrane protein 132B | 2.65 |
| Gm26735 | predicted gene, 26735 | 2.65 |
| Cd34 | CD34 antigen | 2.65 |
| 17238852 | <i>No associated gene</i> | 2.64 |
| Car8 | carbonic anhydrase 8 | 2.64 |
| Gc | group specific component | 2.64 |
| Slc15a3 | solute carrier family 15, member 3 | 2.62 |
| Igtp | interferon gamma induced GTPase | 2.62 |
| Ednra | endothelin receptor type A | 2.62 |
| Ephb2 | Eph receptor B2 | 2.62 |
| Gm20412 | predicted gene 20412 | 2.61 |
| Slc5a10 | solute carrier family 5 (sodium/glucose cotransporter), member 10 | 2.61 |
| Trim9 | tripartite motif-containing 9 | 2.60 |
| Mfap5 | microfibrillar associated protein 5 | 2.60 |
| 17547680 | <i>No associated gene</i> | 2.60 |
| 17238834 | <i>No associated gene</i> | 2.60 |
| 17238844 | <i>No associated gene</i> | 2.59 |
| Fam84a | family with sequence similarity 84, member A | 2.59 |
| Cidea | cell death-inducing DNA fragmentation factor, alpha subunit-like effector A | 2.59 |
| Hist1h3f | histone cluster 1, H3f | 2.58 |
| Irgm2 | immunity-related GTPase family M member 2 | 2.57 |
| Bcl2a1a | B cell leukemia/lymphoma 2 related protein A1a | 2.57 |
| Kl | klotho | 2.56 |
| Gm14446 | predicted gene 14446 | 2.56 |
| Phf11d | PHD finger protein 11D | 2.55 |
| Cdr1 | cerebellar degeneration related antigen 1 | 2.55 |

| | | |
|----------------------|--|------|
| Mmp14 | matrix metalloproteinase 14 (membrane-inserted) | 2.55 |
| Cfb | complement factor B | 2.55 |
| Peak1 | pseudopodium-enriched atypical kinase 1 | 2.54 |
| 17549402 | <i>No associated gene</i> | 2.54 |
| Angptl2 | angiopoietin-like 2 | 2.53 |
| Cdh9 | cadherin 9 | 2.53 |
| Gli3 | GLI-Kruppel family member GLI3 | 2.53 |
| Gbp2b | guanylate binding protein 2b | 2.53 |
| Thy1 | thymus cell antigen 1, theta | 2.52 |
| Prrx1 | paired related homeobox 1 | 2.51 |
| Tgfb1 | transforming growth factor, beta 1 | 2.50 |
| Herc6 | hect domain and RLD 6 | 2.49 |
| 17548193 | <i>No associated gene</i> | 2.49 |
| BC028528 | cDNA sequence BC028528 | 2.48 |
| Tm4sf20 | transmembrane 4 L six family member 20 | 2.47 |
| Tle4 | transducin-like enhancer of split 4 | 2.47 |
| Fxyd3 | FXDY domain-containing ion transport regulator 3 | 2.47 |
| Ppp1r3c | protein phosphatase 1, regulatory (inhibitor) subunit 3C | 2.46 |
| Plaur | plasminogen activator, urokinase receptor | 2.45 |
| Lrrc32 | leucine rich repeat containing 32 | 2.44 |
| AK088706 | <i>No associated gene</i> | 2.44 |
| Aldh1a2 | aldehyde dehydrogenase family 1, subfamily A2 | 2.43 |
| Il4ra | interleukin 4 receptor, alpha | 2.43 |
| Plet1os | placenta expressed transcript 1, opposite strand | 2.43 |
| Rtn1 | reticulon 1 | 2.43 |
| Gm17757 | GTPase, very large interferon inducible 1 pseudogene | 2.42 |
| 17548750 | <i>No associated gene</i> | 2.42 |
| S1pr3 | sphingosine-1-phosphate receptor 3 | 2.42 |
| Csn3 | casein kappa | 2.41 |
| Nebl | nebulin | 2.41 |
| Penk | preproenkephalin | 2.41 |
| Tmprss2 | transmembrane protease, serine 2 | 2.41 |
| A4galt | alpha 1,4-galactosyltransferase | 2.41 |
| Il18 | interleukin 18 | 2.40 |
| Mmp7 | matrix metalloproteinase 7 | 2.40 |
| Arhgap42 | Rho GTPase activating protein 42 | 2.40 |
| Gfra3 | glial cell line derived neurotrophic factor family receptor alpha 3 | 2.39 |
| Necab2 | N-terminal EF-hand calcium binding protein 2 | 2.39 |
| Pld1 | phospholipase D1 | 2.39 |
| 17547505 | <i>No associated gene</i> | 2.39 |
| 4933412E12Rik | RIKEN cDNA 4933412E12 gene | 2.38 |
| Magi2 | membrane associated guanylate kinase, WW and PDZ domain containing 2 | 2.38 |
| H2-Ea-ps | histocompatibility 2, class II antigen E alpha, pseudogene | 2.38 |
| Xaf1 | XIAP associated factor 1 | 2.38 |

| | | |
|-----------------------------|---|------|
| <i>Rnf138rt1</i> | ring finger protein 138, retrogene 1 | 2.37 |
| <i>Krt27</i> | keratin 27 | 2.37 |
| <i>Mfge8</i> | milk fat globule-EGF factor 8 protein | 2.37 |
| <i>Pdgfrb</i> | platelet derived growth factor receptor, beta polypeptide | 2.36 |
| <i>Arhgap10</i> | Rho GTPase activating protein 10 | 2.36 |
| <i>H2-T22</i> | histocompatibility 2, T region locus 22 | 2.35 |
| <i>Ppap2a</i> | phosphatidic acid phosphatase type 2A | 2.35 |
| <i>Fstl1</i> | follistatin-like 1 | 2.35 |
| <i>Ehf</i> | ets homologous factor | 2.35 |
| <i>Tmem47</i> | transmembrane protein 47 | 2.34 |
| <i>1700042O10Rik</i> | RIKEN cDNA 1700042O10 gene | 2.34 |
| <i>Fgf14</i> | fibroblast growth factor 14 | 2.34 |
| <i>Itga6</i> | integrin alpha 6 | 2.34 |
| <i>Tmem173</i> | transmembrane protein 173 | 2.34 |
| <i>Abcg2</i> | ATP-binding cassette, sub-family G (WHITE), member 2 | 2.33 |
| <i>Pdgfra</i> | platelet derived growth factor receptor, alpha polypeptide | 2.33 |
| <i>Syt16</i> | synaptotagmin XVI | 2.32 |
| <i>Spon2</i> | spondin 2, extracellular matrix protein | 2.32 |
| <i>Aif1</i> | allograft inflammatory factor 1 | 2.32 |
| <i>Sncg</i> | synuclein, gamma | 2.32 |
| <i>Il18bp</i> | interleukin 18 binding protein | 2.32 |
| <i>Mkl1</i> | mixed lineage kinase domain-like | 2.32 |
| <i>17238836</i> | <i>No associated gene</i> | 2.31 |
| <i>Timp2</i> | tissue inhibitor of metalloproteinase 2 | 2.31 |
| <i>Gimap4</i> | GTPase, IMAP family member 4 | 2.31 |
| <i>Serping1</i> | serine (or cysteine) peptidase inhibitor, clade G, member 1 | 2.30 |
| <i>Nsg1</i> | neuron specific gene family member 1 | 2.30 |
| <i>Dnm3</i> | dynammin 3 | 2.30 |
| <i>Scn1b</i> | sodium channel, voltage-gated, type I, beta | 2.30 |
| <i>Col6a3</i> | collagen, type VI, alpha 3 | 2.30 |
| <i>Epb4.1l2</i> | erythrocyte protein band 4.1-like 2 | 2.30 |
| <i>Cd9</i> | CD9 antigen | 2.30 |
| <i>Cald1</i> | caldesmon 1 | 2.30 |
| <i>Rasgrf2</i> | RAS protein-specific guanine nucleotide-releasing factor 2 | 2.29 |
| <i>Apbb1ip</i> | amyloid beta (A4) precursor protein-binding, family B, member 1 interacting protein | 2.29 |
| <i>Parp9</i> | poly (ADP-ribose) polymerase family, member 9 | 2.29 |
| <i>Gchfr</i> | GTP cyclohydrolase I feedback regulator | 2.29 |
| <i>Slfn5</i> | schlafen 5 | 2.28 |
| <i>Sox4</i> | SRY (sex determining region Y)-box 4 | 2.27 |
| <i>Arap2</i> | ArfGAP with RhoGAP domain, ankyrin repeat and PH domain 2 | 2.27 |
| <i>Heyl</i> | hairy/enhancer-of-split related with YRPW motif-like | 2.27 |
| <i>Sox18</i> | SRY (sex determining region Y)-box 18 | 2.26 |
| <i>Rnu3a</i> | U3A small nuclear RNA | 2.26 |

| | | |
|-----------------------------|---|------|
| <i>Galnt7</i> | UDP-N-acetyl-alpha-D-galactosamine: polypeptide N-acetylgalactosaminyltransferase 7 | 2.26 |
| <i>Tmem59l</i> | transmembrane protein 59-like | 2.26 |
| <i>Sorcs2</i> | sortilin-related VPS10 domain containing receptor 2 | 2.26 |
| <i>Scn9a</i> | sodium channel, voltage-gated, type IX, alpha | 2.26 |
| <i>Trpm3</i> | transient receptor potential cation channel, subfamily M, member 3 | 2.25 |
| <i>H2-T23</i> | histocompatibility 2, T region locus 23 | 2.25 |
| <i>Pros1</i> | protein S (alpha) | 2.25 |
| <i>Ccl5</i> | chemokine (C-C motif) ligand 5 | 2.25 |
| <i>Slfn9</i> | schlafen 9 | 2.25 |
| <i>Irgm1</i> | immunity-related GTPase family M member 1 | 2.25 |
| <i>Layn</i> | layilin | 2.25 |
| <i>Zfp36l1</i> | zinc finger protein 36, C3H type-like 1 | 2.24 |
| <i>Cntnap5b</i> | contactin associated protein-like 5B | 2.23 |
| <i>Egr2</i> | early growth response 2 | 2.23 |
| <i>Ms4a6d</i> | membrane-spanning 4-domains, subfamily A, member 6D | 2.23 |
| <i>Hspb1</i> | heat shock protein 1 | 2.23 |
| <i>NONMMUT004538</i> | <i>No associated gene</i> | 2.22 |
| <i>Cntn3</i> | contactin 3 | 2.22 |
| <i>17480528</i> | <i>No associated gene</i> | 2.22 |
| <i>F2</i> | coagulation factor II | 2.22 |
| <i>Csf1</i> | colony stimulating factor 1 (macrophage) | 2.21 |
| <i>Rab32</i> | RAB32, member RAS oncogene family | 2.21 |
| <i>Ngf</i> | nerve growth factor | 2.21 |
| <i>Gm15441</i> | predicted gene 15441 | 2.20 |
| <i>Tpd52l1</i> | tumor protein D52-like 1 | 2.20 |
| <i>Rgs16</i> | regulator of G-protein signaling 16 | 2.20 |
| <i>Parp14</i> | poly (ADP-ribose) polymerase family, member 14 | 2.20 |
| <i>Gadd45b</i> | growth arrest and DNA-damage-inducible 45 beta | 2.19 |
| <i>Large</i> | like-glycosyltransferase | 2.19 |
| <i>Fam167b</i> | family with sequence similarity 167, member B | 2.19 |
| <i>NONMMUT004541</i> | <i>No associated gene</i> | 2.18 |
| <i>Cd38</i> | CD38 antigen | 2.18 |
| <i>Thbd</i> | thrombomodulin | 2.18 |
| <i>Cd200</i> | CD200 antigen | 2.18 |
| <i>Aspn</i> | asporin | 2.17 |
| <i>Gbp4</i> | guanylate binding protein 4 | 2.17 |
| <i>Trav9d-3</i> | T cell receptor alpha variable 9D-3 | 2.17 |
| <i>Tmem255a</i> | transmembrane protein 255A | 2.17 |
| <i>Snai1</i> | snail family zinc finger 1 | 2.16 |
| <i>Ptchd1</i> | patched domain containing 1 | 2.16 |
| <i>Gm26719</i> | predicted gene, 26719 | 2.16 |
| <i>C1ql3</i> | C1q-like 3 | 2.16 |
| <i>17548709</i> | <i>No associated gene</i> | 2.16 |

| | | |
|-----------------------------|---|------|
| <i>Pltp</i> | phospholipid transfer protein | 2.16 |
| <i>Anxa3</i> | annexin A3 | 2.16 |
| <i>Tekt2</i> | tektin 2 | 2.16 |
| <i>17548315</i> | <i>No associated gene</i> | 2.16 |
| <i>Ascl1</i> | achaete-scute family bHLH transcription factor 1 | 2.15 |
| <i>Stat2</i> | signal transducer and activator of transcription 2 | 2.15 |
| <i>Fcgrt</i> | Fc receptor, IgG, alpha chain transporter | 2.15 |
| <i>Tgm2</i> | transglutaminase 2, C polypeptide | 2.15 |
| <i>Trim21</i> | tripartite motif-containing 21 | 2.15 |
| <i>Egr1</i> | early growth response 1 | 2.14 |
| <i>Slco2a1</i> | solute carrier organic anion transporter family, member 2a1 | 2.14 |
| <i>Ms4a6c</i> | membrane-spanning 4-domains, subfamily A, member 6C | 2.13 |
| <i>Prrg3</i> | proline rich Gla (G-carboxyglutamic acid) 3 (transmembrane) | 2.13 |
| <i>Itga5</i> | integrin alpha 5 (fibronectin receptor alpha) | 2.13 |
| <i>Arhgdib</i> | Rho, GDP dissociation inhibitor (GDI) beta | 2.13 |
| <i>Klf10</i> | Kruppel-like factor 10 | 2.13 |
| <i>17549810</i> | <i>No associated gene</i> | 2.12 |
| <i>Txnip</i> | thioredoxin interacting protein | 2.12 |
| <i>Clic5</i> | chloride intracellular channel 5 | 2.12 |
| <i>H2-Ab1</i> | histocompatibility 2, class II antigen A, beta 1 | 2.11 |
| <i>Dgkb</i> | diacylglycerol kinase, beta | 2.11 |
| <i>Nrp1</i> | neuropilin 1 | 2.11 |
| <i>P2rx4</i> | purinergic receptor P2X, ligand-gated ion channel 4 | 2.11 |
| <i>Calcr1</i> | calcitonin receptor-like | 2.11 |
| <i>Asic1</i> | acid-sensing (proton-gated) ion channel 1 | 2.11 |
| <i>Cd44</i> | CD44 antigen | 2.10 |
| <i>Rspo3</i> | R-spondin 3 | 2.10 |
| <i>3425401B19Rik</i> | RIKEN cDNA 3425401B19 gene | 2.10 |
| <i>Foxp2</i> | forkhead box P2 | 2.10 |
| <i>Galk1</i> | galactokinase 1 | 2.10 |
| <i>Crip2</i> | cysteine rich protein 2 | 2.09 |
| <i>Nap1l5</i> | nucleosome assembly protein 1-like 5 | 2.09 |
| <i>Dcdc2a</i> | doublecortin domain containing 2a | 2.09 |
| <i>Phlda1</i> | pleckstrin homology like domain, family A, member 1 | 2.09 |
| <i>Sgk1</i> | serum/glucocorticoid regulated kinase 1 | 2.08 |
| <i>Scn3a</i> | sodium channel, voltage-gated, type III, alpha | 2.08 |
| <i>17238864</i> | <i>No associated gene</i> | 2.08 |
| <i>Cd97</i> | CD97 antigen | 2.07 |
| <i>Gbe1</i> | glucan (1,4-alpha-), branching enzyme 1 | 2.07 |
| <i>Cyyr1</i> | cysteine and tyrosine-rich protein 1 | 2.06 |
| <i>17238850</i> | <i>No associated gene</i> | 2.06 |
| <i>Syne1</i> | spectrin repeat containing, nuclear envelope 1 | 2.06 |
| <i>Itp1</i> | inositol 1,4,5-trisphosphate receptor 1 | 2.06 |
| <i>17238888</i> | <i>No associated gene</i> | 2.06 |

| | | |
|-----------------------------|--|------|
| <i>Tle1</i> | transducin-like enhancer of split 1 | 2.06 |
| <i>Rgs5</i> | regulator of G-protein signaling 5 | 2.06 |
| <i>Plvap</i> | plasmalemma vesicle associated protein | 2.06 |
| <i>LOC101055672</i> | nuclear body protein SP140-like, RIKEN cDNA A530032D15Rik gene | 2.05 |
| <i>Cxcl12</i> | chemokine (C-X-C motif) ligand 12 | 2.05 |
| <i>Vim</i> | vimentin | 2.05 |
| <i>Adcyap1</i> | adenylate cyclase activating polypeptide 1 | 2.05 |
| <i>Serpinh1</i> | serine (or cysteine) peptidase inhibitor, clade H, member 1 | 2.05 |
| <i>Dhx58</i> | DEXH (Asp-Glu-X-His) box polypeptide 58 | 2.05 |
| <i>Cck</i> | cholecystokinin | 2.05 |
| <i>Gm8995</i> | predicted gene 8995 | 2.04 |
| <i>Eng</i> | endoglin | 2.04 |
| <i>Serpine1</i> | serine (or cysteine) peptidase inhibitor, clade E, member 1 | 2.04 |
| <i>Dbn1</i> | drebrin 1 | 2.04 |
| <i>Lst1</i> | leukocyte specific transcript 1 | 2.04 |
| <i>Nid1</i> | nidogen 1 | 2.03 |
| <i>Shisa6</i> | shisa family member 6 | 2.03 |
| <i>Arxes1</i> | adipocyte-related X-chromosome expressed sequence 1 | 2.03 |
| <i>Nmnat2</i> | nicotinamide nucleotide adenyltransferase 2 | 2.03 |
| <i>Msn</i> | moesin | 2.03 |
| <i>Dnase1l3</i> | deoxyribonuclease 1-like 3 | 2.01 |
| <i>Hspb8</i> | heat shock protein 8 | 2.01 |
| <i>D330045A20Rik</i> | RIKEN cDNA D330045A20 gene | 2.01 |
| <i>17549478</i> | <i>No associated gene</i> | 2.01 |
| <i>Kcnk16</i> | potassium channel, subfamily K, member 16 | 2.00 |
| <i>Apol9a</i> | apolipoprotein L 9a | 2.00 |
| <i>Lrrn3</i> | leucine rich repeat protein 3, neuronal | 2.00 |
| <i>Rnf213</i> | ring finger protein 213 | 2.00 |
| <i>Kctd12</i> | potassium channel tetramerisation domain containing 12 | 2.00 |
| <i>Col8a1</i> | collagen, type VIII, alpha 1 | 2.00 |
| <i>Cp</i> | ceruloplasmin | 1.99 |
| <i>Slc4a4</i> | solute carrier family 4 (anion exchanger), member 4 | 1.99 |
| <i>Slamf9</i> | SLAM family member 9 | 1.99 |
| <i>Mmrn2</i> | multimerin 2 | 1.99 |
| <i>Ralgds</i> | ral guanine nucleotide dissociation stimulator | 1.99 |
| <i>Tek</i> | endothelial-specific receptor tyrosine kinase | 1.99 |
| <i>LOC102635076</i> | serine/arginine repetitive matrix protein 2-like | 1.99 |
| <i>Mgp</i> | matrix Gla protein | 1.99 |
| <i>17238872</i> | <i>No associated gene</i> | 1.99 |
| <i>B4galt5</i> | UDP-Gal:betaGlcNAc beta 1,4-galactosyltransferase, polypeptide 5 | 1.99 |
| <i>Gpihbp1</i> | GPI-anchored HDL-binding protein 1 | 1.99 |
| <i>17548808</i> | <i>No associated gene</i> | 1.98 |
| <i>Ms4a7</i> | membrane-spanning 4-domains, subfamily A, member 7 | 1.98 |
| <i>Pak7</i> | p21 protein (Cdc42/Rac)-activated kinase 7 | 1.98 |

| | | |
|-----------------------|---|------|
| Syt9 | synaptotagmin IX | 1.98 |
| Flt1 | FMS-like tyrosine kinase 1 | 1.98 |
| Pik3ap1 | phosphoinositide-3-kinase adaptor protein 1 | 1.98 |
| Rsad2 | radical S-adenosyl methionine domain containing 2 | 1.97 |
| Dab2 | disabled 2, mitogen-responsive phosphoprotein | 1.97 |
| Chd5 | chromodomain helicase DNA binding protein 5 | 1.97 |
| Lgmn | legumain | 1.97 |
| Limch1 | LIM and calponin homology domains 1 | 1.96 |
| Cers4 | ceramide synthase 4 | 1.96 |
| Pdk2 | pyruvate dehydrogenase kinase, isoenzyme 2 | 1.96 |
| 17548908 | <i>No associated gene</i> | 1.96 |
| Tagln | transgelin | 1.96 |
| Gimap6 | GTPase, IMAP family member 6 | 1.96 |
| Axl | AXL receptor tyrosine kinase | 1.95 |
| 17242306 | <i>No associated gene</i> | 1.95 |
| Tusc5 | tumor suppressor candidate 5 | 1.95 |
| Cd248 | CD248 antigen, endosialin | 1.95 |
| Naip2 | NLR family, apoptosis inhibitory protein 2 | 1.95 |
| Lxn | latexin | 1.95 |
| Cpne2 | copine II | 1.94 |
| LOC102641603 | cyclin-dependent kinases regulatory subunit 2-like, CDC28 protein kinase regulatory subunit 2 | 1.94 |
| Ano1 | anoctamin 1, calcium activated chloride channel | 1.94 |
| Oas1g | 2'-5' oligoadenylate synthetase 1G | 1.94 |
| Rbms1 | RNA binding motif, single stranded interacting protein 1 | 1.94 |
| Thrb | thyroid hormone receptor beta | 1.94 |
| 9930111J21Rik2 | RIKEN cDNA 9930111J21 gene 2 | 1.93 |
| Rnf122 | ring finger protein 122 | 1.93 |
| 17549490 | <i>No associated gene</i> | 1.93 |
| Foxs1 | forkhead box S1 | 1.93 |
| Aldh1a3 | aldehyde dehydrogenase family 1, subfamily A3 | 1.93 |
| 17229451 | <i>No associated gene</i> | 1.93 |
| Psmb8 | proteasome (prosome, macropain) subunit, beta type 8 (large multifunctional peptidase 7) | 1.93 |
| Clqb | complement component 1, q subcomponent, beta polypeptide | 1.93 |
| Adap2 | ArfGAP with dual PH domains 2 | 1.93 |
| NONMMUT004549 | <i>No associated gene</i> | 1.92 |
| Dtx3l | deltex 3-like, E3 ubiquitin ligase | 1.92 |
| Emcn | endomucin | 1.92 |
| Il13ra1 | interleukin 13 receptor, alpha 1 | 1.92 |
| Ddr2 | discoidin domain receptor family, member 2 | 1.92 |
| Pla1a | phospholipase A1 member A | 1.91 |
| Slc35b3 | solute carrier family 35, member B3 | 1.91 |
| Ifih1 | interferon induced with helicase C domain 1 | 1.91 |

| | | |
|-----------------------------|--|------|
| <i>Gucy1b3</i> | guanylate cyclase 1, soluble, beta 3 | 1.91 |
| <i>Cyp4v3</i> | cytochrome P450, family 4, subfamily v, polypeptide 3 | 1.90 |
| <i>Fam43a</i> | family with sequence similarity 43, member A | 1.90 |
| <i>Cadps2</i> | Ca ²⁺ -dependent activator protein for secretion 2 | 1.90 |
| <i>Ube2l6</i> | ubiquitin-conjugating enzyme E2L 6 | 1.90 |
| <i>Ctla2b</i> | cytotoxic T lymphocyte-associated protein 2 beta | 1.90 |
| <i>Tmem179</i> | transmembrane protein 179 | 1.90 |
| <i>Pak1</i> | p21 protein (Cdc42/Rac)-activated kinase 1 | 1.90 |
| <i>Gm25703</i> | predicted gene, 25703 | 1.90 |
| <i>Ctsf</i> | cathepsin F | 1.90 |
| <i>Cyp1a1</i> | cytochrome P450, family 1, subfamily a, polypeptide 1 | 1.89 |
| <i>Tlr2</i> | toll-like receptor 2 | 1.89 |
| <i>Rai14</i> | retinoic acid induced 14 | 1.89 |
| <i>Gm26809</i> | predicted gene, 26809 | 1.89 |
| <i>Jag1</i> | jagged 1 | 1.89 |
| <i>Capsl</i> | calcyphosine-like | 1.89 |
| <i>Fxyd6</i> | FXDYD domain-containing ion transport regulator 6 | 1.89 |
| <i>Rbp4</i> | retinol binding protein 4, plasma | 1.89 |
| <i>Rgcc</i> | regulator of cell cycle | 1.88 |
| <i>Des</i> | desmin | 1.88 |
| <i>Bcl3</i> | B cell leukemia/lymphoma 3 | 1.88 |
| <i>Prdx4</i> | peroxiredoxin 4 | 1.88 |
| <i>Anxa2</i> | annexin A2 | 1.88 |
| <i>Kdr</i> | kinase insert domain protein receptor | 1.87 |
| <i>Npr1</i> | natriuretic peptide receptor 1 | 1.87 |
| <i>Rasd1</i> | RAS, dexamethasone-induced 1 | 1.87 |
| <i>Rsph4a</i> | radial spoke head 4 homolog A (Chlamydomonas) | 1.87 |
| <i>Esam</i> | endothelial cell-specific adhesion molecule | 1.87 |
| <i>Cd55</i> | CD55 molecule, decay accelerating factor for complement | 1.87 |
| <i>B4galt1</i> | UDP-Gal:betaGlcNAc beta 1,4- galactosyltransferase, polypeptide 1 | 1.87 |
| <i>Usp18</i> | ubiquitin specific peptidase 18 | 1.87 |
| <i>3632451O06Rik</i> | RIKEN cDNA 3632451O06 gene | 1.87 |
| <i>Tns1</i> | tensin 1 | 1.86 |
| <i>Gfra1</i> | glial cell line derived neurotrophic factor family receptor alpha 1 | 1.86 |
| <i>17234896</i> | <i>No associated gene</i> | 1.86 |
| <i>Prex2</i> | phosphatidylinositol-3,4,5-trisphosphate-dependent Rac exchange factor 2 | 1.86 |
| <i>Lmcd1</i> | LIM and cysteine-rich domains 1 | 1.86 |
| <i>Ly6e</i> | lymphocyte antigen 6 complex, locus E | 1.86 |
| <i>Tmlhe</i> | trimethyllysine hydroxylase, epsilon | 1.86 |
| <i>Wfdc18</i> | WAP four-disulfide core domain 18 | 1.86 |
| <i>Nespas</i> | neuroendocrine secretory protein antisense | 1.85 |
| <i>Tbx3</i> | T-box 3 | 1.85 |
| <i>9330136K24Rik</i> | RIKEN cDNA 9330136K24 gene | 1.85 |
| <i>Cyba</i> | cytochrome b-245, alpha polypeptide | 1.85 |

| | | |
|---------------------------|---|------|
| Ifit3 | interferon-induced protein with tetratricopeptide repeats 3 | 1.85 |
| Il17re | interleukin 17 receptor E | 1.85 |
| Plxnb1 | plexin B1 | 1.85 |
| Rpl5 | ribosomal protein L5 | 1.85 |
| Erg | avian erythroblastosis virus E-26 (v-ets) oncogene related | 1.85 |
| Irf9 | interferon regulatory factor 9 | 1.85 |
| Cmtm3 | CKLF-like MARVEL transmembrane domain containing 3 | 1.85 |
| Anpep | alanyl (membrane) aminopeptidase | 1.85 |
| Lyn | LYN proto-oncogene, Src family tyrosine kinase | 1.85 |
| Nckap1l | NCK associated protein 1 like | 1.85 |
| Spred1 | sprouty protein with EVH-1 domain 1, related sequence | 1.85 |
| Rbms3 | RNA binding motif, single stranded interacting protein | 1.84 |
| Myd88 | myeloid differentiation primary response gene 88 | 1.84 |
| Gja4 | gap junction protein, alpha 4 | 1.84 |
| Trim34a | tripartite motif-containing 34A | 1.84 |
| Itpril2 | inositol 1,4,5-triphosphate receptor interacting protein-like 2 | 1.84 |
| 17548166 | <i>No associated gene</i> | 1.84 |
| Arsk | arylsulfatase K | 1.83 |
| Pamr1 | peptidase domain containing associated with muscle regeneration 1 | 1.83 |
| Gm12250 | predicted gene 12250 | 1.83 |
| 17249829 | <i>No associated gene</i> | 1.83 |
| Pon2 | paraoxonase 2 | 1.83 |
| Tesc | tescalcin | 1.83 |
| Itgb2 | integrin beta 2 | 1.83 |
| 5033417F24Rik | RIKEN cDNA 5033417F24 gene | 1.83 |
| Rbm11 | RNA binding motif protein 11 | 1.83 |
| Tlr5 | toll-like receptor 5 | 1.83 |
| Scnn1b | sodium channel, nonvoltage-gated 1 beta | 1.82 |
| Gm16984 | predicted gene, 16984 | 1.82 |
| GENSCAN00000019044 | <i>No associated gene</i> | 1.82 |
| Tspan8 | tetraspanin 8 | 1.82 |
| Nek5 | NIMA (never in mitosis gene a)-related expressed kinase 5 | 1.82 |
| Ppap2b | phosphatidic acid phosphatase type 2B | 1.82 |
| Tmem86a | transmembrane protein 86A | 1.81 |
| Cacnb3 | calcium channel, voltage-dependent, beta 3 subunit | 1.81 |
| Panx1 | pannexin 1 | 1.81 |
| Grem2 | gremlin 2, DAN family BMP antagonist | 1.81 |
| Gvin1 | GTPase, very large interferon inducible 1 | 1.81 |
| Spock3 | sparc/osteonectin, cwcv and kazal-like domains proteoglycan 3 | 1.81 |
| 17398176 | <i>No associated gene</i> | 1.81 |
| Tspan15 | tetraspanin 15 | 1.81 |
| Cd74 | CD74 antigen (invariant polypeptide of major histocompatibility complex, class II antigen-associated) | 1.81 |
| Colla1 | collagen, type I, alpha 1 | 1.81 |

| | | |
|----------------------|---|------|
| <i>Cyth4</i> | cytohesin 4 | 1.81 |
| <i>Lrrc8b</i> | leucine rich repeat containing 8 family, member B | 1.81 |
| <i>Ifi30</i> | interferon gamma inducible protein 30 | 1.80 |
| <i>Parp12</i> | poly (ADP-ribose) polymerase family, member 12 | 1.80 |
| <i>Susd4</i> | sushi domain containing 4 | 1.80 |
| <i>Gm26540</i> | predicted gene, 26540 | 1.80 |
| <i>Gm5124</i> | predicted pseudogene 5124 | 1.80 |
| <i>Flna</i> | filamin, alpha | 1.80 |
| <i>Tnr</i> | tenascin R | 1.79 |
| <i>Bcl2l11</i> | BCL2-like 11 (apoptosis facilitator) | 1.79 |
| <i>Nrp2</i> | neuropilin 2 | 1.79 |
| <i>Rspo4</i> | R-spondin 4 | 1.79 |
| <i>Col4a1</i> | collagen, type IV, alpha 1 | 1.79 |
| <i>Hs6st1</i> | heparan sulfate 6-O-sulfotransferase 1 | 1.79 |
| <i>Ptprd</i> | protein tyrosine phosphatase, receptor type, D | 1.78 |
| <i>Nfkbiz</i> | nuclear factor of kappa light polypeptide gene enhancer in B cells inhibitor, zeta | 1.78 |
| <i>Misp</i> | mitotic spindle positioning | 1.78 |
| <i>Tpm1</i> | tropomyosin 1, alpha | 1.78 |
| <i>Fxyd5</i> | FXYD domain-containing ion transport regulator 5 | 1.78 |
| <i>Il1a</i> | interleukin 1 alpha | 1.78 |
| <i>Sepp1</i> | selenoprotein P, plasma, 1 | 1.78 |
| <i>A930017M01Rik</i> | RIKEN cDNA A930017M01 gene | 1.78 |
| <i>Oas1l</i> | 2'-5' oligoadenylate synthetase-like 1 | 1.78 |
| <i>Gm13420</i> | predicted gene 13420 | 1.77 |
| <i>Kalrn</i> | kalirin, RhoGEF kinase | 1.77 |
| <i>Prp</i> | prolylcarboxypeptidase (angiotensinase C) | 1.77 |
| <i>Ifim2</i> | interferon induced transmembrane protein 2 | 1.77 |
| <i>Ndr2</i> | N-myc downstream regulated gene 2 | 1.77 |
| <i>Pink1</i> | PTEN induced putative kinase 1 | 1.77 |
| <i>Lhfp15</i> | lipoma HMGIC fusion partner-like 5 | 1.77 |
| <i>Cst6</i> | cystatin E/M | 1.77 |
| <i>Tshz3</i> | teashirt zinc finger family member 3 | 1.77 |
| <i>Acp5</i> | acid phosphatase 5, tartrate resistant | 1.77 |
| <i>Wipf1</i> | WAS/WASL interacting protein family, member 1 | 1.77 |
| <i>Apol9b</i> | apolipoprotein L 9b | 1.77 |
| <i>Mex3b</i> | mex3 RNA binding family member B | 1.77 |
| <i>Limk2</i> | LIM motif-containing protein kinase 2 | 1.77 |
| <i>Pgm2l1</i> | phosphoglucomutase 2-like 1 | 1.76 |
| <i>Rasgrp3</i> | RAS, guanyl releasing protein 3 | 1.76 |
| <i>Galnt13</i> | UDP-N-acetyl-alpha-D-galactosamine:polypeptide N-acetylgalactosaminyltransferase 13 | 1.76 |
| <i>Sorbs3</i> | sorbin and SH3 domain containing 3 | 1.76 |
| <i>Sparc</i> | secreted acidic cysteine rich glycoprotein | 1.76 |
| <i>Pmep1</i> | prostate transmembrane protein, androgen induced 1 | 1.76 |

| | | |
|----------------------|--|------|
| <i>Csf2rb</i> | colony stimulating factor 2 receptor, beta, low-affinity (granulocyte-macrophage) | 1.76 |
| <i>Uba7</i> | ubiquitin-like modifier activating enzyme 7 | 1.76 |
| <i>Pcolce2</i> | procollagen C-endopeptidase enhancer 2 | 1.76 |
| <i>Fam105a</i> | family with sequence similarity 105, member A | 1.76 |
| <i>Hs6st3</i> | heparan sulfate 6-O-sulfotransferase 3 | 1.75 |
| <i>Mgst3</i> | microsomal glutathione S-transferase 3 | 1.75 |
| <i>Ctss</i> | cathepsin S | 1.75 |
| <i>Myo1b</i> | myosin IB | 1.75 |
| <i>F2r</i> | coagulation factor II (thrombin) receptor | 1.75 |
| <i>Cd81</i> | CD81 antigen | 1.75 |
| <i>Gm26669</i> | predicted gene, 26669 | 1.75 |
| <i>Gucyl1a2</i> | guanylate cyclase 1, soluble, alpha 2 | 1.75 |
| <i>Tgfb1</i> | transforming growth factor, beta induced | 1.74 |
| <i>Gm25857</i> | predicted gene, 25857 | 1.74 |
| <i>Gm20275</i> | predicted gene, 20275 | 1.74 |
| <i>Cda</i> | cytidine deaminase | 1.74 |
| <i>Tmem140</i> | transmembrane protein 140 | 1.74 |
| <i>17389048</i> | <i>No associated gene</i> | 1.74 |
| <i>Sult4a1</i> | sulfotransferase family 4A, member 1 | 1.74 |
| <i>Fam212a</i> | family with sequence similarity 212, member A | 1.74 |
| <i>Cd151</i> | CD151 antigen | 1.73 |
| <i>St3gal4</i> | ST3 beta-galactoside alpha-2,3-sialyltransferase 4 | 1.73 |
| <i>17548270</i> | <i>No associated gene</i> | 1.73 |
| <i>Mov10</i> | Moloney leukemia virus 10 | 1.73 |
| <i>Rpph1</i> | ribonuclease P RNA component H1 | 1.73 |
| <i>Lrp1</i> | low density lipoprotein receptor-related protein 1 | 1.73 |
| <i>Skil</i> | SKI-like | 1.73 |
| <i>Rnf145</i> | ring finger protein 145 | 1.73 |
| <i>Nxph1</i> | neurexophilin 1 | 1.73 |
| <i>Xdh</i> | xanthine dehydrogenase | 1.72 |
| <i>Cdc42ep3</i> | CDC42 effector protein (Rho GTPase binding) 3 | 1.72 |
| <i>Ptgfrn</i> | prostaglandin F2 receptor negative regulator | 1.72 |
| <i>Ntn4</i> | netrin 4 | 1.72 |
| <i>Dram1</i> | DNA-damage regulated autophagy modulator 1 | 1.72 |
| <i>Sema3e</i> | sema domain, immunoglobulin domain (Ig), short basic domain, secreted, (semaphorin) 3E | 1.72 |
| <i>H2-Q4</i> | histocompatibility 2, Q region locus 4 | 1.72 |
| <i>Pygb</i> | brain glycogen phosphorylase | 1.72 |
| <i>Hbb-b2</i> | hemoglobin, beta adult minor chain | 1.72 |
| <i>P2ry1</i> | purinergic receptor P2Y, G-protein coupled 1 | 1.72 |
| <i>Zdhhc14</i> | zinc finger, DHHC domain containing 14 | 1.72 |
| <i>Olfm3</i> | olfactomedin 3 | 1.72 |
| <i>Gm16277</i> | predicted gene 16277 | 1.72 |
| <i>A330050F15Rik</i> | RIKEN cDNA A330050F15 gene | 1.72 |

| | | |
|-----------------------------|--|------|
| <i>St8sia3</i> | ST8 alpha-N-acetyl-neuraminide alpha-2,8-sialyltransferase 3 | 1.71 |
| <i>Gfod1</i> | glucose-fructose oxidoreductase domain containing 1 | 1.71 |
| <i>Tiparp</i> | TCDD-inducible poly(ADP-ribose) polymerase | 1.71 |
| <i>Parvb</i> | parvin, beta | 1.71 |
| <i>Gprasp2</i> | G protein-coupled receptor associated sorting protein 2 | 1.71 |
| <i>Slc12a4</i> | solute carrier family 12, member 4 | 1.71 |
| <i>Gm17096</i> | predicted gene 17096 | 1.71 |
| <i>Tram2</i> | translocating chain-associating membrane protein 2 | 1.71 |
| <i>Dusp26</i> | dual specificity phosphatase 26 (putative) | 1.71 |
| <i>Cd274</i> | CD274 antigen | 1.71 |
| <i>Gprin3</i> | GPRIN family member 3 | 1.71 |
| <i>Gm12666</i> | predicted gene 12666 | 1.71 |
| <i>Icam1</i> | intercellular adhesion molecule 1 | 1.71 |
| <i>Sema4a</i> | sema domain, immunoglobulin domain (Ig), transmembrane domain (TM) and short cytoplasmic domain, (semaphorin) 4A | 1.71 |
| <i>Tcp11l2</i> | t-complex 11 (mouse) like 2 | 1.71 |
| <i>Tox</i> | thymocyte selection-associated high mobility group box | 1.70 |
| <i>Ucp2</i> | uncoupling protein 2 (mitochondrial, proton carrier) | 1.70 |
| <i>Gm19461</i> | predicted gene, 19461 | 1.70 |
| <i>2700038G22Rik</i> | RIKEN cDNA 2700038G22 gene | 1.70 |
| <i>Fam221a</i> | family with sequence similarity 221, member A | 1.70 |
| <i>Fam183b</i> | family with sequence similarity 183, member B | 1.70 |
| <i>17549304</i> | <i>No associated gene</i> | 1.70 |
| <i>Map4k4</i> | mitogen-activated protein kinase kinase kinase kinase 4 | 1.70 |
| <i>17486956</i> | <i>No associated gene</i> | 1.70 |
| <i>Rb1</i> | RB transcriptional corepressor 1 | 1.70 |
| <i>Wdr72</i> | WD repeat domain 72 | 1.70 |
| <i>Ets1</i> | E26 avian leukemia oncogene 1, 5' domain | 1.70 |
| <i>Clcn5</i> | chloride channel, voltage-sensitive 5 | 1.70 |
| <i>Medag</i> | mesenteric estrogen dependent adipogenesis | 1.70 |
| <i>Gprc5a</i> | G protein-coupled receptor, family C, group 5, member A | 1.70 |
| <i>Pcolce</i> | procollagen C-endopeptidase enhancer protein | 1.69 |
| <i>Myct1</i> | myc target 1 | 1.69 |
| <i>Me2</i> | malic enzyme 2, NAD(+)-dependent, mitochondrial | 1.69 |
| <i>Plxdc2</i> | plexin domain containing 2 | 1.69 |
| <i>Jun</i> | jun proto-oncogene | 1.69 |
| <i>Cdhr2</i> | cadherin-related family member 2 | 1.69 |
| <i>Rhbdl3</i> | rhomboid, veinlet-like 3 (Drosophila) | 1.69 |
| <i>Fcgr1</i> | Fc receptor, IgG, high affinity I | 1.69 |
| <i>Mapkapk3</i> | mitogen-activated protein kinase-activated protein kinase 3 | 1.69 |
| <i>Gm7609</i> | predicted pseudogene 7609 | 1.69 |
| <i>Eltf1</i> | EGF, latrophilin seven transmembrane domain containing 1 | 1.68 |
| <i>Tap1</i> | transporter 1, ATP-binding cassette, sub-family B (MDR/TAP) | 1.68 |
| <i>Trex1</i> | three prime repair exonuclease 1 | 1.68 |

| | | |
|----------------------|---|------|
| <i>Tmem243</i> | transmembrane protein 243, mitochondrial | 1.68 |
| <i>Nfatc1</i> | nuclear factor of activated T cells, cytoplasmic, calcineurin dependent 1 | 1.68 |
| <i>2310015B20Rik</i> | RIKEN cDNA 2310015B20 gene | 1.68 |
| <i>Csrp2</i> | cysteine and glycine-rich protein 2 | 1.68 |
| <i>Dusp6</i> | dual specificity phosphatase 6 | 1.68 |
| <i>Pdlim7</i> | PDZ and LIM domain 7 | 1.68 |
| <i>Cpt1a</i> | carnitine palmitoyltransferase 1a, liver | 1.68 |
| <i>Cit</i> | citron | 1.68 |
| <i>F11r</i> | F11 receptor | 1.68 |
| <i>Mef2c</i> | myocyte enhancer factor 2C | 1.68 |
| <i>Piezo1</i> | piezo-type mechanosensitive ion channel component 1 | 1.68 |
| <i>Ggh</i> | gamma-glutamyl hydrolase | 1.67 |
| <i>Dnm1</i> | dynamitin 1 | 1.67 |
| <i>Map2k4</i> | mitogen-activated protein kinase kinase 4 | 1.67 |
| <i>Il6ra</i> | interleukin 6 receptor, alpha | 1.67 |
| <i>Slc40a1</i> | solute carrier family 40 (iron-regulated transporter), member 1 | 1.67 |
| <i>Gatsl2</i> | GATS protein-like 2 | 1.67 |
| <i>Cd93</i> | CD93 antigen | 1.67 |
| <i>Pianp</i> | PILR alpha associated neural protein | 1.67 |
| <i>Dopey2</i> | dopey family member 2 | 1.67 |
| <i>Trim30d</i> | tripartite motif-containing 30D | 1.67 |
| <i>Srgn</i> | serglycin | 1.67 |
| <i>Nrep</i> | neuronal regeneration related protein | 1.67 |
| <i>Marveld2</i> | MARVEL (membrane-associating) domain containing 2 | 1.67 |
| <i>Tacc2</i> | transforming, acidic coiled-coil containing protein 2 | 1.67 |
| <i>Stat1</i> | signal transducer and activator of transcription 1 | 1.66 |
| <i>Ednrb</i> | endothelin receptor type B | 1.66 |
| <i>Gm5424</i> | predicted gene 5424 | 1.66 |
| <i>Gnb4</i> | guanine nucleotide binding protein (G protein), beta 4 | 1.66 |
| <i>Msh3</i> | mutS homolog 3 | 1.66 |
| <i>Fam210b</i> | family with sequence similarity 210, member B | 1.66 |
| <i>Atp2b4</i> | ATPase, Ca ⁺⁺ transporting, plasma membrane 4 | 1.66 |
| <i>Junb</i> | jun B proto-oncogene | 1.66 |
| <i>Samd9l</i> | sterile alpha motif domain containing 9-like | 1.66 |
| <i>Tlr3</i> | toll-like receptor 3 | 1.66 |
| <i>Smtn</i> | smoothelin | 1.66 |
| <i>Anks1b</i> | ankyrin repeat and sterile alpha motif domain containing 1B | 1.66 |
| <i>Cdh2</i> | cadherin 2 | 1.66 |
| <i>Scnn1g</i> | sodium channel, nonvoltage-gated 1 gamma | 1.66 |
| <i>Gda</i> | guanine deaminase | 1.66 |
| <i>Lgals3bp</i> | lectin, galactoside-binding, soluble, 3 binding protein | 1.66 |
| <i>Tppp3</i> | tubulin polymerization-promoting protein family member 3 | 1.65 |
| <i>Sh3bgr</i> | SH3-binding domain glutamic acid-rich protein | 1.65 |
| <i>Dennd5b</i> | DENN/MADD domain containing 5B | 1.65 |

| | | |
|----------------------|--|------|
| <i>9430020K01Rik</i> | RIKEN cDNA 9430020K01 gene | 1.65 |
| <i>Rit2</i> | Ras-like without CAAX 2 | 1.65 |
| <i>Gpr75</i> | G protein-coupled receptor 75 | 1.65 |
| <i>Bcl2a1b</i> | B cell leukemia/lymphoma 2 related protein A1b | 1.65 |
| <i>Ryr3</i> | ryanodine receptor 3 | 1.65 |
| <i>Hsbp1l1</i> | heat shock factor binding protein 1-like 1 | 1.65 |
| <i>Lcp1</i> | lymphocyte cytosolic protein 1 | 1.65 |
| <i>Pecam1</i> | platelet/endothelial cell adhesion molecule 1 | 1.65 |
| <i>Trim25</i> | tripartite motif-containing 25 | 1.65 |
| <i>Ldb2</i> | LIM domain binding 2 | 1.65 |
| <i>H2-Q5</i> | histocompatibility 2, Q region locus 5 | 1.65 |
| <i>Ddah2</i> | dimethylarginine dimethylaminohydrolase 2 | 1.64 |
| <i>Ccdc80</i> | coiled-coil domain containing 80 | 1.64 |
| <i>Pcdhb10</i> | protocadherin beta 10 | 1.64 |
| <i>Actr6</i> | ARP6 actin-related protein 6 | 1.64 |
| <i>Wnk3</i> | WNK lysine deficient protein kinase 3 | 1.64 |
| <i>Adam23</i> | a disintegrin and metallopeptidase domain 23 | 1.64 |
| <i>Rfx6</i> | regulatory factor X, 6 | 1.64 |
| <i>2310009B15Rik</i> | RIKEN cDNA 2310009B15 gene | 1.64 |
| <i>Fbxo33</i> | F-box protein 33 | 1.64 |
| <i>Mpeg1</i> | macrophage expressed gene 1 | 1.63 |
| <i>Slc36a1</i> | solute carrier family 36 (proton/amino acid symporter), member 1 | 1.63 |
| <i>Gm2a</i> | GM2 ganglioside activator protein | 1.63 |
| <i>Epha7</i> | Eph receptor A7 | 1.63 |
| <i>Mpp1</i> | membrane protein, palmitoylated | 1.63 |
| <i>Ap1s2</i> | adaptor-related protein complex 1, sigma 2 subunit | 1.63 |
| <i>Tmem9</i> | transmembrane protein 9 | 1.63 |
| <i>Uaca</i> | uveal autoantigen with coiled-coil domains and ankyrin repeats | 1.63 |
| <i>Negr1</i> | neuronal growth regulator 1 | 1.63 |
| <i>Crim1</i> | cysteine rich transmembrane BMP regulator 1 (chordin like) | 1.63 |
| <i>Traf4</i> | TNF receptor associated factor 4 | 1.62 |
| <i>Mrap2</i> | melanocortin 2 receptor accessory protein 2 | 1.62 |
| <i>Gm26778</i> | predicted gene, 26778 | 1.62 |
| <i>H2-M2</i> | histocompatibility 2, M region locus 2 | 1.62 |
| <i>Pdia5</i> | protein disulfide isomerase associated 5 | 1.62 |
| <i>Zfp608</i> | zinc finger protein 608 | 1.62 |
| <i>Scgn</i> | secretagogin, EF-hand calcium binding protein | 1.62 |
| <i>Gm10499</i> | predicted gene 10499 | 1.62 |
| <i>Lpar6</i> | lysophosphatidic acid receptor 6 | 1.62 |
| <i>LOC101056100</i> | centrin-4-like /// centrin 4 | 1.62 |
| <i>LOC102641190</i> | uncharacterized LOC102641190 | 1.62 |
| <i>Nap1l2</i> | nucleosome assembly protein 1-like 2 | 1.62 |
| <i>Map3k15</i> | mitogen-activated protein kinase kinase kinase 15 | 1.62 |
| <i>Inpp1</i> | inositol polyphosphate-1-phosphatase | 1.62 |

| | | |
|----------------------|---|------|
| 1700017B05Rik | RIKEN cDNA 1700017B05 gene | 1.61 |
| Pls3 | plastin 3 (T-isoform) | 1.61 |
| Ccdc85a | coiled-coil domain containing 85A | 1.61 |
| Akap2 | A kinase (PRKA) anchor protein 2 | 1.61 |
| Ocln | occludin | 1.61 |
| Tmem45b | transmembrane protein 45b | 1.61 |
| Igfbp7 | insulin-like growth factor binding protein 7 | 1.61 |
| Tcf21 | transcription factor 21 | 1.61 |
| Bcmo1 | beta-carotene 15,15-monooxygenase | 1.61 |
| Adora2a | adenosine A2a receptor | 1.61 |
| Arsj | arylsulfatase J | 1.61 |
| Nfkbia | nuclear factor of kappa light polypeptide gene enhancer in B cells inhibitor, alpha | 1.61 |
| 17549580 | <i>No associated gene</i> | 1.61 |
| Smoc1 | SPARC related modular calcium binding 1 | 1.61 |
| Gsta3 | glutathione S-transferase, alpha 3 | 1.61 |
| Jam3 | junction adhesion molecule 3 | 1.60 |
| Bdkrb2 | bradykinin receptor, beta 2 | 1.60 |
| Oas1b | 2'-5' oligoadenylate synthetase 1B | 1.60 |
| Pnmal2 | PNMA-like 2 | 1.60 |
| Trim30c | tripartite motif-containing 30C | 1.60 |
| Ccl8 | chemokine (C-C motif) ligand 8 | 1.60 |
| Tfpi | tissue factor pathway inhibitor | 1.60 |
| Foxp4 | forkhead box P4 | 1.60 |
| Lsp1 | lymphocyte specific 1 | 1.60 |
| 4930429F24Rik | RIKEN cDNA 4930429F24 gene | 1.60 |
| Mob3b | MOB kinase activator 3B | 1.60 |
| Abhd3 | abhydrolase domain containing 3 | 1.60 |
| Itm2c | integral membrane protein 2C | 1.60 |
| Tstd1 | thiosulfate sulfurtransferase (rhodanese)-like domain containing 1 | 1.60 |
| Arid5b | AT rich interactive domain 5B (MRF1-like) | 1.60 |
| Epb4.1l4b | erythrocyte protein band 4.1-like 4b | 1.59 |
| Ankrd50 | ankyrin repeat domain 50 | 1.59 |
| Arhgef3 | Rho guanine nucleotide exchange factor (GEF) 3 | 1.59 |
| Atox1 | antioxidant 1 copper chaperone | 1.59 |
| 17544689 | <i>No associated gene</i> | 1.59 |
| Pde7b | phosphodiesterase 7B | 1.59 |
| Cep70 | centrosomal protein 70 | 1.59 |
| Bcam | basal cell adhesion molecule | 1.59 |
| Gylt1b | glycosyltransferase-like 1B | 1.59 |
| Gabbr3 | gamma-aminobutyric acid (GABA) A receptor, subunit beta 3 | 1.59 |
| Slc35g1 | solute carrier family 35, member G1 | 1.59 |
| Lrp3 | low density lipoprotein receptor-related protein 3 | 1.59 |
| Rel1 | RELT-like 1 | 1.59 |

| | | |
|-----------------------------|---|------|
| <i>Elf4</i> | E74-like factor 4 (ets domain transcription factor) | 1.58 |
| <i>Rgs17</i> | regulator of G-protein signaling 17 | 1.58 |
| <i>Asic2</i> | acid-sensing (proton-gated) ion channel 2 | 1.58 |
| <i>Ccr7</i> | chemokine (C-C motif) receptor 7 | 1.58 |
| <i>Igh-VJ558</i> | immunoglobulin heavy chain (J558 family) | 1.58 |
| <i>Slc37a1</i> | solute carrier family 37 (glycerol-3-phosphate transporter), member 1 | 1.58 |
| <i>Ccng2</i> | cyclin G2 | 1.58 |
| <i>Ube2h</i> | ubiquitin-conjugating enzyme E2H | 1.58 |
| <i>Aplp1</i> | amyloid beta (A4) precursor-like protein 1 | 1.58 |
| <i>LOC102638331</i> | uncharacterized LOC102638331 | 1.58 |
| <i>17422688</i> | <i>No associated gene</i> | 1.58 |
| <i>Smpd3</i> | sphingomyelin phosphodiesterase 3, neutral | 1.58 |
| <i>E2f7</i> | E2F transcription factor 7 | 1.58 |
| <i>Pphln1</i> | periphilin 1 | 1.58 |
| <i>Aacs</i> | acetoacetyl-CoA synthetase | 1.58 |
| <i>Sh3bp4</i> | SH3-domain binding protein 4 | 1.57 |
| <i>Btd</i> | biotinidase | 1.57 |
| <i>Mkrn2os</i> | makorin, ring finger protein 2, opposite strand | 1.57 |
| <i>Gfpt2</i> | glutamine fructose-6-phosphate transaminase 2 | 1.57 |
| <i>Lamc1</i> | laminin, gamma 1 | 1.57 |
| <i>Olfml3</i> | olfactomedin-like 3 | 1.57 |
| <i>Mcm6</i> | minichromosome maintenance complex component 6 | 1.57 |
| <i>Tspo</i> | translocator protein | 1.57 |
| <i>Cds1</i> | CDP-diacylglycerol synthase 1 | 1.57 |
| <i>Man2b1</i> | mannosidase 2, alpha B1 | 1.57 |
| <i>Cited1</i> | Cbp/p300-interacting transactivator with Glu/Asp-rich carboxy-terminal domain 1 | 1.57 |
| <i>Efemp2</i> | epidermal growth factor-containing fibulin-like extracellular matrix protein 2 | 1.56 |
| <i>Ifi35</i> | interferon-induced protein 35 | 1.56 |
| <i>Pkd1l1</i> | polycystic kidney disease 1 like 1 | 1.56 |
| <i>Pik3r3</i> | phosphatidylinositol 3 kinase, regulatory subunit, polypeptide 3 (p55) | 1.56 |
| <i>Bag3</i> | BCL2-associated athanogene 3 | 1.56 |
| <i>4930524O07Rik</i> | RIKEN cDNA 4930524O07 gene | 1.56 |
| <i>Ogfr</i> | opioid growth factor receptor | 1.56 |
| <i>Scarb1</i> | scavenger receptor class B, member 1 | 1.56 |
| <i>Mtmr12</i> | myotubularin related protein 12 | 1.56 |
| <i>17512654</i> | <i>No associated gene</i> | 1.56 |
| <i>Gcnt2</i> | glucosaminyl (N-acetyl) transferase 2, I-branching enzyme | 1.56 |
| <i>Napepld</i> | N-acyl phosphatidylethanolamine phospholipase D | 1.56 |
| <i>Cd99l2</i> | CD99 antigen-like 2 | 1.56 |
| <i>Fam155a</i> | family with sequence similarity 155, member A | 1.56 |
| <i>Cxx1c</i> | CAAX box 1C | 1.56 |
| <i>Sdcbp2</i> | syndecan binding protein (syntenin) 2 | 1.56 |
| <i>Thbs1</i> | thrombospondin 1 | 1.56 |

| | | |
|----------------------|--|------|
| <i>Cbr3</i> | carbonyl reductase 3 | 1.56 |
| <i>Gadd45a</i> | growth arrest and DNA-damage-inducible 45 alpha | 1.56 |
| <i>Wee1</i> | WEE 1 homolog 1 (<i>S. pombe</i>) | 1.56 |
| <i>D230025D16Rik</i> | RIKEN cDNA D230025D16 gene | 1.56 |
| <i>Dnajc12</i> | DnaJ heat shock protein family (Hsp40) member C12 | 1.55 |
| <i>Antrx2</i> | anthrax toxin receptor 2 | 1.55 |
| <i>Map3k19</i> | mitogen-activated protein kinase kinase kinase 19 | 1.55 |
| <i>Tcrb-J</i> | T cell receptor beta, joining region | 1.55 |
| <i>Usp25</i> | ubiquitin specific peptidase 25 | 1.55 |
| <i>Il10ra</i> | interleukin 10 receptor, alpha | 1.55 |
| <i>Gpr116</i> | G protein-coupled receptor 116 | 1.55 |
| <i>Ndst2</i> | N-deacetylase/N-sulfotransferase (heparan glucosaminyl) 2 | 1.55 |
| <i>Cplx2</i> | complexin 2 | 1.55 |
| <i>Ldb1</i> | LIM domain binding 1 | 1.55 |
| <i>17548713</i> | <i>No associated gene</i> | 1.55 |
| <i>Idh1</i> | isocitrate dehydrogenase 1 (NADP+), soluble | 1.55 |
| <i>Zswim6</i> | zinc finger SWIM-type containing 6 | 1.55 |
| <i>Esm1</i> | endothelial cell-specific molecule 1 | 1.54 |
| <i>Lrig1</i> | leucine-rich repeats and immunoglobulin-like domains 1 | 1.54 |
| <i>Unc5a</i> | unc-5 netrin receptor A | 1.54 |
| <i>Map3k5</i> | mitogen-activated protein kinase kinase kinase 5 | 1.54 |
| <i>March11</i> | membrane-associated ring finger (C3HC4) 11 | 1.54 |
| <i>Glb1</i> | galactosidase, beta 1 | 1.54 |
| <i>Mical2</i> | microtubule associated monooxygenase, calponin and LIM domain containing 2 | 1.54 |
| <i>Rras</i> | related RAS viral (r-ras) oncogene | 1.54 |
| <i>Dapk1</i> | death associated protein kinase 1 | 1.54 |
| <i>Eci2</i> | enoyl-Coenzyme A delta isomerase 2 | 1.54 |
| <i>Shisa5</i> | shisa family member 5 | 1.54 |
| <i>Slc18b1</i> | solute carrier family 18, subfamily B, member 1 | 1.54 |
| <i>Plce1</i> | phospholipase C, epsilon 1 | 1.54 |
| <i>Plekhm1</i> | pleckstrin homology domain containing, family M (with RUN domain) member 1 | 1.54 |
| <i>Slc27a4</i> | solute carrier family 27 (fatty acid transporter), member 4 | 1.54 |
| <i>Kcnh6</i> | potassium voltage-gated channel, subfamily H (eag-related), member 6 | 1.54 |
| <i>Pgbd5</i> | piggyBac transposable element derived 5 | 1.54 |
| <i>Rph3al</i> | rabphilin 3A-like (without C2 domains) | 1.54 |
| <i>Traf1</i> | TRAF type zinc finger domain containing 1 | 1.53 |
| <i>1700025G04Rik</i> | RIKEN cDNA 1700025G04 gene | 1.53 |
| <i>Dusp5</i> | dual specificity phosphatase 5 | 1.53 |
| <i>Ulk1</i> | unc-51 like kinase 1 | 1.53 |
| <i>Sgk3</i> | serum/glucocorticoid regulated kinase 3 | 1.53 |
| <i>Rab8b</i> | RAB8B, member RAS oncogene family | 1.53 |
| <i>Ddx58</i> | DEAD (Asp-Glu-Ala-Asp) box polypeptide 58 | 1.53 |
| <i>Pax6</i> | paired box 6 | 1.53 |

| | | |
|----------------------|--|-------|
| Pvrl2 | poliovirus receptor-related 2 | 1.53 |
| Cmtm7 | CKLF-like MARVEL transmembrane domain containing 7 | 1.53 |
| Igsf1 | immunoglobulin superfamily, member 1 | 1.53 |
| Chst15 | carbohydrate (N-acetylgalactosamine 4-sulfate 6-O) sulfotransferase 15 | 1.53 |
| Samhd1 | SAM domain and HD domain, 1 | 1.53 |
| Gm23555 | predicted gene, 23555 | 1.53 |
| 17549672 | <i>No associated gene</i> | 1.53 |
| 17277267 | <i>No associated gene</i> | 1.52 |
| Lrrc9 | leucine rich repeat containing 9 | 1.52 |
| Ttc30b | tetratricopeptide repeat domain 30B | 1.52 |
| Dock8 | dedicator of cytokinesis 8 | 1.52 |
| Lpcat4 | lysophosphatidylcholine acyltransferase 4 | 1.52 |
| Abcb9 | ATP-binding cassette, sub-family B (MDR/TAP), member 9 | 1.52 |
| Lamb1 | laminin B1 | 1.52 |
| Rhoc | ras homolog family member C | 1.52 |
| Arhgap29 | Rho GTPase activating protein 29 | 1.52 |
| 1810044D09Rik | RIKEN cDNA 1810044D09 gene | 1.51 |
| Golm1 | golgi membrane protein 1 | 1.51 |
| Prdm5 | PR domain containing 5 | 1.51 |
| Procr | protein C receptor, endothelial | 1.51 |
| Nyap2 | neuronal tyrosine-phosphorylated phosphoinositide 3-kinase adaptor 2 | 1.51 |
| H2-K1 | histocompatibility 2, K1, K region | 1.51 |
| Galnt3 | UDP-N-acetyl-alpha-D-galactosamine:polypeptide N-acetylgalactosaminyltransferase 3 | 1.51 |
| Hsd17b11 | hydroxysteroid (17-beta) dehydrogenase 11 | 1.51 |
| Thbs3 | thrombospondin 3 | 1.51 |
| 17268817 | <i>No associated gene</i> | 1.51 |
| Taf1d | TATA-box binding protein associated factor, RNA polymerase I, D | 1.51 |
| Plxna1 | plexin A1 | 1.51 |
| Frmd4b | FERM domain containing 4B | 1.51 |
| Prkch | protein kinase C, eta | 1.51 |
| Ammecr1 | Alport syndrome, mental retardation, midface hypoplasia and elliptocytosis chromosomal region gene 1 | 1.51 |
| Sdc2 | syndecan 2 | 1.51 |
| Irf1 | interferon regulatory factor 1 | 1.51 |
| 1110058L19Rik | RIKEN cDNA 1110058L19 gene | 1.51 |
| Casp8 | caspase 8 | 1.51 |
| Eml1 | echinoderm microtubule associated protein like 1 | 1.51 |
| Arhgef28 | Rho guanine nucleotide exchange factor (GEF) 28 | 1.51 |
| Ambp | alpha 1 microglobulin/bikunin | 1.51 |
| Cpxm1 | carboxypeptidase X 1 (M14 family) | 1.51 |
| Lyplal1 | lysophospholipase-like 1 | -1.51 |
| Gm12059 | predicted gene 12059 | -1.51 |
| Unc13a | unc-13 homolog A (C. elegans) | -1.51 |
| Dgkg | diacylglycerol kinase, gamma | -1.51 |

| | | |
|----------------------|---|-------|
| <i>Raph1</i> | Ras association (RalGDS/AF-6) and pleckstrin homology domains 1 | -1.51 |
| <i>Acot13</i> | acyl-CoA thioesterase 13 | -1.51 |
| <i>Ptpru</i> | protein tyrosine phosphatase, receptor type, U | -1.51 |
| <i>LOC102632031</i> | predicted gene 15728 | -1.51 |
| <i>Larp1b</i> | La ribonucleoprotein domain family, member 1B | -1.51 |
| <i>Cyp4f39</i> | cytochrome P450, family 4, subfamily f, polypeptide 39 | -1.51 |
| <i>Tenn2</i> | teneurin transmembrane protein 2 | -1.51 |
| <i>Gm23962</i> | predicted gene, 23962 | -1.52 |
| <i>Grb10</i> | growth factor receptor bound protein 10 | -1.52 |
| <i>Naaa</i> | N-acylethanolamine acid amidase | -1.52 |
| <i>LOC102632394</i> | predicted gene, 26910 | -1.52 |
| <i>Lrrc16b</i> | leucine rich repeat containing 16B | -1.52 |
| <i>Pofut2</i> | protein O-fucosyltransferase 2 | -1.52 |
| <i>9430021M05Rik</i> | RIKEN cDNA 9430021M05 gene | -1.52 |
| <i>Abhd17c</i> | abhydrolase domain containing 17C | -1.52 |
| <i>Fam110b</i> | family with sequence similarity 110, member B | -1.52 |
| <i>Tcea1</i> | transcription elongation factor A (SII) 1 | -1.52 |
| <i>Gramd3</i> | GRAM domain containing 3 | -1.52 |
| <i>Cad</i> | carbamoyl-phosphate synthetase 2, aspartate transcarbamylase, and dihydroorotase | -1.52 |
| <i>Gm14920</i> | predicted pseudogene 14920 | -1.52 |
| <i>Mettl7a1</i> | methyltransferase like 7A1 | -1.52 |
| <i>Tmem97</i> | transmembrane protein 97 | -1.52 |
| <i>Mars</i> | methionine-tRNA synthetase | -1.52 |
| <i>Ascc2</i> | activating signal cointegrator 1 complex subunit 2 | -1.53 |
| <i>Fkbp5</i> | FK506 binding protein 5 | -1.53 |
| <i>Gm20071</i> | predicted gene, 20071 | -1.53 |
| <i>Gm16440</i> | predicted gene 16440 | -1.53 |
| <i>4931403G20Rik</i> | RIKEN cDNA 4931403G20 gene | -1.53 |
| <i>Ltv1</i> | LTV1 ribosome biogenesis factor | -1.53 |
| <i>6430548M08Rik</i> | RIKEN cDNA 6430548M08 gene | -1.53 |
| <i>Greb1l</i> | growth regulation by estrogen in breast cancer-like | -1.53 |
| <i>Jade1</i> | jade family PHD finger 1 | -1.53 |
| <i>Cdc14b</i> | CDC14 cell division cycle 14B | -1.53 |
| <i>Igh-VX24</i> | immunoglobulin heavy chain (X24 family) | -1.53 |
| <i>Aanat</i> | arylalkylamine N-acetyltransferase | -1.53 |
| <i>Mthfd2</i> | methylenetetrahydrofolate dehydrogenase (NAD+ dependent), methenyltetrahydrofolate cyclohydrolase | -1.53 |
| <i>Gm9767</i> | predicted gene 9767 | -1.53 |
| <i>Ighv9-4</i> | immunoglobulin heavy variable 9-4 | -1.53 |
| <i>AK129341</i> | cDNA sequence AK129341 | -1.54 |
| <i>Psmg2</i> | proteasome (prosome, macropain) assembly chaperone 2 | -1.54 |
| <i>17216244</i> | <i>No associated gene</i> | -1.54 |
| <i>Fam206a</i> | family with sequence similarity 206, member A | -1.54 |
| <i>Tma16</i> | translation machinery associated 16 | -1.54 |

| | | |
|-----------------------------|---|-------|
| <i>Reps2</i> | RALBP1 associated Eps domain containing protein 2 | -1.54 |
| <i>Prdm10</i> | PR domain containing 10 | -1.54 |
| <i>Camk1g</i> | calcium/calmodulin-dependent protein kinase I gamma | -1.54 |
| <i>17442526</i> | <i>No associated gene</i> | -1.54 |
| <i>Msi1</i> | musashi RNA-binding protein 1 | -1.55 |
| <i>Rassf4</i> | Ras association (RalGDS/AF-6) domain family member 4 | -1.55 |
| <i>Gm17232</i> | predicted gene 17232 | -1.55 |
| <i>Per2</i> | period circadian clock 2 | -1.55 |
| <i>Gm6594</i> | predicted pseudogene 6594 | -1.55 |
| <i>Slc6a17</i> | solute carrier family 6 (neurotransmitter transporter), member 17 | -1.55 |
| <i>A930011G23Rik</i> | RIKEN cDNA A930011G23 gene | -1.55 |
| <i>17547596</i> | <i>No associated gene</i> | -1.55 |
| <i>LOC102634708</i> | predicted gene 11695 | -1.55 |
| <i>Robo2</i> | roundabout guidance receptor 2 | -1.55 |
| <i>Gm3558</i> | predicted gene 3558 | -1.55 |
| <i>Pstpip2</i> | proline-serine-threonine phosphatase-interacting protein 2 | -1.55 |
| <i>Wsb2</i> | WD repeat and SOCS box-containing 2 | -1.55 |
| <i>Dnaja3</i> | DnaJ heat shock protein family (Hsp40) member A3 | -1.56 |
| <i>Tmem107</i> | transmembrane protein 107 | -1.56 |
| <i>9330102E08Rik</i> | RIKEN cDNA 9330102E08 gene | -1.56 |
| <i>Sept9</i> | septin 9 | -1.56 |
| <i>AU022751</i> | expressed sequence AU022751 | -1.56 |
| <i>Rhox4c</i> | reproductive homeobox 4C | -1.56 |
| <i>Bag2</i> | BCL2-associated athanogene 2 | -1.56 |
| <i>Hdac4</i> | histone deacetylase 4 | -1.56 |
| <i>Deb1</i> | differentially expressed in B16F10 1 | -1.57 |
| <i>Mir329</i> | microRNA 329 | -1.57 |
| <i>Aard</i> | alanine and arginine rich domain containing protein | -1.57 |
| <i>Kbtbd7</i> | kelch repeat and BTB (POZ) domain containing 7 | -1.57 |
| <i>17290695</i> | <i>No associated gene</i> | -1.57 |
| <i>Hist1h2aa</i> | histone cluster 1, H2aa | -1.57 |
| <i>Car15</i> | carbonic anhydrase 15 | -1.57 |
| <i>A830082N09Rik</i> | RIKEN cDNA A830082N09 gene | -1.57 |
| <i>Slc25a15</i> | solute carrier family 25 (mitochondrial carrier ornithine transporter), member 15 | -1.57 |
| <i>Ankrd10</i> | ankyrin repeat domain 10 | -1.57 |
| <i>Gm25375</i> | predicted gene, 25375 | -1.57 |
| <i>Tmod2</i> | tropomodulin 2 | -1.57 |
| <i>Copz2</i> | coatamer protein complex, subunit zeta 2 | -1.58 |
| <i>Siva1</i> | SIVA1, apoptosis-inducing factor | -1.58 |
| <i>Gm22889</i> | predicted gene, 22889 | -1.58 |
| <i>Gm10406</i> | predicted gene 10406 | -1.58 |
| <i>D730003I15Rik</i> | RIKEN cDNA D730003I15 gene | -1.58 |
| <i>Rapgef4os2</i> | Rap guanine nucleotide exchange factor (GEF) 4, opposite strand 2 | -1.58 |

| | | |
|--------------------------------------|--|-------|
| <i>Neto2</i> | neuropilin (NRP) and tolloid (TLL)-like 2 | -1.58 |
| <i>Gne</i> | glucosamine (UDP-N-acetyl)-2-epimerase/N-acetylmannosamine kinase | -1.58 |
| <i>Xpot</i> | exportin, tRNA (nuclear export receptor for tRNAs) | -1.58 |
| <i>Fa2h</i> | fatty acid 2-hydroxylase | -1.58 |
| <i>Sel1l</i> | sel-1 suppressor of lin-12-like (<i>C. elegans</i>) | -1.59 |
| <i>Abat</i> | 4-aminobutyrate aminotransferase | -1.59 |
| <i>Sars</i> | seryl-aminoacyl-tRNA synthetase | -1.59 |
| <i>Gm12060</i> | predicted gene 12060 | -1.59 |
| <i>Agl</i> | amylase-1,6-glucosidase, 4-alpha-glucanotransferase | -1.59 |
| <i>A430078I02Rik</i> | RIKEN cDNA A430078I02 gene | -1.60 |
| <i>Uhrf1bp1</i> | UHRF1 (ICBP90) binding protein 1 | -1.60 |
| <i>D1Ert448e</i> | DNA segment, Chr 1, ERATO Doi 448, expressed | -1.60 |
| <i>Gm23974</i> | predicted gene, 23974 | -1.60 |
| <i>Tmem150cos</i> | transmembrane protein 150C, opposite strand | -1.60 |
| <i>Galns</i> | galactosamine (N-acetyl)-6-sulfate sulfatase | -1.60 |
| <i>Gm24409</i> | predicted gene, 24409 | -1.60 |
| <i>Gm26148</i> | predicted gene, 26148 | -1.60 |
| <i>Uck2</i> | uridine-cytidine kinase 2 | -1.60 |
| <i>Ankhd1</i> | ankyrin repeat and KH domain containing 1 | -1.60 |
| <i>Vmn2r54</i> | vomer nasal 2, receptor 54 | -1.60 |
| <i>Cbx4</i> | chromobox 4 | -1.61 |
| <i>Crhr1</i> | corticotropin releasing hormone receptor 1 | -1.61 |
| <i>Esrp1</i> | epithelial splicing regulatory protein 1 | -1.61 |
| <i>Eif3c</i> | eukaryotic translation initiation factor 3, subunit C | -1.61 |
| <i>Epb4.1</i> | erythrocyte protein band 4.1 | -1.61 |
| <i>Cttnbp2</i> | cortactin binding protein 2 | -1.61 |
| <i>Cry1l</i> | crystallin, lambda 1 | -1.61 |
| <i>Tubb2b</i> | tubulin, beta 2B class IIB | -1.61 |
| <i>LOC102641575</i> | predicted gene 13507 | -1.61 |
| <i>Tmem141</i> | transmembrane protein 141 | -1.61 |
| <i>Cyb5b</i> | cytochrome b5 type B | -1.61 |
| <i>Idua</i> | iduronidase, alpha-L- | -1.62 |
| <i>Pi4k2a</i> | phosphatidylinositol 4-kinase type 2 alpha | -1.62 |
| <i>Pitrm1</i> | pitrilysin metalloproteinase 1 | -1.62 |
| <i>Hsd17b13</i> | hydroxysteroid (17-beta) dehydrogenase 13 | -1.62 |
| <i>Tatdn3</i> | TatD DNase domain containing 3 | -1.62 |
| <i>Cys1</i> | cystin 1 | -1.63 |
| <i>Mpc1</i> | mitochondrial pyruvate carrier 1 | -1.63 |
| <i>Bcl2l1</i> | BCL2-like 1 | -1.63 |
| <i>Gcat</i> | glycine C-acetyltransferase (2-amino-3-ketobutyrate-coenzyme A ligase) | -1.63 |
| <i>GENSCAN0000000057</i> <i>5</i> | <i>No associated gene</i> | -1.63 |
| <i>Cyp20a1</i> | cytochrome P450, family 20, subfamily a, polypeptide 1 | -1.63 |
| <i>Sdf2l1</i> | stromal cell-derived factor 2-like 1 | -1.63 |

| | | |
|---------------------|--|-------|
| <i>Hax1</i> | HCLS1 associated X-1 | -1.63 |
| <i>Erc2</i> | ELKS/RAB6-interacting/CAST family member 2 | -1.64 |
| <i>Ern1</i> | endoplasmic reticulum (ER) to nucleus signalling 1 | -1.64 |
| <i>LOC102637737</i> | predicted gene 10010 | -1.64 |
| <i>Gm6484</i> | predicted gene 6484 | -1.64 |
| <i>Arhgef2</i> | rho/rac guanine nucleotide exchange factor (GEF) 2 | -1.64 |
| <i>Aox1</i> | aldehyde oxidase 1 | -1.64 |
| <i>Abca5</i> | ATP-binding cassette, sub-family A (ABC1), member 5 | -1.64 |
| <i>Gm25908</i> | predicted gene, 25908 | -1.64 |
| <i>Slc7a1</i> | solute carrier family 7 (cationic amino acid transporter, y+ system), member 1 | -1.65 |
| <i>Timm8a1</i> | translocase of inner mitochondrial membrane 8A1 | -1.65 |
| <i>Rpp25</i> | ribonuclease P/MRP 25 subunit | -1.65 |
| <i>Zcchc12</i> | zinc finger, CCHC domain containing 12 | -1.65 |
| <i>Glp1r</i> | glucagon-like peptide 1 receptor | -1.65 |
| <i>Gm24443</i> | predicted gene, 24443 | -1.65 |
| <i>Snx8</i> | sorting nexin 8 | -1.65 |
| <i>Ccnd2</i> | cyclin D2 | -1.65 |
| <i>Cars</i> | cysteinyl-tRNA synthetase | -1.65 |
| <i>Ccdc130</i> | coiled-coil domain containing 130 | -1.65 |
| <i>Eya1</i> | EYA transcriptional coactivator and phosphatase 1 | -1.66 |
| <i>Nudt7</i> | nudix (nucleoside diphosphate linked moiety X)-type motif 7 | -1.66 |
| <i>Trav16n</i> | T cell receptor alpha variable 16n | -1.66 |
| <i>Lrfn4</i> | leucine rich repeat and fibronectin type III domain containing 4 | -1.66 |
| <i>Folr1</i> | folate receptor 1 (adult) | -1.66 |
| <i>Atp2a2</i> | ATPase, Ca ⁺⁺ transporting, cardiac muscle, slow twitch 2 | -1.66 |
| <i>Mir149</i> | microRNA 149 | -1.66 |
| <i>Cyb5r2</i> | cytochrome b5 reductase 2 | -1.66 |
| <i>LOC102635342</i> | predicted gene 15415 | -1.67 |
| <i>Th</i> | tyrosine hydroxylase | -1.67 |
| <i>Scube2</i> | signal peptide, CUB domain, EGF-like 2 | -1.67 |
| <i>Ccdc47</i> | coiled-coil domain containing 47 | -1.67 |
| <i>Dhdk1</i> | dehydrogenase E1 and transketolase domain containing 1 | -1.67 |
| <i>Isoc2b</i> | isochorismatase domain containing 2b | -1.67 |
| <i>Rab39b</i> | RAB39B, member RAS oncogene family | -1.67 |
| <i>Nrf1</i> | nuclear respiratory factor 1 | -1.67 |
| <i>Snord2</i> | small nucleolar RNA, C/D box 2 | -1.67 |
| <i>Tenn4</i> | teneurin transmembrane protein 4 | -1.67 |
| <i>Ivd</i> | isovaleryl coenzyme A dehydrogenase | -1.68 |
| <i>Gstm4</i> | glutathione S-transferase, mu 4 | -1.68 |
| <i>Yars</i> | tyrosyl-tRNA synthetase | -1.68 |
| <i>Ap3b2</i> | adaptor-related protein complex 3, beta 2 subunit | -1.68 |
| <i>Fam135a</i> | family with sequence similarity 135, member A | -1.68 |
| <i>Lgals6</i> | lectin, galactose binding, soluble 6 | -1.68 |

| | | |
|-----------------------------|--|-------|
| <i>Ccdc173</i> | coiled-coil domain containing 173 | -1.68 |
| <i>1190002F15Rik</i> | RIKEN cDNA 1190002F15 gene | -1.68 |
| <i>A930024N18Rik</i> | RIKEN cDNA A930024N18 gene | -1.69 |
| <i>Gm26584</i> | predicted gene, 26584 | -1.69 |
| <i>Ttc8</i> | tetratricopeptide repeat domain 8 | -1.69 |
| <i>Npas3</i> | neuronal PAS domain protein 3 | -1.69 |
| <i>Snord91a</i> | small nucleolar RNA, C/D box 91A | -1.69 |
| <i>Pck2</i> | phosphoenolpyruvate carboxykinase 2 (mitochondrial) | -1.69 |
| <i>Sqle</i> | squalene epoxidase | -1.70 |
| <i>Coro7</i> | coronin 7 | -1.70 |
| <i>Fh1</i> | fumarate hydratase 1 | -1.70 |
| <i>LOC106740</i> | PHD finger protein 10 | -1.70 |
| <i>Lars</i> | leucyl-tRNA synthetase | -1.70 |
| <i>Ing2</i> | inhibitor of growth family, member 2 | -1.70 |
| <i>Nup160</i> | nucleoporin 160 | -1.70 |
| <i>NONMMUT011248</i> | <i>No associated gene</i> | -1.70 |
| <i>LOC102641857</i> | RIKEN cDNA D630024D03 gene | -1.70 |
| <i>Asns</i> | asparagine synthetase | -1.70 |
| <i>Ift172</i> | intraflagellar transport 172 | -1.70 |
| <i>Mpp6</i> | membrane protein, palmitoylated 6 (MAGUK p55 subfamily member 6) | -1.71 |
| <i>Mir1898</i> | microRNA 1898 | -1.71 |
| <i>4932702P03Rik</i> | RIKEN cDNA 4932702P03 gene | -1.71 |
| <i>Prdm8</i> | PR domain containing 8 | -1.71 |
| <i>17408273</i> | <i>No associated gene</i> | -1.71 |
| <i>17489508</i> | <i>No associated gene</i> | -1.71 |
| <i>Pcdh15</i> | protocadherin 15 | -1.71 |
| <i>Cebpg</i> | CCAAT/enhancer binding protein (C/EBP), gamma | -1.71 |
| <i>Ero1lb</i> | ERO1-like beta (<i>S. cerevisiae</i>) | -1.71 |
| <i>Gars</i> | glycyl-tRNA synthetase | -1.71 |
| <i>Aldh18a1</i> | aldehyde dehydrogenase 18 family, member A1 | -1.72 |
| <i>Dock10</i> | dedicator of cytokinesis 10 | -1.72 |
| <i>Trim37</i> | tripartite motif-containing 37 | -1.72 |
| <i>Gm26508</i> | predicted gene, 26508 | -1.73 |
| <i>Gnpnat1</i> | glucosamine-phosphate N-acetyltransferase 1 | -1.73 |
| <i>Entpd3</i> | ectonucleoside triphosphate diphosphohydrolase 3 | -1.73 |
| <i>Slc7a5</i> | solute carrier family 7 (cationic amino acid transporter, y+ system), member 5 | -1.73 |
| <i>Ero1l</i> | ERO1-like (<i>S. cerevisiae</i>) | -1.73 |
| <i>Dnajc21</i> | DnaJ heat shock protein family (Hsp40) member C21 | -1.73 |
| <i>9030025P20Rik</i> | RIKEN cDNA 9030025P20 gene | -1.73 |
| <i>17549652</i> | <i>No associated gene</i> | -1.73 |
| <i>Rnf186</i> | ring finger protein 186 | -1.74 |
| <i>Gm3286</i> | predicted gene 3286 | -1.74 |
| <i>Scnn1a</i> | sodium channel, nonvoltage-gated 1 alpha | -1.74 |

| | | |
|----------------------|---|-------|
| 2310040G24Rik | RIKEN cDNA 2310040G24 gene | -1.74 |
| Pde5a | phosphodiesterase 5A, cGMP-specific | -1.75 |
| Flnb | filamin, beta | -1.75 |
| Iars | isoleucine-tRNA synthetase | -1.75 |
| Eml5 | echinoderm microtubule associated protein like 5 | -1.75 |
| Igsf11 | immunoglobulin superfamily, member 11 | -1.75 |
| Tmem8 | transmembrane protein 8 (five membrane-spanning domains) | -1.75 |
| Rhobtb2 | Rho-related BTB domain containing 2 | -1.76 |
| 9530034E10Rik | RIKEN cDNA 9530034E10 gene | -1.76 |
| Abcc4 | ATP-binding cassette, sub-family C (CFTR/MRP), member 4 | -1.76 |
| Atp7a | ATPase, Cu ⁺⁺ transporting, alpha polypeptide | -1.76 |
| Fabp3-ps1 | fatty acid binding protein 3, muscle and heart, pseudogene 1 | -1.76 |
| Dus2 | dihydrouridine synthase 2 | -1.77 |
| Ghitm | growth hormone inducible transmembrane protein | -1.77 |
| Nostrin | nitric oxide synthase trafficker | -1.77 |
| Gm26407 | predicted gene, 26407 | -1.77 |
| Rny1 | RNA, Y1 small cytoplasmic, Ro-associated | -1.77 |
| Hspa9 | heat shock protein 9 | -1.78 |
| Rwdd4a | RWD domain containing 4A | -1.78 |
| Ttc28 | tetratricopeptide repeat domain 28 | -1.78 |
| Gm11454 | predicted gene 11454 | -1.78 |
| Pgm3 | phosphoglucomutase 3 | -1.78 |
| Dennd4c | DENN/MADD domain containing 4C | -1.78 |
| Lrrc10b | leucine rich repeat containing 10B | -1.79 |
| Gm15559 | predicted gene 15559 | -1.79 |
| Ica1l | islet cell autoantigen 1-like | -1.79 |
| Zyg11b | zyg-11 family member B, cell cycle regulator | -1.79 |
| Agap1 | ArfGAP with GTPase domain, ankyrin repeat and PH domain 1 | -1.79 |
| Hist2h4 | histone cluster 2, H4 | -1.80 |
| Ptptr | protein tyrosine phosphatase, receptor type, T | -1.80 |
| Fmn1 | formin 1 | -1.80 |
| F2r1l | coagulation factor II (thrombin) receptor-like 1 | -1.80 |
| Vdr | vitamin D receptor | -1.80 |
| 17548581 | <i>No associated gene</i> | -1.80 |
| Dach2 | dachshund 2 (Drosophila) | -1.80 |
| Slc2a2 | solute carrier family 2 (facilitated glucose transporter), member 2 | -1.80 |
| Nme4 | NME/NM23 nucleoside diphosphate kinase 4 | -1.80 |
| Dlgap1 | discs, large (Drosophila) homolog-associated protein 1 | -1.80 |
| Mir143 | microRNA 143 | -1.81 |
| Got1 | glutamic-oxaloacetic transaminase 1, soluble | -1.81 |
| Rapgef4 | Rap guanine nucleotide exchange factor (GEF) 4 | -1.81 |
| Ins1 | insulin I | -1.81 |
| Scd2 | stearoyl-Coenzyme A desaturase 2 | -1.81 |
| Rhbdd1 | rhomboid domain containing 1 | -1.82 |

| | | |
|-----------------|--|-------|
| <i>Sv2a</i> | synaptic vesicle glycoprotein 2 a | -1.82 |
| <i>Gm23609</i> | predicted gene, 23609 | -1.82 |
| <i>Snai2</i> | snail family zinc finger 2 | -1.83 |
| <i>Il6st</i> | interleukin 6 signal transducer | -1.83 |
| <i>Gfra4</i> | glial cell line derived neurotrophic factor family receptor alpha 4 | -1.83 |
| <i>Gm12120</i> | predicted gene 12120 | -1.83 |
| <i>Gpt2</i> | glutamic pyruvate transaminase (alanine aminotransferase) 2 | -1.84 |
| <i>Syce2</i> | synaptonemal complex central element protein 2 | -1.84 |
| <i>17307425</i> | <i>No associated gene</i> | -1.84 |
| <i>Gm13421</i> | predicted gene 13421 | -1.85 |
| <i>Cln6</i> | ceroid-lipofuscinosis, neuronal 6 | -1.85 |
| <i>17299196</i> | <i>No associated gene</i> | -1.85 |
| <i>Gcgr</i> | glucagon receptor | -1.85 |
| <i>Oxct1</i> | 3-oxoacid CoA transferase 1 | -1.86 |
| <i>Lrrfip2</i> | leucine rich repeat (in FLII) interacting protein 2 | -1.86 |
| <i>Tars</i> | threonyl-tRNA synthetase | -1.86 |
| <i>Zmynd10</i> | zinc finger, MYND domain containing 10 | -1.86 |
| <i>Fam101b</i> | family with sequence similarity 101, member B | -1.86 |
| <i>Vipr1</i> | vasoactive intestinal peptide receptor 1 | -1.86 |
| <i>Gm10653</i> | predicted gene 10653 | -1.86 |
| <i>Ky</i> | kyphoscoliosis peptidase | -1.87 |
| <i>Gm6356</i> | predicted gene 6356 | -1.87 |
| <i>Gpm6a</i> | glycoprotein m6a | -1.88 |
| <i>Ntrk2</i> | neurotrophic tyrosine kinase, receptor, type 2 | -1.88 |
| <i>Gm5797</i> | predicted gene 5797 | -1.88 |
| <i>Hmox1</i> | heme oxygenase 1 | -1.88 |
| <i>Tmem206</i> | transmembrane protein 206 | -1.88 |
| <i>Prkcb</i> | protein kinase C, beta | -1.88 |
| <i>Tubb1</i> | tubulin, beta 1 class VI | -1.88 |
| <i>Hs3st6</i> | heparan sulfate (glucosamine) 3-O-sulfotransferase 6 | -1.89 |
| <i>Cabp1</i> | calcium binding protein 1 | -1.89 |
| <i>Cpeb1</i> | cytoplasmic polyadenylation element binding protein 1 | -1.89 |
| <i>Grip1</i> | glutamate receptor interacting protein 1 | -1.89 |
| <i>Reep6</i> | receptor accessory protein 6 | -1.90 |
| <i>Cdh4</i> | cadherin 4 | -1.90 |
| <i>Slc1a4</i> | solute carrier family 1 (glutamate/neutral amino acid transporter), member 4 | -1.91 |
| <i>Scel</i> | sciellin | -1.91 |
| <i>Sec16b</i> | SEC16 homolog B (<i>S. cerevisiae</i>) | -1.92 |
| <i>Gtpbp2</i> | GTP binding protein 2 | -1.92 |
| <i>Tnfrsf23</i> | tumor necrosis factor receptor superfamily, member 23 | -1.92 |
| <i>Phactr1</i> | phosphatase and actin regulator 1 | -1.92 |
| <i>Coro2b</i> | coronin, actin binding protein, 2B | -1.93 |
| <i>Gmpr</i> | guanosine monophosphate reductase | -1.94 |
| <i>Pappa2</i> | pappalysin 2 | -1.95 |

| | | |
|----------------------|--|-------|
| Gm22581 | predicted gene, 22581 | -1.95 |
| Mlph | melanophilin | -1.97 |
| Eif4ebp1 | eukaryotic translation initiation factor 4E binding protein 1 | -1.97 |
| Tmem65 | transmembrane protein 65 | -1.97 |
| Pcsk2os2 | proprotein convertase subtilisin/kexin type 2, opposite strand 2 | -1.97 |
| Slc7a3 | solute carrier family 7 (cationic amino acid transporter, y+ system), member 3 | -1.98 |
| Dusp10 | dual specificity phosphatase 10 | -1.98 |
| Gdap2 | ganglioside-induced differentiation-associated-protein 2 | -1.98 |
| Fam107a | family with sequence similarity 107, member A | -1.98 |
| Erlin1 | ER lipid raft associated 1 | -1.98 |
| 17547897 | <i>No associated gene</i> | -1.99 |
| Morn4 | MORN repeat containing 4 | -1.99 |
| 17534213 | <i>No associated gene</i> | -1.99 |
| Gm7241 | predicted pseudogene 7241 | -1.99 |
| Fam129a | family with sequence similarity 129, member A | -1.99 |
| Lrp5 | low density lipoprotein receptor-related protein 5 | -1.99 |
| Gm8281 | predicted gene, 8281 | -2.00 |
| Taf15 | TATA-box binding protein associated factor 15 | -2.01 |
| Fibin | fin bud initiation factor homolog (zebrafish) | -2.02 |
| Pfkfb2 | 6-phosphofructo-2-kinase/fructose-2,6-biphosphatase 2 | -2.03 |
| 17547971 | <i>No associated gene</i> | -2.03 |
| LOC102639013 | predicted gene 14246 | -2.03 |
| Pycr1 | pyrroline-5-carboxylate reductase 1 | -2.04 |
| Atp4a | ATPase, H+/K+ exchanging, gastric, alpha polypeptide | -2.05 |
| Fmo1 | flavin containing monooxygenase 1 | -2.05 |
| BB557941 | expressed sequence BB557941 | -2.05 |
| Tbc1d31 | TBC1 domain family, member 31 | -2.06 |
| 1700084E18Rik | RIKEN cDNA 1700084E18 gene | -2.06 |
| Cdh7 | cadherin 7, type 2 | -2.06 |
| Olfir887 | olfactory receptor 887 | -2.07 |
| Gm22043 | predicted gene, 22043 | -2.09 |
| Nr1d1 | nuclear receptor subfamily 1, group D, member 1 | -2.09 |
| Scpep1 | serine carboxypeptidase 1 | -2.09 |
| Chac1 | ChaC, cation transport regulator 1 | -2.09 |
| Aldh5a1 | aldehyde dehydrogenase family 5, subfamily A1 | -2.09 |
| Wls | wntless homolog (Drosophila) | -2.10 |
| Dyrk3 | dual-specificity tyrosine-(Y)-phosphorylation regulated kinase 3 | -2.12 |
| Slco1a5 | solute carrier organic anion transporter family, member 1a5 | -2.12 |
| Glce | glucuronyl C5-epimerase | -2.12 |
| Mns1 | meiosis-specific nuclear structural protein 1 | -2.13 |
| Fhdc1 | FH2 domain containing 1 | -2.14 |
| 2610042L04Rik | RIKEN cDNA 2610042L04 gene | -2.15 |
| Gm4791 | predicted gene 4791 | -2.15 |

| | | |
|----------------------|--|-------|
| Gm12119 | predicted gene 12119 | -2.15 |
| Star | steroidogenic acute regulatory protein | -2.15 |
| Adm2 | adrenomedullin 2 | -2.17 |
| Kcnip1 | Kv channel-interacting protein 1 | -2.17 |
| Gm15414 | predicted gene 15414 | -2.18 |
| Trpm5 | transient receptor potential cation channel, subfamily M, member 5 | -2.18 |
| Sv2b | synaptic vesicle glycoprotein 2 b | -2.19 |
| LOC102633750 | zinc finger protein 14-like | -2.19 |
| 17548723 | <i>No associated gene</i> | -2.20 |
| Gm10021 | predicted gene 10021 | -2.20 |
| Edn3 | endothelin 3 | -2.21 |
| Mpp3 | membrane protein, palmitoylated 3 (MAGUK p55 subfamily member 3) | -2.21 |
| Fam159a | family with sequence similarity 159, member A | -2.22 |
| Gcnt1 | glucosaminyl (N-acetyl) transferase 1, core 2 | -2.23 |
| Rragd | Ras-related GTP binding D | -2.24 |
| Asb4 | ankyrin repeat and SOCS box-containing 4 | -2.24 |
| Mir5133 | microRNA 5133 | -2.25 |
| Ccdc6 | coiled-coil domain containing 6 | -2.25 |
| Grin1os | glutamate receptor, ionotropic, NMDA1 (zeta 1), opposite strand | -2.26 |
| Eprs | glutamyl-prolyl-tRNA synthetase | -2.28 |
| Spock1 | sparc/osteonectin, cwcv and kazal-like domains proteoglycan 1 | -2.29 |
| Abcb4 | ATP-binding cassette, sub-family B (MDR/TAP), member 4 | -2.31 |
| Gm4419 | predicted gene 4419 | -2.31 |
| Muc4 | mucin 4 | -2.32 |
| Olfm4 | olfactomedin 4 | -2.32 |
| Etv5 | ets variant 5 | -2.33 |
| Gm10941 | predicted gene 10941 | -2.33 |
| Gpr137b-ps | G protein-coupled receptor 137B, pseudogene | -2.37 |
| Gnpda1 | glucosamine-6-phosphate deaminase 1 | -2.38 |
| Avpi1 | arginine vasopressin-induced 1 | -2.38 |
| Vldlr | very low density lipoprotein receptor | -2.38 |
| 2210019I11Rik | RIKEN cDNA 2210019I11 gene | -2.39 |
| Psat1 | phosphoserine aminotransferase 1 | -2.39 |
| Psph | phosphoserine phosphatase | -2.41 |
| Lonp1 | lon peptidase 1, mitochondrial | -2.42 |
| 4930550C14Rik | RIKEN cDNA 4930550C14 gene | -2.44 |
| Gm25099 | predicted gene, 25099 | -2.44 |
| 17547943 | <i>No associated gene</i> | -2.46 |
| Skap1 | src family associated phosphoprotein 1 | -2.47 |
| Itpkb | inositol 1,4,5-trisphosphate 3-kinase B | -2.47 |
| Papss2 | 3'-phosphoadenosine 5'-phosphosulfate synthase 2 | -2.48 |
| P2ry12 | purinergic receptor P2Y, G-protein coupled 12 | -2.49 |
| A530058N18Rik | RIKEN cDNA A530058N18 gene | -2.49 |
| Gm6999 | predicted gene 6999 | -2.52 |

| | | |
|----------------------|---|-------|
| <i>Gm15407</i> | predicted gene 15407 | -2.53 |
| <i>Angptl6</i> | angiopoietin-like 6 | -2.53 |
| <i>Gpr158</i> | G protein-coupled receptor 158 | -2.57 |
| <i>Maob</i> | monoamine oxidase B | -2.60 |
| <i>Ucn3</i> | urocortin 3 | -2.63 |
| <i>Adora1</i> | adenosine A1 receptor | -2.67 |
| <i>Sult1c2</i> | sulfotransferase family, cytosolic, 1C, member 2 | -2.69 |
| <i>Tfrc</i> | transferrin receptor | -2.72 |
| <i>Ppp1r15a</i> | protein phosphatase 1, regulatory (inhibitor) subunit 15A | -2.72 |
| <i>Dsp</i> | desmoplakin | -2.74 |
| <i>Pcx</i> | pyruvate carboxylase | -2.74 |
| <i>Slco1a6</i> | solute carrier organic anion transporter family, member 1a6 | -2.75 |
| <i>Cntfr</i> | ciliary neurotrophic factor receptor | -2.80 |
| <i>Cyb5r1</i> | cytochrome b5 reductase 1 | -2.80 |
| <i>Gm23134</i> | predicted gene, 23134 | -2.81 |
| <i>Itgb8</i> | integrin beta 8 | -2.84 |
| <i>Syt14</i> | synaptotagmin-like 4 | -2.90 |
| <i>Nnat</i> | neuronatin | -2.93 |
| <i>Grin1</i> | glutamate receptor, ionotropic, NMDA1 (zeta 1) | -2.97 |
| <i>Calml4</i> | calmodulin-like 4 | -2.98 |
| <i>Steap1</i> | six transmembrane epithelial antigen of the prostate 1 | -2.99 |
| <i>Gm15810</i> | predicted gene 15810 | -3.00 |
| <i>Adh1</i> | alcohol dehydrogenase 1 (class I) | -3.01 |
| <i>Prlr</i> | prolactin receptor | -3.04 |
| <i>Sgcz</i> | sarcoglycan zeta | -3.07 |
| <i>Dock5</i> | dedicator of cytokinesis 5 | -3.17 |
| <i>Ptprz1</i> | protein tyrosine phosphatase, receptor type Z, polypeptide 1 | -3.20 |
| <i>Kcnmb1</i> | potassium large conductance calcium-activated channel, subfamily M, beta member 1 | -3.23 |
| <i>Jph3</i> | junctophilin 3 | -3.32 |
| <i>1700016K19Rik</i> | RIKEN cDNA 1700016K19 gene | -3.33 |
| <i>Vgf</i> | VGF nerve growth factor inducible | -3.33 |
| <i>Ipcef1</i> | interaction protein for cytohesin exchange factors 1 | -3.39 |
| <i>Angptl7</i> | angiopoietin-like 7 | -3.40 |
| <i>Dusp4</i> | dual specificity phosphatase 4 | -3.44 |
| <i>Vrk1</i> | vaccinia related kinase 1 | -3.44 |
| <i>Crybb3</i> | crystallin, beta B3 | -3.59 |
| <i>Ttyh1</i> | tweety family member 1 | -3.60 |
| <i>Kcnh5</i> | potassium voltage-gated channel, subfamily H (eag-related), member 5 | -3.64 |
| <i>Prss53</i> | protease, serine 53 | -3.67 |
| <i>Rab3c</i> | RAB3C, member RAS oncogene family | -3.76 |
| <i>Plk3</i> | polo-like kinase 3 | -3.81 |
| <i>Igf1r</i> | insulin-like growth factor I receptor | -3.83 |
| <i>Aldh1l2</i> | aldehyde dehydrogenase 1 family, member L2 | -3.88 |

| | | |
|-----------------|---|--------|
| <i>Tat</i> | tyrosine aminotransferase | -3.94 |
| <i>Serpina7</i> | serine (or cysteine) peptidase inhibitor, clade A (alpha-1 antiproteinase, antitrypsin), member 7 | -3.98 |
| <i>Trib3</i> | tribbles pseudokinase 3 | -3.99 |
| <i>Rasgrf1</i> | RAS protein-specific guanine nucleotide-releasing factor 1 | -4.06 |
| <i>Cbs</i> | cystathionine beta-synthase | -4.31 |
| <i>Pdyn</i> | prodynorphin | -4.34 |
| <i>Slc4a10</i> | solute carrier family 4, sodium bicarbonate cotransporter-like, member 10 | -4.45 |
| <i>Ddit3</i> | DNA-damage inducible transcript 3 | -4.64 |
| <i>Defb1</i> | defensin beta 1 | -4.65 |
| <i>Gm11789</i> | predicted gene 11789 | -4.68 |
| <i>Slitrk6</i> | SLIT and NTRK-like family, member 6 | -4.69 |
| <i>Hspa12a</i> | heat shock protein 12A | -4.84 |
| <i>Nrcam</i> | neuronal cell adhesion molecule | -4.86 |
| <i>17547793</i> | <i>No associated gene</i> | -4.98 |
| <i>Robo1</i> | roundabout guidance receptor 1 | -5.04 |
| <i>Cdh8</i> | cadherin 8 | -5.33 |
| <i>Nell1</i> | NEL-like 1 | -5.99 |
| <i>Ppp1r1a</i> | protein phosphatase 1, regulatory (inhibitor) subunit 1A | -6.28 |
| <i>Ffar3</i> | free fatty acid receptor 3 | -6.58 |
| <i>G6pc2</i> | glucose-6-phosphatase, catalytic, 2 | -6.90 |
| <i>Spc25</i> | SPC25, NDC80 kinetochore complex component, homolog (<i>S. cerevisiae</i>) | -7.81 |
| <i>Tmem215</i> | transmembrane protein 215 | -9.70 |
| <i>Ffar1</i> | free fatty acid receptor 1 | -12.00 |
| <i>Cox6a2</i> | cytochrome c oxidase subunit VIa polypeptide 2 | -14.33 |

Supplementary table 4: ChIP-sequencing for PAX6 in hypothalamic tissue

Differentially bound genomic site assigned genes in hypothalamus of 10 week old male mice using MACS differential peak finding ($P < 10^{-5}$). 0 denotes reduced binding while 1 denotes increased binding.

| Gene symbol | Gene name | Distance to start | Position | Leca2 | WT |
|----------------------|----------------------------|-------------------|------------|-------|----|
| <i>0610009O20Rik</i> | RIKEN cDNA 0610009O20 gene | 5655 | in gene | 0 | 1 |
| <i>1110059E24Rik</i> | RIKEN cDNA 1110059E24 gene | -169 | upstream | 0 | 1 |
| <i>1700036G14Rik</i> | RIKEN cDNA 1700036G14 gene | 22001 | downstream | 0 | 1 |
| <i>1700086O06Rik</i> | RIKEN cDNA 1700086O06 gene | -5339 | upstream | 0 | 1 |
| <i>1810024B03Rik</i> | RIKEN cDNA 1810024B03 gene | -88 | upstream | 0 | 1 |
| <i>1810044D09Rik</i> | RIKEN cDNA 1810044D09 gene | -59 | upstream | 0 | 1 |
| <i>2310033P09Rik</i> | RIKEN cDNA 2310033P09 gene | -5769 | upstream | 0 | 1 |
| <i>2310036O22Rik</i> | RIKEN cDNA 2310036O22 gene | 111 | in gene | 0 | 1 |
| <i>2310057B04Rik</i> | RIKEN cDNA 2310057B04 gene | 8767 | downstream | 0 | 1 |
| <i>2610035D17Rik</i> | RIKEN cDNA 2610035D17 gene | 54286 | in gene | 0 | 1 |
| <i>2610507I01Rik</i> | RIKEN cDNA 2610507I01 gene | -161 | upstream | 0 | 1 |

| | | | | | |
|----------------------|---|--------|------------|---|---|
| <i>4930471M09Rik</i> | RIKEN cDNA 4930471M09 gene | -74 | upstream | 0 | 1 |
| <i>4930527F14Rik</i> | RIKEN cDNA 4930527F14 gene | -3859 | upstream | 0 | 1 |
| <i>4933431G14Rik</i> | RIKEN cDNA 4933431G14 gene | 10429 | downstream | 0 | 1 |
| <i>4933433H22Rik</i> | RIKEN cDNA 4933433H22 gene | 3324 | in gene | 0 | 1 |
| <i>9130011E15Rik</i> | RIKEN cDNA 9130011E15 gene | -5144 | upstream | 0 | 1 |
| <i>Abhd1</i> | abhydrolase domain containing 1 | 3838 | in gene | 0 | 1 |
| <i>Abhd17b</i> | abhydrolase domain containing 17B | -349 | upstream | 0 | 1 |
| <i>Abt1</i> | activator of basal transcription 1 | -8886 | upstream | 0 | 1 |
| <i>Alas1</i> | aminolevulinic acid synthase 1 | -4046 | upstream | 0 | 1 |
| <i>Amd1</i> | S-adenosylmethionine decarboxylase 1 | 1164 | in gene | 0 | 1 |
| <i>Ankrd13c</i> | ankyrin repeat domain 13c | -394 | upstream | 0 | 1 |
| <i>Arf1</i> | ADP-ribosylation factor 1 | 25675 | downstream | 0 | 1 |
| <i>Arhgef10</i> | Rho guanine nucleotide exchange factor (GEF) 10 | 91611 | downstream | 0 | 1 |
| <i>Asna1</i> | arsA arsenite transporter, ATP-binding, homolog 1 (bacterial) | -1666 | upstream | 0 | 1 |
| <i>Auts2</i> | autism susceptibility candidate 2 | 896391 | in gene | 0 | 1 |
| <i>B330016D10Rik</i> | RIKEN cDNA B330016D10 gene | -4114 | upstream | 0 | 1 |
| <i>B3gnt1</i> | UDP-GlcNAc:betaGal beta-1,3-N-acetylglucosaminyltransferase 1 | 2486 | downstream | 0 | 1 |
| <i>B4galt7</i> | xylosylprotein beta1,4-galactosyltransferase, polypeptide 7 (galactosyltransferase I) | -6943 | upstream | 0 | 1 |
| <i>B930041F14Rik</i> | RIKEN cDNA B930041F14 gene | 10794 | downstream | 0 | 1 |
| <i>BC003965</i> | cDNA sequence BC003965 | 15 | in gene | 0 | 1 |
| <i>BC026590</i> | | -57 | upstream | 0 | 1 |
| <i>Bfsp2</i> | beaded filament structural protein 2, phakinin | 200 | in gene | 0 | 1 |
| <i>Bpnt1</i> | bisphosphate 3'-nucleotidase 1 | 30753 | downstream | 0 | 1 |
| <i>Brms1</i> | breast cancer metastasis-suppressor 1 | -92 | upstream | 0 | 1 |
| <i>C230035I16Rik</i> | RIKEN cDNA C230035I16 gene | -1735 | upstream | 0 | 1 |
| <i>Cacna2d1</i> | calcium channel, voltage-dependent, alpha2/delta subunit 1 | 330973 | in gene | 0 | 1 |
| <i>Car11</i> | | 7681 | downstream | 0 | 1 |
| <i>Celf2</i> | CUGBP, Elav-like family member 2 | 848902 | in gene | 0 | 1 |
| <i>Cgref1</i> | cell growth regulator with EF hand domain 1 | -8424 | upstream | 0 | 1 |
| <i>Clp1</i> | CLP1, cleavage and polyadenylation factor I subunit | -124 | upstream | 0 | 1 |
| <i>Coro2b</i> | coronin, actin binding protein, 2B | 67828 | in gene | 0 | 1 |
| <i>Ctnnal1</i> | catenin (cadherin associated protein), alpha-like 1 | 62939 | downstream | 0 | 1 |
| <i>Ctnnb1</i> | catenin, beta like 1 | 14503 | in gene | 0 | 1 |
| <i>Cux1</i> | cut-like homeobox 1 | 163687 | in gene | 0 | 1 |
| <i>Cux2</i> | cut-like homeobox 2 | 109969 | in gene | 0 | 1 |
| <i>Dbc1</i> | deleted in bladder cancer 1 (human) | 47293 | in gene | 0 | 1 |
| <i>Dbp</i> | D site albumin promoter binding protein | 2401 | in gene | 0 | 1 |

| | | | | | |
|----------------|---|--------|------------|---|---|
| <i>Dclk1</i> | doublecortin-like kinase 1 | 288978 | in gene | 0 | 1 |
| <i>Ddx55</i> | DEAD (Asp-Glu-Ala-Asp) box polypeptide 55 | 26208 | downstream | 0 | 1 |
| <i>Dlgap2</i> | discs, large (Drosophila) homolog-associated protein 2 | 636509 | in gene | 0 | 1 |
| <i>Dmrtb1</i> | DMRT-like family B with proline-rich C-terminal, 1 | 9922 | downstream | 0 | 1 |
| <i>Dtna</i> | dystrobrevin alpha | 106761 | in gene | 0 | 1 |
| <i>Dtx1</i> | deltex 1 homolog (Drosophila) | 38901 | downstream | 0 | 1 |
| <i>Dusp6</i> | dual specificity phosphatase 6 | -191 | upstream | 0 | 1 |
| <i>Ebf4</i> | early B cell factor 4 | 56157 | in gene | 0 | 1 |
| <i>Ehbp111</i> | EH domain binding protein 1-like 1 | -5363 | upstream | 0 | 1 |
| <i>Eif2b1</i> | eukaryotic translation initiation factor 2B, subunit 1 (alpha) | -15 | upstream | 0 | 1 |
| <i>Eif2b4</i> | eukaryotic translation initiation factor 2B, subunit 4 delta | 13171 | downstream | 0 | 1 |
| <i>Eprs</i> | glutamyl-prolyl-tRNA synthetase | -183 | upstream | 0 | 1 |
| <i>Fam115a</i> | family with sequence similarity 115, member A | 451 | in gene | 0 | 1 |
| <i>Fam13b</i> | family with sequence similarity 13, member B | -5209 | upstream | 0 | 1 |
| <i>Fam172a</i> | family with sequence similarity 172, member A | -50 | upstream | 0 | 1 |
| <i>Fam193a</i> | family with sequence similarity 193, member A | -301 | upstream | 0 | 1 |
| <i>Fam89b</i> | family with sequence similarity 89, member B | -2014 | upstream | 0 | 1 |
| <i>Fermt2</i> | fermitin family homolog 2 (Drosophila) | -9786 | upstream | 0 | 1 |
| <i>Fnbp1</i> | formin binding protein 1 | 73128 | in gene | 0 | 1 |
| <i>Frmd4a</i> | FERM domain containing 4A | 35841 | in gene | 0 | 1 |
| <i>Gfer</i> | growth factor, erv1 (<i>S. cerevisiae</i>)-like (augmenter of liver regeneration) | 6252 | downstream | 0 | 1 |
| <i>Gm10815</i> | predicted gene 10815 | 9082 | downstream | 0 | 1 |
| <i>Gm12657</i> | predicted gene 12657 | 9646 | downstream | 0 | 1 |
| <i>Gm16630</i> | predicted gene, 16630 | 28960 | in gene | 0 | 1 |
| <i>Gm17750</i> | predicted gene, 17750 | 21186 | in gene | 0 | 1 |
| <i>Gm4123</i> | predicted gene 4123 | 5867 | downstream | 0 | 1 |
| <i>Gtf2h3</i> | general transcription factor IIH, polypeptide 3 | -76 | upstream | 0 | 1 |
| <i>Gtf3c2</i> | general transcription factor IIIC, polypeptide 2, beta | 176 | in gene | 0 | 1 |
| <i>Hdac7</i> | histone deacetylase 7 | 41782 | in gene | 0 | 1 |
| <i>Hic1</i> | hypermethylated in cancer 1 | 4303 | in gene | 0 | 1 |
| <i>Hps6</i> | Hermansky-Pudlak syndrome 6 | 154 | in gene | 0 | 1 |
| <i>Hsf2bp</i> | heat shock transcription factor 2 binding protein | -1924 | upstream | 0 | 1 |
| <i>Ikkkap</i> | inhibitor of kappa light polypeptide enhancer in B cells, kinase complex-associated protein | 59 | in gene | 0 | 1 |
| <i>Inpp5a</i> | inositol polyphosphate-5-phosphatase A | 141867 | in gene | 0 | 1 |
| <i>Kank3</i> | KN motif and ankyrin repeat domains 3 | 14085 | downstream | 0 | 1 |

| | | | | | |
|----------------|--|--------|------------|---|---|
| <i>Kbtbd11</i> | kelch repeat and BTB (POZ) domain containing 11 | -7697 | upstream | 0 | 1 |
| <i>Kcnab2</i> | potassium voltage-gated channel, shaker-related subfamily, beta member 2 | 909 | in gene | 0 | 1 |
| <i>Kdm2a</i> | lysine (K)-specific demethylase 2A | 63157 | in gene | 0 | 1 |
| <i>Kdm3b</i> | KDM3B lysine (K)-specific demethylase 3B | 63680 | downstream | 0 | 1 |
| <i>Kif13a</i> | kinesin family member 13A | 170262 | in gene | 0 | 1 |
| <i>Kif3c</i> | kinesin family member 3C | 25940 | in gene | 0 | 1 |
| <i>Ksr2</i> | kinase suppressor of ras 2 | 290574 | in gene | 0 | 1 |
| <i>L3mbtl3</i> | l(3)mbt-like 3 (Drosophila) | 94993 | in gene | 0 | 1 |
| <i>Ltbp3</i> | latent transforming growth factor beta binding protein 3 | -9224 | upstream | 0 | 1 |
| <i>Magef1</i> | melanoma antigen family F, 1 | -6266 | upstream | 0 | 1 |
| <i>Mir132</i> | microRNA 132 | -7730 | upstream | 0 | 1 |
| <i>Mir212</i> | microRNA 212 | -7436 | upstream | 0 | 1 |
| <i>Mras</i> | muscle and microspikes RAS | -5421 | upstream | 0 | 1 |
| <i>Mrpl55</i> | mitochondrial ribosomal protein L55 | 75 | in gene | 0 | 1 |
| <i>Ncbp1</i> | nuclear cap binding protein subunit 1 | 385 | in gene | 0 | 1 |
| <i>Ndufa7</i> | NADH dehydrogenase (ubiquinone) 1 alpha subcomplex, 7 (B14.5a) | -6 | upstream | 0 | 1 |
| <i>Noxo1</i> | NADPH oxidase organizer 1 | -6330 | upstream | 0 | 1 |
| <i>Nphp4</i> | nephronophthisis 4 (juvenile) homolog (human) | -1502 | upstream | 0 | 1 |
| <i>Nrxn3</i> | neurexin III | 383684 | in gene | 0 | 1 |
| <i>Ntsr2</i> | neurotensin receptor 2 | -9326 | upstream | 0 | 1 |
| <i>Ovca2</i> | candidate tumor suppressor in ovarian cancer 2 | 12856 | downstream | 0 | 1 |
| <i>Pcp4</i> | Purkinje cell protein 4 | 19754 | in gene | 0 | 1 |
| <i>Pdzrn4</i> | PDZ domain containing RING finger 4 | 200310 | in gene | 0 | 1 |
| <i>Plaa</i> | phospholipase A2, activating protein | -49 | upstream | 0 | 1 |
| <i>Preb</i> | prolactin regulatory element binding | 6457 | in gene | 0 | 1 |
| <i>Prss53</i> | protease, serine, 53 | 15034 | downstream | 0 | 1 |
| <i>Rasal1</i> | RAS protein activator like 1 (GAP1 like) | 23946 | in gene | 0 | 1 |
| <i>Rbm12b2</i> | RNA binding motif protein 12 B2 | -1071 | upstream | 0 | 1 |
| <i>Rdh11</i> | retinol dehydrogenase 11 | 587 | in gene | 0 | 1 |
| <i>Reep2</i> | receptor accessory protein 2 | 99 | in gene | 0 | 1 |
| <i>Rin1</i> | | -9496 | upstream | 0 | 1 |
| <i>Rnf130</i> | ring finger protein 130 | -275 | upstream | 0 | 1 |
| <i>Rps28</i> | ribosomal protein S28 | -110 | upstream | 0 | 1 |
| <i>Rrp1b</i> | ribosomal RNA processing 1 homolog B (S. cerevisiae) | 270 | in gene | 0 | 1 |
| <i>Samd3</i> | sterile alpha motif domain containing 3 | 50485 | downstream | 0 | 1 |
| <i>Scarf1</i> | scavenger receptor class F, member 1 | 18683 | downstream | 0 | 1 |
| <i>Scarna2</i> | small Cajal body-specific RNA 2 | -8062 | upstream | 0 | 1 |

| | | | | | |
|-----------------|---|--------|------------|---|---|
| <i>Slc20a2</i> | solute carrier family 20, member 2 | 68228 | in gene | 0 | 1 |
| <i>Slc22a23</i> | solute carrier family 22, member 23 | 152398 | in gene | 0 | 1 |
| <i>Slc29a2</i> | solute carrier family 29 (nucleoside transporters), member 2 | 17306 | downstream | 0 | 1 |
| <i>Slc43a2</i> | solute carrier family 43, member 2 | 530 | in gene | 0 | 1 |
| <i>Slc48a1</i> | solute carrier family 48 (heme transporter), member 1 | 18355 | downstream | 0 | 1 |
| <i>Smg6</i> | Smg-6 homolog, nonsense mediated mRNA decay factor (<i>C. elegans</i>) | 240080 | downstream | 0 | 1 |
| <i>Snrnp200</i> | small nuclear ribonucleoprotein 200 (U5) | -36 | upstream | 0 | 1 |
| <i>Spn</i> | SPEN homolog, transcriptional regulator (<i>Drosophila</i>) | -3451 | upstream | 0 | 1 |
| <i>Sphk2</i> | sphingosine kinase 2 | 10354 | downstream | 0 | 1 |
| <i>Sssca1</i> | Sjogren's syndrome/scleroderma autoantigen 1 homolog (human) | 41 | in gene | 0 | 1 |
| <i>Ssu72</i> | Ssu72 RNA polymerase II CTD phosphatase homolog (yeast) | 321 | in gene | 0 | 1 |
| <i>St3gal5</i> | ST3 beta-galactoside alpha-2,3-sialyltransferase 5 | 15155 | in gene | 0 | 1 |
| <i>Syng3</i> | | 45 | in gene | 0 | 1 |
| <i>Taf13</i> | TAF13 RNA polymerase II, TATA box binding protein (TBP)-associated factor | -9235 | upstream | 0 | 1 |
| <i>Tbccd1</i> | TBCC domain containing 1 | 13153 | in gene | 0 | 1 |
| <i>Tmed9</i> | transmembrane emp24 protein transport domain containing 9 | 33 | in gene | 0 | 1 |
| <i>Tmem108</i> | transmembrane protein 108 | 281709 | downstream | 0 | 1 |
| <i>Tmem167b</i> | transmembrane protein 167B | 2 | in gene | 0 | 1 |
| <i>Tmem67</i> | transmembrane protein 67 | -342 | upstream | 0 | 1 |
| <i>Tmx1</i> | thioredoxin-related transmembrane protein 1 | 24574 | downstream | 0 | 1 |
| <i>Tnik</i> | TRAF2 and NCK interacting kinase | 268194 | in gene | 0 | 1 |
| <i>Tnpo2</i> | transportin 2 (importin 3, karyopherin beta 2b) | -9971 | upstream | 0 | 1 |
| <i>Tnr</i> | tenascin R | 70055 | in gene | 0 | 1 |
| <i>Tns3</i> | tensin 3 | 210951 | in gene | 0 | 1 |
| <i>Tstd2</i> | thiosulfate sulfurtransferase (rhodanese)-like domain containing 2 | -421 | upstream | 0 | 1 |
| <i>Ttc22</i> | tetratricopeptide repeat domain 22 | 8191 | in gene | 0 | 1 |
| <i>Tuba1c</i> | tubulin, alpha 1C | 11741 | downstream | 0 | 1 |
| <i>Ube2f</i> | ubiquitin-conjugating enzyme E2F (putative) | 1 | in gene | 0 | 1 |
| <i>Unkl</i> | unkempt-like (<i>Drosophila</i>) | -3824 | upstream | 0 | 1 |
| <i>Uqcrfs1</i> | ubiquinol-cytochrome c reductase, Rieske iron-sulfur polypeptide 1 | 68 | in gene | 0 | 1 |
| <i>Vangl1</i> | vang-like 1 (van gogh, <i>Drosophila</i>) | 35269 | in gene | 0 | 1 |
| <i>Wdr70</i> | WD repeat domain 70 | 9 | in gene | 0 | 1 |

| | | | | | |
|----------------------|--|--------|------------|---|---|
| <i>Ypel4</i> | yippee-like 4 (Drosophila) | -6812 | upstream | 0 | 1 |
| <i>Zbtb16</i> | zinc finger and BTB domain containing 16 | 112201 | in gene | 0 | 1 |
| <i>Zfp51</i> | zinc finger protein 51 | -48 | upstream | 0 | 1 |
| <i>Zfp598</i> | zinc finger protein 598 | 20152 | downstream | 0 | 1 |
| <i>Zfp646</i> | zinc finger protein 646 | -1765 | upstream | 0 | 1 |
| <i>Zfp668</i> | zinc finger protein 668 | 887 | in gene | 0 | 1 |
| <i>Zhx2</i> | zinc fingers and homeoboxes 2 | 34101 | in gene | 0 | 1 |
| <i>1700067K01Rik</i> | RIKEN cDNA 1700067K01 gene | 9675 | downstream | 1 | 0 |
| <i>2210011C24Rik</i> | RIKEN cDNA 2210011C24 gene | 775 | in gene | 1 | 0 |
| <i>2410018M08Rik</i> | RIKEN cDNA 2410018M08 gene | 13045 | downstream | 1 | 0 |
| <i>2500004C02Rik</i> | RIKEN cDNA 2500004C02 gene | -910 | upstream | 1 | 0 |
| <i>4930478P22Rik</i> | RIKEN cDNA 4930478P22 gene | 15359 | downstream | 1 | 0 |
| <i>4930542N06Rik</i> | RIKEN cDNA 4930542N06 gene | 176 | in gene | 1 | 0 |
| <i>9530059O14Rik</i> | RIKEN cDNA 9530059O14 gene | -3509 | upstream | 1 | 0 |
| <i>Add3</i> | adducin 3 (gamma) | 1795 | in gene | 1 | 0 |
| <i>Asx11</i> | | 581 | in gene | 1 | 0 |
| <i>Cadm2</i> | cell adhesion molecule 2 | 492 | in gene | 1 | 0 |
| <i>Cdyl2</i> | chromodomain protein, Y chromosome-like 2 | 95 | in gene | 1 | 0 |
| <i>Cgnl1</i> | cingulin-like 1 | 274 | in gene | 1 | 0 |
| <i>E130018O15Rik</i> | RIKEN cDNA E130018O15 gene | 11564 | downstream | 1 | 0 |
| <i>Foxo1</i> | forkhead box O1 | 303 | in gene | 1 | 0 |
| <i>Gm20290</i> | predicted gene, 20290 | -9244 | upstream | 1 | 0 |
| <i>Grin2d</i> | glutamate receptor, ionotropic, NMDA2D (epsilon 4) | 9241 | in gene | 1 | 0 |
| <i>Grsf1</i> | G-rich RNA sequence binding factor 1 | 43 | in gene | 1 | 0 |
| <i>Hnrpl1</i> | heterogeneous nuclear ribonucleoprotein L-like | -226 | upstream | 1 | 0 |
| <i>Hrasls5</i> | HRAS-like suppressor family, member 5 | 167 | in gene | 1 | 0 |
| <i>Itm2b</i> | integral membrane protein 2B | 247 | in gene | 1 | 0 |
| <i>Lgals12</i> | lectin, galactose binding, soluble 12 | -5560 | upstream | 1 | 0 |
| <i>Lrrc8b</i> | leucine rich repeat containing 8 family, member B | -287 | upstream | 1 | 0 |
| <i>Lysmd2</i> | LysM, putative peptidoglycan-binding, domain containing 2 | 444 | in gene | 1 | 0 |
| <i>Mir1199</i> | microRNA 1199 | 252 | downstream | 1 | 0 |
| <i>Mob4</i> | MOB family member 4, phocein | 419 | in gene | 1 | 0 |
| <i>Nupr11</i> | nuclear protein transcriptional regulator 1 like | 228 | in gene | 1 | 0 |
| <i>Palm3</i> | | -10093 | upstream | 1 | 0 |
| <i>Parvb</i> | parvin, beta | 90997 | downstream | 1 | 0 |
| <i>Parvg</i> | parvin, gamma | -1680 | upstream | 1 | 0 |
| <i>Rab22a</i> | RAB22A, member RAS oncogene family | 347 | in gene | 1 | 0 |
| <i>Rnf217</i> | ring finger protein 217 | 189 | in gene | 1 | 0 |
| <i>Sbspon</i> | somatomedin B and thrombospondin, type 1 domain containing | -6574 | upstream | 1 | 0 |

| | | | | | |
|-------------------|---|--------|----------|---|---|
| <i>Sh3pxd2a</i> | SH3 and PX domains 2A | 120843 | in gene | 1 | 0 |
| <i>Spock1</i> | sparc/osteonectin, cwcv and kazal-like domains proteoglycan 1 | 378700 | in gene | 1 | 0 |
| <i>Srebf2</i> | sterol regulatory element binding factor 2 | 22139 | in gene | 1 | 0 |
| <i>St6galnac3</i> | ST6 (alpha-N-acetyl-neuraminyl-2,3-beta-galactosyl-1,3)-N-acetylgalactosaminide alpha-2,6-sialyltransferase 3 | 240269 | in gene | 1 | 0 |
| <i>Tle4</i> | transducin-like enhancer of split 4, homolog of Drosophila E(spl) | -769 | upstream | 1 | 0 |
| <i>Trim36</i> | tripartite motif-containing 36 | 607 | in gene | 1 | 0 |
| <i>Wwox</i> | WW domain-containing oxidoreductase | 393212 | in gene | 1 | 0 |
| <i>Zc2hc1a</i> | zinc finger, C2HC-type containing 1A | 5150 | in gene | 1 | 0 |
| <i>Zfp703</i> | zinc finger protein 703 | -376 | upstream | 1 | 0 |

6. REFERENCES

1. Langerhans, P., *Beitrage zur mikroskopischen anatomie der bauchspeichel druse*. 1869, Berlin: Gustav Lange.
2. Minkowski, J.v.M.a.O., *Diabetes mellitus nach Pankreasekstirpation*. Centralblatt für klinische Medicin, Leipzig, 1889, 10 (23): 393-394. Archiv für experimentelle Pathologie und Pharmakologie, Leipzig, 1890, 26: 37.
3. Banting, F.G., et al., *Pancreatic Extracts in the Treatment of Diabetes Mellitus*. Can Med Assoc J, 1922. **12**(3): p. 141-6.
4. Banting FG, B.C., *Pancreatic extracts*. J Lab Clin Med, 1922. **7**: p. 464-472.
5. McEvoy, R.C., *Changes in the volumes of the A-, B-, and D-cell populations in the pancreatic islets during the postnatal development of the rat*. Diabetes, 1981. **30**(10): p. 813-7.
6. Steiner, D.J., et al., *Pancreatic islet plasticity: interspecies comparison of islet architecture and composition*. Islets, 2010. **2**(3): p. 135-45.
7. Rahier, J., R.M. Goebbels, and J.C. Henquin, *Cellular composition of the human diabetic pancreas*. Diabetologia, 1983. **24**(5): p. 366-71.
8. Orci, L. and R.H. Unger, *Functional subdivision of islets of Langerhans and possible role of D cells*. Lancet, 1975. **2**(7947): p. 1243-4.
9. Bosco, D., et al., *Unique arrangement of alpha- and beta-cells in human islets of Langerhans*. Diabetes, 2010. **59**(5): p. 1202-10.
10. Ahlgren, U., J. Jonsson, and H. Edlund, *The morphogenesis of the pancreatic mesenchyme is uncoupled from that of the pancreatic epithelium in IPF1/PDX1-deficient mice*. Development, 1996. **122**(5): p. 1409-16.
11. Jonsson, J., et al., *Insulin-promoter-factor 1 is required for pancreas development in mice*. Nature, 1994. **371**(6498): p. 606-9.
12. Kawaguchi, Y., et al., *The role of the transcriptional regulator Ptf1a in converting intestinal to pancreatic progenitors*. Nat Genet, 2002. **32**(1): p. 128-34.
13. Seymour, P.A., et al., *SOX9 is required for maintenance of the pancreatic progenitor cell pool*. Proc Natl Acad Sci U S A, 2007. **104**(6): p. 1865-70.
14. Gittes, G.K., *Developmental biology of the pancreas: a comprehensive review*. Dev Biol, 2009. **326**(1): p. 4-35.
15. Pictet, R.L., et al., *An ultrastructural analysis of the developing embryonic pancreas*. Dev Biol, 1972. **29**(4): p. 436-67.
16. Gu, G., J. Dubauskaite, and D.A. Melton, *Direct evidence for the pancreatic lineage: NGN3+ cells are islet progenitors and are distinct from duct progenitors*. Development, 2002. **129**(10): p. 2447-57.
17. Haumaitre, C., et al., *Lack of TCF2/vHNF1 in mice leads to pancreas agenesis*. Proc Natl Acad Sci U S A, 2005. **102**(5): p. 1490-5.
18. Arda, H.E., C.M. Benitez, and S.K. Kim, *Gene regulatory networks governing pancreas development*. Dev Cell, 2013. **25**(1): p. 5-13.
19. Maestro, M.A., et al., *Hnf6 and Tcf2 (MODY5) are linked in a gene network operating in a precursor cell domain of the embryonic pancreas*. Hum Mol Genet, 2003. **12**(24): p. 3307-14.
20. Gradwohl, G., et al., *neurogenin3 is required for the development of the four endocrine cell lineages of the pancreas*. Proc Natl Acad Sci U S A, 2000. **97**(4): p. 1607-11.
21. Habener, J.F., D.M. Kemp, and M.K. Thomas, *Minireview: transcriptional regulation in pancreatic development*. Endocrinology, 2005. **146**(3): p. 1025-34.
22. Zhou, Q., et al., *A multipotent progenitor domain guides pancreatic organogenesis*. Dev Cell, 2007. **13**(1): p. 103-14.
23. Oliver-Krasinski, J.M. and D.A. Stoffers, *On the origin of the beta cell*. Genes Dev, 2008. **22**(15): p. 1998-2021.
24. Naya, F.J., et al., *Diabetes, defective pancreatic morphogenesis, and abnormal enteroendocrine differentiation in BETA2/neuroD-deficient mice*. Genes Dev, 1997. **11**(18): p. 2323-34.

25. Gierl, M.S., et al., *The zinc-finger factor Insm1 (IA-1) is essential for the development of pancreatic beta cells and intestinal endocrine cells*. *Genes Dev*, 2006. **20**(17): p. 2465-78.
26. Mellitzer, G., et al., *IA1 is NGN3-dependent and essential for differentiation of the endocrine pancreas*. *EMBO J*, 2006. **25**(6): p. 1344-52.
27. St-Onge, L., et al., *Pax6 is required for differentiation of glucagon-producing alpha-cells in mouse pancreas*. *Nature*, 1997. **387**(6631): p. 406-9.
28. Sander, M., et al., *Genetic analysis reveals that PAX6 is required for normal transcription of pancreatic hormone genes and islet development*. *Genes Dev*, 1997. **11**(13): p. 1662-73.
29. Sosa-Pineda, B., et al., *The Pax4 gene is essential for differentiation of insulin-producing beta cells in the mammalian pancreas*. *Nature*, 1997. **386**(6623): p. 399-402.
30. Collombat, P., et al., *Opposing actions of Arx and Pax4 in endocrine pancreas development*. *Genes Dev*, 2003. **17**(20): p. 2591-603.
31. Wang, J., et al., *The concerted activities of Pax4 and Nkx2.2 are essential to initiate pancreatic beta-cell differentiation*. *Dev Biol*, 2004. **266**(1): p. 178-89.
32. Sussel, L., et al., *Mice lacking the homeodomain transcription factor Nkx2.2 have diabetes due to arrested differentiation of pancreatic beta cells*. *Development*, 1998. **125**(12): p. 2213-21.
33. Nelson, S.B., A.E. Schaffer, and M. Sander, *The transcription factors Nkx6.1 and Nkx6.2 possess equivalent activities in promoting beta-cell fate specification in Pdx1+ pancreatic progenitor cells*. *Development*, 2007. **134**(13): p. 2491-500.
34. Sander, M., et al., *Homeobox gene Nkx6.1 lies downstream of Nkx2.2 in the major pathway of beta-cell formation in the pancreas*. *Development*, 2000. **127**(24): p. 5533-40.
35. Matsuoka, T.A., et al., *The MafA transcription factor appears to be responsible for tissue-specific expression of insulin*. *Proc Natl Acad Sci U S A*, 2004. **101**(9): p. 2930-3.
36. Artner, I., et al., *MafB is required for islet beta cell maturation*. *Proc Natl Acad Sci U S A*, 2007. **104**(10): p. 3853-8.
37. Zhang, C., et al., *MafA is a key regulator of glucose-stimulated insulin secretion*. *Mol Cell Biol*, 2005. **25**(12): p. 4969-76.
38. Nishimura, W., S. Takahashi, and K. Yasuda, *MafA is critical for maintenance of the mature beta cell phenotype in mice*. *Diabetologia*, 2015. **58**(3): p. 566-74.
39. Artner, I., et al., *MafB: an activator of the glucagon gene expressed in developing islet alpha- and beta-cells*. *Diabetes*, 2006. **55**(2): p. 297-304.
40. Gittes, G.K. and W.J. Rutter, *Onset of cell-specific gene expression in the developing mouse pancreas*. *Proc Natl Acad Sci U S A*, 1992. **89**(3): p. 1128-32.
41. Prado, C.L., et al., *Ghrelin cells replace insulin-producing beta cells in two mouse models of pancreas development*. *Proc Natl Acad Sci U S A*, 2004. **101**(9): p. 2924-9.
42. Teitelman, G., et al., *Precursor cells of mouse endocrine pancreas coexpress insulin, glucagon and the neuronal proteins tyrosine hydroxylase and neuropeptide Y, but not pancreatic polypeptide*. *Development*, 1993. **118**(4): p. 1031-9.
43. Morahan, F.-X.J.a.G., *Pancreatic Stem Cells: Unresolved Business*, in *Stem Cells in Clinic and Research*. 2011.
44. Schisler, J.C., et al., *The Nkx6.1 homeodomain transcription factor suppresses glucagon expression and regulates glucose-stimulated insulin secretion in islet beta cells*. *Proc Natl Acad Sci U S A*, 2005. **102**(20): p. 7297-302.
45. Gauthier, B.R., et al., *The beta-cell specific transcription factor Nkx6.1 inhibits glucagon gene transcription by interfering with Pax6*. *Biochem J*, 2007. **403**(3): p. 593-601.
46. R. Pictet, W.R., *Development of the embryonic endocrine pancreas*. D.F. Steiner, N. Freinkel (Eds.), Section 7: Endocrinology Handbook of Physiology: American Physiologic Society, Washington, D.C. , 1972. **1**(7): p. 67-76.
47. Brissova, M., et al., *Assessment of human pancreatic islet architecture and composition by laser scanning confocal microscopy*. *J Histochem Cytochem*, 2005. **53**(9): p. 1087-97.
48. Jo, J., M.Y. Choi, and D.S. Koh, *Size distribution of mouse Langerhans islets*. *Biophys J*, 2007. **93**(8): p. 2655-66.
49. Rorsman, P., et al., *Failure of glucose to elicit a normal secretory response in fetal pancreatic beta cells results from glucose insensitivity of the ATP-regulated K+ channels*. *Proc Natl Acad Sci U S A*, 1989. **86**(12): p. 4505-9.

50. Otonkoski, T., et al., *Maturation of insulin response to glucose during human fetal and neonatal development. Studies with perfusion of pancreatic isletlike cell clusters.* Diabetes, 1988. **37**(3): p. 286-91.
51. Bliss, C.R. and G.W. Sharp, *Glucose-induced insulin release in islets of young rats: time-dependent potentiation and effects of 2-bromostearate.* Am J Physiol, 1992. **263**(5 Pt 1): p. E890-6.
52. Sherman, A., J. Rinzel, and J. Keizer, *Emergence of organized bursting in clusters of pancreatic beta-cells by channel sharing.* Biophys J, 1988. **54**(3): p. 411-25.
53. Stolovich-Rain, M., et al., *Weaning triggers a maturation step of pancreatic beta cells.* Dev Cell, 2015. **32**(5): p. 535-45.
54. De Vos, A., et al., *Human and rat beta cells differ in glucose transporter but not in glucokinase gene expression.* J Clin Invest, 1995. **96**(5): p. 2489-95.
55. Matschinsky, F.M., *Glucokinase as glucose sensor and metabolic signal generator in pancreatic beta-cells and hepatocytes.* Diabetes, 1990. **39**(6): p. 647-52.
56. Herzig, S., et al., *Identification and functional expression of the mitochondrial pyruvate carrier.* Science, 2012. **337**(6090): p. 93-6.
57. Bricker, D.K., et al., *A mitochondrial pyruvate carrier required for pyruvate uptake in yeast, Drosophila, and humans.* Science, 2012. **337**(6090): p. 96-100.
58. Kennedy, H.J., et al., *Glucose generates sub-plasma membrane ATP microdomains in single islet beta-cells. Potential role for strategically located mitochondria.* J Biol Chem, 1999. **274**(19): p. 13281-91.
59. Ashcroft, F.M., D.E. Harrison, and S.J. Ashcroft, *Glucose induces closure of single potassium channels in isolated rat pancreatic beta-cells.* Nature, 1984. **312**(5993): p. 446-8.
60. Cook, D.L. and C.N. Hales, *Intracellular ATP directly blocks K⁺ channels in pancreatic B-cells.* Nature, 1984. **311**(5983): p. 271-3.
61. Meissner, H.P. and H. Schmelz, *Membrane potential of beta-cells in pancreatic islets.* Pflugers Arch, 1974. **351**(3): p. 195-206.
62. Mitchell, K.J., T. Tsuboi, and G.A. Rutter, *Role for plasma membrane-related Ca²⁺-ATPase-1 (ATP2C1) in pancreatic beta-cell Ca²⁺ homeostasis revealed by RNA silencing.* Diabetes, 2004. **53**(2): p. 393-400.
63. Gustafsson, A.J., et al., *Ryanodine receptor-operated activation of TRP-like channels can trigger critical Ca²⁺ signaling events in pancreatic beta-cells.* FASEB J, 2005. **19**(2): p. 301-3.
64. Rutter, G.A., et al., *Pancreatic beta-cell identity, glucose sensing and the control of insulin secretion.* Biochem J, 2015. **466**(2): p. 203-18.
65. Rorsman, P., et al., *The Cell Physiology of Biphasic Insulin Secretion.* News Physiol Sci, 2000. **15**: p. 72-77.
66. Drucker, D.J., et al., *Glucagon-like peptide I stimulates insulin gene expression and increases cyclic AMP levels in a rat islet cell line.* Proc Natl Acad Sci U S A, 1987. **84**(10): p. 3434-8.
67. Thorens, B., *Expression cloning of the pancreatic beta cell receptor for the gluco-incretin hormone glucagon-like peptide 1.* Proc Natl Acad Sci U S A, 1992. **89**(18): p. 8641-5.
68. Usdin, T.B., et al., *Gastric inhibitory polypeptide receptor, a member of the secretin-vasoactive intestinal peptide receptor family, is widely distributed in peripheral organs and the brain.* Endocrinology, 1993. **133**(6): p. 2861-70.
69. Drucker, D.J., *The biology of incretin hormones.* Cell Metab, 2006. **3**(3): p. 153-65.
70. Ding, W.G. and J. Gromada, *Protein kinase A-dependent stimulation of exocytosis in mouse pancreatic beta-cells by glucose-dependent insulinotropic polypeptide.* Diabetes, 1997. **46**(4): p. 615-21.
71. Holz, G.G., *Epac: A new cAMP-binding protein in support of glucagon-like peptide-1 receptor-mediated signal transduction in the pancreatic beta-cell.* Diabetes, 2004. **53**(1): p. 5-13.
72. Seino, Y., M. Fukushima, and D. Yabe, *GIP and GLP-1, the two incretin hormones: Similarities and differences.* J Diabetes Investig, 2010. **1**(1-2): p. 8-23.
73. Dupre, J., et al., *Stimulation of insulin secretion by gastric inhibitory polypeptide in man.* J Clin Endocrinol Metab, 1973. **37**(5): p. 826-8.

74. Kreymann, B., et al., *Glucagon-like peptide-1 7-36: a physiological incretin in man*. *Lancet*, 1987. **2**(8571): p. 1300-4.
75. Schmidt, W.E., E.G. Siegel, and W. Creutzfeldt, *Glucagon-like peptide-1 but not glucagon-like peptide-2 stimulates insulin release from isolated rat pancreatic islets*. *Diabetologia*, 1985. **28**(9): p. 704-7.
76. Miki, T., et al., *Distinct effects of glucose-dependent insulinotropic polypeptide and glucagon-like peptide-1 on insulin secretion and gut motility*. *Diabetes*, 2005. **54**(4): p. 1056-63.
77. Chambers, A.P., et al., *The Role of Pancreatic Preproglucagon in Glucose Homeostasis in Mice*. *Cell Metab*, 2017. **25**(4): p. 927-934 e3.
78. Itoh, Y., et al., *Free fatty acids regulate insulin secretion from pancreatic beta cells through GPR40*. *Nature*, 2003. **422**(6928): p. 173-6.
79. Verspohl, E.J., et al., *Evidence that cholecystokinin interacts with specific receptors and regulates insulin release in isolated rat islets of Langerhans*. *Diabetes*, 1986. **35**(1): p. 38-43.
80. Moens, K., et al., *Expression and functional activity of glucagon, glucagon-like peptide I, and glucose-dependent insulinotropic peptide receptors in rat pancreatic islet cells*. *Diabetes*, 1996. **45**(2): p. 257-61.
81. Turner, D.S. and N. McIntyre, *Stimulation by glucagon of insulin release from rabbit pancreas in vitro*. *Lancet*, 1966. **1**(7433): p. 351-2.
82. Wollheim, C.B., et al., *Somatostatin- and epinephrine-induced modifications of $^{45}\text{Ca}^{++}$ fluxes and insulin release in rat pancreatic islets maintained in tissue culture*. *J Clin Invest*, 1977. **60**(5): p. 1165-73.
83. Gerich, J.E., R. Lovinger, and G.M. Grodsky, *Inhibition by somatostatin of glucagon and insulin release from the perfused rat pancreas in response to arginine, isoproterenol and theophylline: evidence for a preferential effect on glucagon secretion*. *Endocrinology*, 1975. **96**(3): p. 749-54.
84. Schuit, F.C. and D.G. Pipeleers, *Differences in adrenergic recognition by pancreatic A and B cells*. *Science*, 1986. **232**(4752): p. 875-7.
85. Gilman, A.G., *G proteins: transducers of receptor-generated signals*. *Annu Rev Biochem*, 1987. **56**: p. 615-49.
86. Rorsman, P., et al., *Activation by adrenaline of a low-conductance G protein-dependent K^{+} channel in mouse pancreatic B cells*. *Nature*, 1991. **349**(6304): p. 77-9.
87. Itoh, M. and J.E. Gerich, *Adrenergic modulation of pancreatic somatostatin, insulin, and glucagon secretion: evidence for differential sensitivity of islet A, B, and D cells*. *Metabolism*, 1982. **31**(7): p. 715-20.
88. Samols, E. and G.C. Weir, *Adrenergic modulation of pancreatic A, B, and D cells alpha-Adrenergic suppression and beta-adrenergic stimulation of somatostatin secretion, alpha-adrenergic stimulation of glucagon secretion in the perfused dog pancreas*. *J Clin Invest*, 1979. **63**(2): p. 230-8.
89. Curry, D.L., L.L. Bennett, and G.M. Grodsky, *Dynamics of insulin secretion by the perfused rat pancreas*. *Endocrinology*, 1968. **83**(3): p. 572-84.
90. Cerasi, E. and R. Luft, *Plasma-Insulin Response to Sustained Hyperglycemia Induced by Glucose Infusion in Human Subjects*. *Lancet*, 1963. **2**(7322): p. 1359-61.
91. Porksen, N., et al., *Pulsatile insulin secretion: detection, regulation, and role in diabetes*. *Diabetes*, 2002. **51 Suppl 1**: p. S245-54.
92. Opara, E.C., I. Atwater, and V.L. Go, *Characterization and control of pulsatile secretion of insulin and glucagon*. *Pancreas*, 1988. **3**(4): p. 484-7.
93. Lang, D.A., et al., *Pulsatile, synchronous basal insulin and glucagon secretion in man*. *Diabetes*, 1982. **31**(1): p. 22-6.
94. Ohneda, K., H. Ee, and M. German, *Regulation of insulin gene transcription*. *Semin Cell Dev Biol*, 2000. **11**(4): p. 227-33.
95. Melloul, D., S. Marshak, and E. Cerasi, *Regulation of insulin gene transcription*. *Diabetologia*, 2002. **45**(3): p. 309-26.
96. Pullen, T.J., et al., *Identification of genes selectively disallowed in the pancreatic islet*. *Islets*, 2010. **2**(2): p. 89-95.

97. Gu, C., et al., *Pancreatic beta cells require NeuroD to achieve and maintain functional maturity*. Cell Metab, 2010. **11**(4): p. 298-310.
98. Hart, A.W., et al., *The developmental regulator Pax6 is essential for maintenance of islet cell function in the adult mouse pancreas*. PLoS One, 2013. **8**(1): p. e54173.
99. Swisa, A., et al., *PAX6 maintains beta cell identity by repressing genes of alternative islet cell types*. J Clin Invest, 2017. **127**(1): p. 230-243.
100. Mitchell, R.K., et al., *The transcription factor Pax6 is required for pancreatic beta cell identity, glucose-regulated ATP synthesis and Ca²⁺ dynamics in adult mice*. J Biol Chem, 2017.
101. Ahmad, Z., et al., *Pax6 Inactivation in the Adult Pancreas Reveals Ghrelin as Endocrine Cell Maturation Marker*. PLoS One, 2015. **10**(12): p. e0144597.
102. Ohlsson, H., K. Karlsson, and T. Edlund, *IPF1, a homeodomain-containing transactivator of the insulin gene*. EMBO J, 1993. **12**(11): p. 4251-9.
103. Guo, L., et al., *PDX1 in ducts is not required for postnatal formation of beta-cells but is necessary for their subsequent maturation*. Diabetes, 2013. **62**(10): p. 3459-68.
104. Gao, T., et al., *Pdx1 maintains beta cell identity and function by repressing an alpha cell program*. Cell Metab, 2014. **19**(2): p. 259-71.
105. Taylor, B.L., F.F. Liu, and M. Sander, *Nkx6.1 is essential for maintaining the functional state of pancreatic beta cells*. Cell Rep, 2013. **4**(6): p. 1262-75.
106. Taylor, B.L., J. Benthuisen, and M. Sander, *Postnatal beta-cell proliferation and mass expansion is dependent on the transcription factor Nkx6.1*. Diabetes, 2015. **64**(3): p. 897-903.
107. Eto, K., et al., *MafA is required for postnatal proliferation of pancreatic beta-cells*. PLoS One, 2014. **9**(8): p. e104184.
108. Ait-Lounis, A., et al., *Novel function of the ciliogenic transcription factor RFX3 in development of the endocrine pancreas*. Diabetes, 2007. **56**(4): p. 950-9.
109. Soyer, J., et al., *Rfx6 is an Ngn3-dependent winged helix transcription factor required for pancreatic islet cell development*. Development, 2010. **137**(2): p. 203-12.
110. Ait-Lounis, A., et al., *The transcription factor Rfx3 regulates beta-cell differentiation, function, and glucokinase expression*. Diabetes, 2010. **59**(7): p. 1674-85.
111. Smith, S.B., et al., *Rfx6 directs islet formation and insulin production in mice and humans*. Nature, 2010. **463**(7282): p. 775-80.
112. Piccand, J., et al., *Rfx6 maintains the functional identity of adult pancreatic beta cells*. Cell Rep, 2014. **9**(6): p. 2219-32.
113. *International Diabetes Federation. IDF Diabetes Atlas Update 2014*.
114. Ashcroft, F.M. and P. Rorsman, *Diabetes mellitus and the beta cell: the last ten years*. Cell, 2012. **148**(6): p. 1160-71.
115. American Diabetes, A., *Diagnosis and classification of diabetes mellitus*. Diabetes Care, 2014. **37 Suppl 1**: p. S81-90.
116. Rubio-Cabezas, O., et al., *ISPAD Clinical Practice Consensus Guidelines 2014. The diagnosis and management of monogenic diabetes in children and adolescents*. Pediatr Diabetes, 2014. **15 Suppl 20**: p. 47-64.
117. Donath, M.Y. and P.A. Halban, *Decreased beta-cell mass in diabetes: significance, mechanisms and therapeutic implications*. Diabetologia, 2004. **47**(3): p. 581-9.
118. Hosker, J.P., et al., *Similar reduction of first- and second-phase B-cell responses at three different glucose levels in type II diabetes and the effect of gliclazide therapy*. Metabolism, 1989. **38**(8): p. 767-72.
119. Matthews, D.R., et al., *Control of pulsatile insulin secretion in man*. Diabetologia, 1983. **24**(4): p. 231-7.
120. O'Rahilly, S., R.C. Turner, and D.R. Matthews, *Impaired pulsatile secretion of insulin in relatives of patients with non-insulin-dependent diabetes*. N Engl J Med, 1988. **318**(19): p. 1225-30.
121. Polonsky, K.S., et al., *Abnormal patterns of insulin secretion in non-insulin-dependent diabetes mellitus*. N Engl J Med, 1988. **318**(19): p. 1231-9.
122. Talchai, C., et al., *Pancreatic beta cell dedifferentiation as a mechanism of diabetic beta cell failure*. Cell, 2012. **150**(6): p. 1223-34.

123. Cinti, F., et al., *Evidence of beta-Cell Dedifferentiation in Human Type 2 Diabetes*. J Clin Endocrinol Metab, 2016. **101**(3): p. 1044-54.
124. Dahan, T., et al., *Pancreatic beta-Cells Express the Fetal Islet Hormone Gastrin in Rodent and Human Diabetes*. Diabetes, 2017. **66**(2): p. 426-436.
125. Segerstolpe, A., et al., *Single-Cell Transcriptome Profiling of Human Pancreatic Islets in Health and Type 2 Diabetes*. Cell Metab, 2016. **24**(4): p. 593-607.
126. Xin, Y., et al., *RNA Sequencing of Single Human Islet Cells Reveals Type 2 Diabetes Genes*. Cell Metab, 2016. **24**(4): p. 608-615.
127. Guo, S., et al., *Inactivation of specific beta cell transcription factors in type 2 diabetes*. J Clin Invest, 2013. **123**(8): p. 3305-16.
128. Hunter, C.S. and R.W. Stein, *Evidence for Loss in Identity, De-Differentiation, and Trans-Differentiation of Islet beta-Cells in Type 2 Diabetes*. Front Genet, 2017. **8**: p. 35.
129. Jonas, J.C., et al., *Chronic hyperglycemia triggers loss of pancreatic beta cell differentiation in an animal model of diabetes*. J Biol Chem, 1999. **274**(20): p. 14112-21.
130. Brereton, M.F., et al., *Reversible changes in pancreatic islet structure and function produced by elevated blood glucose*. Nat Commun, 2014. **5**: p. 4639.
131. Ding, J., et al., *Pax6 haploinsufficiency causes abnormal metabolic homeostasis by down-regulating glucagon-like peptide 1 in mice*. Endocrinology, 2009. **150**(5): p. 2136-44.
132. Kuroda, A., et al., *Mutation of the Pax6 gene causes impaired glucose-stimulated insulin secretion*. Diabetologia, 2004. **47**(11): p. 2039-41.
133. Mako, M.E., J.I. Starr, and A.H. Rubenstein, *Circulating proinsulin in patients with maturity onset diabetes*. Am J Med, 1977. **63**(6): p. 865-9.
134. Kahn, S.E. and P.A. Halban, *Release of incompletely processed proinsulin is the cause of the disproportionate proinsulinemia of NIDDM*. Diabetes, 1997. **46**(11): p. 1725-32.
135. Kahn, S.E., *Clinical review 135: The importance of beta-cell failure in the development and progression of type 2 diabetes*. J Clin Endocrinol Metab, 2001. **86**(9): p. 4047-58.
136. Mergenthaler, P., et al., *Sugar for the brain: the role of glucose in physiological and pathological brain function*. Trends Neurosci, 2013. **36**(10): p. 587-97.
137. Mutel, E., et al., *Control of blood glucose in the absence of hepatic glucose production during prolonged fasting in mice: induction of renal and intestinal gluconeogenesis by glucagon*. Diabetes, 2011. **60**(12): p. 3121-31.
138. Saltiel, A.R. and J.E. Pessin, *Insulin signaling pathways in time and space*. Trends Cell Biol, 2002. **12**(2): p. 65-71.
139. Winnick, J.J., et al., *A physiological increase in the hepatic glycogen level does not affect the response of net hepatic glucose uptake to insulin*. Am J Physiol Endocrinol Metab, 2009. **297**(2): p. E358-66.
140. Samols, E., G. Marri, and V. Marks, *Interrelationship of glucagon, insulin and glucose. The insulinogenic effect of glucagon*. Diabetes, 1966. **15**(12): p. 855-66.
141. Authier, F. and B. Desbuquois, *Glucagon receptors*. Cell Mol Life Sci, 2008. **65**(12): p. 1880-99.
142. Quesada, I., et al., *Physiology of the pancreatic alpha-cell and glucagon secretion: role in glucose homeostasis and diabetes*. J Endocrinol, 2008. **199**(1): p. 5-19.
143. Jiang, G. and B.B. Zhang, *Glucagon and regulation of glucose metabolism*. Am J Physiol Endocrinol Metab, 2003. **284**(4): p. E671-8.
144. Perry, R.J., et al., *Hepatic acetyl CoA links adipose tissue inflammation to hepatic insulin resistance and type 2 diabetes*. Cell, 2015. **160**(4): p. 745-58.
145. Lei, K.J., et al., *Glucose-6-phosphatase dependent substrate transport in the glycogen storage disease type-1a mouse*. Nat Genet, 1996. **13**(2): p. 203-9.
146. Mutel, E., et al., *Targeted deletion of liver glucose-6 phosphatase mimics glycogen storage disease type 1a including development of multiple adenomas*. J Hepatol, 2011. **54**(3): p. 529-37.
147. Gomez-Valades, A.G., et al., *Pck1 gene silencing in the liver improves glycemia control, insulin sensitivity, and dyslipidemia in db/db mice*. Diabetes, 2008. **57**(8): p. 2199-210.
148. Vieira, E., A. Salehi, and E. Gylfe, *Glucose inhibits glucagon secretion by a direct effect on mouse pancreatic alpha cells*. Diabetologia, 2007. **50**(2): p. 370-9.

149. Gerich, J.E., M.A. Charles, and G.M. Grodsky, *Regulation of pancreatic insulin and glucagon secretion*. *Annu Rev Physiol*, 1976. **38**: p. 353-88.
150. Salehi, A., E. Vieira, and E. Gylfe, *Paradoxical stimulation of glucagon secretion by high glucose concentrations*. *Diabetes*, 2006. **55**(8): p. 2318-23.
151. Cryer, P.E., *Hypoglycaemia: the limiting factor in the glycaemic management of Type I and Type II diabetes*. *Diabetologia*, 2002. **45**(7): p. 937-48.
152. Taniguchi, C.M., B. Emanuelli, and C.R. Kahn, *Critical nodes in signalling pathways: insights into insulin action*. *Nat Rev Mol Cell Biol*, 2006. **7**(2): p. 85-96.
153. Brunet, A., et al., *Akt promotes cell survival by phosphorylating and inhibiting a Forkhead transcription factor*. *Cell*, 1999. **96**(6): p. 857-68.
154. Biggs, W.H., 3rd, et al., *Protein kinase B/Akt-mediated phosphorylation promotes nuclear exclusion of the winged helix transcription factor FKHR1*. *Proc Natl Acad Sci U S A*, 1999. **96**(13): p. 7421-6.
155. Puigserver, P., et al., *Insulin-regulated hepatic gluconeogenesis through FOXO1-PGC-1alpha interaction*. *Nature*, 2003. **423**(6939): p. 550-5.
156. Schilling, M.M., et al., *Gluconeogenesis: re-evaluating the FOXO1-PGC-1alpha connection*. *Nature*, 2006. **443**(7111): p. E10-1.
157. Rhee, J., et al., *Regulation of hepatic fasting response by PPARgamma coactivator-1alpha (PGC-1): requirement for hepatocyte nuclear factor 4alpha in gluconeogenesis*. *Proc Natl Acad Sci U S A*, 2003. **100**(7): p. 4012-7.
158. Matsumoto, M., et al., *Impaired regulation of hepatic glucose production in mice lacking the forkhead transcription factor Foxo1 in liver*. *Cell Metab*, 2007. **6**(3): p. 208-16.
159. Lu, M., et al., *Insulin regulates liver metabolism in vivo in the absence of hepatic Akt and Foxo1*. *Nat Med*, 2012. **18**(3): p. 388-95.
160. Braissant, O., et al., *Differential expression of peroxisome proliferator-activated receptors (PPARs): tissue distribution of PPAR-alpha, -beta, and -gamma in the adult rat*. *Endocrinology*, 1996. **137**(1): p. 354-66.
161. Guerre-Millo, M., et al., *PPAR-alpha-null mice are protected from high-fat diet-induced insulin resistance*. *Diabetes*, 2001. **50**(12): p. 2809-14.
162. Koo, S.H., et al., *PGC-1 promotes insulin resistance in liver through PPAR-alpha-dependent induction of TRB-3*. *Nat Med*, 2004. **10**(5): p. 530-4.
163. Lundasen, T., et al., *PPARalpha is a key regulator of hepatic FGF21*. *Biochem Biophys Res Commun*, 2007. **360**(2): p. 437-40.
164. Galman, C., et al., *The circulating metabolic regulator FGF21 is induced by prolonged fasting and PPARalpha activation in man*. *Cell Metab*, 2008. **8**(2): p. 169-74.
165. Badman, M.K., et al., *Hepatic fibroblast growth factor 21 is regulated by PPARalpha and is a key mediator of hepatic lipid metabolism in ketotic states*. *Cell Metab*, 2007. **5**(6): p. 426-37.
166. Kharitonov, A., et al., *FGF-21 as a novel metabolic regulator*. *J Clin Invest*, 2005. **115**(6): p. 1627-35.
167. Potthoff, M.J., et al., *FGF21 induces PGC-1alpha and regulates carbohydrate and fatty acid metabolism during the adaptive starvation response*. *Proc Natl Acad Sci U S A*, 2009. **106**(26): p. 10853-8.
168. Markan, K.R., et al., *Circulating FGF21 is liver derived and enhances glucose uptake during refeeding and overfeeding*. *Diabetes*, 2014. **63**(12): p. 4057-63.
169. Montagner, A., et al., *Liver PPARalpha is crucial for whole-body fatty acid homeostasis and is protective against NAFLD*. *Gut*, 2016. **65**(7): p. 1202-14.
170. Woods, S.C., et al., *Chronic intracerebroventricular infusion of insulin reduces food intake and body weight of baboons*. *Nature*, 1979. **282**(5738): p. 503-5.
171. McGowan, M.K., et al., *Chronic intrahypothalamic insulin infusion in the rat: behavioral specificity*. *Physiol Behav*, 1993. **54**(5): p. 1031-4.
172. Pocai, A., et al., *Hypothalamic K(ATP) channels control hepatic glucose production*. *Nature*, 2005. **434**(7036): p. 1026-31.
173. Obici, S., et al., *Decreasing hypothalamic insulin receptors causes hyperphagia and insulin resistance in rats*. *Nat Neurosci*, 2002. **5**(6): p. 566-72.

174. Obici, S., et al., *Hypothalamic insulin signaling is required for inhibition of glucose production*. Nat Med, 2002. **8**(12): p. 1376-82.
175. Bruning, J.C., et al., *Role of brain insulin receptor in control of body weight and reproduction*. Science, 2000. **289**(5487): p. 2122-5.
176. Koch, L., et al., *Central insulin action regulates peripheral glucose and fat metabolism in mice*. J Clin Invest, 2008. **118**(6): p. 2132-47.
177. Frederich, R.C., et al., *Leptin levels reflect body lipid content in mice: evidence for diet-induced resistance to leptin action*. Nat Med, 1995. **1**(12): p. 1311-4.
178. Friedman, J.M., *The function of leptin in nutrition, weight, and physiology*. Nutr Rev, 2002. **60**(10 Pt 2): p. S1-14; discussion S68-84, 85-7.
179. Plum, L., B.F. Belgardt, and J.C. Bruning, *Central insulin action in energy and glucose homeostasis*. J Clin Invest, 2006. **116**(7): p. 1761-6.
180. Konner, A.C., T. Klockener, and J.C. Bruning, *Control of energy homeostasis by insulin and leptin: targeting the arcuate nucleus and beyond*. Physiol Behav, 2009. **97**(5): p. 632-8.
181. Niswender, K.D., et al., *Intracellular signalling. Key enzyme in leptin-induced anorexia*. Nature, 2001. **413**(6858): p. 794-5.
182. Aponte, Y., D. Atasoy, and S.M. Sternson, *AGRP neurons are sufficient to orchestrate feeding behavior rapidly and without training*. Nat Neurosci, 2011. **14**(3): p. 351-5.
183. Kim, M.S., et al., *Role of hypothalamic Foxo1 in the regulation of food intake and energy homeostasis*. Nat Neurosci, 2006. **9**(7): p. 901-6.
184. Kitamura, T., et al., *Forkhead protein FoxO1 mediates Agrp-dependent effects of leptin on food intake*. Nat Med, 2006. **12**(5): p. 534-40.
185. Ropelle, E.R., et al., *Inhibition of hypothalamic Foxo1 expression reduced food intake in diet-induced obesity rats*. J Physiol, 2009. **587**(Pt 10): p. 2341-51.
186. Konner, A.C., et al., *Insulin action in AgRP-expressing neurons is required for suppression of hepatic glucose production*. Cell Metab, 2007. **5**(6): p. 438-49.
187. Plum, L., M. Schubert, and J.C. Bruning, *The role of insulin receptor signaling in the brain*. Trends Endocrinol Metab, 2005. **16**(2): p. 59-65.
188. Chi, N. and J.A. Epstein, *Getting your Pax straight: Pax proteins in development and disease*. Trends Genet, 2002. **18**(1): p. 41-7.
189. Blake, J.A. and M.R. Ziman, *Pax genes: regulators of lineage specification and progenitor cell maintenance*. Development, 2014. **141**(4): p. 737-51.
190. Soleimani, V.D., et al., *Transcriptional dominance of Pax7 in adult myogenesis is due to high-affinity recognition of homeodomain motifs*. Dev Cell, 2012. **22**(6): p. 1208-20.
191. Martin-Montalvo, A., et al., *Targeting pancreatic expressed PAX genes for the treatment of diabetes mellitus and pancreatic neuroendocrine tumors*. Expert Opin Ther Targets, 2017. **21**(1): p. 77-89.
192. Robson, E.J., S.J. He, and M.R. Eccles, *A PANorama of PAX genes in cancer and development*. Nat Rev Cancer, 2006. **6**(1): p. 52-62.
193. Lorenzo, P.I., et al., *PAX4 Defines an Expandable beta-Cell Subpopulation in the Adult Pancreatic Islet*. Sci Rep, 2015. **5**: p. 15672.
194. Simpson, T.I. and D.J. Price, *Pax6; a pleiotropic player in development*. Bioessays, 2002. **24**(11): p. 1041-51.
195. Epstein, J., et al., *Identification of a Pax paired domain recognition sequence and evidence for DNA-dependent conformational changes*. J Biol Chem, 1994. **269**(11): p. 8355-61.
196. Wilson, D., et al., *Cooperative dimerization of paired class homeo domains on DNA*. Genes Dev, 1993. **7**(11): p. 2120-34.
197. Tang, H.K., S. Singh, and G.F. Saunders, *Dissection of the transactivation function of the transcription factor encoded by the eye developmental gene PAX6*. J Biol Chem, 1998. **273**(13): p. 7210-21.
198. Epstein, J.A., et al., *Two independent and interactive DNA-binding subdomains of the Pax6 paired domain are regulated by alternative splicing*. Genes Dev, 1994. **8**(17): p. 2022-34.
199. Kozmik, Z., T. Czerny, and M. Busslinger, *Alternatively spliced insertions in the paired domain restrict the DNA sequence specificity of Pax6 and Pax8*. EMBO J, 1997. **16**(22): p. 6793-803.

200. Ton, C.C., H. Miwa, and G.F. Saunders, *Small eye (Sey): cloning and characterization of the murine homolog of the human aniridia gene*. Genomics, 1992. **13**(2): p. 251-6.
201. Hill, R.E., et al., *Mouse small eye results from mutations in a paired-like homeobox-containing gene*. Nature, 1991. **354**(6354): p. 522-5.
202. Matsuo, T., et al., *A mutation in the Pax-6 gene in rat small eye is associated with impaired migration of midbrain crest cells*. Nat Genet, 1993. **3**(4): p. 299-304.
203. Hogan, B.L., et al., *Small eye (Sey): a mouse model for the genetic analysis of craniofacial abnormalities*. Development, 1988. **103 Suppl**: p. 115-9.
204. Glaser, T., et al., *PAX6 gene dosage effect in a family with congenital cataracts, aniridia, anophthalmia and central nervous system defects*. Nat Genet, 1994. **7**(4): p. 463-71.
205. Quiring, R., et al., *Homology of the eyeless gene of Drosophila to the Small eye gene in mice and Aniridia in humans*. Science, 1994. **265**(5173): p. 785-9.
206. Glaser, T., D.S. Walton, and R.L. Maas, *Genomic structure, evolutionary conservation and aniridia mutations in the human PAX6 gene*. Nat Genet, 1992. **2**(3): p. 232-9.
207. Ashery-Padan, R., et al., *Conditional inactivation of Pax6 in the pancreas causes early onset of diabetes*. Dev Biol, 2004. **269**(2): p. 479-88.
208. Dames, P., et al., *Relative roles of the different Pax6 domains for pancreatic alpha cell development*. BMC Dev Biol, 2010. **10**: p. 39.
209. Yasuda, T., et al., *PAX6 mutation as a genetic factor common to aniridia and glucose intolerance*. Diabetes, 2002. **51**(1): p. 224-30.
210. Mitchell, T.N., et al., *Polymicrogyria and absence of pineal gland due to PAX6 mutation*. Annals of Neurology, 2003. **53**(5): p. 658-663.
211. Nishi, M., et al., *A case of novel de novo paired box gene 6 (PAX6) mutation with early-onset diabetes mellitus and aniridia*. Diabet Med, 2005. **22**(5): p. 641-4.
212. Wen, J.H., et al., *Paired box 6 (PAX6) regulates glucose metabolism via proinsulin processing mediated by prohormone convertase 1/3 (PC1/3)*. Diabetologia, 2009. **52**(3): p. 504-13.
213. Gosmain, Y., et al., *Pax6 is crucial for beta-cell function, insulin biosynthesis, and glucose-induced insulin secretion*. Mol Endocrinol, 2012. **26**(4): p. 696-709.
214. Liu, T., et al., *Pax6 directly down-regulates Pcsk1n expression thereby regulating PC1/3 dependent proinsulin processing*. PLoS One, 2012. **7**(10): p. e46934.
215. Ahlqvist, E., et al., *A common variant upstream of the PAX6 gene influences islet function in man*. Diabetologia, 2012. **55**(1): p. 94-104.
216. Chen, Y., et al., *Mutant PAX6 downregulates prohormone convertase 2 expression in mouse islets*. Exp Biol Med (Maywood), 2013. **238**(11): p. 1259-64.
217. Gosmain, Y., et al., *Pax6 is a key component of regulated glucagon secretion*. Endocrinology, 2012. **153**(9): p. 4204-15.
218. Hill, M.E., S.L. Asa, and D.J. Drucker, *Essential requirement for Pax6 in control of enteroendocrine proglucagon gene transcription*. Mol Endocrinol, 1999. **13**(9): p. 1474-86.
219. Trinh, D.K., et al., *Pax-6 activates endogenous proglucagon gene expression in the rodent gastrointestinal epithelium*. Diabetes, 2003. **52**(2): p. 425-33.
220. Kim, J. and J.D. Lauderdale, *Analysis of Pax6 expression using a BAC transgene reveals the presence of a paired-less isoform of Pax6 in the eye and olfactory bulb*. Dev Biol, 2006. **292**(2): p. 486-505.
221. Chen, R., et al., *Single-Cell RNA-Seq Reveals Hypothalamic Cell Diversity*. Cell Rep, 2017. **18**(13): p. 3227-3241.
222. Azuma, N., et al., *PAX6 missense mutation in isolated foveal hypoplasia*. Nat Genet, 1996. **13**(2): p. 141-2.
223. Yamaguchi, Y., et al., *Autoregulation of Pax6 transcriptional activation by two distinct DNA-binding subdomains of the paired domain*. Genes Cells, 1997. **2**(4): p. 255-61.
224. Thaug, C., et al., *Novel ENU-induced eye mutations in the mouse: models for human eye disease*. Hum Mol Genet, 2002. **11**(7): p. 755-67.
225. Walcher, T., et al., *Functional dissection of the paired domain of Pax6 reveals molecular mechanisms of coordinating neurogenesis and proliferation*. Development, 2013. **140**(5): p. 1123-36.

226. Cavanna, D., *In vivo and in vitro analysis of Dll1 and Pax6 function in the adult mouse pancreas*. 2013, Technische Universität München.
227. Ayala, J.E., et al., *Standard operating procedures for describing and performing metabolic tests of glucose homeostasis in mice*. *Dis Model Mech*, 2010. **3**(9-10): p. 525-34.
228. Neschen, S., et al., *Metformin supports the antidiabetic effect of a sodium glucose cotransporter 2 inhibitor by suppressing endogenous glucose production in diabetic mice*. *Diabetes*, 2015. **64**(1): p. 284-90.
229. R Development Core Team (2004) *r: A language and environment for statistical computing*. ISBN 3-900051-00-3, h.w.R.-p.o.
230. Rainer, J., et al., *CARMAweb: comprehensive R- and bioconductor-based web service for microarray data analysis*. *Nucleic Acids Res*, 2006. **34**(Web Server issue): p. W498-503.
231. Dreja, T., et al., *Diet-induced gene expression of isolated pancreatic islets from a polygenic mouse model of the metabolic syndrome*. *Diabetologia*, 2010. **53**(2): p. 309-20.
232. Livak, K.J. and T.D. Schmittgen, *Analysis of relative gene expression data using real-time quantitative PCR and the 2(-Delta Delta C(T)) Method*. *Methods*, 2001. **25**(4): p. 402-8.
233. Blum, B., et al., *Functional beta-cell maturation is marked by an increased glucose threshold and by expression of urocortin 3*. *Nat Biotechnol*, 2012. **30**(3): p. 261-4.
234. Yin, D.D., et al., *Mesothelin promotes cell proliferation in the remodeling of neonatal rat pancreas*. *World J Gastroenterol*, 2014. **20**(22): p. 6884-96.
235. Schwitzgebel, V.M., et al., *Expression of neurogenin3 reveals an islet cell precursor population in the pancreas*. *Development*, 2000. **127**(16): p. 3533-42.
236. Rozman, J., M. Klingenspor, and M. Hrabe de Angelis, *A review of standardized metabolic phenotyping of animal models*. *Mamm Genome*, 2014. **25**(9-10): p. 497-507.
237. Kelley, D.E. and L.J. Mandarino, *Fuel selection in human skeletal muscle in insulin resistance: a reexamination*. *Diabetes*, 2000. **49**(5): p. 677-83.
238. Kubeck, R., et al., *Dietary fat and gut microbiota interactions determine diet-induced obesity in mice*. *Mol Metab*, 2016. **5**(12): p. 1162-1174.
239. van Schaftingen, E. and I. Gerin, *The glucose-6-phosphatase system*. *Biochem J*, 2002. **362**(Pt 3): p. 513-32.
240. Alessi, D.R., et al., *Mechanism of activation of protein kinase B by insulin and IGF-1*. *EMBO J*, 1996. **15**(23): p. 6541-51.
241. Nakae, J., et al., *The forkhead transcription factor Foxo1 (Fkhr) confers insulin sensitivity onto glucose-6-phosphatase expression*. *J Clin Invest*, 2001. **108**(9): p. 1359-67.
242. Witters, L.A. and J. Avruch, *Insulin regulation of hepatic glycogen synthase and phosphorylase*. *Biochemistry*, 1978. **17**(3): p. 406-10.
243. Zeigerer, A., et al., *Functional properties of hepatocytes in vitro are correlated with cell polarity maintenance*. *Exp Cell Res*, 2017. **350**(1): p. 242-252.
244. Chypre, M., N. Zaidi, and K. Smans, *ATP-citrate lyase: a mini-review*. *Biochem Biophys Res Commun*, 2012. **422**(1): p. 1-4.
245. Kim, K.H., *Regulation of mammalian acetyl-coenzyme A carboxylase*. *Annu Rev Nutr*, 1997. **17**: p. 77-99.
246. Shimano, H., et al., *Sterol regulatory element-binding protein-1 as a key transcription factor for nutritional induction of lipogenic enzyme genes*. *J Biol Chem*, 1999. **274**(50): p. 35832-9.
247. Zhang, Y., et al., *The link between fibroblast growth factor 21 and sterol regulatory element binding protein 1c during lipogenesis in hepatocytes*. *Mol Cell Endocrinol*, 2011. **342**(1-2): p. 41-7.
248. Williams, K.W. and J.K. Elmquist, *From neuroanatomy to behavior: central integration of peripheral signals regulating feeding behavior*. *Nat Neurosci*, 2012. **15**(10): p. 1350-5.
249. Bandah, D., et al., *A complex expression pattern of Pax6 in the pigeon retina*. *Invest Ophthalmol Vis Sci*, 2007. **48**(6): p. 2503-9.
250. Rezanejad, H., et al., *In vitro differentiation of adipose-tissue-derived mesenchymal stem cells into neural retinal cells through expression of human PAX6 (5a) gene*. *Cell Tissue Res*, 2014. **356**(1): p. 65-75.
251. Lein, E.S., et al., *Genome-wide atlas of gene expression in the adult mouse brain*. *Nature*, 2007. **445**(7124): p. 168-76.

252. Kristensen, P., et al., *Hypothalamic CART is a new anorectic peptide regulated by leptin*. Nature, 1998. **393**(6680): p. 72-6.
253. Krude, H., et al., *Severe early-onset obesity, adrenal insufficiency and red hair pigmentation caused by POMC mutations in humans*. Nat Genet, 1998. **19**(2): p. 155-7.
254. Perry, R.J., et al., *Leptin reverses diabetes by suppression of the hypothalamic-pituitary-adrenal axis*. Nat Med, 2014. **20**(7): p. 759-63.
255. Ahima, R.S., et al., *Role of leptin in the neuroendocrine response to fasting*. Nature, 1996. **382**(6588): p. 250-2.
256. Barrachina, M.D., et al., *Leptin-induced decrease in food intake is not associated with changes in gastric emptying in lean mice*. Am J Physiol, 1997. **272**(3 Pt 2): p. R1007-11.
257. Heinz, S., et al., *Simple combinations of lineage-determining transcription factors prime cis-regulatory elements required for macrophage and B cell identities*. Mol Cell, 2010. **38**(4): p. 576-89.
258. Wang, Z., et al., *Pancreatic beta cell dedifferentiation in diabetes and redifferentiation following insulin therapy*. Cell Metab, 2014. **19**(5): p. 872-82.
259. Swisa, A., B. Glaser, and Y. Dor, *Metabolic Stress and Compromised Identity of Pancreatic Beta Cells*. Front Genet, 2017. **8**: p. 21.
260. Manuel, M., et al., *Controlled overexpression of Pax6 in vivo negatively autoregulates the Pax6 locus, causing cell-autonomous defects of late cortical progenitor proliferation with little effect on cortical arealization*. Development, 2007. **134**(3): p. 545-55.
261. Samaras, S.E., et al., *Conserved sequences in a tissue-specific regulatory region of the pdx-1 gene mediate transcription in Pancreatic beta cells: role for hepatocyte nuclear factor 3 beta and Pax6*. Mol Cell Biol, 2002. **22**(13): p. 4702-13.
262. Raum, J.C., et al., *Islet beta-cell-specific MafA transcription requires the 5'-flanking conserved region 3 control domain*. Mol Cell Biol, 2010. **30**(17): p. 4234-44.
263. Quintens, R., et al., *Why expression of some genes is disallowed in beta-cells*. Biochem Soc Trans, 2008. **36**(Pt 3): p. 300-5.
264. Gao, N., et al., *Foxa1 and Foxa2 maintain the metabolic and secretory features of the mature beta-cell*. Mol Endocrinol, 2010. **24**(8): p. 1594-604.
265. van der Meulen, T., et al., *Virgin Beta Cells Persist throughout Life at a Neogenic Niche within Pancreatic Islets*. Cell Metab, 2017. **25**(4): p. 911-926 e6.
266. Pound, L.D., et al., *G6PC2: a negative regulator of basal glucose-stimulated insulin secretion*. Diabetes, 2013. **62**(5): p. 1547-56.
267. O'Brien, R.M., *Moving on from GWAS: functional studies on the G6PC2 gene implicated in the regulation of fasting blood glucose*. Curr Diab Rep, 2013. **13**(6): p. 768-77.
268. Arden, C., et al., *A role for PFK-2/FBPase-2, as distinct from fructose 2,6-bisphosphate, in regulation of insulin secretion in pancreatic beta-cells*. Biochem J, 2008. **411**(1): p. 41-51.
269. Gomi, H., et al., *Granuphilin molecularly docks insulin granules to the fusion machinery*. J Cell Biol, 2005. **171**(1): p. 99-109.
270. Li, C., et al., *Urocortin 3 regulates glucose-stimulated insulin secretion and energy homeostasis*. Proc Natl Acad Sci U S A, 2007. **104**(10): p. 4206-11.
271. Kulkarni, R.N., et al., *beta-cell-specific deletion of the Igf1 receptor leads to hyperinsulinemia and glucose intolerance but does not alter beta-cell mass*. Nat Genet, 2002. **31**(1): p. 111-5.
272. Sorensen, H., et al., *Glucagon receptor knockout mice display increased insulin sensitivity and impaired beta-cell function*. Diabetes, 2006. **55**(12): p. 3463-9.
273. Flamez, D., et al., *Mouse pancreatic beta-cells exhibit preserved glucose competence after disruption of the glucagon-like peptide-1 receptor gene*. Diabetes, 1998. **47**(4): p. 646-52.
274. Sunahara, R.K., C.W. Dessauer, and A.G. Gilman, *Complexity and diversity of mammalian adenylyl cyclases*. Annu Rev Pharmacol Toxicol, 1996. **36**: p. 461-80.
275. Arumugam, R., et al., *Regulation of islet beta-cell pyruvate metabolism: interactions of prolactin, glucose, and dexamethasone*. Endocrinology, 2010. **151**(7): p. 3074-83.
276. Zhang, C.Y., et al., *Uncoupling protein-2 negatively regulates insulin secretion and is a major link between obesity, beta cell dysfunction, and type 2 diabetes*. Cell, 2001. **105**(6): p. 745-55.

277. Stark, R., et al., *Phosphoenolpyruvate cycling via mitochondrial phosphoenolpyruvate carboxykinase links anaplerosis and mitochondrial GTP with insulin secretion*. J Biol Chem, 2009. **284**(39): p. 26578-90.
278. Boschero, A.C., et al., *D-glucose and L-leucine metabolism in neonatal and adult cultured rat pancreatic islets*. Mol Cell Endocrinol, 1990. **73**(1): p. 63-71.
279. Graw, J., et al., *Three novel Pax6 alleles in the mouse leading to the same small-eye phenotype caused by different consequences at target promoters*. Invest Ophthalmol Vis Sci, 2005. **46**(12): p. 4671-83.
280. Storlien, L., N.D. Oakes, and D.E. Kelley, *Metabolic flexibility*. Proc Nutr Soc, 2004. **63**(2): p. 363-8.
281. Estivill-Torres, G., et al., *The transcription factor Pax6 is required for development of the diencephalic dorsal midline secretory radial glia that form the subcommissural organ*. Mech Dev, 2001. **109**(2): p. 215-24.
282. Macchi, M.M. and J.N. Bruce, *Human pineal physiology and functional significance of melatonin*. Front Neuroendocrinol, 2004. **25**(3-4): p. 177-95.
283. Abouzeid, H., et al., *PAX6 aniridia and interhemispheric brain anomalies*. Mol Vis, 2009. **15**: p. 2074-83.
284. Marcheva, B., et al., *Disruption of the clock components CLOCK and BMAL1 leads to hypoinsulinaemia and diabetes*. Nature, 2010. **466**(7306): p. 627-31.
285. Bass, J. and J.S. Takahashi, *Circadian integration of metabolism and energetics*. Science, 2010. **330**(6009): p. 1349-54.
286. Turek, F.W., et al., *Obesity and metabolic syndrome in circadian Clock mutant mice*. Science, 2005. **308**(5724): p. 1043-5.
287. Lamia, K.A., K.F. Storch, and C.J. Weitz, *Physiological significance of a peripheral tissue circadian clock*. Proc Natl Acad Sci U S A, 2008. **105**(39): p. 15172-7.
288. Moore, M.C., et al., *Regulation of hepatic glucose uptake and storage in vivo*. Adv Nutr, 2012. **3**(3): p. 286-94.
289. Virtanen, K.A., et al., *Glucose uptake and perfusion in subcutaneous and visceral adipose tissue during insulin stimulation in nonobese and obese humans*. J Clin Endocrinol Metab, 2002. **87**(8): p. 3902-10.
290. Ng, J.M., et al., *PET imaging reveals distinctive roles for different regional adipose tissue depots in systemic glucose metabolism in nonobese humans*. Am J Physiol Endocrinol Metab, 2012. **303**(9): p. E1134-41.
291. Rui, L., *Energy metabolism in the liver*. Compr Physiol, 2014. **4**(1): p. 177-97.
292. She, P., et al., *Mechanisms by which liver-specific PEPCCK knockout mice preserve euglycemia during starvation*. Diabetes, 2003. **52**(7): p. 1649-54.
293. Gelling, R.W., et al., *Lower blood glucose, hyperglucagonemia, and pancreatic alpha cell hyperplasia in glucagon receptor knockout mice*. Proc Natl Acad Sci U S A, 2003. **100**(3): p. 1438-43.
294. Chen, C., et al., *The effects of fasting and refeeding on liver glycogen synthase and phosphorylase in obese and lean mice*. Horm Metab Res, 1992. **24**(4): p. 161-6.
295. Straub, L. and C. Wolfrum, *FGF21, energy expenditure and weight loss - How much brown fat do you need?* Mol Metab, 2015. **4**(9): p. 605-9.
296. Xu, J., et al., *Fibroblast growth factor 21 reverses hepatic steatosis, increases energy expenditure, and improves insulin sensitivity in diet-induced obese mice*. Diabetes, 2009. **58**(1): p. 250-9.
297. Shimomura, I., Y. Bashmakov, and J.D. Horton, *Increased levels of nuclear SREBP-1c associated with fatty livers in two mouse models of diabetes mellitus*. J Biol Chem, 1999. **274**(42): p. 30028-32.
298. Wang, Q., et al., *Abrogation of hepatic ATP-citrate lyase protects against fatty liver and ameliorates hyperglycemia in leptin receptor-deficient mice*. Hepatology, 2009. **49**(4): p. 1166-75.
299. Sachdeva, M.M. and D.A. Stoffers, *Minireview: Meeting the demand for insulin: molecular mechanisms of adaptive postnatal beta-cell mass expansion*. Mol Endocrinol, 2009. **23**(6): p. 747-58.

300. Tamemoto, H., et al., *Insulin resistance and growth retardation in mice lacking insulin receptor substrate-1*. Nature, 1994. **372**(6502): p. 182-6.
301. Araki, E., et al., *Alternative pathway of insulin signalling in mice with targeted disruption of the IRS-1 gene*. Nature, 1994. **372**(6502): p. 186-90.
302. Withers, D.J., et al., *Disruption of IRS-2 causes type 2 diabetes in mice*. Nature, 1998. **391**(6670): p. 900-4.
303. Kubota, N., et al., *Disruption of insulin receptor substrate 2 causes type 2 diabetes because of liver insulin resistance and lack of compensatory beta-cell hyperplasia*. Diabetes, 2000. **49**(11): p. 1880-9.
304. Champy, M.F., et al., *Genetic background determines metabolic phenotypes in the mouse*. Mamm Genome, 2008. **19**(5): p. 318-31.
305. Gerich, J.E., et al., *Prevention of human diabetic ketoacidosis by somatostatin. Evidence for an essential role of glucagon*. N Engl J Med, 1975. **292**(19): p. 985-9.
306. Quant, P.A., P.K. Tubbs, and M.D. Brand, *Treatment of rats with glucagon or mannoheptulose increases mitochondrial 3-hydroxy-3-methylglutaryl-CoA synthase activity and decreases succinyl-CoA content in liver*. Biochem J, 1989. **262**(1): p. 159-64.
307. Meek, T.H., et al., *Evidence That in Uncontrolled Diabetes, Hyperglucagonemia Is Required for Ketosis but Not for Increased Hepatic Glucose Production or Hyperglycemia*. Diabetes, 2015. **64**(7): p. 2376-87.
308. Mountjoy, K.G. and J. Wong, *Obesity, diabetes and functions for proopiomelanocortin-derived peptides*. Mol Cell Endocrinol, 1997. **128**(1-2): p. 171-7.
309. Butler, A.A. and R.D. Cone, *The melanocortin receptors: lessons from knockout models*. Neuropeptides, 2002. **36**(2-3): p. 77-84.
310. Pritchard, L.E., A.V. Turnbull, and A. White, *Pro-opiomelanocortin processing in the hypothalamus: impact on melanocortin signalling and obesity*. J Endocrinol, 2002. **172**(3): p. 411-21.
311. Gantz, I., et al., *Molecular cloning, expression, and gene localization of a fourth melanocortin receptor*. J Biol Chem, 1993. **268**(20): p. 15174-9.
312. Huszar, D., et al., *Targeted disruption of the melanocortin-4 receptor results in obesity in mice*. Cell, 1997. **88**(1): p. 131-41.
313. Vaisse, C., et al., *Melanocortin-4 receptor mutations are a frequent and heterogeneous cause of morbid obesity*. J Clin Invest, 2000. **106**(2): p. 253-62.
314. Balthasar, N., et al., *Divergence of melanocortin pathways in the control of food intake and energy expenditure*. Cell, 2005. **123**(3): p. 493-505.
315. Coll, A.P., I.S. Farooqi, and S. O'Rahilly, *The hormonal control of food intake*. Cell, 2007. **129**(2): p. 251-62.
316. Ahima, R.S. and J.S. Flier, *Leptin*. Annu Rev Physiol, 2000. **62**: p. 413-37.
317. Saladin, R., et al., *Transient increase in obese gene expression after food intake or insulin administration*. Nature, 1995. **377**(6549): p. 527-9.
318. Barr, V.A., et al., *Insulin stimulates both leptin secretion and production by rat white adipose tissue*. Endocrinology, 1997. **138**(10): p. 4463-72.
319. Vong, L., et al., *Leptin action on GABAergic neurons prevents obesity and reduces inhibitory tone to POMC neurons*. Neuron, 2011. **71**(1): p. 142-54.
320. Wu, Q., M.P. Boyle, and R.D. Palmiter, *Loss of GABAergic signaling by AgRP neurons to the parabrachial nucleus leads to starvation*. Cell, 2009. **137**(7): p. 1225-34.
321. Tong, Q., et al., *Synaptic release of GABA by AgRP neurons is required for normal regulation of energy balance*. Nat Neurosci, 2008. **11**(9): p. 998-1000.
322. Chauhan, B.K., et al., *A comparative cDNA microarray analysis reveals a spectrum of genes regulated by Pax6 in mouse lens*. Genes Cells, 2002. **7**(12): p. 1267-83.
323. Hsueh, H., W. Pan, and A.J. Kastin, *The fasting polypeptide FGF21 can enter brain from blood*. Peptides, 2007. **28**(12): p. 2382-6.
324. Liang, Q., et al., *FGF21 maintains glucose homeostasis by mediating the cross talk between liver and brain during prolonged fasting*. Diabetes, 2014. **63**(12): p. 4064-75.

325. Kurosu, H., et al., *Tissue-specific expression of betaKlotho and fibroblast growth factor (FGF) receptor isoforms determines metabolic activity of FGF19 and FGF21*. J Biol Chem, 2007. **282**(37): p. 26687-95.
326. Bookout, A.L., et al., *FGF21 regulates metabolism and circadian behavior by acting on the nervous system*. Nat Med, 2013. **19**(9): p. 1147-52.
327. Shah, B.P., et al., *MC4R-expressing glutamatergic neurons in the paraventricular hypothalamus regulate feeding and are synaptically connected to the parabrachial nucleus*. Proc Natl Acad Sci U S A, 2014. **111**(36): p. 13193-8.
328. Millington, G.W., *The role of proopiomelanocortin (POMC) neurones in feeding behaviour*. Nutr Metab (Lond), 2007. **4**: p. 18.
329. Padilla, S.L., D. Reef, and L.M. Zeltser, *Defining POMC neurons using transgenic reagents: impact of transient Pomc expression in diverse immature neuronal populations*. Endocrinology, 2012. **153**(3): p. 1219-31.
330. Unger, J., et al., *Distribution of insulin receptor-like immunoreactivity in the rat forebrain*. Neuroscience, 1989. **31**(1): p. 143-57.
331. Tepper, B.J. and R.B. Kanarek, *2-DG-induced glucopenia does elicit feeding in rats with lesions of the zona incerta*. Physiol Behav, 1984. **32**(3): p. 441-6.
332. Walsh, L.L. and S.P. Grossman, *Loss of feeding in response to 2-deoxy-D-glucose but not insulin after zona incerta lesions in the rat*. Physiol Behav, 1975. **15**(5): p. 481-5.
333. Qu, D., et al., *A role for melanin-concentrating hormone in the central regulation of feeding behaviour*. Nature, 1996. **380**(6571): p. 243-7.
334. Nahon, J.L., *The melanin-concentrating hormone: from the peptide to the gene*. Crit Rev Neurobiol, 1994. **8**(4): p. 221-62.
335. Bittencourt, J.C., et al., *The melanin-concentrating hormone system of the rat brain: an immuno- and hybridization histochemical characterization*. J Comp Neurol, 1992. **319**(2): p. 218-45.
336. Marsh, D.J., et al., *Melanin-concentrating hormone 1 receptor-deficient mice are lean, hyperactive, and hyperphagic and have altered metabolism*. Proc Natl Acad Sci U S A, 2002. **99**(5): p. 3240-5.
337. *Illustration of a Liver*; <http://www.healthline.com/health/hepatic-failure#overview1>.
338. *Illustration of a pancreas*; <http://pancreaspictures.org/>.
339. Zaret, K.S. and M. Grompe, *Generation and regeneration of cells of the liver and pancreas*. Science, 2008. **322**(5907): p. 1490-4.
340. Deutsch, G., et al., *A bipotential precursor population for pancreas and liver within the embryonic endoderm*. Development, 2001. **128**(6): p. 871-81.
341. Bader, E., et al., *Identification of proliferative and mature beta-cells in the islets of Langerhans*. Nature, 2016. **535**(7612): p. 430-4.
342. Li, H. and R. Durbin, *Fast and accurate short read alignment with Burrows-Wheeler transform*. Bioinformatics, 2009. **25**(14): p. 1754-60.
343. Zhang, Y., et al., *Model-based analysis of ChIP-Seq (MACS)*. Genome Biol, 2008. **9**(9): p. R137.

V. ACKNOWLEDGEMENT

Even though this degree is awarded to a single person, numerous people participate behind the scenes in making it a success but more than that, memorable. First and foremost, I would like to convey my gratitude to Prof. Dr. Martin Hrabě de Angelis for giving me the opportunity to venture into the field of diabetes and metabolism. His constant guidance and keen judgment brought my aims and aspirations into focus and helped me keep on track.

I would like to extend my heartiest thanks go to Dr. Gerhard Przemeczek who kept a constant check on my progress and provided mentorship on a daily basis. I greatly appreciate his supervision and patience for going through my thesis and manuscripts. I am also grateful for having Dr. Heiko Lickert as part of my thesis committee who suggested interesting ideas and supported me in technical hindrances at all times.

I was lucky to have started this journey with Marina Fütterer, my partner in crime. In all these years, we went through a series of emotional rollercoasters. We certainly had a dubious start but still came out the other side to tell the tale of success.

I am especially grateful to Dr. Peter Huypens for being ever-ready to indulge me in highly stimulating conversations and illuminating my mistakes. Thank you for being such a persistent teacher and being a source of immense motivation. In the same light, I would also like to thank Dr. Jan Rozman for his patience with my somewhat naive questions and sharing my enthusiasm as he guided me throughout.

I would also like to thank Dr. Andras Franko, Dr. Susanne Neschen, Dr. Rafaele Teperino and Dr. Jonatan Darr for their willingness to discuss my data and providing constructive criticism. Furthermore, I would like to thank Dr. Paul Pfluger, Katrin Pfuhlmann, Dr. Anja Zeigerer, Bahar Najafi, Sebastian Krämer and Dr. Frauke Neff for engaging in important discourses and collaborations. Special thanks go to Moya Wu, Dr. Birgit Rathkolb, Dr. Martin Irmeler and Prof. Dr. Johannes Beckers for providing expert assistance in certain techniques, which were pertinent to the project. Thank you all for supporting me in shaping my project and therefore this thesis.

On an everyday basis, excellent technical help was provided by Michael Schulz, Andreas Mayer, Sandra Hoffman and Ann-Elizabeth Schwarz. Thank you so much for all the help and

for patiently accepting my bad German and keeping things in good humor. To all the other members of the IEG, I would like to thank for sharing such a remarkable time and making me part of an incredible research team.

I would like to further acknowledge some friends I made throughout the period as a PhD student. The coffee breaks with Sasha and Tommi will always have a special place in heart. Countless times we found ourselves ranting at each other and at our projects in search for answers. Susi, who I befriended later in my PhD period, was always there to lend a helping hand. I had a great time working with you and enjoyed indulging in nonsensical conversations.

I especially enjoyed my days in the office with Selina and Daniela with our non-scientific chats about basically everything under the sun. I thoroughly relished my time working alongside fellow PhD students in the DINI group (Meike, Maria, Christian, Matea, Moritz, Dennis etc.), and these words would probably not be enough to aptly express the friendship and love I found in you, but thank you for making this period of my life unforgettable and helping me get through some ever-recurring and at times infuriating difficulties.

Last, but certainly not the least, I am thankful to my friends and family back home as well as my dearest Vittoria that kept my spirits high and constantly asked after my wellbeing. I am grateful to my parents for regularly checking up on me and helping me to translate parts of this thesis. Thank you all for your faith and love which was an essential source for my confidence in the midst of all the fluster and frustration.

VI. AFFIRMATION

Ich erkläre hiermit an Eides statt, dass ich die vorliegende Arbeit selbstständig, ohne unzulässige fremde Hilfe und ausschließlich mit den angegebenen Quellen und Hilfsmitteln angefertigt habe.

Die verwendeten Literaturquellen sind im Literaturverzeichnis (References) vollständig zitiert.

Diese Arbeit hat in dieser oder ähnlicher Form noch keiner anderen Prüfungsbehörde vorgelegen.



München, den 12.05.2017

Nirav Florian Chhabra

VII. PUBLICATIONS, TALKS AND POSTERS

Publications related to this thesis;

Nirav F Chhabra, Davide Cavanna, Daniel Gradinger, Marina Fütterer, Moya Wu, Birgit Rathkolb, Magdalena Götz, Jovica Ninkovic, Katrin Pfuhlmann, Paul Pfluger, Susanne Seitz, Anja Zeigerer, Peter Huypens, Martin Irmeler, Johannes Beckers, Jan Rozman, Gerhard K. H. Przemeck, Martin Hrabě de Angelis.

Role of *Pax6* in glucose homeostasis and energy metabolism in adult mouse

Manuscript in preparation

Other publications;

Nirav F Chhabra, Sibylle Sabrautzki, Laura Brachthäuser, Fütterer Marina, Gerhard Przemeck, Bettina Lorenz-Depiereux, Susanne Diener, Thomas Wieland, Birgit Rathkolb, Tim-Matthias Strom, Frauke Neff, Martin Hrabě de Angelis

Severe defects in pancreatic islets, hyperglycemia and reduced survival time in *Pdia6* mutant mice

Manuscript in preparation

Marina Fütterer, Nirav F Chhabra, Davide Cavanna, Daniel Gradinger, Martin Irmeler, Johannes Beckers, Gerhard K. H. Przemeck, Martin Hrabě de Angelis.

Dll1- and Dll4-mediated Notch signaling in adult pancreatic β -cells is essential for insulin secretion downstream of the adenylyl cyclase

Manuscript in preparation

Poster and oral presentations;

Nirav F. Chhabra, Marina Fütterer, Moya Wu, Jan Rozman, Martin Irmeler, Johannes Beckers, Katrin Pfuhlmann, Paul Pfluger, Birgit Rathkolb, Susanne Seitz, Anya Zeigerer, Gerhard K. H. Przemeck, Martin Hrabě de Angelis

Systemic metabolic effects exerted by a point mutation in the RED subdomain of PAX6

EASD Munich 2016, poster presentation

Nirav F. Chhabra, Marina Fütterer, Moya Wu, Jan Rozman, Martin Irmeler, Johannes Beckers, Birgit Rathkolb, Katrin Pfuhlmann, Paul Pfluger, Gerhard K. H. Przemeck, Martin Hrabě de Angelis

Systemic metabolic effects exerted by a point mutation in the RED subdomain of PAX6

TAGC Orlando, FL 2016, poster presentation;

Award: travel grant and outstanding poster presentation

Nirav F. Chhabra, Moya Wu, Moya Wu, Jan Rozman, Martin Irmeler, Johannes Beckers, Katrin Pfuhlmann, Paul Pfluger, Gerhard K. H. Przemeck, Martin Hrabě de Angelis

Systemic metabolic effects exerted by a point mutation in the RED subdomain of PAX6

DZD satellite workshop Düsseldorf 2016, oral presentation

Nirav F. Chhabra, Martin Irmeler, Johannes Beckers, Jan Rozman, Gerhard K. H. Przemeck, Martin Hrabě de Angelis

β -cell dedifferentiation and increased insulin sensitivity in a *Pax6* mouse model

Thementag Helmholtz München 2015, oral presentation

Nirav F. Chhabra, Davide Cavanna, Daniel Gradinger, Nina Schieven, Gerhard K. H. Przemeck, Martin Hrabě de Angelis

Molecular and metabolic assessment of PAX6 mutation on pancreatic β -cell

DZD satellite workshop Tübingen 2014, poster presentation

VIII. CURRICULUM VITAE

| | |
|-----------------------|---|
| Name | Nirav Florian Chhabra |
| Geburtsdatum | 6 November 1989 |
| Geburtsort | Neu Delhi |
| Nationalität | Deutsch |
| | |
| April 2013 – Mai 2017 | Promotion Institut für Experimentelle Genetik, Helmholtz Zentrum München AG Prof. Martin Hrabě de Angelis Titel: <i>Developmental gene Pax6 in adult pancreas homeostasis and energy metabolism</i> |
| Aug 2012 – Nov 2012 | Forschungspraktikum Institut für Immunologie, Universität Regensburg AG Prof. Dr. Daniela N. Männel Titel: <i>Investigation of T-cell function in mouse models of sepsis</i> |
| Sept 2010 – Sept 2011 | Master of Research in Biological Sciences Faculty of Life Science, University of Manchester, Manchester, Großbritannien Abschluss: Master of Research (M.Res.) |
| Aug 2007 – Juni 2010 | Bachelor of Biotechnology Manipal Life Sciences Centre, Manipal University, Manipal, Indien Abschluss: Bachelor of Biotechnology (B.Sc.) |
| Bis März 2007 | Gymnasium Rajghat Besant School, Krishnamurti Foundation, Indien Abschluss: Abitur |